

The Ames Stereo Pipeline:
NASA's Open Source Automated Stereogrammetry Software
A part of the NASA NeoGeography Toolkit
Version 2.5.2

Intelligent Robotics Group
NASA Ames Research Center
stereo-pipeline-owner@lists.nasa.gov

July 16, 2016

Credits

The Ames Stereo Pipeline (ASP) was developed by the Intelligent Robotics Group (IRG), in the Intelligent Systems Division at the National Aeronautics and Space Administration (NASA) Ames Research Center in Moffett Field, CA. It builds on over ten years of IRG experience developing surface reconstruction tools for terrestrial robotic field tests and planetary exploration.

Project Lead

- Dr. Ross Beyer (NASA/SETI Institute)

Development Team

- Oleg Alexandrov (NASA/Stinger-Ghaffarian Technologies)
- Scott McMichael (NASA/Stinger-Ghaffarian Technologies)

Former Developers

- Zachary Moratto (NASA/Stinger-Ghaffarian Technologies)
- Michael J. Broxton (NASA/Carnegie Mellon University)
- Dr. Ara Nefian (NASA/Carnegie Mellon University)
- Matthew Hancher (NASA)
- Mike Lundy (NASA/Stinger-Ghaffarian Technologies)
- Vinh To (NASA/Stinger-Ghaffarian Technologies)

Contributing Developer & Former IRG Terrain Reconstruction Lead

- Dr. Laurence Edwards (NASA)

A number of student interns have made significant contributions to this project over the years: Kyle Husmann (California Polytechnic State University), Sasha Aravkin (Washington State University), Aleksandr Segal (Stanford), Patrick Mihelich (Stanford University), Melissa Bunte (Arizona State University), Matthew Faulkner (Massachusetts Institute of Technology), Todd Templeton (UC Berkeley), Morgan Kanter (Bard College), Kerri Cahoy (Stanford University), and Ian Saxton (UC San Diego).

The open source Stereo Pipeline leverages stereo image processing work, past and present, led by Michael J. Broxton (NASA/CMU), Dr. Laurence Edwards (NASA), Eric Zbinden (formerly NASA/QSS Inc.), Dr. Michael Sims (NASA), and others in the Intelligent Systems Division at NASA Ames Research Center. It has benefited substantially from the contributions of Dr. Keith Nishihara (formerly NASA/Stanford), Randy Sargent (NASA/Carnegie Mellon University), Dr. Judd Bowman (formerly NASA/QSS Inc.), Clay Kunz (formerly NASA/QSS Inc.), and Dr. Matthew Deans (NASA).

Acknowledgments

The initial adaptation of Ames' stereo surface reconstruction tools to orbital imagers was a result of a NASA funded, industry led project to develop automated digital elevation model (DEM) generation techniques for the Mars Global Surveyor (MGS) mission. Our work with that project's Principal Investigator, Dr. Michael Malin of Malin Space Science Systems (MSSS), and Co-Investigator, Dr. Laurence Edwards of NASA Ames, inspired the idea of making stereo surface reconstruction technology available and accessible to a broader community. We thank Dr. Malin and Dr. Edwards for providing the initial impetus that in no small way made this open source stereo pipeline possible, and we thank Dr. Michael Caplinger, Joe Fahle and others at MSSS for their help and technical assistance.

We'd also like to thank our friends and collaborators Dr. Randolph Kirk, Dr. Brent Archinal, Trent Hare, and Mark Rosiek of the United States Geological Survey's (USGS's) Astrogeology Science Center in Flagstaff, AZ, for their encouragement and willingness to share their experience and expertise by answering many of our technical questions. We also thank them for their ongoing support and efforts to help us evaluate our work. Thanks also to the USGS Integrated Software for Imagers and Spectrometers (ISIS) team, especially Jeff Anderson and Kris Becker, for their help in integrating stereo pipeline with the USGS ISIS software package.

Thanks go also to Dr. Mark Robinson, Jacob Danton, Ernest Bowman-Cisneros, Dr. Sam Laurence, and Melissa Bunte at Arizona State University for their help in adapting the Ames Stereo Pipeline to lunar data sets including the Apollo Metric Camera.

We'd also like to thank David Shean, Dr. Ben Smith, and Dr. Ian Joughin of the Applied Physics Laboratory at the University of Washington for providing design direction for adapting Ames Stereo Pipeline to Earth sciences.

Finally, we thank Dr. Ara Nefian, and Dr. Laurence Edwards for their contributions to this software, and Dr. Terry Fong (IRG Group Lead) for his management and support of the open source and public software release process.

Portions of this software were developed with support from the following NASA Science Mission Directorate (SMD) and Exploration Systems Mission Directorate (ESMD) funding sources: the Mars Technology Program, the Mars Critical Data Products Initiative, the Mars Reconnaissance Orbiter mission, the Applied Information Systems Research program grant #06-AISRP06-0142, the Lunar Advanced Science and Exploration Research (LASER) program grants #07-LASER07-0148 and #11-LASER11-0112, the ESMD Lunar Mapping and Modeling Program (LMMP), and the SMD Cryosphere Program.

Any opinions, findings, and conclusions or recommendations expressed in this documentation are those of the authors and do not necessarily reflect the views of the National Aeronautics and Space Administration.

Contents

1	Introduction	1
1.1	Background	1
1.2	Human vs. Computer: When to Choose Automation?	2
1.3	Software Foundations	3
1.3.1	NASA Vision Workbench	3
1.3.2	The USGS Integrated Software for Imagers and Spectrometers	3
1.4	Getting Help and Reporting Bugs	4
1.5	Typographical Conventions	4
1.6	Referencing the Ames Stereo Pipeline in Your Work	5
1.7	Warnings to Users of the Ames Stereo Pipeline	5
I	Getting Started	7
2	Installation	9
2.1	Binary Installation	9
2.1.1	Quick Start for ISIS Users	9
2.1.2	Quick Start for Digital Globe Users	10
2.1.3	Quick Start for Aerial and Historical Imagery	10
2.1.4	Common Errors	10
2.2	Installation from Source	11
2.3	Settings Optimization	11
2.3.1	Performance Settings	13
2.3.2	Logging Settings	13
3	Tutorial: Processing Mars Orbiter Camera Imagery	15
3.1	Quick Start	15
3.2	Preparing the Data	15
3.2.1	Loading and Calibrating Images using ISIS	16
3.2.2	Aligning Images	16

4 Tutorial: Processing Earth Digital Globe Imagery	19
4.1 Processing Raw	20
4.2 Processing Map-Projected Imagery	21
4.3 Handling CCD Boundary Artifacts	21
4.4 Managing Camera Jitter	21
4.5 Dealing with Terrain Lacking Large-Scale Features	23
4.6 Processing Multi-Spectral Images	24
5 The Next Steps	25
5.1 Stereo Pipeline in More Detail	25
5.1.1 Setting Options in the <code>stereo.default</code> File	25
5.1.2 Performing Stereo Correlation	26
5.1.3 Running the GUI Frontend	27
5.1.4 Specifying Settings on the Command Line	27
5.1.5 Stereo on Multiple Machines	27
5.1.6 Running Stereo with Map-projected Images	27
5.1.7 Multi-View Stereo	31
5.1.8 Diagnosing Problems	32
5.1.9 Dealing with Long Run-times	34
5.2 Visualizing and Manipulating the Results	34
5.2.1 Building a 3D Mesh Model	34
5.2.2 Building a Digital Elevation Model and Ortho Image	34
5.2.3 Orthorectification of an Image From a Different Source	35
5.2.4 Correcting Camera Positions and Orientations	37
5.2.5 Alignment to Point Clouds From a Different Source	37
5.2.6 Creating DEMs Relative to the Geoid/Areoid	38
5.2.7 Converting to the LAS Format	38
5.2.8 Generating Color Hillshade Maps	38
5.2.9 Building Overlays for Moon and Mars Mode in Google Earth	39
5.2.10 Using DERT to Visualize Terrain Models	40
6 Tips and Tricks	41
II The Stereo Pipeline in Depth	43
7 Stereo Correlation	45
7.1 Pre-Processing	45

7.2	Disparity Map Initialization	47
7.2.1	Debugging Disparity Map Initialization	48
7.2.2	Search Range Determination	50
7.2.3	Local Homography	51
7.3	Sub-pixel Refinement	51
7.4	Triangulation	52
8	Bundle Adjustment	55
8.1	Overview	55
8.2	Bundle adjustment using ASP	56
8.3	Bundle adjustment using ISIS	56
8.3.1	Tutorial: Processing Mars Orbital Camera Imagery	58
9	Solving for Camera Poses Based on Images	63
9.1	Camera Solve Overview	63
9.2	Example: Apollo 15 Metric Camera	64
9.3	Example: IceBridge DMS Camera	67
10	Shape-from-Shading	71
10.1	How to get good test imagery	71
10.2	Running sfs at 1 meter/pixel using a single image	72
10.3	SfS with multiple images in the presence of shadows	74
10.4	Insights for getting the most of SfS	75
11	Data Processing Examples	77
11.1	Guidelines for Selecting Stereo Pairs	77
11.2	Mars Reconnaissance Orbiter HiRISE	77
11.2.1	Columbia Hills	78
11.3	Mars Reconnaissance Orbiter CTX	79
11.3.1	North Terra Meridiani	80
11.4	Mars Global Surveyor MOC-NA	81
11.4.1	Ceraunius Tholus	81
11.5	Mars Exploration Rovers	82
11.5.1	PANCAM, NAVCAM, HAZCAM	82
11.6	K10	84
11.7	Lunar Reconnaissance Orbiter LROC NAC	85
11.7.1	Lee-Lincoln Scarp	85

11.8 Apollo 15 Metric Camera Images	86
11.8.1 Ansgarius C	86
11.9 Cassini ISS NAC	88
11.9.1 Rhea	88
11.10 Digital Globe Imagery	90
11.11 GeoEye and Astrium Imagery / RPC Imagery	90
11.12 SPOT5 Imagery	91
11.13 Dawn (FC) Framing Camera	92
11.14 ASTER Imagery	93
III Appendices	97
A Tools	99
A.1 stereo	99
A.1.1 Entry Points	100
A.1.2 Decomposition of Stereo	100
A.2 stereo_gui	101
A.2.1 Use as an Image Viewer	102
A.2.2 Other Functionality	102
A.3 parallel_stereo	104
A.3.1 Advanced usage	105
A.4 bundle_adjust	107
A.4.1 Ground control points	109
A.5 point2dem	110
A.5.1 Comparing with MOLA Data	111
A.5.2 Post Spacing	111
A.5.3 Using with LAS or CSV Clouds	112
A.6 point2mesh	115
A.7 dem_mosaic	117
A.8 dem_geoid	120
A.9 dg_mosaic	120
A.10 mapproject	122
A.11 disparitydebug	124
A.12 orbitviz	124
A.13 cam2map4stereo.py	126

A.14	pansharpen	127
A.15	datum_convert	127
A.16	point2las	128
A.17	pc_align	128
A.17.1	The input point clouds	128
A.17.2	Alignment method	129
A.17.3	File formats	129
A.17.4	The alignment transform	129
A.17.5	Applying a previous transform	130
A.17.6	Error metrics and outliers	130
A.17.7	Output point clouds and convergence history	130
A.17.8	Manual alignment	131
A.17.9	Troubleshooting	131
A.18	pc_merge	133
A.19	wv_correct	133
A.20	lronac2mosaic.py	134
A.21	image_calc	134
A.22	colormap	135
A.23	hillshade	136
A.24	image2qtree	136
A.25	geodiff	138
A.26	aster2asp	138
A.27	sfs	139
A.28	undistort_image	140
A.29	camera_calibrate	141
A.30	camera_solve	142
A.31	icebridge_kmz_to_csv	143
A.32	lvis2kml	143
A.33	GDAL Tools	144
B	The stereo.default File	145
B.1	Preprocessing	145
B.2	Correlation	146
B.3	Subpixel Refinement	148
B.4	Filtering	149
B.5	Post-Processing (Triangulation)	150

C	Guide to Output Files	153
D	Pinhole Models	157
D.1	File Format	159
E	Papers that used ASP	163
	Bibliography	166

Chapter 1

Introduction

The NASA Ames Stereo Pipeline (ASP) is a suite of free and open source automated geodesy and stereogrammetry tools designed for processing stereo imagery captured from satellites (around Earth and other planets), robotic rovers, aerial cameras, and historical imagery, with and without accurate camera pose information. It produces cartographic products, including digital elevation models (DEMs), ortho-projected imagery, 3D models, and bundle-adjusted networks of cameras. ASP's data products are suitable for science analysis, mission planning, and public outreach.

1.1 Background

The Intelligent Robotics Group (IRG) at the NASA Ames Research Center has been developing 3D surface reconstruction and visualization capabilities for planetary exploration for more than a decade. First demonstrated during the Mars Pathfinder Mission, the IRG has delivered tools providing these capabilities to the science operations teams of the Mars Polar Lander (MPL) mission, the Mars Exploration Rover (MER) mission, the Mars Reconnaissance Orbiter (MRO) mission, and most recently the Lunar Reconnaissance Orbiter (LRO) mission. A critical component technology enabling this work is the Ames Stereo Pipeline (ASP). The Stereo Pipeline generates high quality, dense, texture-mapped 3D surface models from stereo image pairs. In addition, ASP provides tools to perform many other cartography tasks including map projection, point cloud and DEM registration, automatic registration of cameras, data format conversion, and data visualization.

Although initially developed for ground control and scientific visualization applications, the Stereo Pipeline has evolved to address orbital stereogrammetry and cartographic applications. In particular, long-range mission planning requires detailed knowledge of planetary topography, and high resolution topography is often derived from stereo pairs captured from orbit. Orbital mapping satellites are sent as precursors to planetary bodies in advance of landers and rovers. They return a wealth of imagery and other data that helps mission planners and scientists identify areas worthy of more detailed study. Topographic information often plays a central role in this planning and analysis process.

Our recent development of the Stereo Pipeline coincides with a period of time when NASA orbital mapping missions are returning orders of magnitude more data than ever before. Data volumes from the Mars and Lunar Reconnaissance Orbiter missions now measure in the tens of terabytes. There is growing consensus that existing processing techniques, which are still extremely human intensive and expensive, are no longer adequate to address the data processing needs of NASA and the Planetary Science community. To pick an example of particular relevance, the High Resolution Imaging Science Experiment (HiRISE) instrument has captured a few thousand stereo pairs. Of these, only about two hundred stereo pairs have been processed to date; mostly on human-operated, high-end photogrammetric workstations. It is clear that much more value

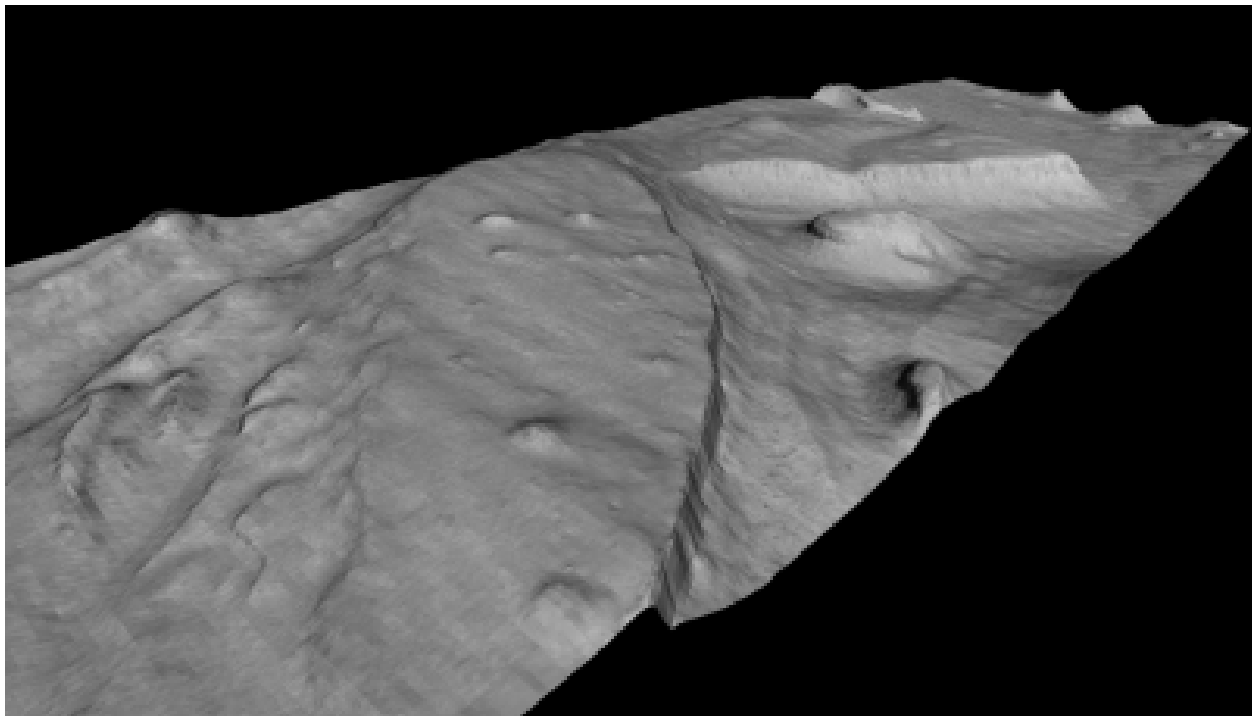


Figure 1.1: This 3D model was generated from a Mars Orbiter Camera (MOC) image pair M01/00115 and E02/01461 (34.66N, 141.29E). The complete stereo reconstruction process takes approximately thirty minutes on a 3.0 GHz workstation for input images of this size (1024×8064 pixels). This model, shown here without vertical exaggeration, is roughly 2 km wide in the cross-track dimension.

could be extracted from this valuable raw data if a more streamlined, efficient process could be developed.

The Stereo Pipeline was designed to address this very need. By applying recent advances in computer vision, we have created an *automated* process that is capable of generating high quality digital elevation models (DEMs) with minimal human intervention. Users of the Stereo Pipeline can expect to spend some time picking a handful of settings when they first start processing a new type of imagery, but once this is done, the Stereo Pipeline can be used to process tens, hundreds, or even thousands of stereo pairs without further adjustment. With the release of this software, we hope to encourage the adoption of this tool chain at institutions that run and support these remote sensing missions. Over time, we hope to see this tool incorporated into ground data processing systems alongside other automated image processing pipelines. As this tool continues to mature, we believe that it will be capable of producing digital elevation models of exceptional quality without any human intervention.

1.2 Human vs. Computer: When to Choose Automation?

When is it appropriate to choose automated stereo mapping over the use of a conventional, human-operated photogrammetric workstation? This is a philosophical question with an answer that is likely to evolve over the coming years as automated data processing technologies become more robust and widely adopted. For now, our opinion is that you should *always* rely on human-guided, manual data processing techniques for producing mission critical data products for missions where human lives or considerable capital resources are at risk. In particular, maps for landing site analysis and precision landing absolutely require the benefit of an expert human operator to eliminate obvious errors in the DEMs, and also to guarantee that the proper procedures have been followed to correct satellite telemetry errors so that the data have the best possible geodetic control.

When it comes to using DEMs for scientific analysis, both techniques have their merits. Human-guided stereo reconstruction produces DEMs of unparalleled quality that benefit from the intuition and experience of an expert. The process of building and validating these DEMs is well-established and accepted in the scientific community.

However, only a limited number of DEMs can be processed to this level of quality. For the rest, automated stereo processing can be used to produce DEMs at a fraction of the cost. The results are not necessarily less accurate than those produced by the human operator, but they will not benefit from the same level of scrutiny and quality control. As such, users of these DEMs must be able to identify potential issues, and be on the lookout for errors that may result from the improper use of these tools.

We recommend that all users of the Stereo Pipeline take the time to thoroughly read this documentation and build an understanding of how stereo reconstruction and bundle adjustment can be best used together to produce high quality results. You are welcome to contact us if you have any questions (section 1.4).

1.3 Software Foundations

1.3.1 NASA Vision Workbench

The Stereo Pipeline is built upon the Vision Workbench software which is a general purpose image processing and computer vision library also developed by the IRG. Some of the tools discussed in this document are actually Vision Workbench programs, and any distribution of the Stereo Pipeline requires the Vision Workbench. This distinction is important only if compiling this software.

1.3.2 The USGS Integrated Software for Imagers and Spectrometers

For processing non-terrestrial NASA satellite imagery, Stereo Pipeline must be installed alongside a copy of United States Geological Survey (USGS) Integrated Software for Imagers and Spectrometers (ISIS). ISIS is however not required for processing Digital Globe images of Earth.

ISIS is widely used in the planetary science community for processing raw spacecraft imagery into high level data products of scientific interest such as map-projected and mosaicked imagery [5, 26, 99]. We chose ISIS because (1) it is widely adopted by the planetary science community, (2) it contains the authoritative collection of geometric camera models for planetary remote sensing instruments, and (3) it is open source software that is easy to leverage.

By installing the Stereo Pipeline, you will be adding an advanced stereo image processing capability that can be used in your existing ISIS workflow. The Stereo Pipeline supports the ISIS “cube” (`.cub`) file format, and can make use of the ISIS camera models and ancillary information (i.e. SPICE kernels) for imagers on many NASA spacecraft. The use of this single standardized set of camera models ensures consistency between products generated in the Stereo Pipeline and those generated by ISIS. Also by leveraging ISIS camera models, the Stereo Pipeline can process stereo pairs captured by just about any NASA mission.

1.4 Getting Help and Reporting Bugs

All bugs, feature requests, and general discussion should be sent to the Ames Stereo Pipeline user mailing list:

stereo-pipeline@lists.nasa.gov

To subscribe to this list, send an empty email message with the subject ‘subscribe’ (without the quotes) to:

stereo-pipeline-request@lists.nasa.gov

To contact the developers and project manager directly, send mail to:

stereo-pipeline-owner@lists.nasa.gov

When you submit a bug report, it may be helpful to attach the logs output by `stereo` and other tools (section 2.3.2).

1.5 Typographical Conventions

Names of programs that are meant to be run on the command line are written in a constant-width font, like the `stereo` program, as are options to those programs.

An indented line of constant-width text can be typed into your terminal, these lines will either begin with a ‘>’ to denote a regular shell, or with ‘**ISIS**’ which denotes an ISIS-enabled shell (which means you have to set the `ISISROOT` environment variable and sourced the appropriate ISIS 3 Startup script, as detailed in the ISIS 3 instructions).

```
> ls
ISIS 3> pds2isis
```

Italicized constant-width text denotes an option or argument that a user will need to supply. For example, ‘`stereo E0201461.map.cub M0100115.map.cub out`’ is specific, but ‘`stereo left-image right-image out`’ indicates that `left-image` and `right-image` are not the names of specific files, but dummy parameters which need to be replaced with actual file names.

Square brackets denote optional options or values to a command, and items separated by a vertical bar are either aliases for each other, or different, specific options. Default arguments are prefixed by an equals sign within parentheses, and line continuation with a backslash:

```
point2dem [--help|-h] [-r moon|mars] [-s float(=0)] \
           [-o output-filename] pointcloud-PC.tif
```

The above indicates a run of the `point2dem` program. The only argument that it requires is a point cloud file, which is produced by the `stereo` program and ends in `-PC.tif`, although its prefix could be anything (hence the italics for that part). Everything else is in square brackets indicating that they are optional.

Here, `--help` and `-h` refer to the same thing. Similarly, the argument to the `-r` option must be either `moon` or `mars`. The `-s` option takes a floating point value as its argument, and has a default value of zero. The `-o` option takes a filename that will be used as the output DEM.

Although there are two lines of constant-width text, the backslash at the end of the first line indicates that the command continues on the second line. You can either type everything into one long line on your own terminal, or use the backslash character and a return to continue typing on a second line in your terminal.

1.6 Referencing the Ames Stereo Pipeline in Your Work

A recent peer-reviewed paper on using ASP (for Earth imagery) that may be cited in your work is:

Shean, D. E., O. Alexandrov, Z. Moratto, B. E. Smith, I. R. Joughin, C. C. Porter, Morin, P. J. 2016. An automated, open-source pipeline for mass production of digital elevation models (DEMs) from very high-resolution commercial stereo satellite imagery. *ISPRS Journal of Photogrammetry and Remote Sensing.* **116**.

Other publications which detail applications to non-terrestrial planetary bodies are:

Moratto, Z. M., M. J. Broxton, R. A. Beyer, M. Lundy, and K. Husmann. 2010. Ames Stereo Pipeline, NASA's Open Source Automated Stereogrammetry Software. *Lunar and Planetary Science Conference 41*, abstract #2364. [\[ADS Abstract\]](#).

Broxton, M. J. and L. J. Edwards. 2008. The Ames Stereo Pipeline: Automated 3D Surface Reconstruction from Orbital Imagery. *Lunar and Planetary Science Conference 39*, abstract #2419. [\[ADS Abstract\]](#).

If you publish a paper using ASP, please let us know. We'll cite your work in this document, in chapter E.

1.7 Warnings to Users of the Ames Stereo Pipeline

Ames Stereo Pipeline is a **research** product. There may be bugs or incomplete features. We reserve the ability to change the API and command line options of the tools we provide. Although we hope you will find this release helpful, you may use it at your own risk. Please check each release's **NEWS** file to see a summary of our recent changes.

While we are confident that the algorithms used by this software are robust, they have not been systematically tested or rigorously compared to other methods in the peer-reviewed literature. We *strongly recommend* that you consult us first before publishing any results based on the cartographic products produced by this software.

Part I

Getting Started

Chapter 2

Installation

2.1 Binary Installation

This is the recommended method. Only the Stereo Pipeline binaries are required. ISIS is required only for users who wish to process NASA non-terrestrial imagery. A full ISIS installation is not required for operation of Stereo Pipeline programs (only the ISIS data directory is needed), but is required for certain preprocessing steps before Stereo Pipeline programs are run for planetary data. If you only want to process terrestrial Digital Globe imagery, skip to section 2.1.2.

Stereo Pipeline Tarball

The main Stereo Pipeline page is <http://irg.arc.nasa.gov/ngt/stereo>. Download the option that matches the platform you wish to use. The recommended, but optional, ISIS version is listed next to the name.

USGS ISIS

If you are working with non-terrestrial imagery, you will need to install ISIS so that you can perform preprocessing such as radiometric calibration and ephemeris attachment. The ISIS installation guide is at <http://isis.astrogeology.usgs.gov/documents/InstallGuide>. You must use their binaries as-is; if you need to recompile, you can follow the *Source Installation* guide for the Stereo Pipeline in Section 2.2. Note also that the USGS provides only the current version of ISIS and the previous version (denoted with a ‘_OLD’ suffix) via their `rsync` service. If the current version is newer than the version of ISIS that the Stereo Pipeline is compiled against, be assured that we’re working on rolling out a new version. However, since Stereo Pipeline has its own self-contained version of ISIS’s libraries built internally, you should be able to use a newer version of ISIS with the now dated version of ASP. This is assuming no major changes have taken place in the data formats or camera models by USGS. At the very least, you should be able to `rsync` the previous version of ISIS if a break is found. To do so, view the listing of modules that is provided via the ‘`rsync isisdist.astrogeology.usgs.gov::`’ command. You should see several modules listed with the ‘_OLD’ suffix. Select the one that is appropriate for your system, and `rsync` according to the instructions.

In closing, running the Stereo Pipeline executables only requires that you have downloaded the ISIS secondary data and have appropriately set the `ISIS3DATA` environment variable. This is normally performed for the user by ISIS startup script, `$ISISROOT/scripts/isis3Startup.sh`.

2.1.1 Quick Start for ISIS Users

Fetch Stereo Pipeline

Download the Stereo Pipeline from <http://irg.arc.nasa.gov/ngt/stereo>.

Fetch ISIS Binaries

As detailed at <http://isis.astrogeology.usgs.gov/documents/InstallGuide>.

Fetch ISIS Data

As detailed at <http://isis.astrogeology.usgs.gov/documents/InstallGuide>.

Untar Stereo Pipeline

```
tar xzvf StereoPipeline-VERSION-ARCH-OS.tar.gz
```

Add Stereo Pipeline to Path (optional)

```
bash: export PATH="/path/to/StereoPipeline/bin:${PATH}"  
csh: setenv PATH "/path/to/StereoPipeline/bin:${PATH}"
```

Set Up ISIS

bash:

```
export ISISROOT=/path/to/isisroot  
source $ISISROOT/scripts/isis3Startup.sh
```

csh:

```
setenv ISISROOT /path/to/isisroot  
source $ISISROOT/scripts/isis3Startup.csh
```

Try It Out

See Chapter 3 for an example.

2.1.2 Quick Start for Digital Globe Users

Fetch Stereo Pipeline

Download the Stereo Pipeline from <http://irg.arc.nasa.gov/ngt/stereo>.

Untar Stereo Pipeline

```
tar xvzf StereoPipeline-VERSION-ARCH-OS.tar.gz
```

Try It Out

Processing Earth imagery is described in the data processing tutorial in chapter 4.

2.1.3 Quick Start for Aerial and Historical Imagery

Fetch the software as before. Processing imagery without accurate camera pose information is described in chapter 9.

2.1.4 Common Errors

Here are some errors you might see, and what it could mean. Treat these as templates for problems. In practice, the error messages might be slightly different.

```
**I/O ERROR** Unable to open [$ISIS3DATA/Some/Path/Here].  
Stereo step 0: Preprocessing failed
```

You need to set up your ISIS environment or manually set the correct location for **ISIS3DATA**.

```
point2mesh stereo-output-PC.tif stereo-output-L.tif
[...]
99% Vertices: [*****] Complete!
    > size: 82212 vertices
Drawing Triangle Strips
Attaching Texture Data
zsh: bus error  point2mesh stereo-output-PC.tif stereo-output-L.tif
```

The source of this problem is an old version of OpenSceneGraph in your library path. Check your LD_LIBRARY_PATH (for Linux), DYLD_LIBRARY_PATH (for OSX), or your DYLD_FALLBACK_LIBRARY_PATH (for OSX) to see if you have an old version listed, and remove it from the path if that is the case. It is not necessary to remove the old versions from your computer, you just need to remove the reference to them from your library path.

```
bash: stereo: command not found
```

You need to add the bin directory of your deployed Stereo Pipeline installation to the environmental variable PATH.

2.2 Installation from Source

This method is for advanced users. You will need to fetch the Stereo Pipeline source code from GitHub at <https://github.com/NeoGeographyToolkit/StereoPipeline> and then follow the instructions specified in INSTALLGUIDE.

2.3 Settings Optimization

Finally, the last thing to be done for Stereo Pipeline is to setup up Vision Workbench's render and logging settings. This step is optional, but for best performance some thought should be applied here.

Vision Workbench is a multi-threaded image processing library used by Stereo Pipeline. The settings by which Vision Workbench processes is configurable by having a .vwrc file hidden in your home directory. Below is an example.

```

1 # This is an example VW configuration file. Save this file to ~/.vwrc
2 # to adjust the VW log settings, even if the program is already running.
3
4 # General settings
5 [general]
6 default_num_threads = 16
7 write_pool_size = 40
8 system_cache_size = 1024000000 # ~ 1 GB
9
10 # The following integers are associated with the log levels throughout the
11 # Vision Workbench. Use these in the log rules below.
12 #
13 #     ErrorMessage = 0
14 #     WarningMessage = 10
15 #     InfoMessage = 20
16 #     DebugMessage = 30
17 #     VerboseDebugMessage = 40
18 #     EveryMessage = 100
19 #
20 # You can create a new log file or adjust the settings
21 # for the console log:
22 #     logfile <filename>
23 #         - or -
24 #     logfile console
25
26 # Once you have created a logfile (or selected the console), you can
27 # add log rules using the following syntax. (Note that you can use
28 # wildcard characters '*' to catch all log_levels for a given
29 # log_namespace, or vice versa.)
30
31 # <log_level> <log_namespace>
32
33 # Below are examples of using the log settings.
34
35 # Turn on various logging levels for several subsystems, with the
36 # output going to the console (standard output).
37 [logfile console]
38 # Turn on error and warning messages for the thread subsystem.
39 10 = thread
40 # Turn on error, warning, and info messages for the asp subsystem.
41 20 = asp
42 # Turn on error, warning, info, and debug messages for the stereo subsystem.
43 30 = stereo
44 # Turn on every single message for the cache subsystem (this will be
45 # extremely verbose and is not recommended).
46 # 100 = cache
47 # Turn off all progress bars to the console (not recommended).
48 # 0 = *.progress
49
50 # Turn on logging of error and warning messages to a file for the
51 # stereo subsystem. Warning: This file will be always appended to, so
52 # it should be deleted periodically.
53 # [logfile /tmp/vw_log.txt]
54 # 10 = stereo

```

There are a lot of possible options that can be implemented in the above example. Let's cover the most important options and the concerns the user should have when selecting a value.

2.3.1 Performance Settings

default_num_threads (default=2)

This sets the maximum number of threads that can be used for rendering. When stereo's `subpixel_rfne` is running you'll probably notice 10 threads are running when you have `default_num_threads` set to 8. This is not an error, you are seeing 8 threads being used for rendering, 1 thread for holding `main()`'s execution, and finally 1 optional thread acting as the interface to the file driver.

It is usually best to set this parameter equal to the number of processors on your system. Be sure to include the number of logical processors in your arithmetic if your system supports hyper-threading.

Adding more threads for rasterization increases the memory demands of Stereo Pipeline. If your system is memory limited, it might be best to lower the `default_num_threads` option. Remember that 32 bit systems can only allocate 4 GB of memory per process. Despite Stereo Pipeline being a multi-threaded application, it is still a single process.

write_pool_size (default=21)

The `write_pool_size` option represents the max waiting pool size of tiles waiting to be written to disk. Most file formats do not allow tiles to be written arbitrarily out of order. Most however will let rows of tiles to be written out of order, while tiles inside a row must be written in order. Because of the previous constraint, after a tile is rasterized it might spend some time waiting in the 'write pool' before it can be written to disk. If the 'write pool' fills up, only the next tile in order can be rasterized. That makes Stereo Pipeline perform like it is only using a single processor.

Increasing the `write_pool_size` makes Stereo Pipeline more able to use all processing cores in the system. Having this value too large can mean excessive use of memory. For 32 bit systems again, they can run out of memory if this value is too high for the same reason as described for `default_num_threads`.

system_cache_size (default=805306368)

Accessing a file from the hard drive can be very slow. It is especially bad if an application needs to make multiple passes over an input file. To increase performance, Vision Workbench will usually leave an input file stored in memory for quick access. This file storage is known as the 'system cache' and its max size is dictated by `system_cache_size`. The default value is 768 MB.

Setting this value too high can cause your application to crash. It is usually recommend to keep this value around 1/4 of the maximum available memory on the system. For 32 bit systems, this means don't set this value any greater than 1 GB. The units of this property is in bytes.

2.3.2 Logging Settings

The messages displayed in the console by Stereo Pipeline are grouped into several namespaces, and by level of verbosity. An example of customizing Stereo Pipeline's output is given in the `.vwrc` file shown above.

Several of the tools in Stereo Pipeline, including `stereo`, automatically append the information displayed in the console to a log file in the current output directory. These logs contain in addition some data about your system and settings, which may be helpful in resolving problems with the tools.

It is also possible to specify a global log file to which all tools will append to, as illustrated in `.vwrc`.

Chapter 3

Tutorial: Processing Mars Orbiter Camera Imagery

3.1 Quick Start

The Stereo Pipeline package contains GUI and command-line programs that convert a stereo pair in the ISIS *cube* format into a 3D “point cloud” image. This is an intermediate format that can be passed along to one of several programs that convert a point cloud into a mesh for 3D viewing, a gridded digital elevation model (DEM) for GIS purposes, or a LAS/LAZ point cloud.

There are a number of ways to fine-tune parameters and analyze the results, but ultimately this software suite takes images and builds models in a mostly automatic way. To create a point cloud file, you simply pass two image files to the `stereo` command:

```
ISIS 3> stereo left_input_image.cub right_input_image.cub stereo-output
```

Alternatively, the `stereo_gui` frontend can be invoked, with the same options, as described in section A.2. This tool makes it possible to select small clips on which to run `stereo`.

The string `stereo-output` is an arbitrary output prefix, it is used when generating names for `stereo` output files. For example, it can be set to `results/output`, in which case all output files will be in the `results` directory and start with the prefix `output`. See section 5.1 for a more detailed discussion.

You can then make a visualizable mesh or a DEM file with the following commands (the `stereo-output-PC.tif` and `stereo-output-L.tif` files are created by the `stereo` program above):

```
ISIS 3> point2mesh stereo-output-PC.tif stereo-output-L.tif
ISIS 3> point2dem stereo-output-PC.tif
```

More details are provided in section 5.2.

3.2 Preparing the Data

The data set that is used in the tutorial and examples below is a pair of Mars Orbital Camera (MOC) [59, 58] images whose Planetary Data System (PDS) Product IDs are M01/00115 and E02/01461. This data can be downloaded from the PDS directly, or they can be found in the `examples/MOC` directory of your Stereo Pipeline distribution.

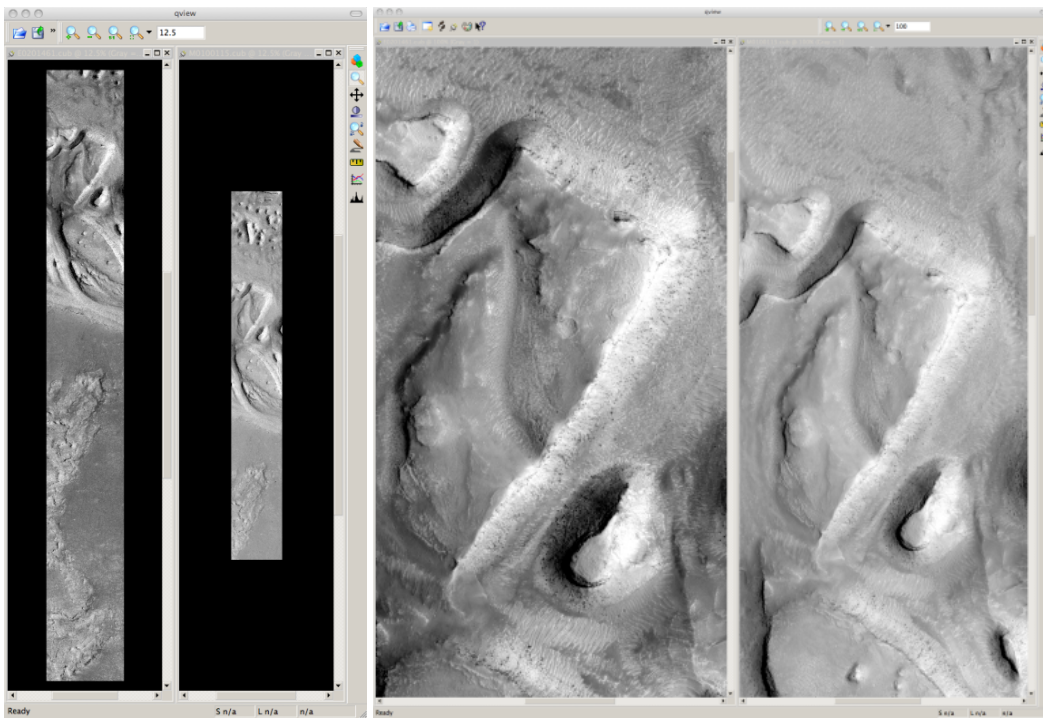


Figure 3.1:
This figure shows E0201461.cub and M0100115.cub open in ISIS's qview program. The view on the left shows their full extents at the same zoom level, showing how they have different ground scales. The view on the right shows both images zoomed in on the same feature.

3.2.1 Loading and Calibrating Images using ISIS

These raw PDS images (M0100115.img and E0201461.img) need to be imported into the ISIS environment and radiometrically calibrated. You will need to be in an ISIS environment (have set the **ISISROOT** environment variable and sourced the appropriate ISIS 3 startup script, as detailed in the ISIS 3 instructions; we will denote this state with the ‘**ISIS 3>**’ prompt). Then you can use the **mocproc** program, as follows:

```
ISIS 3> mocproc from=M0100115.img to=M0100115.cub Mapping=NO
ISIS 3> mocproc from=E0201461.img to=E0201461.cub Mapping=NO
```

There are also **Ingestion** and **Calibration** parameters whose defaults are ‘**YES**’ which will bring the image into the ISIS format and perform radiometric calibration. By setting the **Mapping** parameter to ‘**NO**’, the resultant file will be an ISIS cube file that is calibrated, but not map-projected. Note that while we have not explicitly run **spiceinit**, the Ingestion portion of **mocproc** quietly ran **spiceinit** for you (you’ll find the record of it in the ISIS Session Log, usually written out to a file named **print.prt**). Refer to Figure 3.1 to see the results at this stage of processing.

Datasets for other type of cameras or other planets can be pre-processed similarly, using the ISIS tools specific to them.

3.2.2 Aligning Images

Once the .cub files are obtained, it is possible to run stereo right away, as

```
ISIS 3> stereo E0201461.cub M0100115.cub \
--alignment-method affineepipolar \
-s stereo.default.example results/output
```

In this case, the first thing `stereo` does is to internally align (or rectify the images), which helps with finding stereo matches. Here we have used `affineepipolar` alignment. Another option is to use `homography` alignment, as described in section 5.1.1.

Alternatively, the images can be aligned externally, by map-projecting them in ISIS. External alignment can sometimes give better results than the simple internal alignment described earlier, especially if the images are taken from very different perspectives, or if the curvature of the planet/body being imaged is non-negligible.

We will now describe how to do this alignment, but we also provide the `cam2map4stereo.py` program (page 126) which performs this work automatically for you. (Also note that ASP has its own internal way of map-projecting images, which we believe is preferable. That approach is described in section 5.1.6.)

The ISIS `cam2map` program will map-project these images:

```
ISIS 3> cam2map from=M0100115.cub to=M0100115.map.cub
ISIS 3> cam2map from=E0201461.cub to=E0201461.map.cub map=M0100115.map.cub matchmap=true
```

Notice the order in which the images were run through `cam2map`. The first projection with `M0100115.cub` produced a map-projected image centered on the center of that image. The projection of `E0201461.cub` used the `map=` parameter to indicate that `cam2map` should use the same map projection parameters as those of `M0100115.map.cub` (including center of projection, map extents, map scale, etc.) in creating the projected image. By map-projecting the image with the worse resolution first, and then matching to that, we ensure two things: (1) that the second image is summed or scaled down instead of being magnified up, and (2) that we are minimizing the file sizes to make processing in the Stereo Pipeline more efficient.

Technically, the same end result could be achieved by using the `mocproc` program alone, and using its `map=M0100115.map.cub` option for the run of `mocproc` on `E0201461.cub` (it behaves identically to `cam2map`). However, this would not allow for determining which of the two images had the worse resolution and extracting their minimum intersecting bounding box (see below). Furthermore, if you choose to conduct bundle adjustment (see Chapter 8, page 55) as a pre-processing step, you would do so between `mocproc` (as run above) and `cam2map`.

The above procedure is in the case of two images which cover similar real estate on the ground. If you have a pair of images where one image has a footprint on the ground that is much larger than the other, only the area that is common to both (the intersection of their areas) should be kept to perform correlation (since non-overlapping regions don't contribute to the stereo solution). If the image with the larger footprint size also happens to be the image with the better resolution (i.e. the image run through `cam2map` second with the `map=` parameter), then the above `cam2map` procedure with `matchmap=true` will take care of it just fine. Otherwise you'll need to figure out the latitude and longitude boundaries of the intersection boundary (with the ISIS `camrange` program). Then use that smaller boundary as the arguments to the `MINLAT`, `MAXLAT`, `MINLON`, and `MAXLON` parameters of the first run of `cam2map`. So in the above example, after `mocproc` with `Mapping= NO` you'd do this:

```
ISIS 3> camrange from=M0100115.cub
      ... lots of camrange output omitted ...
Group = UniversalGroundRange
LatitudeType      = Planetocentric
LongitudeDirection = PositiveEast
LongitudeDomain   = 360
MinimumLatitude   = 34.079818835324
MaximumLatitude   = 34.436797628116
MinimumLongitude  = 141.50666207418
```

```

MaximumLongitude    = 141.62534719278
End_Group
    ... more output of camrange omitted ...

ISIS 3> camrange from=E0201461.cub
        ... lots of camrange output omitted ...
Group = UniversalGroundRange
    LatitudeType      = Planetocentric
    LongitudeDirection = PositiveEast
    LongitudeDomain   = 360
    MinimumLatitude   = 34.103893080982
    MaximumLatitude   = 34.547719435156
    MinimumLongitude   = 141.48853937384
    MaximumLongitude   = 141.62919740048
End_Group
    ... more output of camrange omitted ...

```

Now compare the boundaries of the two above and determine the intersection to use as the boundaries for `cam2map`:

```

ISIS 3> cam2map from=M0100115.cub to=M0100115.map.cub DEFaulTRANGE=CAMERA \
          MINLAT=34.10 MAXLAT=34.44 MINLON=141.50 MAXLON=141.63
ISIS 3> cam2map from=E0201461.cub to=E0201461.map.cub map=M0100115.map.cub matchmap=true

```

You only have to do the boundaries explicitly for the first run of `cam2map`, because the second one uses the `map=` parameter to mimic the map-projection of the first. These two images are not radically different in spatial coverage, so this is not really necessary for these images, it is just an example.

Again, unless you are doing something complicated, using the `cam2map4stereo.py` program (page 126) will take care of all these steps for you.

At this stage we can run the stereo program with map-projected images:

```

ISIS 3> stereo E0201461.map.cub M0100115.map.cub --alignment-method none \
          -s stereo.default.example results/output

```

Here we have used `alignment-method none` since `cam2map4stereo.py` brought the two images into the same perspective and using the same resolution. If you invoke `cam2map` independently on the two images, without `matchmap=true`, their resolutions may differ, and using an alignment method rather than `none` to correct for that is still necessary.

Now you may skip to chapter 5 which will discuss the `stereo` program in more detail and the other tools in ASP.

Chapter 4

Tutorial: Processing Earth Digital Globe Imagery

In this chapter we will focus on how to process Earth imagery, or more specifically Digital Globe data. This is different from our previous chapter in that at no point will we be using ISIS utilities. This is because ISIS only supports NASA instruments, while most Earth imagery comes from commercial providers.

In addition to Digital Globe's satellites, ASP supports any Earth imagery that uses the RPC camera model format. How to process such data is described in section 11.11, although following this tutorial may still be insightful even if your data is not from Digital Globe.

Digital Globe provides imagery from Quick Bird and the three World View satellites. These are the hardest images to process with Ames Stereo Pipeline because they are exceedingly large, much larger than HiRISE imagery (the GUI interface can be used to run stereo on just a portion of the images). There is also a wide range of terrain challenges and atmospheric effects that can confuse ASP. Trees are particularly difficult for us since their texture is nearly nadir and perpendicular to our line of sight. It is important to know that the driving force behind our support for Digital Globe imagery is to create models of ice and bare rock. That is the type of imagery that we have tested with and have focused on. If we can make models of wooded or urban areas, that is a bonus, but we can't provide any advice for how to perform or improve the results if you choose to use ASP in that way.

ASP can only process Level 1B satellite imagery, and cannot process Digital Globe's aerial images.

The camera information for Digital Globe images is contained in an XML file for each image. In addition to the exact linear camera model, the XML file also has its RPC approximation. In this chapter we will focus only on processing data using the linear camera model. For more detail on RPC camera models we refer as before to section 11.11.

Our implementation of the linear camera model only models the geometry of the imaging hardware itself and velocity aberration. We do not currently model refraction due to light bending in Earth's atmosphere. It is our understanding that this could represent misplacement of points up to a meter for some imagery. However this is still smaller error than the error from measurement of the spacecraft's position and orientation. The latter can be corrected using bundle adjustment, ideally used with ground control points (section A.4). Alternatively, the `pc_align` tool discussed in section 5.2.5 can be used to align the terrain obtained from ASP to an accurate set of ground measurements.

In the next two sections we will show how to process unmodified and map-projected variants of World View imagery. This steps will be the same for Digital Globe's other satellites. The imagery we are using are from the free stereo pair example of Lucknow, India available from Digital Globe's website [30]. These images represent a non-ideal problem for us since this is an urban location, but at least you should be able

to download this imagery yourself and follow along.

4.1 Processing Raw

After you have downloaded the example stereo imagery of India, you will find a directory titled

```
052783824050_01_P001_PAN
```

It has a lot of files and many of them contain redundant information just displayed in different formats. We are interested only in the TIF or NTF imagery and the similarly named XML files.

Further investigation of the files downloaded will show that there are in fact 4 image files. This is because Digital Globe breaks down a single observation into multiple files for what we assume are size reasons. These files have a pattern string of “_R[N]C1-”, where N increments for every subframe of the full observation. The tool named `dg_mosaic` can be used to mosaic (and optionally reduce the resolution of) such a set of sub-observations into a single image file and create an appropriate camera file

```
> dg_mosaic 12FEB12053305*TIF --output-prefix 12FEB12053305 --reduce-percent 50
```

and analogously for the second set. See section A.9 for more details. The `stereo` program can use either the original or the mosaicked images.

Since we are ingesting these images raw, it is strongly recommended that you use affine epipolar alignment to reduce the search range. The `stereo` command and a rendering in QGIS are shown below.

```
> stereo -t dg --subpixel-mode 1 --alignment-method affineepipolar \
  12FEB12053305-P1BS_R2C1-052783824050_01_P001.TIF \
  12FEB12053341-P1BS_R2C1-052783824050_01_P001.TIF \
  12FEB12053305-P1BS_R2C1-052783824050_01_P001.XML \
  12FEB12053341-P1BS_R2C1-052783824050_01_P001.XML dg/dg
```

Alternatively, the `stereo_gui` frontend can be invoked, with the same options, as described in section A.2.

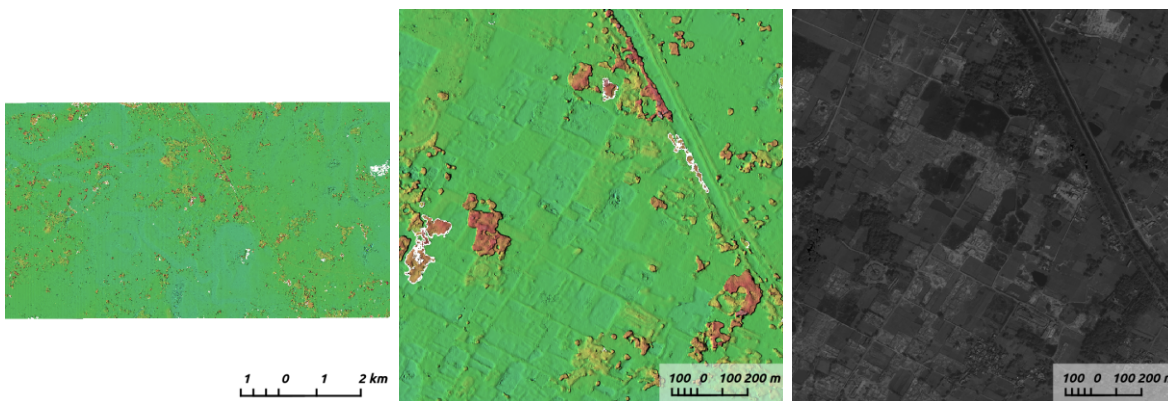


Figure 4.1: Example colorized height map and ortho image output.

Above, we have used `subpixel-mode 1` which is less accurate but reasonably fast. More details about how to set this and other `stereo` parameters can be found in section 5.1.1.

It is important to note that we could have performed stereo using the approximate RPC model instead of the exact linear camera model (both models are in the same XML file), by switching the session in the `stereo` command above from `-t dg` to `-t rpc`. The RPC model is somewhat less accurate, so the results will not be the same, in our experiments we've seen differences in the 3D terrains using the two approaches of 5 meters or more.

4.2 Processing Map-Projected Imagery

ASP computes the highest quality 3D terrain if used with images map-projected onto a low-resolution DEM that is used as an initial guess. This process is described in section 5.1.6.

4.3 Handling CCD Boundary Artifacts

Digital Globe World View images [29] may exhibit slight subpixel artifacts which manifest themselves as discontinuities in the 3D terrain obtained using ASP. We provide a tool named `wv_correct`, that can largely correct such artifacts for World View-1 and World View-2 images for most TDI. It can be invoked as follows:

```
> wv_correct image_in.ntf image.xml image_out.tif
```

The corrected images can be used just as the originals, and the camera models do not change. When working with such imagery, we recommend that CCD artifact correction happen first, on original un-projected imagery. Afterward images can be mosaicked with `dg_mosaic`, map-projected, and the resulting data used to run stereo and create terrain models.

This tool is described in section A.19, and an example of using it is in Figure 4.2.

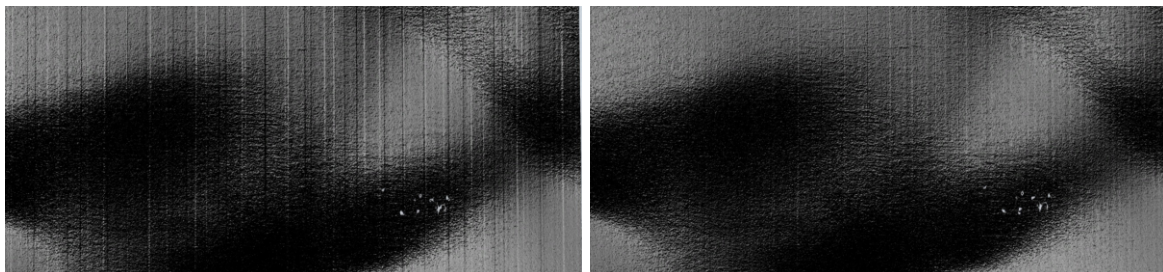


Figure 4.2: Example of a hill-shaded terrain obtained using stereo without (left) and with (right) CCD boundary artifact corrections applied using `wv_correct`.

4.4 Managing Camera Jitter

In this section we will talk about the second largest source of inaccuracies in Digital Globe imagery, after CCD artifacts, namely jitter, and how to correct it.

It is very important to note, right from the beginning, that the order in which these corrections need to be handled is the following. First, CCD artifacts are corrected. Then, optionally, images are mosaicked with `dg_mosaic` and map-projected. And jitter should be handled last, during stereo. An exception is made for WV03 images, for which CCD artifacts do not appear to have a significant effect.

Camera jitter has its origin in the fact that the measured position and orientation of the image-acquiring line sensor as specified in a camera XML file is usually not perfectly accurate, the sensor in fact wiggles slightly from where it is assumed to be as it travels through space and appends rows of pixels to the image. This results in slight errors in the final DEM created using stereo. Those are most clearly seen in the intersection error map output by invoking `point2dem --errorimage`.

ASP provides support for correcting this jitter, at least its lower-frequency component. During stereo, right before the triangulation step, so after the left-to-right image disparity is computed, it can solve for adjustments to apply to the satellite position and orientation. Those adjustments are placed along-track (hence at several lines in the image) with interpolation between them. This is quite analogous to what `bundle_adjust` is doing, except that the latter uses just one adjustment for each image.

This process can be triggered by invoking `stereo` with `--image-lines-per-piecewise-adjustment arg`. A recommended value here is 1000, though it is suggested to try several values. A smaller value of `arg` will result in more adjustments being used (each adjustment being responsible for fewer image lines), hence providing finer-grained control, though making this number too small may result in over-fitting and instability. A smaller value here will also require overall more interest point matches (as computed from the disparity), which is set via `--num-matches-for-piecewise-adjustment`.

Jitter correction is more effective if `stereo` is preceded by bundle adjustment, with the adjusted cameras then being passed to `stereo` via `--bundle-adjust-prefix`.

If it appears that the adjustments show some instability at the starting and ending lines due to not enough matches being present (as deduced from examining the intersection error image), the locations of the first and last adjustment (and everything in between) may be brought closer to each other, by modifying `--piecewise-adjustment-percentiles`. Its values are by default 5 and 95, and could be set for example to 10 and 90. For very tall images, it may be desirable to use instead values closer to 0 and 100.

Section B.5 has the full list of parameters used in jitter correction.

In order for jitter correction to be successful, the disparity map (`*-F.tif`) should be of good quality. If that is not the case, it is suggested to redo stereo, and use, for example, map-projected images, and in the case of terrain lacking large scale features, the value `corr-seed-mode 3` (section 4.5).

An illustration of jitter correction is given in figure 4.3.

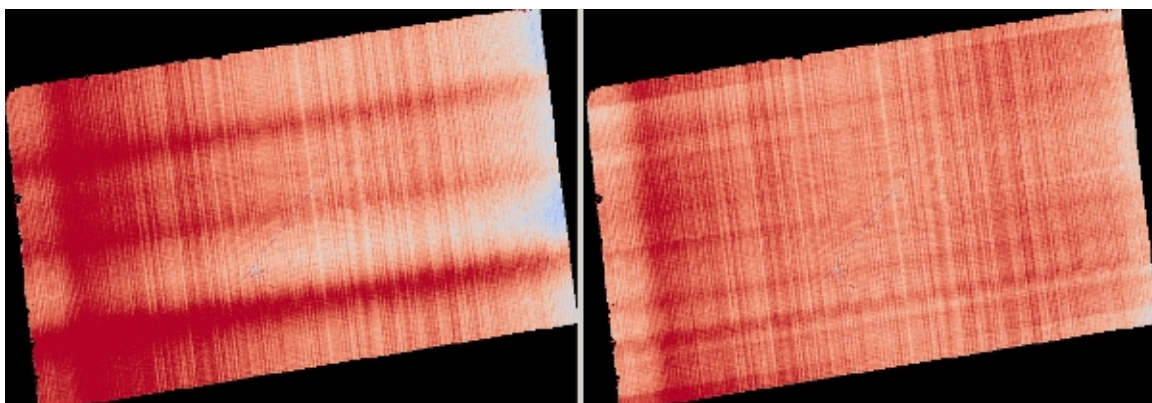


Figure 4.3: Example of a colorized intersection error map before (left) and after jitter correction.

4.5 Dealing with Terrain Lacking Large-Scale Features

Stereo Pipeline's approach to performing correlation is a two-step pyramid algorithm, in which low-resolution versions of the input images are created, the disparity map (*output_prefix-D_sub.tif*) is found, and then this disparity map is refined using increasingly higher-resolution versions of the input images (section 7.2).

This approach usually works quite well for rocky terrain but may fail for snowy landscapes, whose only features may be small-scale grooves or ridges sculpted by wind (so-called *zastrugi*) that disappear at low resolution.

Stereo Pipeline handles such terrains by using a tool named **sparse_disp** to create *output_prefix-D_sub.tif* at full resolution, yet only at a sparse set of pixels for reasons of speed. This low-resolution disparity is then refined as earlier using a pyramid approach.

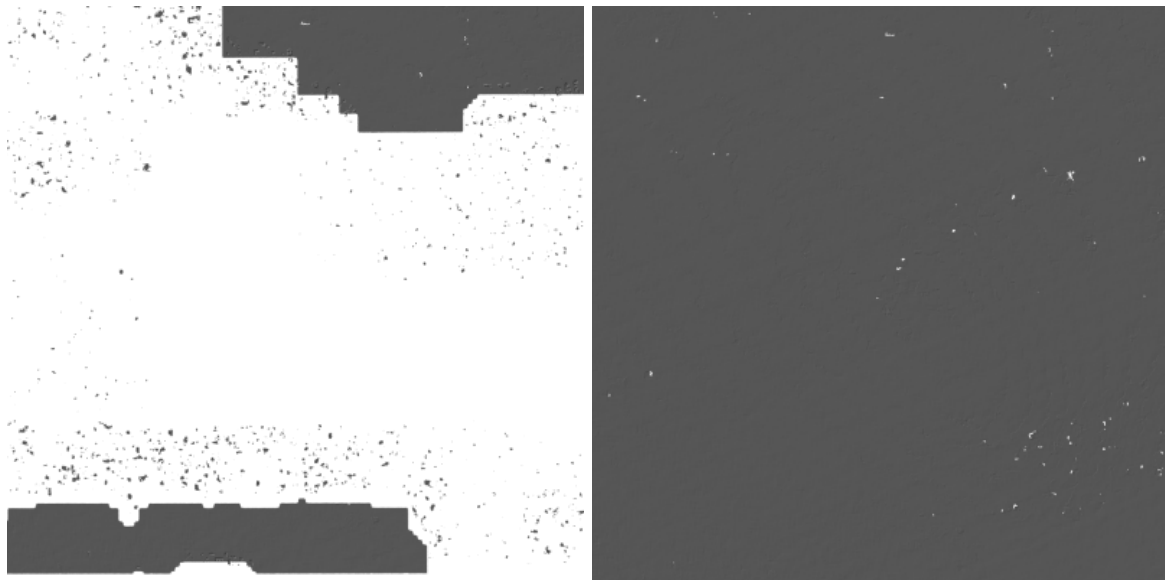


Figure 4.4: Example of a difficult terrain obtained without (left) and with (right) **sparse_disp**. (In these DEMs there is very little elevation change, hence the flat appearance.)

This mode can be invoked by passing to **stereo** the option **--corr-seed-mode 3**. Also, during pyramid correlation it is suggested to use somewhat fewer levels than the default **--corr-max-levels 5**, to again not subsample the images too much and lose the features.

Here is an example:

```
> stereo -t dg --corr-seed-mode 3 --corr-max-levels 2      \
    left_mapped.tif right_mapped.tif                      \
    12FEB12053305-P1BS_R2C1-052783824050_01_P001.XML \
    12FEB12053341-P1BS_R2C1-052783824050_01_P001.XML \
    dg/dg srtm_53_07.tif
```

It is important to note that **sparse_disp** is written in Python and depends on a variety of binary Python modules. These modules cannot be distributed with Stereo Pipeline as they depend on the version of Python installed on your system.

We provide a script which will download and compile the dependencies of this tool for your platform. The script and instructions are at

https://github.com/NeoGeographyToolkit/BinaryBuilder/tree/master/build_python_modules

After building the `sparse_disp` dependencies, per the instructions, the path to the Python modules must be set, for example as:

```
export ASP_PYTHON_MODULES_PATH=<path to python modules>
```

4.6 Processing Multi-Spectral Images

In addition to panchromatic (grayscale) imagery, the Digital Globe satellites also produce lower-resolution multi-spectral (multi-band) images. Stereo Pipeline is designed to process single-band images only. If invoked on multi-spectral data, it will quietly process the first band and ignore the rest. To use one of the other bands it can be singled out by invoking `dg_mosaic` (section 4.1) with the `--band <num>` option. We have evaluated ASP with Digital Globe's multi-spectral images, but support for it is still experimental. We recommend using the panchromatic imagery whenever possible.

Chapter 5

The Next Steps

This chapter will discuss in more detail ASP’s stereo process and other tools available to either pre-process the input images/cameras or to manipulate `stereo`’s outputs, both in the context of planetary ISIS data and for Earth imagery. This includes how to (a) customize `stereo`’s settings (b) use `point2dem` to create 3D terrain models, (c) visualize the results, (d) align the obtained point clouds to another data source, (e) perform 3D terrain adjustments in respect to a geoid, etc.

5.1 Stereo Pipeline in More Detail

5.1.1 Setting Options in the `stereo.default` File

The `stereo` program requires a `stereo.default` file that contains settings that affect the stereo reconstruction process. Its contents can be altered for your needs; details are found in appendix B on page 145. You may find it useful to save multiple versions of the `stereo.default` file for various processing needs. If you do this, be sure to specify the desired settings file by invoking `stereo` with the `-s` option. If this option is not given, the `stereo` program will search for a file named `stereo.default` in the current working directory. If `stereo` does not find `stereo.default` in the current working directory and no file was given with the `-s` option, `stereo` will assume default settings and continue.

An example `stereo.default` file is available in the `examples/` directory of ASP. The actual file has a lot of comments to show you what options and values are possible. Here’s a trimmed version of the important values in that file.

```
alignment-method affineepipolar
cost-mode 2
corr-kernel 21 21
subpixel-mode 1
subpixel-kernel 21 21
```

All these options can be overridden from the command line, as described in section 5.1.4.

Alignment Method

The most important line in `stereo.default` is the first one, specifying the alignment method. For raw images, alignment is always necessary, as the left and right images are from different perspectives. Several alignment methods are supported, including `affineepipolar` and `homography` (see section B.1 for details).

Alternatively, stereo can be performed with map-projected images (section 5.1.6). In effect we take a smooth low-resolution terrain and map both the left and right raw images onto that terrain. This automatically brings both images into the same perspective, and as such, for map-projected images the alignment method is always set to `none`.

Correlation Parameters

The second and third lines in `stereo.default` define what correlation metric (*normalized cross correlation*) we'll be using and how big the template or kernel size should be (*21 pixels square*). A pixel in the left image will be matched to a pixel in the right image by comparing the windows of this size centered at them.

Making the kernel sizes smaller, such as 15×15 , or even 11×11 , may improve results on more complex features, such as steep cliffs, at the expense of perhaps introducing more false matches or noise.

Subpixel Refinement Parameters

A highly critical parameter in ASP is the value of `subpixel-mode`, on the fourth line. When set to 1, `stereo` performs parabola subpixel refinement, which is very fast but not very accurate. When set to 2, it produces very accurate results, but it is about an order of magnitude slower. When set to 3, the accuracy and speed will be somewhere in between the other methods.

The fifth line sets the kernel size to use during subpixel refinement (*also 21 pixels square*).

Search Range Determination

Using these settings alone, ASP will attempt to work out the minimum and maximum disparity it will search for automatically. However if you wish to, you can explicitly set the extent of the search range by adding the option:

```
corr-search -80 -2 20 2
```

More details about this option and the inner workings of stereo correlation can be found in chapter 7.

5.1.2 Performing Stereo Correlation

As already mentioned, the `stereo` program can be invoked for ISIS images as

```
ISIS 3> stereo left_image.cub right_image.cub \
           -s stereo.default results/output
```

For Digital Globe imagery the cameras need to be specified separately:

```
> stereo left.tif right.tif left.xml right.xml \
           -s stereo.default results/output
```

As stated in section 3.1, the string `results/output` is arbitrary, and in this case we will simply make all outputs go to the `results` directory.

When `stereo` finishes, it will have produced a point cloud image. Section 5.2 describes how to convert it to a digital elevation model (DEM) or other formats.

The `stereo` command can also take multiple input images, performing multi-view stereo (section 5.1.7).



Figure 5.1: These are the four viewable .tif files created by the `stereo` program. On the left are the two aligned, pre-processed images: (`results/output-L.tif` and `results/output-R.tif`). The next two are mask images (`results/output-lMask.tif` and `results/output-rMask.tif`), which indicate which pixels in the aligned images are good to use in stereo correlation. The image on the right is the “Good Pixel map”, (`results/output-GoodPixelMap.tif`), which indicates (in gray) which were successfully matched with the correlator, and (in red) those that were not matched.

5.1.3 Running the GUI Frontend

The `stereo_gui` program is a GUI frontend to `stereo`. It is invoked with the same options as `stereo`. It displays the input images, and makes it possible to zoom in and select smaller regions to run `stereo` on. The GUI is described in section A.2.

5.1.4 Specifying Settings on the Command Line

All the settings given via the `stereo.default` file can be over-ridden from the command line. Just add a double hyphen (--) in front the option’s name and then fill out the option just as you would in the configuration file. For options in the `stereo.default` file that take multiple numbers, they must be separated by spaces (like ‘`corr-kernel 25 25`’) on the command line. Here is an example in which we override the search range and subpixel mode from the command line.

```
ISIS 3> stereo E0201461.map.cub M0100115.map.cub \
           -s stereo.map --corr-search -70 -4 40 4 \
           --subpixel-mode 0 results/output
```

5.1.5 Stereo on Multiple Machines

If the input images are really large it may desirable to distribute the work over several computing nodes. ASP provides a tool named `parallel_stereo` for that purpose. Its usage is described in section A.3.

5.1.6 Running Stereo with Map-projected Images

The way `stereo` correlation works is by matching a neighborhood of each pixel in the left image to a similar neighborhood in the right image. This matching process can fail or become unreliable if the two images are too different, which can happen for example if the perspectives of the two cameras are very different or the underlying terrain has steep portions. This will result in ASP producing terrains with noise or missing data.

ASP can mitigate this by *map-projecting* the left and right images onto some pre-existing low-resolution smooth terrain model without holes, and using the output images to do stereo. In effect, this makes the images much more similar and more likely for stereo correlation to succeed.

In this mode, ASP does not create a terrain model from scratch, but rather uses an existing terrain model as an initial guess, and improves on it.

For Earth, an existing terrain model can be, for example, NASA SRTM, GMTED2010, USGS's NED data, or NGA's DTED data. There exist pre-made terrain models for other planets as well, for example the Moon LRO LOLA global DEM and the Mars MGS MOLA DEM.

Alternatively, a low-resolution smooth DEM can be obtained by running ASP itself as described in previous sections. In such a run, subpixel mode may be set to parabola (`subpixel-mode 1`) for speed. To make it sufficiently coarse and smooth, the resolution can be set to about 40 times coarser than either the default `point2dem` resolution or the resolution of the input images. If the resulting DEM turns out to be noisy or have holes, one could change in `point2dem` the search radius factor, use hole-filling, invoke more aggressive outlier removal, and erode pixels at the boundary (those tend to be less reliable). Alternatively, holes can be filled with `dem_mosaic`.

The tool used for map-projecting the images is called `mapproject` (section A.10). It is very important to specify correctly the output resolution (the `--tr` option for `mapproject`) when creating map-projected images. For example, if the input images are about 1 meter/pixel, the same number should be used in `mapproject` (if the desired projection is in degrees, this value should be converted to degrees). If the output resolution is not correct, there will be artifacts in the stereo results.

Some experimentation on a small area may be necessary to obtain the best results.

Example for ISIS images

In this example we illustrate how to run stereo with map-projected images for ISIS data. We start with LRO NAC Lunar images M1121224102LE and M1121209902LE from ASU's LRO NAC web site, <http://lroc.sese.asu.edu/>. We convert them to ISIS cubes using the ISIS program `lronac2isis`, then we use the ISIS tools `spiceinit`, `lronaccal`, and `lrononacecho` to update the SPICE kernels and to do radiometric and echo correction. We name the two obtained .cub files `left.cub` and `right.cub`.

Here we decided to run ASP to create the low-resolution DEM needed for map-projection, rather than get them from an external source. For speed, we process just a small portion of the images:

```
parallel_stereo left.cub right.cub          \
--left-image-crop-win 1984 11602 4000 5000 \
--right-image-crop-win 3111 11027 4000 5000 \
--job-size-w 1024 --job-size-h 1024        \
--subpixel-mode 1                           \
run_nomap/run
```

The input images have resolution of about 1 meter, or 3.3×10^{-5} degrees on the Moon. We create the low-resolution DEM using a resolution 40 times as coarse, so we use a grid size of 0.0013 degrees (we use degrees since the default `point2dem` projection invoked here is `longlat`).

```
point2dem -r moon --nodata-value -32768 --tr 0.0013 run_nomap/run-PC.tif
```

As mentioned earlier, some tweaks to the parameters used by `point2dem` may be necessary for this low-resolution DEM to be smooth enough and with no holes.

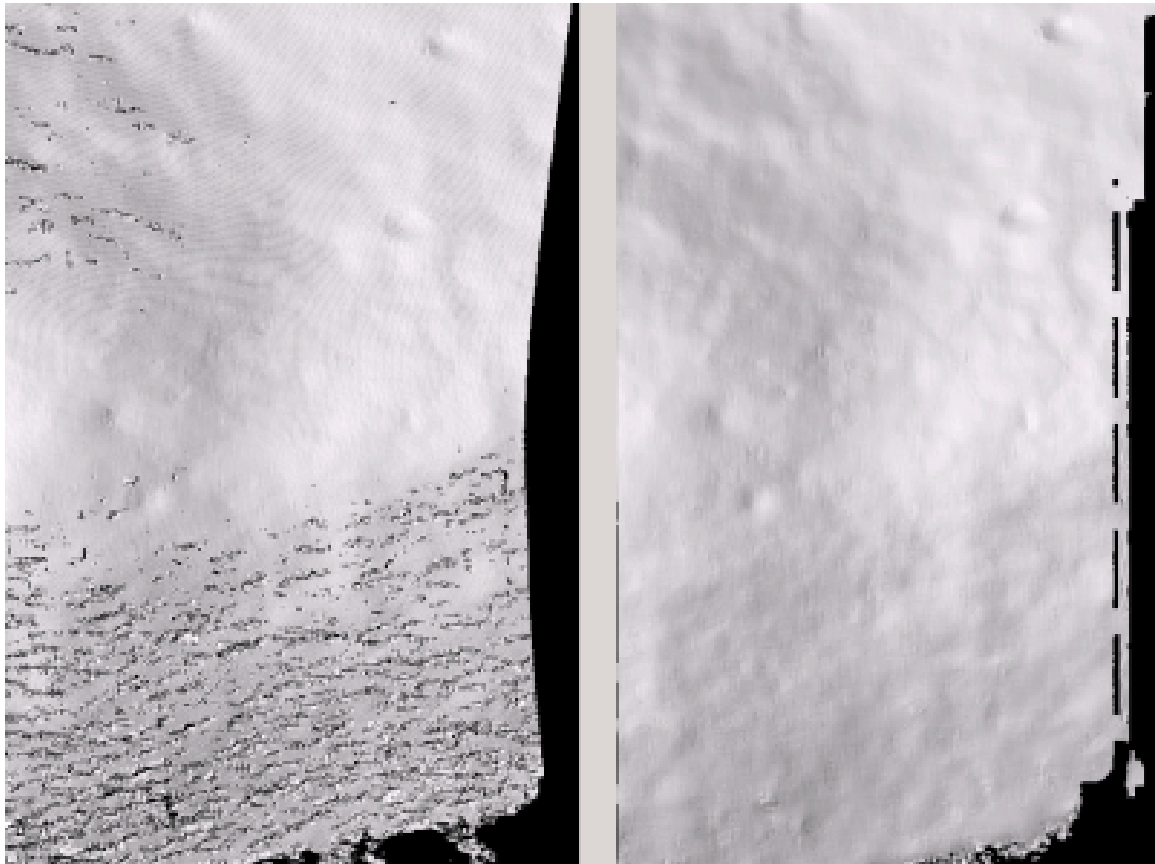


Figure 5.2: A DEM obtained using plain stereo (left) and stereo with map-projected images (right). Their quality will be comparable for relatively flat terrain and the second will be much better for rugged terrain. The right image has some artifacts, but those are limited to areas close to the boundary.

Next, we map-project the images onto this DEM, using the original resolution of 3.3×10^{-5} degrees.

```
mapproject --tr 0.000033 run_nomap/run-DEM.tif left.cub left_proj.tif \
--t_projwin 3.6175120 25.5669989 3.6653695 25.4952127
mapproject --tr 0.000033 run_nomap/run-DEM.tif right.cub right_proj.tif \
--t_projwin 3.6175120 25.5669989 3.6653695 25.4952127
```

Notice that we restricted the area of computation using `--t_projwin` to again make the process faster.

Next, we do stereo with these map-projected images.

```
parallel_stereo --job-size-w 1024 --job-size-h 1024 \
--subpixel-mode 3 \
left_proj.tif right_proj.tif left.cub right.cub \
run_map/run_nomap/run-DEM.tif
```

Notice that even though we use map-projected images, we still specified the original images as the third and fourth arguments. That because we need the camera information from those files. The fifth argument is the output prefix, while the sixth is the low-resolution DEM we used for map-projection. We have used here `--subpixel-mode 3` as this will be the final point cloud and we want the increased accuracy.

Lastly, we create a DEM at 1 meter resolution:

```
point2dem -r moon --nodata-value -32768 --tr 0.000033 run_map/run-PC.tif
```

Note here that we could have used a coarser resolution for the final DEM, such as 4 meters/pixel, since we won't see detail at the level of 1 meter in this DEM, as the stereo process is lossy. This is explained in more detail in section A.5.2.

In figure 5.2 we show the effect of using map-projected images on accuracy of the final DEM.

It is important to note that we could have map-projected the images using the ISIS tool `cam2map`, as described in section 3.2.2. The current approach could be preferable since it allows us to choose the DEM to map-project onto, and it is much faster, since ASP's `mapproject` uses multiple processes, while `cam2map` is restricted to one process and one thread.

Example for Digital Globe Images

In this section we will describe how to run stereo with map-projected images for Digital Globe cameras for Earth. The same process can be used with very minor modifications for any satellite imagery that uses the the RPC camera model. All that is needed is to replace the stereo session when invoking `stereo` below with `rpcmaprpc` from `dgmaprpc`.

Unlike the previous section, here we will use an external DEM to map-project onto, rather than creating our own. We will use a variant of NASA SRTM data with no holes. Other choices have been mentioned earlier.

It is important to note that ASP expects the input low-resolution DEM to be in reference to a datum ellipsoid, such as WGS84 or NAD83. If the DEM is in respect to either the EGM96 or NAVD88 geoids, the ASP tool `dem_geoid` can be used to convert the DEM to WGS84 or NAD83 (section A.8). (The same tool can be used to convert back the final output ASP DEM to be in reference to a geoid, if desired.)

Not applying this conversion might not properly negate the parallax seen between the two images, though it will not corrupt the triangulation results. In other words, sometimes one may be able to ignore the vertical datums on the input but we do not recommend doing that. Also, you should note that the geoheader attached to those types of files usually does not describe the vertical datum they used. That can only be understood by careful reading of your provider's documents.

In this example we use as an input low-resolution DEM the file `srtm_53_07.tif`, a 90 meter resolution tile from the CGIAR-CSI modification of the original NASA SRTM product [25]. The NASA SRTM square for this example spot in India is N26E080.

Below are the commands for map-projecting the input and then running through stereo. You can use any projection you like as long as it preserves detail in the imagery. Note that the last parameter in the stereo call is the input low-resolution DEM. The dataset is the same as the one used in section 4.1.

Commands

```
mapproject -t rpc --t_srs "+proj=eqc +units=m +datum=WGS84" \
--tr 0.5 srtm_53_07.tif \
12FEB12053305-P1BS_R2C1-052783824050_01_P001.TIF \
12FEB12053305-P1BS_R2C1-052783824050_01_P001.XML \
left_mapped.tif
mapproject -t rpc --t_srs "+proj=eqc +units=m +datum=WGS84" \
--tr 0.5 srtm_53_07.tif \
12FEB12053341-P1BS_R2C1-052783824050_01_P001.TIF \

```

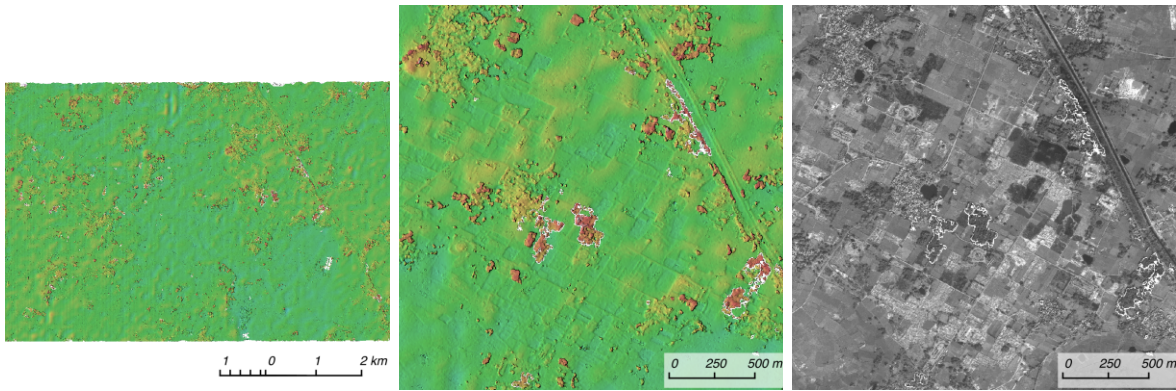


Figure 5.3: Example colorized height map and ortho image output.

```
12FEB12053341-P1BS_R2C1-052783824050_01_P001.XML \
right_mapped.tif
stereo -t dgmaprpc --subpixel-mode 1 --alignment-method none \
left_mapped.tif right_mapped.tif \
12FEB12053305-P1BS_R2C1-052783824050_01_P001.XML \
12FEB12053341-P1BS_R2C1-052783824050_01_P001.XML \
dg/dg srtm_53_07.tif
```

If the `--t_srs` option is not specified, it will be read from the low-resolution input DEM.

The complete list of options for `mapproject` is described in section A.10.

In the `stereo` command, we have used `subpixel-mode 1` which is less accurate but reasonably fast. We have also used `alignment-method none`, since the images are map-projected onto the same terrain with the same resolution, thus no additional alignment is necessary. More details about how to set these and other `stereo` parameters can be found in section 5.1.1.

It is important to note here that any Digital Globe camera file has two models in it, the exact linescan model (which we name `DG`), and its `RPC` approximation. Above, we have used the approximate `RPC` model for map-projection, since map-projection is just a pre-processing step to make the images more similar to each other, this step will be undone during stereo triangulation, and hence using the `RPC` model is good enough, while being much faster than the exact `DG` model. At the stereo stage, we see above that we invoked the `dgmaprpc` session, which suggests that we have used the `RPC` model during map-projection, but we would like to use the accurate `DG` model when performing actual triangulation from the cameras to the ground.

RPC and Pinhole Camera Models

Map-projected images can also be used with `RPC` and `Pinhole` camera models. The `mapproject` command needs to be invoked with `-t rpc` and `-t pinhole` respectively. As earlier, when invoking `stereo` the first two arguments should be the map-projected images, followed by the camera models, output prefix, and the name of the DEM used for map-projection. The session name passed to `stereo` should be `rpccmaprpc` and `pinholemappinhole` respectively.

5.1.7 Multi-View Stereo

ASP supports multi-view stereo at the triangulation stage. In this scenario, the first image is set as reference, disparities are computed from it to all the other images, and then joint triangulation is performed [89]. A

single point cloud is generated with one 3D point for each pixel in the first image. The inputs to multi-view stereo and its output point cloud are handled in the same way as for two-view stereo (e.g., inputs can be map-projected, the output can be converted to a DEM, etc.).

It is suggested that images be bundle-adjusted (section section 8.2) before running multi-view stereo.

Example (for ISIS with three images):

```
stereo file1.cub file2.cub file3.cub results/run
```

Example (for Digital Globe data with three map-projected images):

```
stereo file1.tif file2.tif file3.tif file1.xml file2.xml file3.xml \
results/run input-DEM.tif
```

The `parallel_stereo` tool can also be used with multiple images (section A.3).

For a sequence of images, multi-view stereo can be run several times with each image as a reference, and the obtained point clouds combined into a single DEM using `point2dem` (section A.5).

The ray intersection error, the fourth band in the point cloud file, is computed as twice the mean of distances from the optimally computed intersection point to the individual rays. For two rays, this agrees with the intersection error for two-view stereo which is defined as the minimal distance between rays. For multi-view stereo this error is much less amenable to interpretation than for two-view stereo, since the number of valid rays corresponding to a given feature can vary across the image, which results in discontinuities in the intersection error.

Other ways of combining multiple images

As an alternative to multi-view stereo, point clouds can be generated from multiple stereo pairs, and then a single DEM can be created with `point2dem` (section 5.2.2). Or, multiple DEMs can be created, then combined into a single DEM with `dem_mosaic` (section A.7).

In both of these approaches, the point clouds could be registered to a trusted dataset using `pc_align` before creating a combined terrain model (section 5.2.5).

5.1.8 Diagnosing Problems

Once invoked, `stereo` proceeds through several stages that are detailed on page 100. Intermediate and final output files are generated as it goes. See Appendix C, page 153 for a comprehensive listing. Many of these files are useful for diagnosing and debugging problems. For example, as Figure 5.1 shows, a quick look at some of the TIFF files in the `results/` directory provides some insight into the process.

Perhaps the most accessible file for assessing the quality of your results is the good pixel image, (`results/output-GoodPixelMap.tif`). If this file shows mostly good, gray pixels in the overlap area (the area that is white in both the `results/output-lMask.tif` and `results/output-rMask.tif` files), then your results are just fine. If the good pixel image shows lots of failed data, signified by red pixels in the overlap area, then you need to go back and tune your `stereo.default` file until your results improve. This might be a good time to make a copy of `stereo.default` as you tune the parameters to improve the results.

Whenever `stereo`, `point2dem`, and other executables are run, they create log files in given tool's results directory, containing a copy of the configuration file, the command that was run, your system settings, and

tool's console output. This will help track what was performed so that others in the future can recreate your work.

Another handy debugging tool is the `disparitydebug` program, which allows you to generate viewable versions of the intermediate results from the stereo correlation algorithm. `disparitydebug` converts information in the disparity image files into two TIFF images that contain horizontal and vertical components of the disparity (i.e. matching offsets for each pixel in the horizontal and vertical directions). There are actually three flavors of disparity map: the `-D.tif`, the `-RD.tif`, and `-F.tif`. You can run `disparitydebug` on any of them. Each shows the disparity map at the different stages of processing.

```
> disparitydebug results/output-F.tif
```

If the output H and V files from `disparitydebug` look good, then the point cloud image is most likely ready for post-processing. You can proceed to make a mesh or a DEM by processing `results/output-PC.tif` using the `point2mesh` or `point2dem` tools, respectively.

Figure 5.4 shows the outputs of `disparitydebug`.

If the input images are map-projected (georeferenced) and the alignment method is `none`, all images output by stereo are georeferenced as well, such as `GoodPixelMap`, `D_sub`, `disparity`, etc. As such, all these data can be overlayed in `stereo_gui`. `disparitydebug` also preserves any georeference.

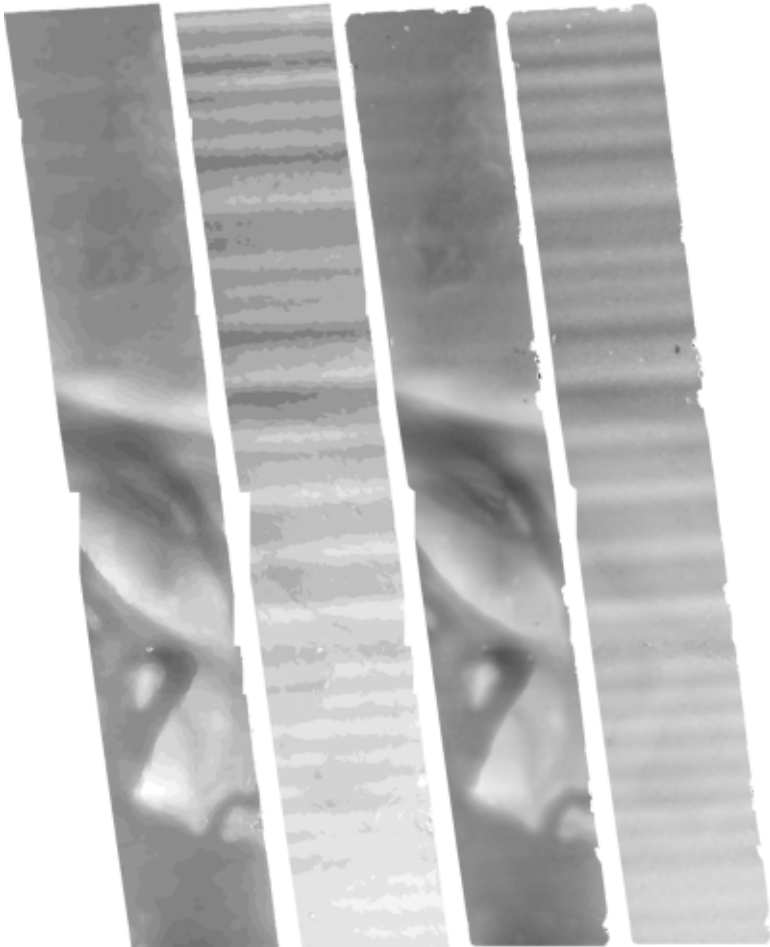


Figure 5.4: Disparity images produced using the `disparitydebug` tool. The two images on the left are the `results/output-D-H.tif` and `results/output-D-V.tif` files, which are normalized horizontal and vertical disparity components produced by the disparity map initialization phase. The two images on the right are `results/output-F-H.tif` and `results/output-F-V.tif`, which are the final filtered, sub-pixel-refined disparity maps that are fed into the Triangulation phase to build the point cloud image. Since these MOC images were acquired by rolling the spacecraft across-track, most of the disparity that represents topography is present in the horizontal disparity map. The vertical disparity map shows disparity due to “washboarding,” which is not from topography but from spacecraft movement. Note however that the horizontal and vertical disparity images are normalized independently. Although both have the same range of gray values from white to black, they represent significantly different absolute ranges of disparity.

5.1.9 Dealing with Long Run-times

If `stereo_corr` takes unreasonably long, it may have encountered a portion of the image where, due to noise (such as clouds, shadows, etc.) the determined search range is much larger than what it should be. The option `--corr-timeout integer` can be used to limit how long each 1024×1024 pixel tile can take. A good value here could be 300 (seconds) or more if your terrain is expected to have large height variations.

5.2 Visualizing and Manipulating the Results

When `stereo` finishes, it will have produced a point cloud image. At this point, many kinds of data products can be built from the `results/output-PC.tif` point cloud file.

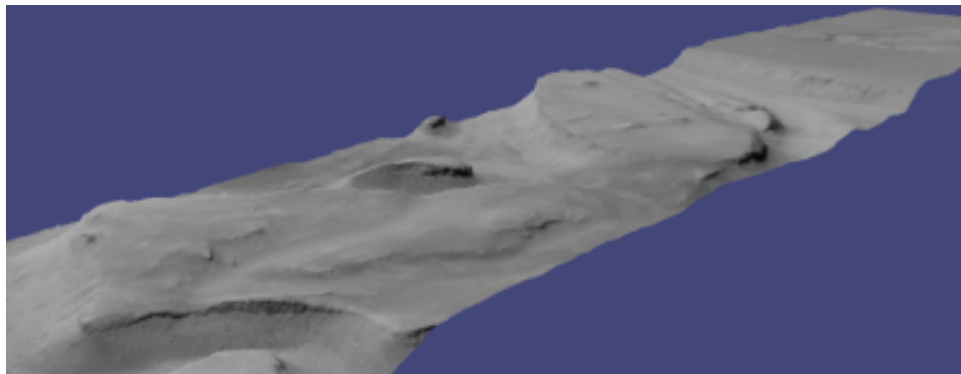


Figure 5.5: The `results/output.osgb` file displayed in the OSG Viewer.

5.2.1 Building a 3D Mesh Model

If you wish to see the data in an interactive 3D browser, then you can generate a 3D object file using the `point2mesh` command (page 115). The resulting file is stored in Open Scene Graph binary format [18]. It can be viewed with `osgviewer` (the Open Scene Graph Viewer program, distributed with the binary version of the Stereo Pipeline). The `point2mesh` program takes the point cloud file and the left normalized image as inputs:

```
> point2mesh results/output-PC.tif results/output-L.tif
> osgviewer results/output.osgb
```

The image displayed by `osgviewer` is shown in figure 5.5.

When the `osgviewer` program starts, you may want to toggle the lighting with the 'L' key, toggle texturing with the 'T' key, and toggle wireframe mode with the 'W'. Press '?' to see a variety of other interactive options.

If you already have a DEM and an ortho image (section 5.2.2), they can be used to build a mesh as well, in the same way as done above:

```
> point2mesh results/output-DEM.tif results/output-DRG.tif
```

5.2.2 Building a Digital Elevation Model and Ortho Image

The `point2dem` program (page 110) creates a Digital Elevation Model (DEM) from the point cloud file.

```
> point2dem results/output-PC.tif
```

The resulting TIFF file is map-projected and will contain georeferencing information stored as GeoTIFF tags.

The tool will infer the datum and projection from the input images, if present. You can explicitly specify a coordinate system (e.g., mercator, sinusoidal) and a reference spheroid (i.e., calculated for the Moon, Mars, or Earth). Alternatively, the datum semi-axes can be set or a PROJ.4 string can be passed in.

```
> point2dem -r mars results/output-PC.tif
```

The output DEM will be named `results/output-DEM.tif`. It can be imported into a variety of GIS platforms. The DEM can be transformed into a hill-shaded image for visualization (section 5.2.8). Both the DEM itself and its hill-shaded version can be examined in `stereo_gui`.

The `point2dem` program can also be used to orthoproject raw satellite imagery onto the DEM. To do this, invoke `point2dem` just as before, but add the `--orthoimage` option and specify the use of the left image file as the texture file to use for the projection:

```
> point2dem -r mars results/output-PC.tif --orthoimage results/output-L.tif
```

The texture file must always be specified after the point cloud file. See figure 5.6 on the right for the output of this command.

If the DEM has holes, which can be inevitable, those holes will also show up in the orthoimage. They can be filled in using the option `--orthoimage-hole-fill-len` with a value passed to it.

The `point2dem` program is also able to accept output projection options the same way as the tools in GDAL. Well-known EPSG, IAU2000 projections, and custom PROJ.4 strings can applied with the target spatial reference set flag, `--t_srs`. If the target spatial reference flag is applied with any of the reference spheroid options, the reference spheroid option will overwrite the datum defined in the target spatial reference set. The following examples produce the same output.

```
> point2dem --t_srs IAU2000:49900 results/output-PC.tif
> point2dem --t_srs "+proj=longlat +a=3396190 +b=3376200"
   results/output-PC.tif
```

The `point2dem` program can be used in many different ways. The complete documentation is in section A.5.

5.2.3 Orthorectification of an Image From a Different Source

If you have already obtained a DEM, using ASP or some other approach, and have an image and camera pair which you would like to overlay on top of this terrain, use the `mapproject` tool (section A.10).

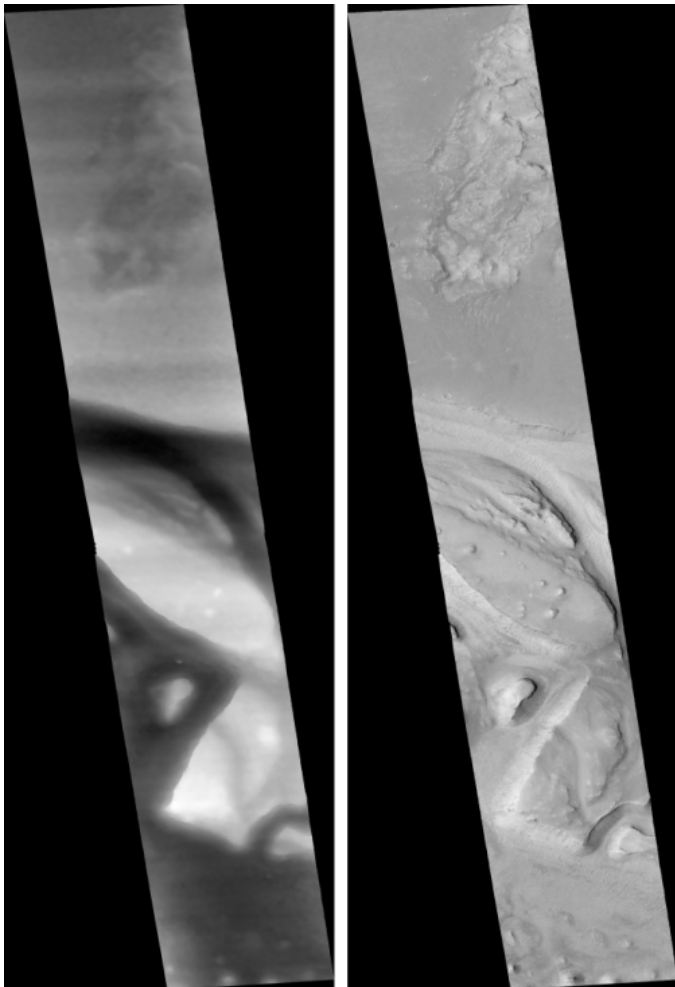


Figure 5.6: The image on the left is a normalized DEM (generated using `point2dem`'s `-n` option), which shows low terrain values as black and high terrain values as white. The image on the right is the left input image projected onto the DEM (created using the `--orthoimage` option to `point2dem`).

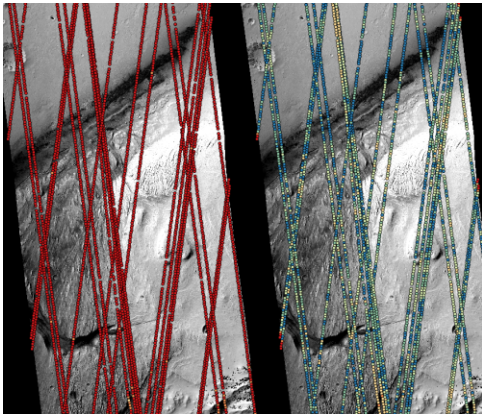


Figure 5.7: Example of using `pc_align` to align a DEM obtained using stereo from CTX images to a set of MOLA tracks. The MOLA points are colored by the offset error initially (left) and after `pc_align` was applied (right) to the terrain model. The red dots indicate more than 100 m of error and blue less than 5 m. The `pc_align` algorithm determined that by moving the terrain model approximately 40 m south, 70 m west, and 175 m vertically, goodness of fit between MOLA and the CTX model was increased substantially.

5.2.4 Correcting Camera Positions and Orientations

The `bundle_adjust` program can be used to adjust the camera positions and orientations before running `stereo`. These adjustments only make the cameras self-consistent. For the adjustments to be absolute, it is necessary to use `bundle_adjust` with ground control points. This tool is described in section A.4.

5.2.5 Alignment to Point Clouds From a Different Source

Often the 3D terrain models output by `stereo` (point clouds and DEMs) can be intrinsically quite accurate yet their actual position on the planet may be off by several meters or several kilometers, depending on the spacecraft. This can result from small errors in the position and orientation of the satellite cameras taking the pictures.

Such errors can be corrected in advance using bundle adjustment, as described in the previous section. That requires using ground control points, that may not be easy to collect. Alternatively, the images and cameras can be used as they are, and the absolute position of the output point clouds can be corrected in post-processing. For that, ASP provides a tool named `pc_align`. It aligns a 3D terrain to a much more accurately positioned (if potentially sparser) dataset. Such datasets can be made up of GPS measurements (in the case of Earth), or from laser altimetry instruments on satellites, such as ICESat/GLASS for Earth, LRO/LOLA on the Moon, and MGS/MOLA on Mars. Under the hood, `pc_align` uses the Iterative Closest Point algorithm (ICP) (both the point-to-plane and point-to-point flavors are supported, and with point-to-point ICP it is also possible to solve for a scale change).

The `pc_align` tool requires another input, an *a priori* guess for the maximum displacement we expect to see as result of alignment, i.e., by how much the points are allowed to move when the alignment transform is applied. If not known, a large (but not unreasonably so) number can be specified. It is used to remove most of the points in the source (movable) point cloud which have no chance of having a corresponding point in the reference (fixed) point cloud.

Here is how `pc_align` can be called (the denser cloud is specified first).

```
> pc_align --max-displacement 200 --datum MOLA \
    --save-inv-transformed-reference-points \
    --csv-format '1:lon 2:lat 3:radius_m' \
    stereo-PC.tif mola.csv
```

It is important to note here that there are two widely used Mars datums, and if your CSV file has, unlike above, the heights relative to a datum, the correct datum name must be specified via `--datum`. Section A.5.1 talks in more detail about the Mars datums.

Figure 5.7 shows an example of using `pc_align`. The complete documentation for this program is in section A.17.

5.2.6 Creating DEMs Relative to the Geoid/Areoid

The DEMs generated using `point2dem` are in reference to a datum ellipsoid. If desired, the `dem_geoid` program can be used to convert this DEM to be relative to a geoid/areoid on Earth/Mars respectively. Example usage:

```
> dem_geoid results/output-DEM.tif
```

5.2.7 Converting to the LAS Format

If it is desired to use the `stereo` generated point cloud outside of ASP, it can be converted to the LAS file format, which is a public file format for the interchange of 3-dimensional point cloud data. The tool `point2las` can be used for that purpose (section A.16). Example usage:

```
> point2las --compressed -r Earth results/output-PC.tif
```

5.2.8 Generating Color Hillshade Maps

Once you have generated a DEM file, you can use the `colormap` and `hillshade` tools to create colorized and/or shaded relief images.

To create a colorized version of the DEM, you need only specify the DEM file to use. The colormap is applied to the full range of the DEM, which is computed automatically. Alternatively you can specify your own min and max range for the color map.

```
> colormap results/output-DEM.tif -o hrad-colorized.tif
```

To create a hillshade of the DEM, specify the DEM file to use. You can control the azimuth and elevation of the light source using the `-a` and `-e` options.

```
> hillshade results/output-DEM.tif -o hrad-shaded.tif -e 25 -a 300
```

To create a colorized version of the shaded relief file, specify the DEM and the shaded relief file that should be used:

```
> colormap results/output-DEM.tif -s hrad-shaded.tif -o hrad-color-shaded.tif
```

See figure 5.8 showing the images obtained with these commands.

The complete documentation for `colormap` is in section A.22, and for `hillshade` in section A.23.

5.2.9 Building Overlays for Moon and Mars Mode in Google Earth

Sometimes it may be convenient to see how the DEMs and orthoimages generated by ASP look on top of existing imagery in Google Earth. ASP provides a tool named `image2qtree` for that purpose. It creates multi-resolution image tiles and a metadata tree in KML format that can be loaded into Google Earth from your local hard drive or streamed from a remote server over the Internet.

The `image2qtree` program can only be used on 8-bit image files with georeferencing information (e.g. grayscale or RGB GeoTIFF images). In this example, it can be used to process

`results/output-DEM-normalized.tif`, `results/output-DRG.tif`, `hrad-shaded.tif`, `hrad-colorized.tif`, and `hrad-shaded-colorized.tif`.

These images were generated respectively by using `point2dem` with the `-n` option creating a normalized DEM, the `--orthoimage` option to `point2dem` which projects the left image onto the DEM, and the images created earlier with `colormap`.

Here's an example of how to invoke this program.

```
> image2qtree hrad-shaded-colorized.tif -m kml --draw-order 100
```

Figure 5.9 shows the obtained KML files in Google Earth.

The complete documentation is in section A.24.

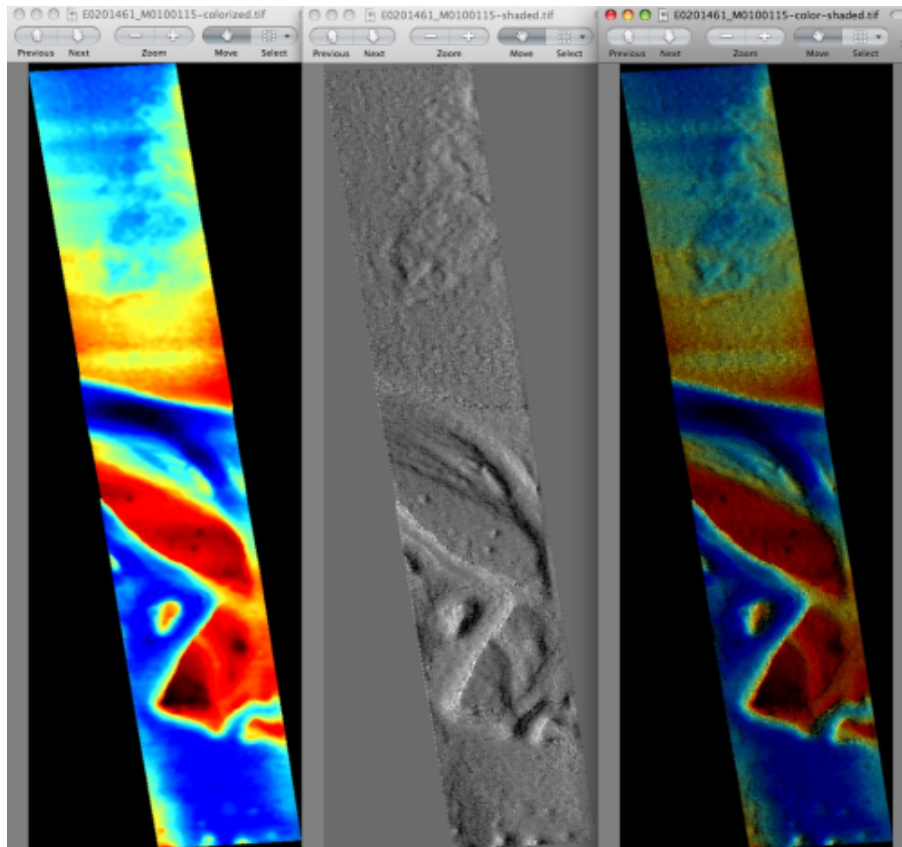


Figure 5.8: The colorized DEM, the shaded relief image, and the colorized hillshade.

5.2.10 Using DERT to Visualize Terrain Models

The open source Desktop Exploration of Remote Terrain (DERT) software tool can be used to explore large digital terrain models, like those created by the Ames Stereo Pipeline. For more information, visit <https://github.com/nasa/DERT>.

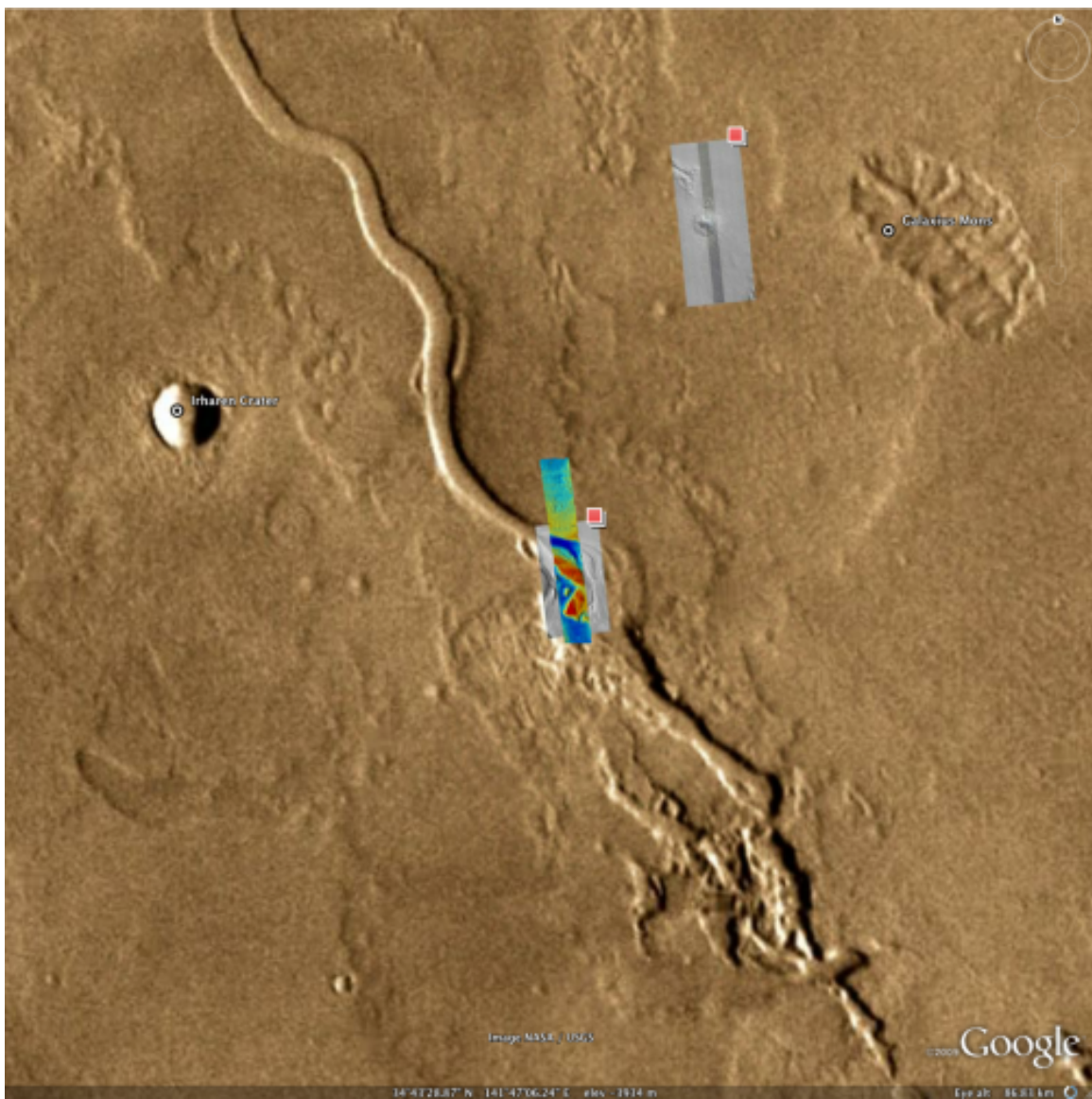


Figure 5.9: The colorized hillshade DEM as a KML overlay.

Chapter 6

Tips and Tricks

Here we summarize, in one place, some insights in how to get the most from ASP, particularly the highest quality results in the smallest amount of time.

- Ask for help or if you have questions. We're always glad to share what we know, implement suggestions, and fix issues (section 1.4).
- Use the GUI (section A.2) to get comfortable with ASP on a small region and to tune parameters (section A.2). A solution specific to ISIS imagery is to crop your stereo pair (using the ISIS `crop` command) to a small region of interest.
- The highest quality results with ASP can be obtained with map-projected images (section 5.1.6).
- Run stereo on multiple machines (section A.3).
- Improve the quality of the inputs to get better outputs. Bundle-adjustment can be used to find out the camera positions more accurately (section 8.2). CCD artifact correction can be used to remove artifacts from WorldView images (section 4.3). Jitter correction can be used for Digital Globe imagery (section 4.4).
- Align the output point cloud to some known absolute reference with `pc_align` (section 5.2.5).
- Remove noise from the output point cloud. During stereo triangulation, points that are further or closer than given distances from planet center or left camera center can be removed as outliers (section B.5). During DEM generation (section A.5), points with large triangulation error can be removed using `--remove-outliers-params`. Spikes can be removed with `--median-filter-params`. Points close to the boundary, that tend to be less accurate, can be eroded (`--erode-length`).
- During stereo filtering, islands can be removed with `--erode-max-size`.
- Remove noise from the low-resolution disparity (`D_sub`) that can greatly slow down a run using `--rm-quantile-percentile` and `--rm-quantile-multiple`. Some care is needed with these to not remove too much information.
- Fill holes in output orthoimages for nicer display (also in DEMs), during DEM and orthoimage generation with `point2dem` (section A.5). Holes in an existing DEM can also be filled using `dem_mosaic` (section A.7).
- To get good results if the images lack large-scale features (such as for ice plains) use a different way to get the low-resolution disparity (section 4.5).

- If a run takes unreasonably long, decreasing the timeout parameter may be in order (section 5.1.9).
- Manually set the search range if the automated approach fails (section 7.2.2).
- To increase speed, the image pair can be subsampled. For ISIS imagery, the ISIS `reduce` command can be used, while for Digital Globe data one can invoke the `dg_mosaic` tool (section A.9, though note that this tool may introduce aliasing). With subsampling, you are trading resolution for speed, so this probably only makes sense for debugging or “previewing” 3D terrain. That said, subsampling will tend to increase the signal to noise ratio, so it may also be helpful for obtaining 3D terrain out of noisy, low quality images.
- Photometric calibration (using the ISIS tools) can be used to improve the input images and hence get higher quality stereo results.
- If your images have missing or inaccurate camera pose information, and they were acquired with frame (pinhole cameras), such data can be solved for using structure-from-motion and bundle adjustment (chapter 9).
- Shape-from-shading (chapter 10) can be used to further increase the level of detail of a DEM obtained from stereo, though this is a computationally expensive process and its results are not easy to validate.

We'll be happy to add here more suggestions from community's accumulated wisdom on using ASP.

Part II

The Stereo Pipeline in Depth

Chapter 7

Stereo Correlation

In this chapter we will dive much deeper into understanding the core algorithms in the Stereo Pipeline. We start with an overview of the five stages of stereo reconstruction. Then we move into an in-depth discussion and exposition of the various correlation algorithms.

The goal of this chapter is to build an intuition for the stereo correlation process. This will help users to identify unusual results in their DEMs and hopefully eliminate them by tuning various parameters in the `stereo.default` file (appendix B). For scientists and engineers who are using DEMs produced with the Stereo Pipeline, this chapter may help to answer the question, “What is the Stereo Pipeline doing to the raw data to produce this DEM?”

A related question that is commonly asked is, “How accurate is a DEM produced by the Stereo Pipeline?” This chapter does not yet address matters of accuracy and error, however we have several efforts underway to quantify the accuracy of Stereo Pipeline-derived DEMs, and will be publishing more information about that shortly. Stay tuned.

The entire stereo correlation process, from raw input images to a point cloud or DEM, can be viewed as a multistage pipeline as depicted in Figure 7.1, and detailed in the following sections.

7.1 Pre-Processing

The first optional (but recommended) step in the process is least squares Bundle Adjustment, which is described in detail in Chapter 8.

Next, the left and right images are roughly aligned using one of the four methods: (1) a homography transform of the right image based on automated tie-point measurements, (2) an affine epipolar transform of both the left and right images (also based on tie-point measurements as earlier), the effect of which is equivalent to rotating the original cameras which took the pictures, (3) a 3D rotation that achieves epipolar rectification (*only implemented for Pinhole sessions for missions like MER or K10 – see sections 11.5 and 11.6*) or (4) map-projection of both the left and right images using the ISIS `cam2map` command or through the more general `mapproject` tool that works for any cameras supported by ASP (see section 5.1.6 for the latter). The first three options can be applied automatically by the Stereo Pipeline when the `alignment-method` variable in the `stereo.default` file is set to `affineepipolar`, `homography`, or `epipolar`, respectively.

The latter option, running `cam2map`, `cam2map4stereo.py`, or `mapproject` must be carried out by the user prior to invoking the `stereo` command. Map-projecting the images using ISIS eliminates any unusual distortion in the image due to the unusual camera acquisition modes (e.g. pitching “ROTO” maneuvers during image acquisition for MOC, or highly elliptical orbits and changing line exposure times for the High

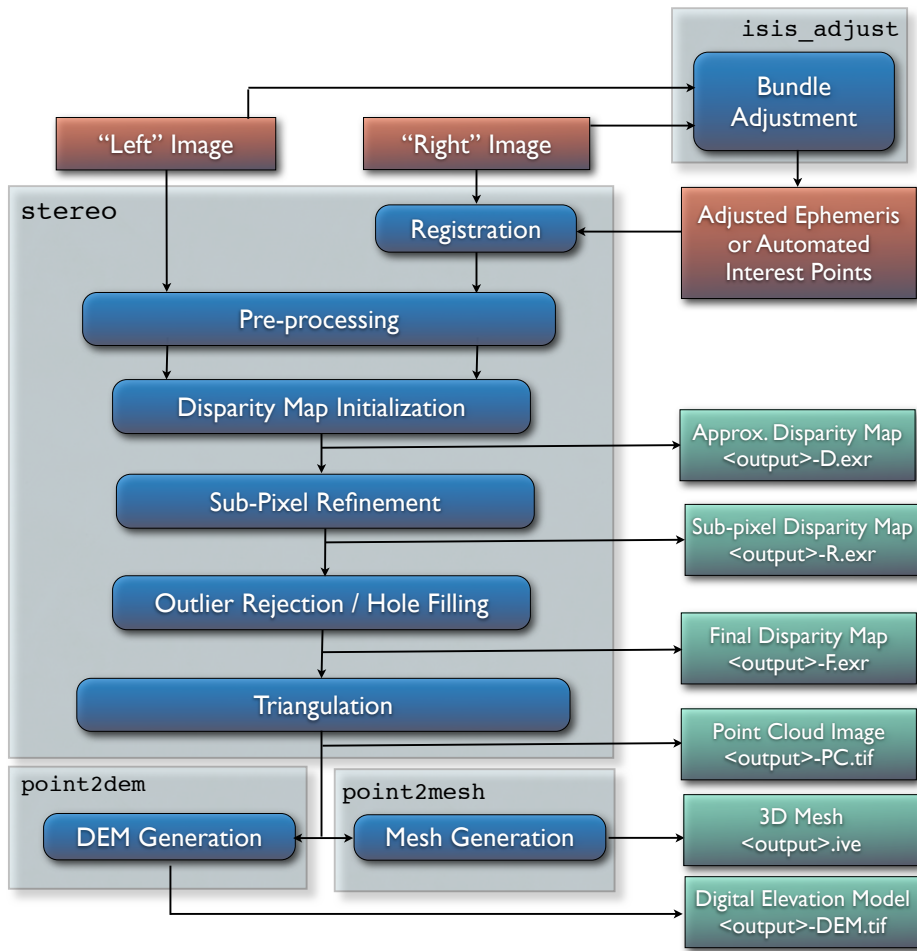


Figure 7.1: Flow of data through the Stereo Pipeline.

Resolution Stereo Camera, HRSC). It also eliminates some of the perspective differences in the image pair that are due to large terrain features by taking the existing low-resolution terrain model into account (e.g., the Mars Orbiter Laser Altimeter, MOLA; Lunar Orbiter Laser Altimeter, LOLA; National Elevation Dataset, NED; or Unified Lunar Coordinate Network, ULCN, 2005 models).

In essence, map-projecting the images results in a pair of very closely matched images that are as close to ideal as possible given existing information. This leaves only small perspective differences in the images, which are exactly the features that the stereo correlation process is designed to detect.

For this reason, we recommend map-projection for pre-alignment of most stereo pairs. Its only cost is longer triangulation times as more math must be applied to work back through the transforms applied to the images. In either case, the pre-alignment step is essential for performance because it ensures that the disparity search space is bounded to a known area. In both cases, the effects of pre-alignment are taken into account later in the process during triangulation, so you do not need to worry that pre-alignment will compromise the geometric integrity of your DEM.

In some cases the pre-processing step may also normalize the pixel values in the left and right images to bring them into the same dynamic range. Various options in the `stereo.default` file affect whether or how normalization is carried out, including `individually-normalize` and `force-use-entire-range`. Although the defaults work in most cases, the use of these normalization steps can vary from data set to data set, so we recommend you refer to the examples in Chapter 11 to see if these are necessary in your use case.

Finally, pre-processing can perform some filtering of the input images (as determined by `prefilter-mode`) to reduce noise and extract edges in the images. When active, these filters apply a kernel with a sigma of `prefilter-kernel-width` pixels that can improve results for noisy images (`prefilter-mode` must be chosen carefully in conjunction with `cost-mode`, see Appendix B). The pre-processing modes that extract image edges are useful for stereo pairs that do not have the same lighting conditions, contrast, and absolute brightness [73]. We recommend that you use the defaults for these parameters to start with, and then experiment only if your results are sub-optimal.

7.2 Disparity Map Initialization

Correlation is the process at the heart of the Stereo Pipeline. It is a collection of algorithms that compute correspondences between pixels in the left image and pixels in the right image. The map of these correspondences is called a *disparity map*. You can think of a disparity map as an image whose pixel locations correspond to the pixel (u, v) in the left image, and whose pixel values contain the horizontal and vertical offsets (d_u, d_v) to the matching pixel in the right image, which is $(u + d_u, v + d_v)$.

The correlation process attempts to find a match for every pixel in the left image. The only pixels skipped are those marked invalid in the mask images. For large images (e.g. from HiRISE, Lunar Reconnaissance Orbiter Camera, LROC, or WorldView), this is very expensive computationally, so the correlation process is split into two stages. The disparity map initialization step computes approximate correspondences using a pyramid-based search that is highly optimized for speed, but trades resolution for speed. The results of disparity map initialization are integer-valued disparity estimates. The sub-pixel refinement step takes these integer estimates as initial conditions for an iterative optimization and refines them using the algorithm discussed in the next section.

We employ several optimizations to accelerate disparity map initialization: (1) a box filter-like accumulator that reduces duplicate operations during correlation [94]; (2) a coarse-to-fine pyramid based approach where disparities are estimated using low-resolution images, and then successively refined at higher resolutions; and (3) partitioning of the disparity search space into rectangular sub-regions with similar values of disparity determined in the previous lower resolution level of the pyramid [94].

Naive correlation itself is carried out by moving a small, rectangular template window from the left image over the specified search region of the right image, as in Figure 7.2. The “best” match is determined by applying a cost function that compares the two windows. The location at which the window evaluates to the lowest cost compared to all the other search locations is reported as the disparity value. The `cost-mode` variable allows you to choose one of three cost functions, though we recommend normalized cross correlation [62], since it is most robust to slight lighting and contrast variations between a pair of images. Try the others if you need more speed at the cost of quality.

Our implementation of pyramid correlation is a little unique in that it is actually split into two levels of pyramid searching. There is a `output_prefix-D_sub.tif` disparity image that is computed from the greatly reduced input images `*-L_sub.tif` and `output_prefix-R_sub.tif`. Those “sub” images have their size chosen so that their area is around 2.25 mega pixels, a size that is easily viewed on the screen unlike the raw source imagery. The low-resolution disparity image then defines the per thread search range of the higher resolution disparity, `output_prefix-D.tif`.

This solution is imperfect but comes from our model of multi-threaded processing. ASP processes individual tiles of the output disparity in parallel. The smaller the tiles, the easier it is to distribute evenly among the CPU cores. The size of the tile unfortunately limits the max number of pyramid levels we can process. We’ve struck a balance where every 1024 by 1024 pixel area is processed individually in a tile. This practice allows only 5 levels of pyramid processing. With the addition of the second tier of pyramid searching with `output_prefix-D_sub.tif`, we are allowed to process beyond that limitation.

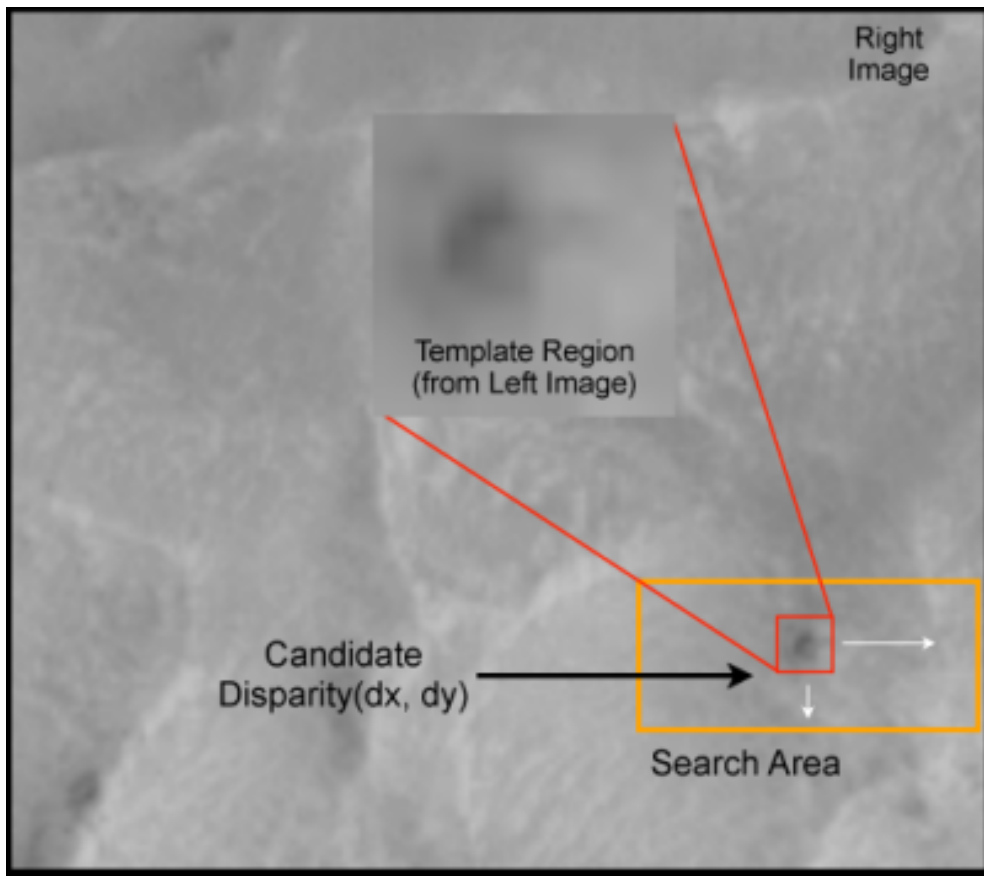


Figure 7.2: The correlation algorithm in disparity map initialization uses a sliding template window from the left image to find the best match in the right image. The size of the template window can be adjusted using the `H_KERN` and `V_KERN` parameters in the `stereo.default` file, and the search range can be adjusted using the `{H,V}_CORR_{MIN/MAX}` parameters.

Any large failure in the low-resolution disparity image will be detrimental to the performance of the higher resolution disparity. In the event that the low-resolution disparity is completely unhelpful, it can be skipped by adding `corr-seed-mode 0` in the `stereo.default` file and using a manual search range (section 7.2.2). This should only be considered in cases where the texture in an image is completely lost when subsampled. An example would be satellite imagery of fresh snow in the Arctic. Alternatively, `output_prefix-D_sub.tif` can be computed at a sparse set of pixels at full resolution, as described in section 4.5.

An alternative to computing `output_prefix-D.tif` from sub-sampled images (`corr-seed-mode 1`) or skipping it altogether (`corr-seed-mode 0`), is to compute it from a lower-resolution DEM of the area (`corr-seed-mode 2`). In this situation, the low-resolution DEM needs to be specified together with its estimated error. See section B.2 for more detailed information as to how to specify these options. In our experiments, if the input DEM has a resolution of 1 km, a good value for the DEM error is about 10 m, or higher if the terrain is very variable.

7.2.1 Debugging Disparity Map Initialization

Never will all pixels be successfully matched during stereo matching. Though a good chunk of the image should be correctly processed. If you see large areas where matching failed, this could be due to a variety of reasons:

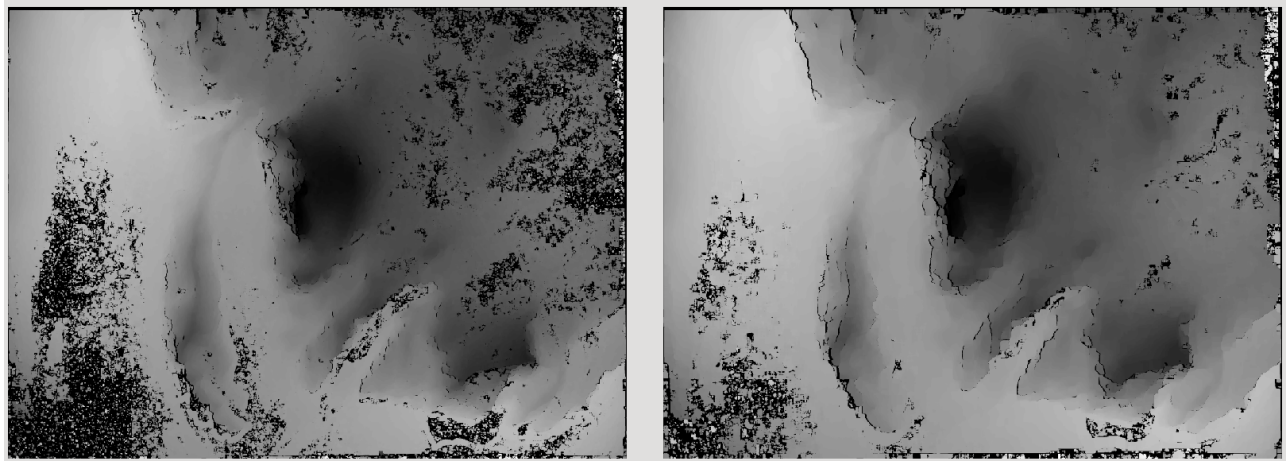


Figure 7.3: The effect of increasing the correlation kernel size from 35 (left) to 75 (right). This location is covered in snow and several regions lack texture for the correlator to use but a large kernel increases the chances of finding useful texture for a given pixel.

- In regions where the images do not overlap, there should be no valid matches in the disparity map.
- Match quality may be poor in regions of the images that have different lighting conditions, contrast, or specular properties of the surface.
- Areas that have image content with very little texture or extremely low contrast may have an insufficient signal to noise ratio, and will be rejected by the correlator.
- Areas that are highly distorted due to different image perspective, such as crater and canyon walls, may exhibit poor matching performance. This could also be due to failure of the preprocessing step in aligning the images. The correlator can not match images that are rotated differently from each other or have different scale/resolution. Map projection is used to at least partially rectify these issues (section 5.1.6).

Bad matches, often called “blunders” or “artifacts” are also common, and can happen for many of the same reasons listed above. The Stereo Pipeline does its best to automatically detect and eliminate these blunders, but the effectiveness of these outlier rejection strategies does vary depending on the quality of the input imagery.

When tuning up your `stereo.default` file, you will find that it is very helpful to look at the raw output of the disparity map initialization step. This can be done using the `disparitydebug` tool, which converts the `output_prefix-D.tif` file into a pair of normal images that contain the horizontal and vertical components of disparity. You can open these in a standard image viewing application and see immediately which pixels were matched successfully, and which were not. Stereo matching blunders are usually also obvious when inspecting these images. With a good intuition for the effects of various `stereo.default` parameters and a good intuition for reading the output of `disparitydebug`, it is possible to quickly identify and address most problems.

If you are seeing too many holes in your disparity images, one option that may give good results is to increase the size of the correlation kernel used by `stereo_corr` with the `-corr-kernel` option. Increasing the kernel size will increase the processing time but should help fill in regions of the image where no match was found.

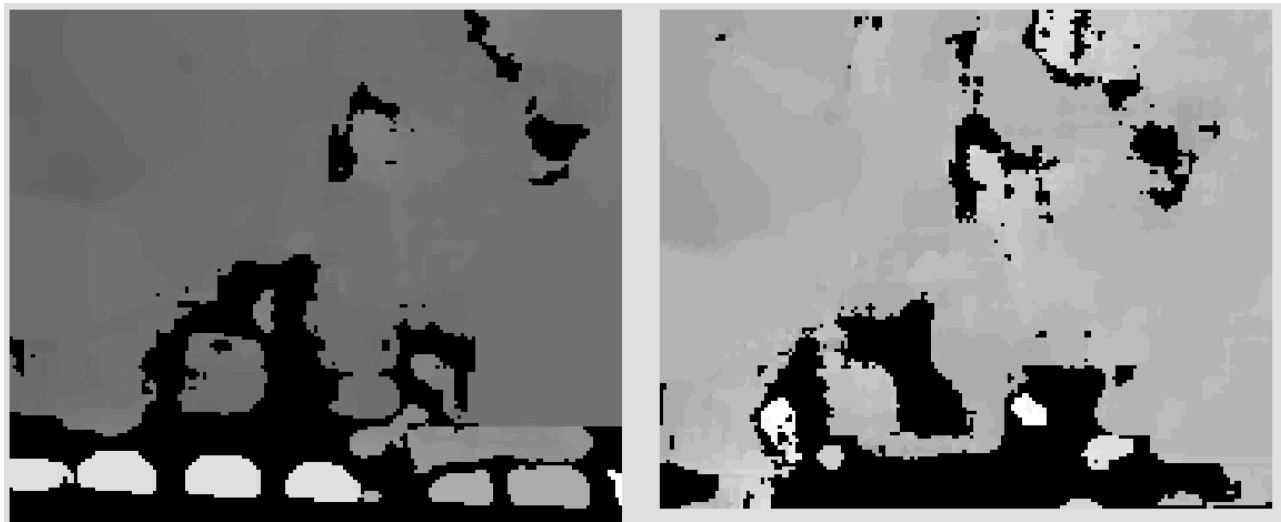


Figure 7.4: The effect of using the `rm-quantile` filtering option in `stereo_corr`. In the left image there are a series of high disparity "islands" at the bottom of the image. In the right image quantile filtering has removed those islands while leaving the rest of the image intact.

7.2.2 Search Range Determination

In some circumstances, the low-resolution disparity `D_sub.tif` may fail to get computed, or it may be inaccurate. This can happen for example if only very small features are present in the original images, and they disappear during the resampling that is necessary to obtain `D_sub.tif`. In this case, it is possible to set `corr-seed-mode` to 0, and manually set a search range to use for full-resolution correlation via the parameter `corr-search`. In `stereo.default` this parameter's entry will look like:

```
corr-search -80 -2 20 2
```

The exact values to use with this option you'll have to discover yourself. The numbers right of `corr-search` represent the horizontal minimum boundary, vertical minimum boundary, horizontal maximum boundary, and finally the horizontal maximum boundary within which we will search for the disparity during correlation.

It can be tricky to select a good search range for the `stereo.default` file. That's why the best way is to let `stereo` perform an automated guess for the search range. If you find that you can do a better estimate of the search range, take look at the intermediate disparity images using the `disparitydebug` program to figure out which search directions can be expanded or contracted. The output images will clearly show good data or bad data depending on whether the search range is correct.

The worst case scenario is to determine the search range manually. For example, for ISIS images, both images could be opened in `qview` and the coordinates of points that can be matched visually can be compared. Subtract line,sample locations in the first image from the coordinates of the same feature in the second image, and this will yield offsets that can be used in the search range. Make several of these offset measurements and use them to define a line,sample bounding box, then expand this by 50% and use it for `corr-search`. This will produce good results in most images.

Also, if you are using an alignment option, you'll instead want to make those disparity measurements against the written L.tif and R.tif files (see chapter C) instead of the original input files.

7.2.3 Local Homography

Correlation works by decomposing the left image into tiles, and for each pixel in each tile finding the best-matching pixel in the right image.

Depending on user's choices, by this stage either the left or the right image (or both) may already be transformed so that they are very similar, making the matching process more likely to succeed.

Whether that is the case or not, Stereo Pipeline can estimate, based on the low-resolution disparity `output_prefix-D_sub.tif`, a local homography transform for every left image tile, which, when applied to the right image, improves the similarity of the right image to the current left image tile. This option can be turned on with the flag `use-local-homography`.

This local homography transform comes in most useful when a global homography transform could not be applied (for example, if interest point matching failed). The input low-resolution disparity can be computed in several ways, as described earlier in the section.

7.3 Sub-pixel Refinement

Once disparity map initialization is complete, every pixel in the disparity map will either have an estimated disparity value, or it will be marked as invalid. All valid pixels are then adjusted in the sub-pixel refinement stage based on the `subpixel-mode` setting.

The first mode is parabola-fitting sub-pixel refinement (`subpixel-mode 1`). This technique fits a 2D parabola to points on the correlation cost surface in an 8-connected neighborhood around the cost value that was the “best” as measured during disparity map initialization. The parabola’s minimum can then be computed analytically and taken as as the new sub-pixel disparity value.

This method is easy to implement and extremely fast to compute, but it exhibits a problem known as pixel-locking: the sub-pixel disparities tend toward their integer estimates and can create noticeable “stair steps” on surfaces that should be smooth [91, 96]. See for example Figure 7.5(b). Furthermore, the parabola subpixel mode is not capable of refining a disparity estimate by more than one pixel, so although it produces smooth disparity maps, these results are not much more accurate than the results that come out of the disparity map initialization in the first place. However, the speed of this method makes it very useful as a “draft” mode for quickly generating a DEM for visualization (i.e. non-scientific) purposes. It is also beneficial in the event that a user will simply downsample their DEM after generation in Stereo Pipeline.

For high quality results, we recommend `subpixel-mode 2`: the Bayes EM weighted affine adaptive window correlator. This advanced method produces extremely high quality stereo matches that exhibit a high degree of immunity to image noise. For example Apollo Metric Camera images are affected by two types of noise inherent to the scanning process: (1) the presence of film grain and (2) dust and lint particles present on the film or scanner. The former gives rise to noise in the DEM values that wash out real features, and the latter causes incorrect matches or hard to detect blemishes in the DEM. Attenuating the effect of these scanning artifacts while simultaneously refining the integer disparity map to sub-pixel accuracy has become a critical goal of our system, and is necessary for processing real-world data sets such as the Apollo Metric Camera data.

The Bayes EM subpixel correlator also features a deformable template window from the left image that can be rotated, scaled, and translated as it zeros in on the correct match in the right image. This adaptive window is essential for computing accurate matches on crater or canyon walls, and on other areas with significant perspective distortion due to foreshortening.

This affine-adaptive behavior is based on the Lucas-Kanade template tracking algorithm, a classic algorithm in the field of computer vision [7]. We have extended this technique; developing a Bayesian model that

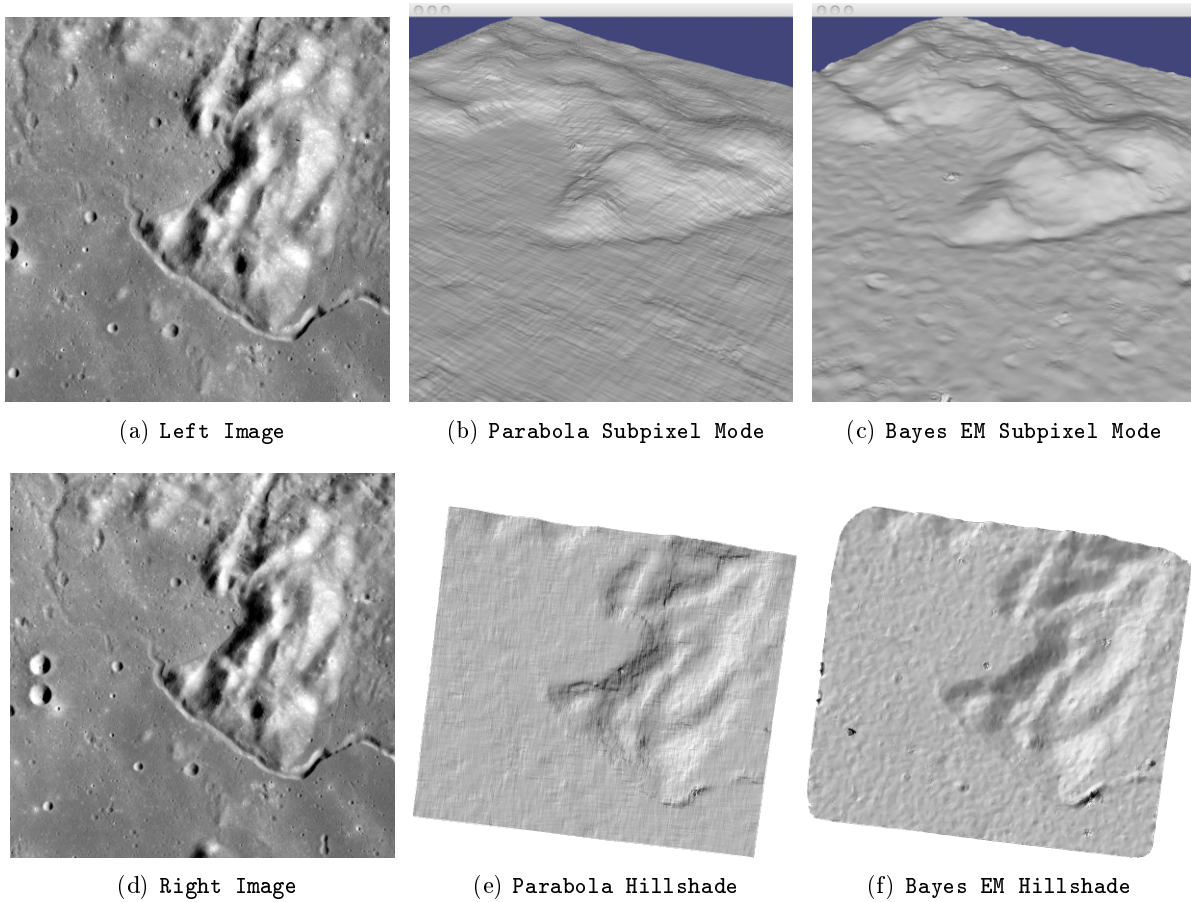


Figure 7.5: Left: Input images. Center: results using the parabola draft subpixel mode (`subpixel-mode = 1`). Right: results using the Bayes EM high quality subpixel mode (`subpixel-mode = 2`).

treats the Lucas-Kanade parameters as random variables in an Expectation Maximization (EM) framework. This statistical model also includes a Gaussian mixture component to model image noise that is the basis for the robustness of our algorithm. We will not go into depth on our approach here, but we encourage interested readers to read our papers on the topic [68, 12].

However we do note that, like the computations in the disparity map initialization stage, we adopt a multi-scale approach for sub-pixel refinement. At each level of the pyramid, the algorithm is initialized with the disparity determined in the previous lower resolution level of the pyramid, thereby allowing the subpixel algorithm to shift the results of the disparity initialization stage by many pixels if a better match can be found using the affine, noise-adapted window. Hence, this sub-pixel algorithm is able to significantly improve upon the results to yield a high quality, high resolution result.

Another option when run time is important is **subpixel-mode 3**: the simple affine correlator. This is essentially the Bayes EM mode with the noise correction features removed in order to decrease the required run time. In data sets with little noise this mode can yield results similar to Bayes EM mode in approximately one fifth the time.

7.4 Triangulation

When running an ISIS session, the Stereo Pipeline uses geometric camera models available in ISIS [6]. These highly accurate models are customized for each instrument that ISIS supports. Each ISIS “cube”

file contains all of the information that is required by the Stereo Pipeline to find and use the appropriate camera model for that observation.

Other sessions such as DG (*Digital Globe*) or Pinhole, require that their camera model be provided as additional arguments to the `stereo` command. Those camera models come in the form of an XML document for DG and as `*.pinhole`, `*.tsai`, `*.cahv`, `*.cahvor` for Pinhole sessions. Those files must be the third and forth arguments or immediately follow after the 2 input images for `stereo`.

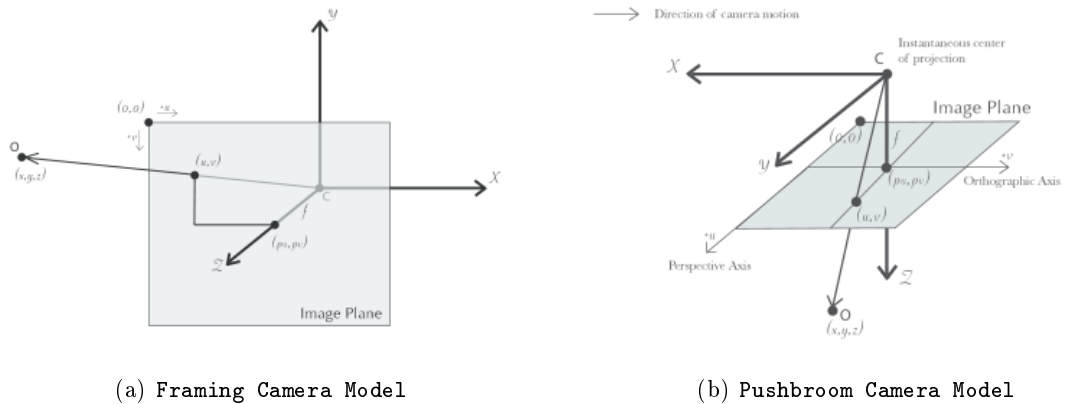


Figure 7.6: Most remote sensing cameras fall into two generic categories based on their basic geometry. Framing cameras (left) capture an instantaneous two-dimensional image. Linescan cameras (right) capture images one scan line at a time, building up an image over the course of several seconds as the satellite moves through the sky.

ISIS camera models account for all aspects of camera geometry, including both intrinsic (i.e. focal length, pixel size, and lens distortion) and extrinsic (e.g. camera position and orientation) camera parameters. Taken together, these parameters are sufficient to “forward project” a 3D point in the world onto the image plane of the sensor. It is also possible to “back project” from the camera’s center of projection through a pixel corresponding to the original 3D point.

Notice, however, that forward and back projection are not symmetric operations. One camera is sufficient to “image” a 3D point onto a pixel located on the image plane, but the reverse is not true. Given only a single camera and a pixel location $x = (u, v)$, that is the image of an unknown 3D point $P = (x, y, z)$, it

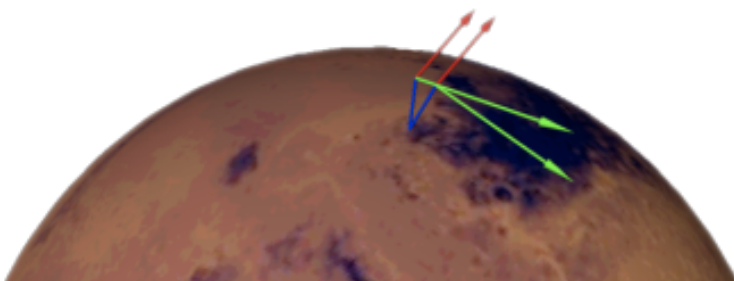


Figure 7.7: Once a disparity map has been generated and refined, it can be used in combination with the geometric camera models to compute the locations of 3D points on the surface of Mars. This figure shows the position (at the origins of the red, green, and blue vectors) and orientation of the Mars Global Surveyor at two points in time where it captured images in a stereo pair.

is only possible to determine that P lies somewhere along a ray that emanates from the camera's center of projection through the pixel location x on the image plane (see Figure 7.6).

Alas, once images are captured, the route from image pixel back to 3D points in the real world is through back projection, so we must bring more information to bear on the problem of uniquely reconstructing our 3D point. In order to determine P using back projection, we need *two* cameras that both contain pixel locations x_1 and x_2 where P was imaged. Now, we have two rays that converge on a point in 3D space (see Figure 7.7). The location where they meet must be the original location of P .

In practice, the two rays rarely intersect perfectly because any slight error in the camera position or pointing information will effect the rays' positions as well. Instead, we take the *closest point of intersection* of the two rays as the location of point P .

Additionally, the actual distance between the rays at this point is an interesting and important error metric that measures how self-consistent our two camera models are for this point. You will learn in the next chapter that this information, when computed and averaged over all reconstructed 3D points, can be a valuable statistic for determining whether to carry out bundle adjustment. Distance between the two rays at their closest intersection is recorded in the fourth channel of the point cloud file, *output-prefix-PC.tif*. This information can be brought to the same perspective as the output DEM by using the `--error` argument on the `point2dem` command.

This error in the triangulation, the distance between two rays, *is not the true accuracy of the DEM*. It is only another indirect measure of quality. A DEM with high triangulation error is always bad and should have its images bundle-adjusted. A DEM with low triangulation error is at least self consistent but could still be bad. A map of the triangulation error should only be interpreted as a relative measurement. Where small areas are found with high triangulation error came from correlation mistakes and large areas of error came from camera model inadequacies.

Chapter 8

Bundle Adjustment

8.1 Overview

Satellite position and orientation errors have a direct effect on the accuracy of digital elevation models produced by the Stereo Pipeline. If they are not corrected, these uncertainties will result in systematic errors in the overall position and slope of the DEM. Severe distortions can occur as well, resulting in twisted or “taco shaped” DEMs, though in most cases these effects are quite subtle and hard to detect. In the worst case, such as with old mission data like Voyager or Apollo, these gross camera misalignments can inhibit Stereo Pipeline’s internal interest point matcher and block auto search range detection.

Errors in camera position and orientation can be corrected using a process called *bundle adjustment*. Bundle adjustment is the process of simultaneously adjusting the properties of many cameras and the 3D locations of the objects they see in order to minimize the error between the estimated, back-projected pixel locations of the 3D objects and their actual measured locations in the captured images.

This complex process can be boiled down to this simple idea: bundle adjustment ensures that the observations in multiple images of a single ground feature are self-consistent. If they are not consistent, then the position and orientation of the cameras as well as the 3D position of the feature must be adjusted until they are. This optimization is carried out along with thousands (or more) of similar constraints involving many different features observed in other images. Bundle adjustment is very powerful and versatile: it can operate on just two overlapping images, or on thousands. It is also a dangerous tool. Careful consideration

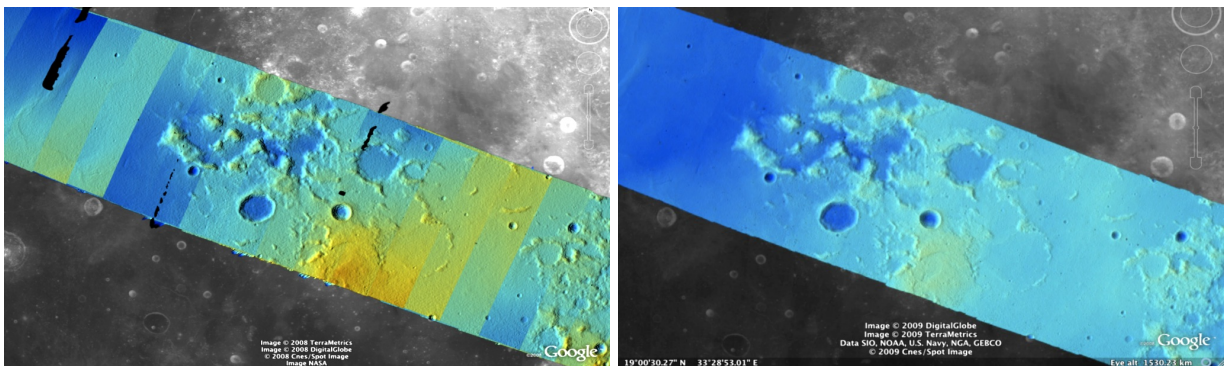


Figure 8.1: Bundle adjustment is illustrated here using a color-mapped, hill-shaded DEM mosaic from Apollo 15, Orbit 33, imagery. (a) Prior to bundle adjustment, large discontinuities can exist between overlapping DEMs made from different images. (b) After bundle adjustment, DEM alignment errors are minimized and no longer visible.

is required to insure and verify that the solution does represent reality.

Bundle adjustment can also take advantage of ground control points (GCPs), which are 3D locations of features that are known a priori (often by measuring them by hand in another existing DEM). GCPs can improve the internal consistency of your DEM or align your DEM to an existing data product. Finally, even though bundle adjustment calculates the locations of the 3D objects it views, only the final properties of the cameras are recorded for use by the Ames Stereo Pipeline. Those properties can be loaded into the `stereo` program which uses its own method for triangulating 3D feature locations.

When using the Stereo Pipeline, bundle adjustment is an optional step between the capture of images and the creation of DEMs. The bundle adjustment process described below should be completed prior to running the `stereo` command.

Although bundle adjustment is not a required step for generating DEMs, it is *highly recommended* for users who plan to create DEMs for scientific analysis and publication. Incorporating bundle adjustment into the stereo work flow not only results in DEMs that are more internally consistent, it is also the correct way to co-register your DEMs with other existing data sets and geodetic control networks.

At the moment however, Bundle Adjustment does not automatically work against outside DEMs from sources such as laser altimeters. Hand-picked GCPs are the only way for ASP to register to those types of sources.

8.2 Bundle adjustment using ASP

Recently, Stereo Pipeline started providing its own bundle adjustment tool, named `bundle_adjust`. Its usage is described in section A.4.

Here is an example of using this tool on a couple of Apollo 15 images, and its effect on decreasing the stereo triangulation error.

Running `stereo` without using bundle-adjusted camera models.

```
stereo AS15-M-1134.cub AS15-M-1135.cub run_noadjust/run
```

Performing bundle adjustment.

```
bundle_adjust AS15-M-1134.cub AS15-M-1135.cub -o run_ba/run
```

Running stereo while using the bundle-adjusted camera models.

```
stereo AS15-M-1134.cub AS15-M-1135.cub run_adjust/run \
--bundle-adjust-prefix run_ba/run
```

A comparison of the two ways of doing stereo is shown in figure 8.2.

8.3 Bundle adjustment using ISIS

In what follows we describe how to do bundle adjustment using ISIS's toolchain. It also serves to describe bundle adjustment in more detail, which is applicable to other bundle adjustment tools as well, including Stereo Pipeline's own tool.

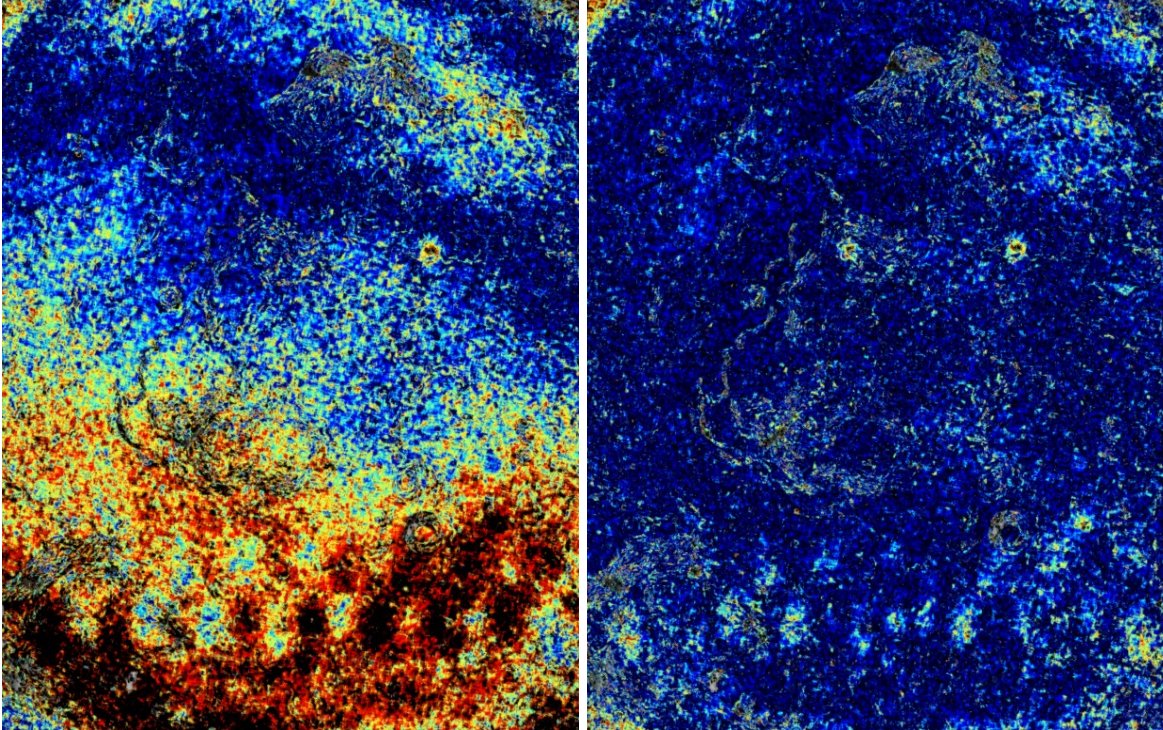


Figure 8.2: Illustration of the triangulation error map for a pair of images before (left) and after (right) using Stereo Pipeline’s `bundle_adjust`. Red and black colors suggest higher error.

In bundle adjustment, the position and orientation of each camera station are determined jointly with the 3D position of a set of image tie-points points chosen in the overlapping regions between images. Tie points, as suggested by the name, tie multiple camera images together. Their physical manifestation would be a rock or small crater than can be observed across more than one image.

Tie-points are automatically extracted using ISIS’s `autoseed` and `pointreg` (alternatively one could use a number of outside methods such as the famous SURF[8]). Creating a collection of tie points, called a *control network*, is a three step process. First, a general geographic layout of the points must be decided upon. This is traditionally just a grid layout that has some spacing that allows for about 20-30 measurements to be made per image. This shows up in slightly different projected locations in each image due to their slight misalignments. The second step is to have an automatic registration algorithm try to find the same feature in all images using the prior grid as a starting location. The third step is to manually verify all measurements visually, checking to insure that each measurement is looking at the same feature.

Bundle Adjustment in ISIS is performed with the `jigsaw` executable. It generally follows the method described in [97] and determines the best camera parameters that minimize the projection error given by $\epsilon = \sum_k \sum_j (I_k - I(C_j, X_k))^2$ where I_k are the tie points on the image plane, C_j are the camera parameters, and X_k are the 3D positions associated with features I_k . $I(C_j, X_k)$ is an image formation model (i.e. forward projection) for a given camera and 3D point. To recap, it projects the 3D point, X_k , into the camera with parameters C_j . This produces a predicted image location for the 3D point that is compared against the observed location, I_k . It then reduces this error with the Levenberg-Marquardt algorithm (LMA). Speed is improved by using sparse methods as described in Hartley and Zisserman [36], Konolige [45], and Chen et al. [14].

Even though the arithmetic for bundle adjustment sounds clever, there are faults with the base implementation. Imagine a case where all cameras and 3D points were collapsed into a single point. If you evaluate the above cost function, you’ll find that the error is indeed zero. This is not the correct solution if the

images were taken from orbit. Another example is if a translation was applied equally to all 3D points and camera locations. This again would not affect the cost function. This fault comes from bundle adjustment's inability to control the scale and translation of the solution. It will correct the geometric shape of the problem, yet it cannot guarantee that the solution will have correct scale and translation.

ISIS attempts to fix this problem by adding two additional cost functions to bundle adjustment. First of which is $\epsilon = \sum_j (C_j^{initial} - C_j)^2$. This constrains camera parameters to stay relatively close to their initial values. Second, a small handful of 3D ground control points can be chosen by hand and added to the error metric as $\epsilon = \sum_k (X_k^{gcp} - X_k)^2$ to constrain these points to known locations in the planetary coordinate frame. A physical example of a ground control point could be the location of a lander that has a well known location. GCPs could also be hand-picked points against a highly regarded and prior existing map such as the THEMIS Global Mosaic or the LRO-WAC Global Mosaic.

Like other iterative optimization methods, there are several conditions that will cause bundle adjustment to terminate. When updates to parameters become insignificantly small or when the error, ϵ , becomes insignificantly small, then the algorithm has converged and the result is most likely as good as it will get. However, the algorithm will also terminate when the number of iterations becomes too large in which case bundle adjustment may or may not have finished refining the parameters of the cameras.

8.3.1 Tutorial: Processing Mars Orbital Camera Imagery

This tutorial for ISIS's bundle adjustment tools is taken from [65] and [66]. These tools are not a product of NASA nor the authors of Stereo Pipeline. They were created by USGS and their documentation is available

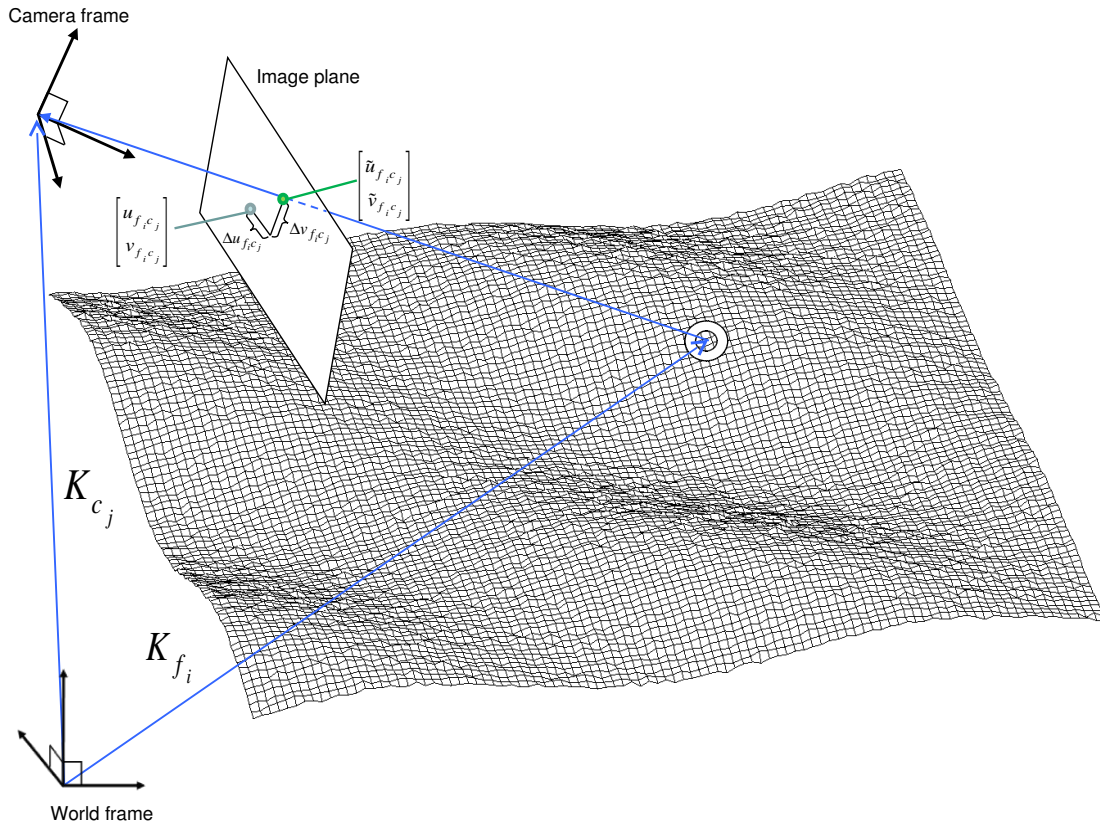


Figure 8.3: A feature observation in bundle adjustment, from Moore et al. [63]

at [13].

What follows is an example of bundle adjustment using two MOC images of Hrad Vallis. We use images E02/01461 and M01/00115, the same as used in Chapter 3. These images are available from NASA's PDS (the ISIS `mocproc` program will operate on either the IMQ or IMG format files, we use the `.imq` below in the example). For reference, the following ISIS commands are how to convert the MOC images to ISIS cubes.

```
ISIS 3> mocproc from=e0201461.imq to=e0201461.cub mapping=no
ISIS 3> mocproc from=m0100115.imq to=m0100115.cub mapping=no
```

Note that the resulting images are not map-projected. Bundle adjustment requires the ability to project arbitrary 3D points into the camera frame. The process of map-projecting an image dissociates the camera model from the image. Map-projecting can be perceived as the generation of a new infinitely large camera sensor that may be parallel to the surface, a conic shape, or something more complex. That makes it extremely hard to project a random point into the camera's original model. The math would follow the transformation from projection into the camera frame, then projected back down to surface that ISIS uses, then finally up into the infinitely large sensor. `Jigsaw` does not support this and thus does not operate on map-projected imagery.

Before we can dive into creating our tie-point measurements we must finish prepping these images. The following commands will add a vector layer to the cube file that describes its outline on the globe. It will also create a data file that describes the overlapping sections between files.

```
ISIS 3> footprintinit from=e0201461.cub
ISIS 3> footprintinit from=m0100115.cub
ISIS 3> echo *cub | xargs -n1 echo > cube.lis
ISIS 3> findimageoverlaps from=cube.lis overlaplist=overlap.lis
```

At this point, we are ready to start generating our measurements. This is a three step process that requires defining a geographic pattern for the layout of the points on the groups, an automatic registration pass, and finally a manual clean up of all measurements. Creating the ground pattern of measurements is performed with `autoseed`. It requires a settings file that defines the spacing in meters between measurements. For this example, write the following text into a `autoseed.def` file.

```
Group = PolygonSeederAlgorithm
  Name = Grid
  MinimumThickness = 0.01
  MinimumArea = 1
  XSpacing = 1000
  YSpacing = 2000
End_Group
```

The minimum thickness defines the minimum ratio between the sides of the region that can have points applied to it. A choice of 1 would define a square and anything less defines thinner and thinner rectangles. The minimum area argument defines the minimum square meters that must be in an overlap region. The last two are the spacing in meters between control points. Those values were specifically chosen for this pair so that about 30 measurements would be produced from `autoseed`. Having more control points just makes for more work later on in this process. Run `autoseed` with the following instruction.

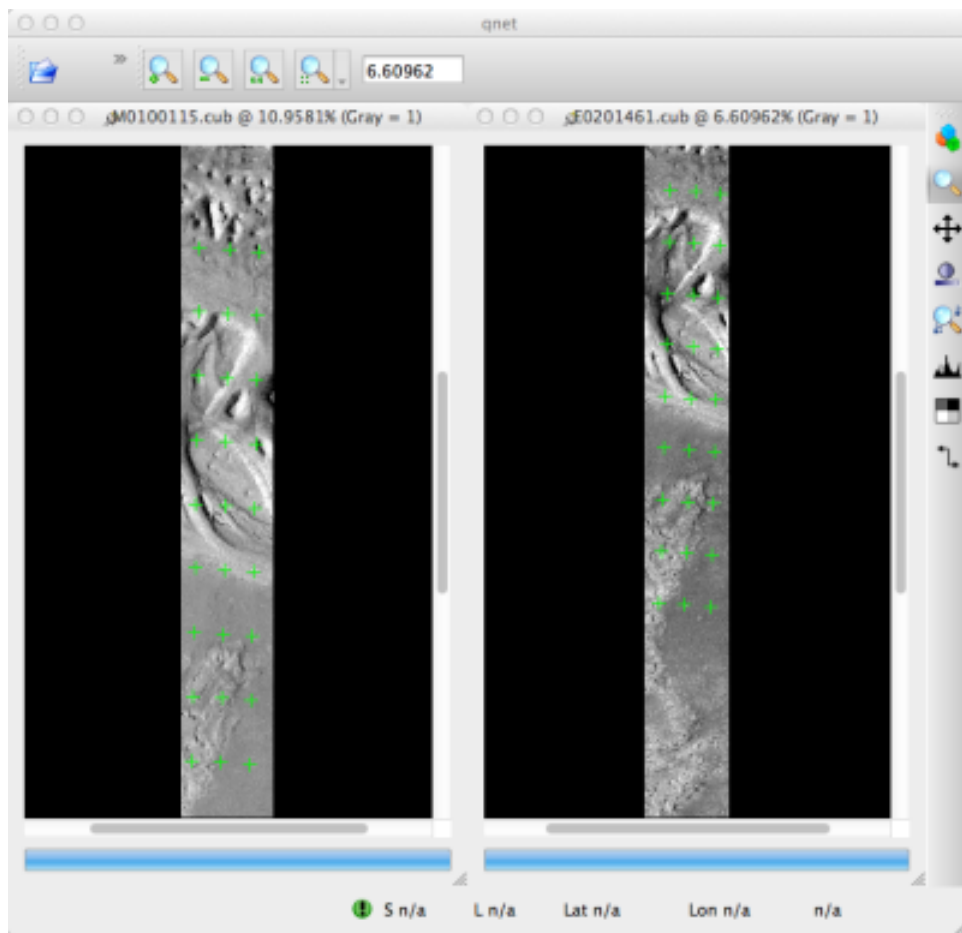


Figure 8.4: A visualization of the features laid out by `autoseed` in `qnet`. Note that the marks do not cover the same features between images. This is due to the poor initial spice data for MOC imagery.

```
ISIS 3> autoseed fromlist=cube.lis overlaplist=overlap.lis \
          onet=control.net deffile=autoseed.def networkid=moc \
          pointid=???? description=hrad_vallis
```

The next step is to perform auto registration of these features between the two images using `pointreg`. This program also requires a settings file that describes how to do the automatic search. Copy the text box below into a `autoRegTemplate.def` file.

```
Object = AutoRegistration
Group = Algorithm
  Name      = MaximumCorrelation
  Tolerance = 0.7
EndGroup

Group = PatternChip
  Samples = 21
  Lines   = 21
  MinimumZScore = 1.5
  ValidPercent = 80
EndGroup
```

```
Group = SearchChip
Samples = 75
Lines   = 1000
EndGroup
EndObject
```

The search chip defines the search range for which `pointreg` will look for matching imagery. The pattern chip is simply the kernel size of the matching template. The search range is specific for this image pair. The control network result after `autoseed` had a large vertical offset in the ball park of 500 px. The large misalignment dictated the need for the large search in the lines direction. Use `qnet` to get an idea for what the pixel shifts look like in your stereo pair to help you decide on a search range. In this example, only one measurement failed to match automatically. Here are the arguments to use in this example of `pointreg`.

```
ISIS 3> pointreg fromlist=cube.lis cnet=control.net \
          onet=control_pointreg.net deffile=autoRegTemplate.def \
```

The third step is to manually edit the control and verify the measurements in `qnet`. Type `qnet` in the terminal and then open `cube.lis` and lastly `control_pointreg.net`. From the Control Network Navigator window, click on the first point listed as *0001*. That opens a third window called the Qnet Tool. That window will allow you to play a flip animation that shows alignment of the feature between the two images. Correcting a measurement is performed by left clicking in the right image, then clicking *Save Measure*, and finally finishing by clicking *Save Point*.

In this tutorial, measurement *0025* ended up being incorrect. Your number may vary if you used different settings than the above or if MOC spice data has improved since this writing. When finished, go back to the main Qnet window. Save the final control network as `control_qnet.net` by clicking on *File*, and then *Save As*.

Once the control network is finished, it is finally time to start bundle adjustment. Here's what the call to `jigsaw` looks like:

```
ISIS 3> jigsaw fromlist=cube.lis update=yes twist=no radius=yes \
          cnet=control_qnet.net onet=control_ba.net \
```

The `update` option defines that we would like to update the camera pointing, if our bundle adjustment converges. The `twist=no` says to not solve for the camera rotation about the camera bore. That property is usually very well known as it is critical for integrating an image with a line-scan camera. The `radius=yes` means that the radius of the 3D features can be solved for. Using no will force the points to use height values from another source, usually LOLA or MOLA.

The above command will spew out a bunch of diagnostic information from every iteration of the optimization algorithm. The most important feature to look at is the `sigma0` value. It represents the mean of pixel errors in the control network. In our run, the initial error was 1065 px and the final solution had an error of 1.1 px.

Producing a DEM using the newly created camera corrections is the same as covered in the Tutorial on page 15. When using `jigsaw`, it modifies a copy of the spice data that is stored internally to the cube file. Thus when we want to create a DEM using the correct camera geometry, no extra information needs to be given to `stereo` since it is already contained in the file. In the event a mistake has been made, `spiceinit` will overwrite the spice data inside a cube file and provide the original uncorrected camera pointing.

```
ISIS 3> stereo E0201461.cub M0100115.cub bundled/bundled
```

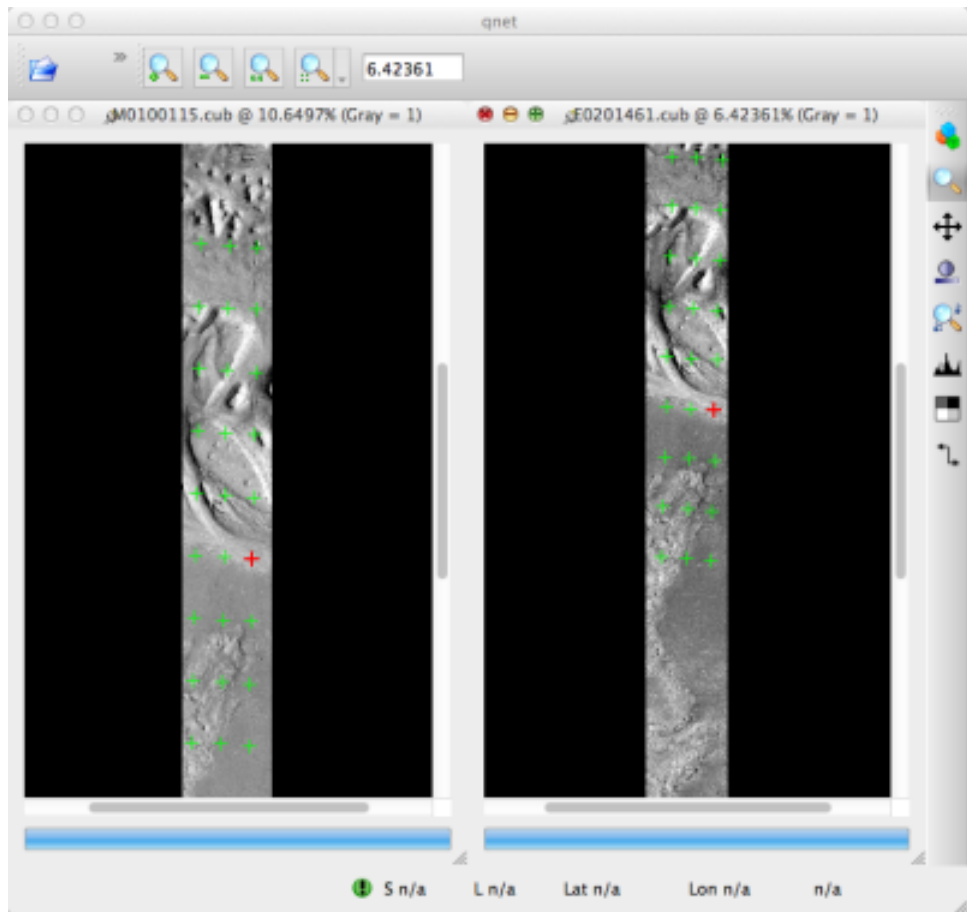


Figure 8.5: A visualization of the features after manual editing in *qnet*. Note that the marks now appear in the same location between images.

Chapter 9

Solving for Camera Poses Based on Images

The ASP tool `camera_solve` offers several ways to find the true position of frame camera images that do not come with any attached pose metadata. This can be useful with aerial, hand-held, and historical imagery for which such information may be incomplete or inaccurate.

An overview of the tool and examples are provided in this chapter. Reference information for this tool can be found in Appendix A.30.

9.1 Camera Solve Overview

The `camera_solve` tool is implemented as a Python wrapper around two other tools. The first of these is the THEIA software library, which is used to generate initial camera position estimates in a local coordinate space. You can learn more about THEIA at <http://www.theia-sfm.org/index.html>. The second tool is ASP's own `bundle_adjust` tool. The second step improves the solution to account for lens distortion and transforms the solution from local to global coordinates by making use of additional input data.

Currently the tool only solves for the extrinsic camera parameters and the user must provide intrinsic camera information. You can use the `camera_calibrate` tool (see Appendix A.29) or other camera calibration software to solve for intrinsic parameters if you have access to the camera in question. The camera calibration information must be contained in a .tsai pinhole camera model file and must be passed in using the `--calib-file` option. You can find descriptions of our supported pinhole camera models in Appendix D.

In order to transform the camera models from local to world coordinates, one of three pieces of information may be used. These sources are listed below and described in more detail in the examples that follow:

- A set of ground control points of the same type used by `pc_align`. The easiest way to generate these points is to use the ground control point writer tool available in the `stereo-gui` tool.
- A set of estimated camera positions (perhaps from a GPS unit) stored in a csv file.
- A DEM which a local point cloud can be registered to using `pc_align`. This method can be more accurate if estimated camera positions are also used. The user must perform alignment to a DEM, that step is not handled by `camera_solve`.

Power users can tweak the individual steps that `camera_solve` goes through to optimize their results. This primarily involves setting up a custom flag file for THEIA and/or passing in settings to `bundle_adjust`.

9.2 Example: Apollo 15 Metric Camera

To demonstrate the ability of the Ames Stereo Pipeline to process a generic frame camera we use images from the Apollo 15 Metric camera. The calibration information for this camera is available online and we have accurate digital terrain models we can use to verify our results.

First download a pair of images:

```
> wget http://apollo.sese.asu.edu/data/metric/AS15/png/AS15-M-0414_MED.png
> wget http://apollo.sese.asu.edu/data/metric/AS15/png/AS15-M-1134_MED.png
```

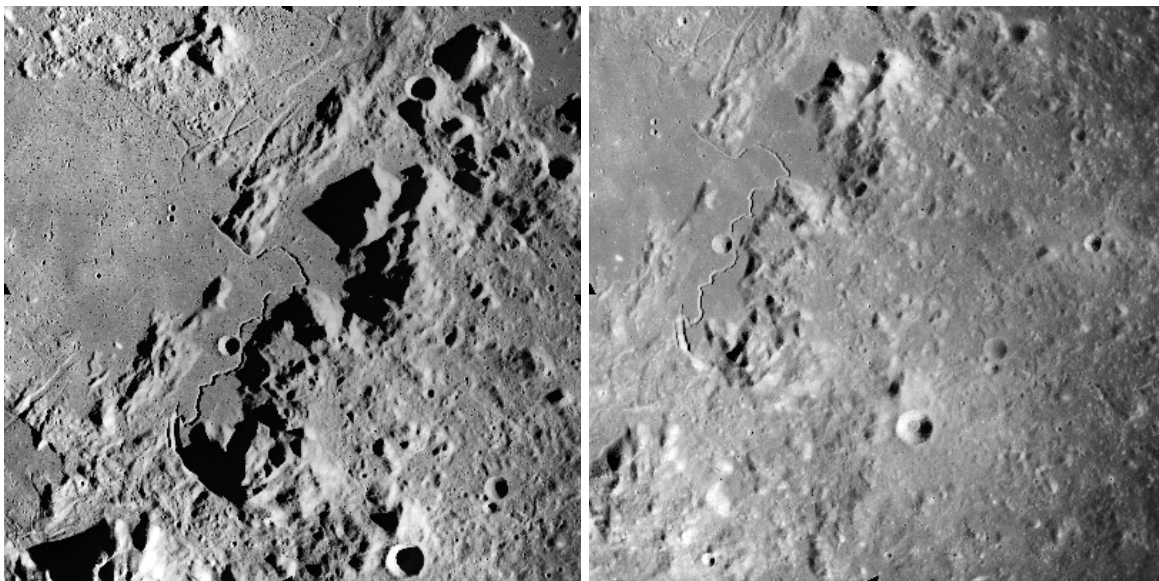


Figure 9.1: The two Apollo 15 images.

In order to make the example run faster we use downsampled versions of the original images. The images at those links have already been downsampled by a factor of $4\sqrt{2}$ from the original images. This means that the effective pixel size has increased from five microns (0.005 millimeters) to 0.028284 millimeters.

The next step is to fill out the rest of the pinhole camera model information we need. Using the data sheets available at http://apollo.sese.asu.edu/SUPPORT_DATA/AS15_SIMBAY_SUMMARY.pdf we can find the lens distortion parameters for metric camera. Looking at the ASP lens distortion models in Appendix D, we see that the description matches ASP's Brown-Conrady model. Using the example in the appendix we can fill out the rest of the sensor model file (metric_model.tsai) so it looks as follows:

```
VERSION_3
fu = 76.080
fv = 76.080
cu = 57.246816
cv = 57.246816
u_direction = 1 0 0
v_direction = 0 1 0
w_direction = 0 0 1
C = 0 0 0
R = 1 0 0 0 1 0 0 0 0 1
```

```
pitch = 0.028284
BrownConrad
xp = -0.006
yp = -0.002
k1 = -0.13361854e-5
k2 = 0.52261757e-09
k3 = -0.50728336e-13
p1 = -0.54958195e-06
p2 = -0.46089420e-10
phi = 2.9659070
```

These parameters use units of millimeters so we have to convert the nominal center point of the images from 2024 pixels to units of millimeters. Note that for some older images like these the nominal image center can be checked by looking for some sort of marking around the image borders that indicates where the center should lie. For these pictures there are black triangles at the center positions and they line up nicely with the center of the image. Before we try to solve for the camera positions we can run a simple tool to check the quality of our camera model file:

```
> undistort_image AS15-M-0414_MED.png metric_model.tsai -o corrected_414.tif
```

It is difficult to tell if the distortion model is correct by using this tool but it should be obvious if there are any gross errors in your camera model file such as incorrect units or missing parameters. In this case the tool will fail to run or will produce a significantly distorted image. For certain distortion models the `undistort_image` tool may take a long time to run.

If your input images are not all from the same camera or were scanned such that the center point is not at the same pixel, you can run `camera_solve` with one camera model file per input image. To do so pass a space-separated list of files surrounded by quotes to the `-calib-file` option such as `-calib-file "c1.tsai c2.tsai c3.tsai"`.

If we do not see any obvious problems we can go ahead and run the `camera_solve` tool:

```
> camera_solve out/ AS15-M-0414_MED.png AS15-M-1134_MED.png --datum D_MOON \
--calib-file metric_model.tsai
```

We should get some camera models in the output folder and see a printout of the final bundle adjustment error among the program output information:

Cost:	
Initial	1.450385e+01
Final	7.461198e+00
Change	7.042649e+00

We can't generate a DEM with these local camera models but we can run stereo anyways and look at the intersection error in the fourth band of the `PC.tif` file. While there are many speckles in this example where stereo correlation failed the mean intersection error is low and we don't see any evidence of lens distortion error.

```
> stereo AS15-M-0414_MED.png AS15-M-1134_MED.png out/AS15-M-0414_MED.png.final.tsai \
out/AS15-M-1134_MED.png.final.tsai -t pinhole s_local/out --corr-timeout 300 \
--erode-max-size 100
```

```
> gdalinfo -stats s_local/out-PC.tif
...
Band 4 Block=256x256 Type=Float32, ColorInterp=Undefined
    Minimum=0.000, Maximum=56.845, Mean=0.340, StdDev=3.512
Metadata:
    STATISTICS_MAXIMUM=56.844654083252
    STATISTICS_MEAN=0.33962282293374
    STATISTICS_MINIMUM=0
    STATISTICS_STDDEV=3.5124044818554
```

In order to generate a useful DEM, we need to move our cameras from local coordinates to global coordinates. The easiest way to do this is to obtain known ground control points (GCPs) which can be identified in the frame images. This will allow an accurate positioning of the cameras provided that the GCPs and the camera model parameters are accurate. To create GCPs see the instructions for the `stereo_gui` tool in appendix A.2.2. For the moon there are several ways to get DEMs and in this case we generated GCPs using `stereo_gui` and a DEM generated from LRONAC images.

After running this command:

```
> camera_solve out_gcp/ AS15-M-0414_MED.png AS15-M-1134_MED.png --datum D_MOON \
--calib-file metric_model.tsai --gcp-file ground_control_points.gcp
```

we end up with results that can be compared with the a DEM created from LRONAC images. The stereo results on the Apollo 15 images leave something to be desired but the DEM they produced has been moved to the correct location. You can easily visualize the output camera positions using the `orbitviz` tool with the `-load-camera-solve` option as shown below. Green lines between camera positions mean that a sufficient number of matching interest points were found between those two images.

```
> stereo AS15-M-0414_MED.png AS15-M-1134_MED.png out_gcp/AS15-M-0414_MED.png.final.tsai \
out_gcp/AS15-M-1134_MED.png.final.tsai -t nadirpinhole s_global/out --corr-timeout 300 \
--erode-max-size 100
> orbitviz -t nadirpinhole -r moon out_gcp --load-camera-solve
```

ASP also supports the method of initializing the `camera_solve` tool with estimated camera positions. This method will not move the cameras to exactly the right location but it should get them fairly close and at the correct scale, hopefully close enough to be used as-is or to be refined using `pc_align` or some other method. To use this method, pass additional bundle adjust parameters to `camera_solve` similar to the following line:

```
--bundle-adjust-params '--camera-positions nav.csv \
--csv-format "1:file 12:lat 13:lon 14:height_above_datum" --camera-weight 0.2'
```

The nav data file you use must have a column (the "file" column) containing a string that can be matched to the input image files passed to `camera_solve`. The tool looks for strings that are fully contained inside one of the image file names, so for example the field value 2009_10_20_0778 would be matched with the input file 2009_10_20_0778.JPG.

Chapter 5 will discuss the `stereo` program in more detail and the other tools in ASP.

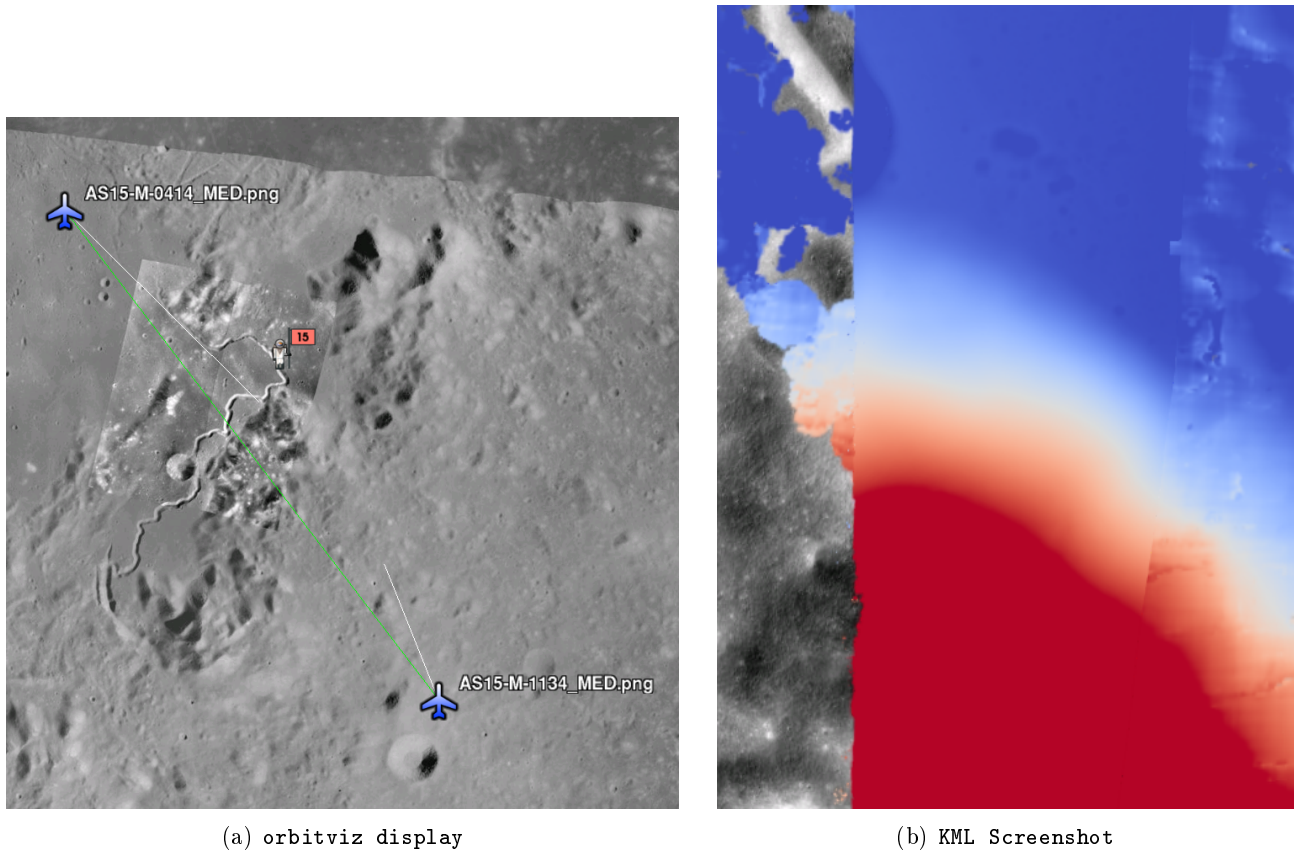


Figure 9.2: (a) Solved for camera positions plotted using orbitviz. (b) A narrow LRONAC DEM overlaid on the resulting DEM, both colormapped to the same elevation range.

9.3 Example: IceBridge DMS Camera

The DMS (Digital Mapping System) Camera is a frame camera flown on as part of the NASA IceBridge program to collect digital terrain imagery of polar and Antarctic terrain. To process this data the steps are very similar to the steps described above for the Apollo Metric camera but there are some aspects which are particular to IceBridge. You can download DMS images from ftp://n5eil01u.ecs.nsidc.org/SAN2/ICEBRIDGE_FTP/IODMS0_DMSraw_v01/. A list of the available data types can be found at https://nsidc.org/data/icebridge/instr_data_summary.html. This example uses data from the November 5, 2009 flight over Antarctica. The following camera model (icebridge_model.tsai) was used:

```
VERSION_3
fu = 28.429
fv = 28.429
cu = 17.9712
cv = 11.9808
u_direction = 1 0 0
v_direction = 0 1 0
w_direction = 0 0 1
C = 0 0 0
R = 1 0 0 0 1 0 0 0 1
pitch = 0.0064
Photometrix
```

```

xp = 0.004
yp = -0.191
k1 = 1.31024e-04
k2 = -2.05354e-07
k3 = -5.28558e-011
p1 = 7.2359e-006
p2 = 2.2656e-006
b1 = 0.0
b2 = 0.0

```

Note that these images are RGB format which is not supported by all ASP tools. To use the files with ASP, first convert them to single channel images using a tool such as ImageMagick's `convert`, `gdal_translate`, or `gdal_edit.py`. Different conversion methods may produce slightly different results depending on the contents of your input images. Some conversion command examples are shown below:

```

convert rgb.jpg -colorspace Gray gray.jpg
gdal_calc.py -A rgb.tif --A_band=1 -B rgb.tif --B_band=2 -C rgb.tif
--C_band=3 --outfile=gray.tif --calc="A*0.2989+B*0.5870+C*0.1140"
gdal_translate -b 1 rgb.jpg gray.jpg

```

Obtaining ground control points for icy locations on Earth can be particularly difficult because they are not well surveyed or because the terrain shifts over time. This may force you to use estimated camera positions to convert the local camera models into global coordinates. To make this easier for IceBridge data sets, ASP provides the `icebridge_kmz_to_csv` tool (see appendix A.31) which extracts a list of estimated camera positions from the kmz files available for each IceBridge flight at <http://asapdata.arc.nasa.gov/dms/missions.html>.

Another option which is useful when processing IceBridge data is the `--position-filter-dist` option for `bundle_adjust`. IceBridge data sets contain a large number of images and when processing many at once you can significantly decrease your processing time by using this option to limit interest-point matching to image pairs which are actually close enough to overlap. A good way to determine what distance to use is to load the camera position kmz file from their website into Google Earth and use the ruler tool to measure the distance between a pair of frames that are as far apart as you want to match. Commands using these options may look like this:

```

icebridge_kmz_to_csv 1000123_DMS_Frame_Events.kmz camera_positions.csv
camera_solve out 2009_11_05_00667.JPG 2009_11_05_00668.JPG \
2009_11_05_00669.JPG 2009_11_05_00670.JPG 2009_11_05_02947.JPG 2009_11_05_02948.JPG \
2009_11_05_02949.JPG 2009_11_05_02950.JPG 2009_11_05_01381.JPG 2009_11_05_01382.JPG \
--datum WGS84 --calib-file icebridge_model.tsai \
--bundle-adjust-params '--camera-positions camera_positions.csv' \
--csv-format "1:file 2:lon 3:lat 4:height_above_datum" --position-filter-dist 2000'
orbitviz out --load-camera-solve --hide-labels -r wgs84 -t nadirpinhole

```

A final tip for processing IceBridge data is that Land, Vegetation, and Ice Sensor (LVIS) lidar data available for some flights can be used to register DEMs created using DMS imagery. LVIS data can be downloaded at <ftp://n5eil01u.ecs.nsidc.org/SAN2/ICEBRIDGE/ILVIS2.001/>. The lidar data comes in plain text files that `pc_align` and `point2dem` can parse using the following option:

```
--csv-format "5:lat 4:lon 6:height_above_datum"
```

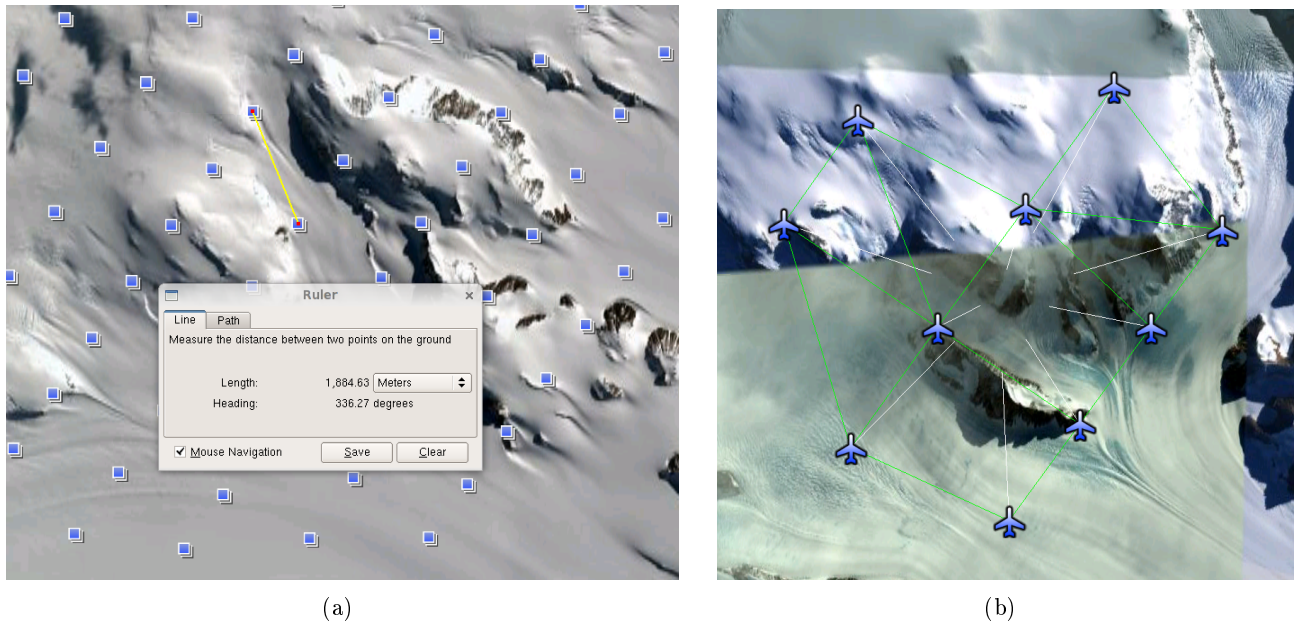


Figure 9.3: (a) Measuring the distance between estimated frame locations using Google Earth and an IceBridge kmz file. The kmz file is from the IceBridge website with no modifications. Using a position filter distance of 2000 meters will mostly limit image IP matching in this case to each image's immediate "neighbors". (b) Display of `camera_solve` results for ten IceBridge images using `orbitviz`.

ASP provides the `lvis2kml` tool to help visualize the coverage and terrain contained in LVIS files, see Appendix A.32 for details. The LVIS lidar coverage is sparse compared to the image coverage and you will have difficulty getting a good registration unless the region has terrain features such as hills or you are registering very large point clouds that overlap with the lidar coverage across a wide area. Otherwise `pc_align` will simply slide the flat terrain to an incorrect location to produce a low-error fit with the narrow lidar tracks. This test case was specifically chosen to provide strong terrain features to make alignment more accurate but `pc_align` still failed to produce a good fit until the lidar point cloud was converted into a smoothed DEM.

```

stereo 2009_11_05_02948.JPG 2009_11_05_02949.JPG out/2009_11_05_02948.JPG.final.tsai \
out/2009_11_05_02949.JPG.final.tsai st_run/out -t nadirpinhole
point2dem ILVIS2_AQ2009_1105_R1408_055812.TXT --datum WGS_1984 \
--t_srs "+proj=stere +lat_0=-90 +lon_0=0 +k=1 +x_0=0 +y_0=0 +datum=WGS84 +units=m +no_defs" \
--csv-format "5:lat 4:lon 6:height_above_datum" --tr 30 \
--search-radius-factor 2.0 -o lvis
pc_align --max-displacement 1000 lvis-DEM.tif st_run/out-PC.tif -o align_run/out \
--save-transformed-source-points --datum wgs84 --outlier-ratio 0.55
point2dem align_run/out-trans_source.tif --datum WGS_1984 \
--t_srs "+proj=stere +lat_0=-90 +lon_0=0 +k=1 +x_0=0 +y_0=0 +datum=WGS84 +units=m +no_defs"
colormap align_run_big/out-trans_source-DEM.tif --min 200 --max 1500
colormap lvis-DEM.tif --min 200 --max 1500
image2qtree lvis-DEM_CMAP.tif
image2qtree align_run_big/out-trans_source-DEM_CMAP.tif

```

Chapter 5 will discuss the `stereo` program in more detail and the other tools in ASP.

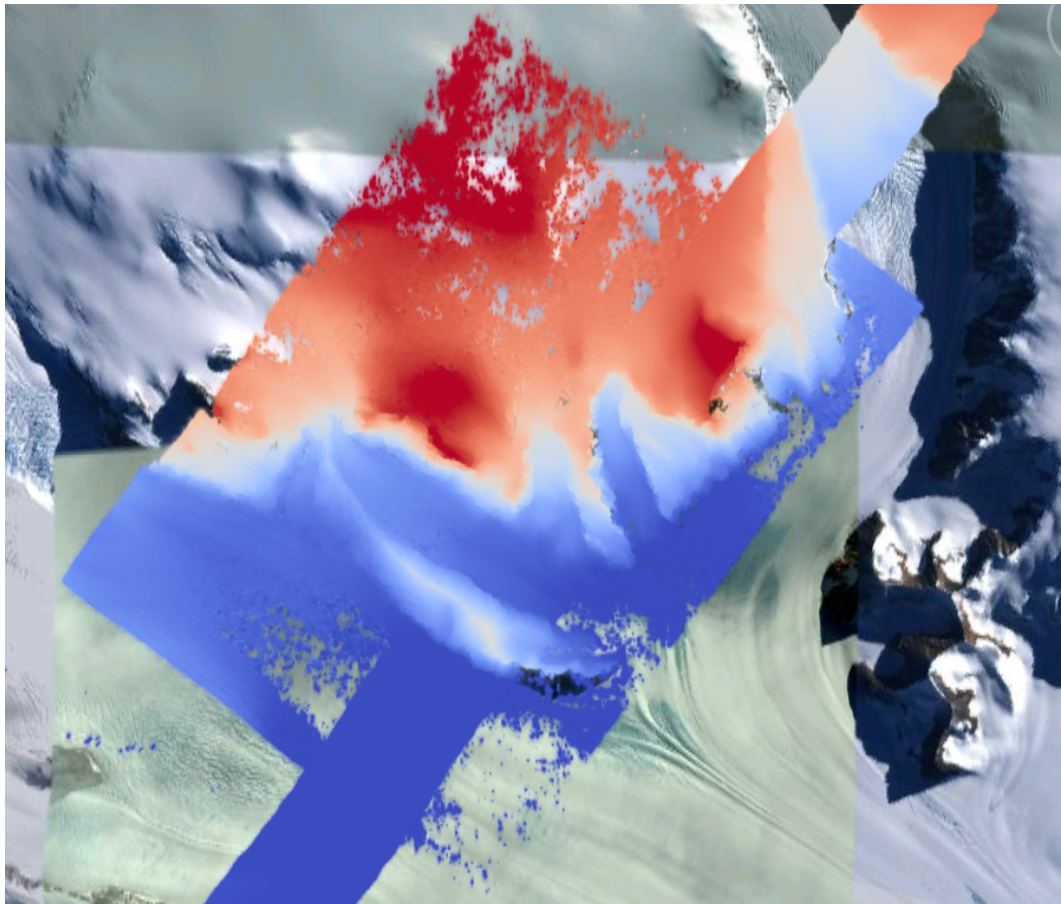


Figure 9.4: LVIS lidar DEM overlaid on the ASP created DEM, both colormapped to the same elevation range. The ASP DEM could be improved but the registration is accurate. Notice how narrow the LVIS lidar coverage is compared to the field of view of the camera.

Chapter 10

Shape-from-Shading

ASP provides a tool, named **sfs**, that can improve the level of detail of DEMs created by ASP or any other source using *shape-from-shading* (SfS).

The tool takes as input one or more camera images, a DEM at roughly the same resolution as the images, and returns a refined DEM.

sfs works only with ISIS cub images. It has been tested only for Lunar LRO NAC datasets. As seen later in the text, it returns reasonable results as far as 85° South on the Moon.

Currently, **sfs** is computationally expensive, and is practical only for DEMs of size up to 1000×1000 pixels. It can be very sensitive to errors in the position and orientation of the cameras, the accuracy of the initial DEM, and to the value of the smoothing term used to ensure that the output DEM is not overly noisy.

The **sfs** program can model position-dependent albedo, different exposure values for each camera, shadows in the input images, and regions in the DEM occluded from the Sun. It can refine the positions and orientations of the cameras, and supports the Lambertian and Lunar-Lambertian reflectance models.

The tool works by minimizing the cost function

$$\iint \sum_k [I_k(\phi)(x, y) - T_k A(x, y) R_k(\phi)(x, y)]^2 + \mu \|\nabla^2 \phi(x, y)\|^2 dx dy$$

Here, $I_k(\phi)(x, y)$ is the k -th camera image interpolated at pixels obtained by projecting into the camera 3D points from the terrain $\phi(x, y)$, T_k is the k -th image exposure, $A(x, y)$ is the per-pixel albedo, $R_k(\phi)(x, y)$ is the reflectance computed from the terrain for k -th image, $\|\nabla^2 \phi\|^2$ is the sum of squares all second-order partial derivatives of ϕ , and $\mu > 0$ is a smoothing term. We use either the regular Lambertian reflectance model, or the Lunar-Lambertian model [60].

Below we show two examples of running **sfs**, first for one image, and then for multiple images with bundle-adjustment and modeling the shadow threshold.

10.1 How to get good test imagery

We obtain the images from <http://wms.lroc.asu.edu/lroc/search> (we search for EDR images of type NACL and NACR).

A faster (but not as complete) interface is provided by <http://ode.rsl.wustl.edu/moon/indexproductsearch.aspx>. The related site <http://ode.rsl.wustl.edu/moon/indextools.aspx?displaypage=lolardr> can provide LOLA datasets which can be used as ground truth.

We advise the following strategy for picking images. First choose a small longitude-latitude window in which to perform a search for imagery. Pick two images that are very close in time and with a big amount of overlap. Those will create a stereo pair and an initial DEM. Then search for other images close to the center of the maximum overlap of the first two images. Pick one or more of those, ideally with different illumination conditions than the first two, and run SfS for example with the first and the third image.

To locate the area of spatial overlap, the images can be map-projected (either with `cam2map` with a coarse resolution) or with `mapproject` (using say the LOLA DEM as the terrain to project onto, or the DEM obtained from running `stereo` on those images). Then the images can be examined in `stereo_gui` while turning on the mode to render them using their georeferences.

10.2 Running sfs at 1 meter/pixel using a single image

In both this and the next section we will work with LRO NAC images taken close to the Lunar South Pole, at 85° of latitude (the tool was tested on equatorial regions as well). We will use four images, M139939938LE, M139946735RE, M173004270LE, and M122270273LE.

We first retrieve the data sets, convert them to ISIS cubes, initialize the SPICE kernels, and perform radiometric calibration and echo correction. Here are the steps, illustrated on the first image:

```
wget http://lroc.sese.asu.edu/data/LRO-L-LROC-2-EDR-V1.0/\
LROLRC_0005/DATA/SCI/2010267/NAC/M139939938LE.IMG
lronac2isis from = M139939938LE.IMG to = M139939938LE.cub
spiceinit from = M139939938LE.cub
lronaccal from = M139939938LE.cub to = M139939938LE.cal.cub
lronacecho from = M139939938LE.cal.cub to = M139939938LE.cal.echo.cub
```

We rename, for simplicity, the obtained four processed datasets to A.cub, B.cub, C.cub, and D.cub.

The first step is to run `stereo` to create an initial guess DEM. We picked for this the first two of these images. These form a stereo pair, that is, they have a reasonable baseline and sufficiently close times of acquisition (hence very similar illuminations). These conditions are necessary to obtain a good stereo result.

```
parallel_stereo --job-size-w 1024 --job-size-h 1024 A.cub B.cub \
--left-image-crop-win 0 7998 2728 2696 \
--right-image-crop-win 0 9377 2733 2505 \
--threads 16 --corr-seed-mode 1 --subpixel-mode 3 \
run_full1/run
```

Next we create a DEM at 1 meter/pixel, which is about the resolution of the input images. We use the stereographic projection since this dataset is very close to the South Pole. Then we crop it to the region we'd like to do SfS on.

```
point2dem -r moon --stereographic --proj-lon 0 \
--proj-lat -90 run_full1/run-PC.tif
gdal_translate -projwin -15471.9 150986 -14986.7 150549 \
run_full1/run-DEM.tif run_full1/run-crop-DEM.tif
```

This creates a DEM of size 456 × 410 pixels.

Then we run `sfs`:

```
sfs -i run_full1/run-crop-DEM.tif A.cub -o sfs/run \
--smoothness-weight 0.08 --reflectance-type 0 \
--max-iterations 100 --use-approx-camera-models
```

This run should take an hour or more, but just after 10 iterations it should be clear how the solution is behaving.

The smoothness weight is a parameter that needs tuning. If it is too small, SfS will return noisy results, if it is too large, too much detail will be blurred. We have chosen to use here the plain Lambertian model (reflectance-type 0), as the Lunar Lambertian broke down so far South (an issue to be investigated). The meaning of the other `sfs` options can be looked up in section A.27.

We show the results of running this program in figure 10.1. The left-most figure is the hill-shaded original DEM, which was obtained by running:

```
hillshade --azimuth 300 --elevation 20 run_full1/run-crop-DEM.tif \
-o run_full1/run-crop-hill.tif
```

The second image is the hill-shaded DEM obtained after running `sfs` for 15 iterations.

The third image is, for comparison, the map-projection of `A.cub` onto the original DEM, obtained via the command:

```
mapproject --tr 1 run_full1/run-crop-DEM.tif A.cub A_map.tif --tile-size 128
```

The forth image is the colored absolute difference between the original DEM and the SfS output, obtained by running:

```
geodiff --absolute sfs/run-DEM-iter15.tif run_full1/run-crop-DEM.tif
colormap --min 0 --max 2 --colormap-style binary-red-blue \
run-DEM-iter15_run-crop-DEM-diff.tif
```

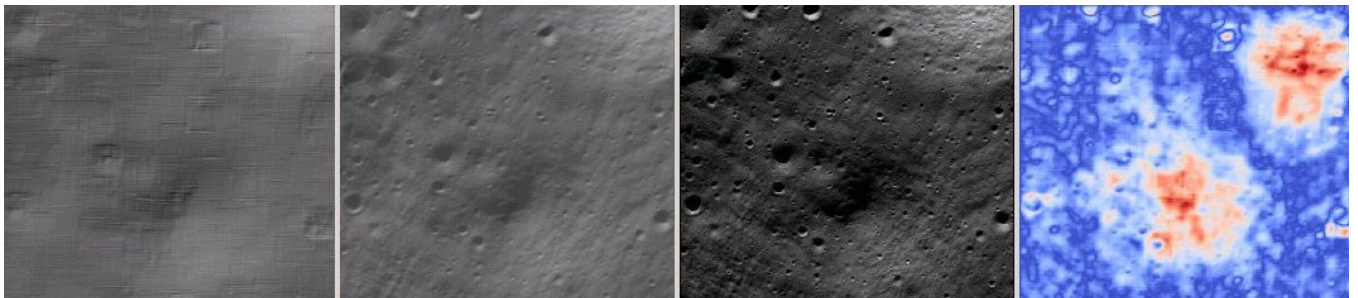


Figure 10.1: An illustration of `sfs`. The images are, from left to right, the original hill-shaded DEM, the hill-shaded DEM obtained from `sfs`, the image `A.cub` map-projected onto the original DEM, and the absolute difference of the original and final DEM, where the brightest shade of red corresponds to a 2 meter height difference.

It can be seen that the optimized DEM provides a wealth of detail and looks quite similar to the input image. It also did not diverge significantly from the input DEM. We will see in the next section that SfS is in fact able to make the refined DEM more accurate than the initial guess (as compared to some known ground truth), though that is not guaranteed, and most likely did not happen here where just one image was used.

10.3 SfS with multiple images in the presence of shadows

In this section we will run **sfs** with multiple images. We would like to be able to see if SfS improves the accuracy of the DEM rather than just adding detail to it. We evaluate this using the following (admittedly imperfect) approach. We resample the original images by a factor of 10, run stereo with them, followed by SfS using the stereo result as an initial guess and with the resampled images. As ground truth, we create a DEM from the original images at 1 meter/pixel, which we bring closer to the initial guess for SfS using **pc_align**. We would like to know if running SfS brings us even closer to this “ground truth” DEM.

The most significant challenge in running SfS with multiple images is that shape-from-shading is highly sensitive to errors in camera position and orientation. The **sfs** tool can improve these by floating them during optimization and by using a coarse-to-fine scheme, where the problem is first solved using subsampled images and terrain then it is successively refined.

If possible, it may still be desirable to bundle-adjust the cameras first (section A.4). It is important to note that bundle adjustment may fail if the images have sufficiently different illumination, as it will not be able to find matches among images. In that case, it can be used at least among the images forming the stereo pair that is used to create the initial DEM, and one of these images should be specified as the first input to SfS (as the tool keeps the camera pose of the first image fixed while optimizing the poses of the other cameras to it). Alternatively, **stereo_gui** tool can be used to create the matches manually (section A.2).

To make bundle adjustment and stereo faster, we first crop the images, such as shown below (the crop parameters can be determined via **stereo_gui**).

```
crop from = A.cub to = A_crop.cub sample = 1 line = 6644 nsamples = 2192 nlines = 4982
crop from = B.cub to = B_crop.cub sample = 1 line = 7013 nsamples = 2531 nlines = 7337
crop from = C.cub to = C_crop.cub sample = 1 line = 1 nsamples = 2531 nlines = 8305
crop from = D.cub to = D_crop.cub sample = 1 line = 1 nsamples = 2531 nlines = 2740
```

Then we bundle-adjust and run stereo

```
bundle_adjust A_crop.cub B_crop.cub C_crop.cub D_crop.cub \
--min-matches 10 -o run_ba/run
stereo A_crop.cub B_crop.cub run_full2/run --subpixel-mode 3 \
--bundle-adjust-prefix run_ba/run
```

This will result in a point cloud, **run_full2/run-PC.tif**, which will lead us to the “ground truth” DEM. As mentioned before, we’ll in fact run SfS with images subsampled by a factor of 10. Subsampling is done by running the ISIS **reduce** command

```
reduce from = A_crop.cub to = A_crop_sub10.cub sscale = 10 lscale = 10
```

and the same for the other images.

We run bundle adjustment and stereo with the subsampled images using commands analogous to the above:

```
bundle_adjust A_crop_sub10.cub B_crop_sub10.cub C_crop_sub10.cub D_crop_sub10.cub \
--min-matches 1 -o run_ba_sub10/run --ip-per-tile 100000
stereo A_crop_sub10.cub B_crop_sub10.cub run_sub10/run --subpixel-mode 3 \
--bundle-adjust-prefix run_ba_sub10/run
```

We’ll obtain a point cloud named **run_sub10/run-PC.tif**.

We’ll bring the “ground truth” point cloud closer to the initial guess for SfS using **pc_align**:

```
pc_align --max-displacement 200 run_full2/run-PC.tif run_sub10/run-PC.tif \
-o run_full2/run --save-inv-transformed-reference-points
```

This step is extremely important. Since we ran two bundle adjustment steps, and both were without ground control points, the resulting clouds may differ by a large translation, which we correct here. Hence we would like to make the “ground truth” terrain aligned with the datasets on which we will perform SfS.

Next we create the “ground truth” DEM from the aligned high-resolution point cloud, and crop it to a desired region:

```
point2dem -r moon --tr 10 --stereographic --proj-lon 0 --proj-lat -90 \
run_full2/run-trans_reference.tif
gdal_translate -projwin -15540.7 151403 -14554.5 150473 \
run_full2/run-trans_reference-DEM.tif run_full2/run-crop-DEM.tif
```

We repeat the same steps for the initial guess for SfS:

```
point2dem -r moon --tr 10 --stereographic --proj-lon 0 --proj-lat -90 \
run_sub10/run-PC.tif
gdal_translate -projwin -15540.7 151403 -14554.5 150473 \
run_sub10/run-DEM.tif run_sub10/run-crop-DEM.tif
```

Next we run `sfs` itself. Since our dataset has many shadows, we found that specifying the shadow thresholds for the tool improves the results. The thresholds can be determined using `stereo_gui`.

```
sfs -i run_sub10/run-crop-DEM.tif A_crop_sub10.cub C_crop_sub10.cub \
D_crop_sub10.cub -o sfs/run --threads 1 --smoothness-weight 0.12 \
--max-iterations 100 --reflectance-type 0 --float-exposure \
--float-cameras --use-approx-camera-models \
--bundle-adjust-prefix run_ba_sub10/run \
--shadow-thresholds "0.00162484 0.0012166 0.000781663"
```

We compare the initial guess to `sfs` to the “ground truth” DEM obtained earlier and the same for the final refined DEM using `geodiff` as in the previous section. The mean error goes from 2.65 meters to 1.34 meters. Visually the refined DEM looks more detailed as well as seen in figure 10.2.

We also show in this figure the first of the images used for SfS, `A_crop_sub10.cub`, map-projected upon the optimized DEM. Note that we use the previously computed bundle-adjusted cameras when map-projecting, otherwise the image will show as shifted from its true location:

```
mapproject sfs/run-DEM-iter28.tif A_crop_sub10.cub A_crop_sub10_map.tif \
--bundle-adjust-prefix run_ba_sub10/run
```

10.4 Insights for getting the most of SfS

Here are a few suggestions we have found helpful when running `sfs`:

- First determine the appropriate smoothing term, by running a small clip, and using just one image.

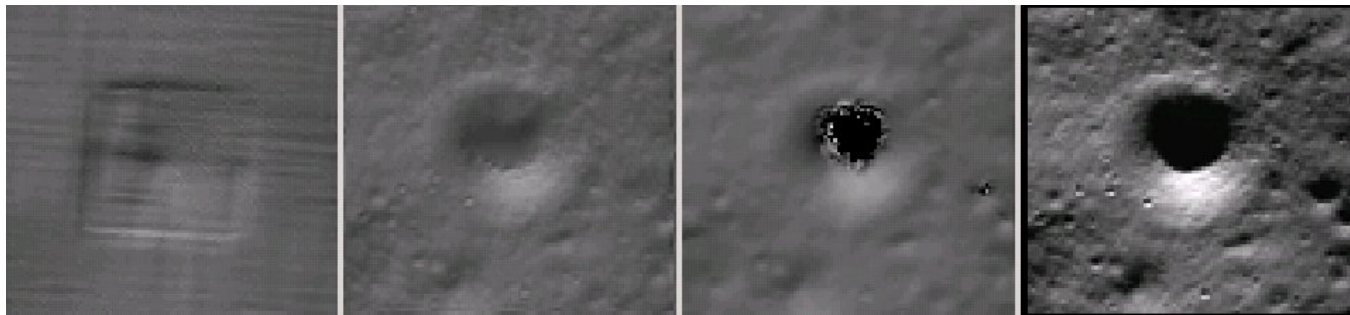


Figure 10.2: An illustration of `sfs`. The images are, from left to right, the hill-shaded initial guess DEM for SfS, the hill-shaded DEM obtained from `sfs`, the “ground truth” DEM, and the first of the images used in SfS map-projected onto the optimized DEM.

- Bundle-adjustment for multiple images is crucial. It is suggested to examine the measured intensity images output by `sfs` for some iterations using `stereo_gui` with the options `--single-window` and `--use-georef` to see if the images overlay correctly, and if the overlay error appears to go down as the tool is running. If not, the cameras have a pose error that is too big for the algorithm to correct it.
- If bundle adjustment is not successful, the option `--coarse-levels` is very helpful in fixing errors in camera positions. It first runs SfS at a coarse resolution, and progressively refines the results. A good value for the number of levels can be 3 to 5 (downsampling the images by a factor of 32 and 128 respectively), larger values are suggested for larger camera errors.
- Floating the albedo (option `--float-albedo`) can introduce instability and divergence, it should be avoided unless albedo variation is seen in the images.
- Floating the DEM at the boundary (option `--float-dem-at-boundary`) is also suggested to be avoided.
- Overall, the best strategy is to first use SfS for a single image and not float any variables except the DEM being optimized, and then gradually add images and float more variables and select whichever approach seems to give better results.

Chapter 11

Data Processing Examples

This chapter showcases a variety of results that are possible when processing different data sets with the Stereo Pipeline. It is also a shortened guide that shows the commands used to process specific mission data. There is no definitive method yet for making elevation models as each stereo pair is unique. We hope that the following sections serve as a cookbook for strategies that will get you started in processing your own data. We recommend that you second check your results against another source.

11.1 Guidelines for Selecting Stereo Pairs

When choosing image pairs to process, images that are taken with similar viewing angles, lighting conditions, and significant surface coverage overlap are best suited for creating terrain models. Depending on the characteristics of the mission data set and the individual images, the degree of acceptable variation will differ. Significant differences between image characteristics increases the likelihood of stereo matching error and artifacts, and these errors will propagate through to the resulting data products.

Although images do not need to be map-projected before running the `stereo` program, we recommend that you do run `cam2map` (or `cam2map4stereo.py`) beforehand, especially for image pairs that contain large topographic variation (and therefore large disparity differences across the scene, e.g., Valles Marineris). Map-projection is especially necessary when processing HiRISE images. This removes the large disparity differences between HiRISE images and leaves only the small detail for the Stereo Pipeline to compute. Remember that ISIS can work backwards through a map-projection when applying the camera model, so the geometric integrity of your images will not be sacrificed if you map-project first.

An alternative way of map-projection, that applies to non-ISIS imagery as well, is with the `mapproject` tool (section 5.1.6).

Excessively noisy images will not correlate well, so images should be photometrically calibrated in whatever fashion suits your purposes. If there are photometric problems with the images, those photometric defects can be misinterpreted as topography.

Remember, in order for `stereo` to process stereo pairs in ISIS cube format, the images must have had SPICE data associated by running ISIS's `spiceinit` program run on them first.

11.2 Mars Reconnaissance Orbiter HiRISE

HiRISE is one of the most challenging cameras to use when making 3D models because HiRISE exposures can be several gigabytes each. Working with this data requires patience as it will take time.

One important fact to know about HiRISE is that it is composed of multiple linear CCDs that are arranged side by side with some vertical offsets. These offsets mean that the CCDs will view some of the same terrain but at a slightly different time and a slightly different angle. Mosaicking the CCDs together to a single image is not a simple process and involves living with some imperfections.

One cannot simply use the HiRISE RDR products, as they do not have the required geometric stability. Instead, the HiRISE EDR products must be assembled using ISIS `noproj`. The USGS distributes a script in use by the HiRISE team that works forward from the team-produced ‘balance’ cubes, which provides a de-jittered, `noproj`’ed mosaic of a single observation, which is perfectly suitable for use by the Stereo Pipeline (this script was originally engineered to provide input for SOCET SET). However, the ‘balance’ cubes are not available to the general public, and so we include a program (`hiedr2mosaic.py`, written in [Python](#)) that will take PDS available HiRISE EDR products and walk through the processing steps required to provide good input images for `stereo`.

The program takes all the red CCDs and projects them using the ISIS `noproj` command into the perspective of the RED5 CCD. From there, `hijitreg` is performed to work out the relative offsets between CCDs. Finally the CCDs are mosaicked together using the average offset listed from `hijitreg` using the `handmos` command, and the mosaic is normalized with `cubenorm`. Below is an outline of the processing.

```
hi2isis          # Import HiRISE IMG to Isis
hical           # Calibrate
histitch         # Assemble whole-CCD images from the channels
spiceinit
spicefit         # For good measure
noproj          # Project all images into perspective of RED5
hijitreg         # Work out alignment between CCDs
handmos          # Mosaic to single file
cubenorm         # Normalize the mosaic
```

To use our script, first go to the directory where you have downloaded the HiRISE’s RED EDR IMG files. You can run the `hiedr2mosaic.py` program without any arguments to view a short help statement, with the `-h` option to view a longer help statement, or just run the program on the EDR files like so:

```
hiedr2mosaic.py *.IMG
```

If you have more than one observation’s worth of EDRs in that directory, then limit the program to just one observation’s EDRs at a time, e.g. `hiedr2mosaic.py PSP_001513_1655*IMG`. If you run into problems, try using the `-k` option to retain all of the intermediary image files to help track down the issue. The `hiedr2mosaic.py` program will create a single mosaic file with the extension `.mos_hijitreged.norm.cub`. Be warned that the operations carried out by `hiedr2mosaic.py` can take many hours to complete on the very large HiRISE images.

An example of using ASP with HiRISE data is included in the `examples/HiRISE` directory (just type ‘make’ there).

11.2.1 Columbia Hills

HiRISE observations [PSP_001513_1655](#) and [PSP_001777_1650](#) are on the floor of Gusev Crater and cover the area where the MER Spirit landed and has roved, including the Columbia Hills.

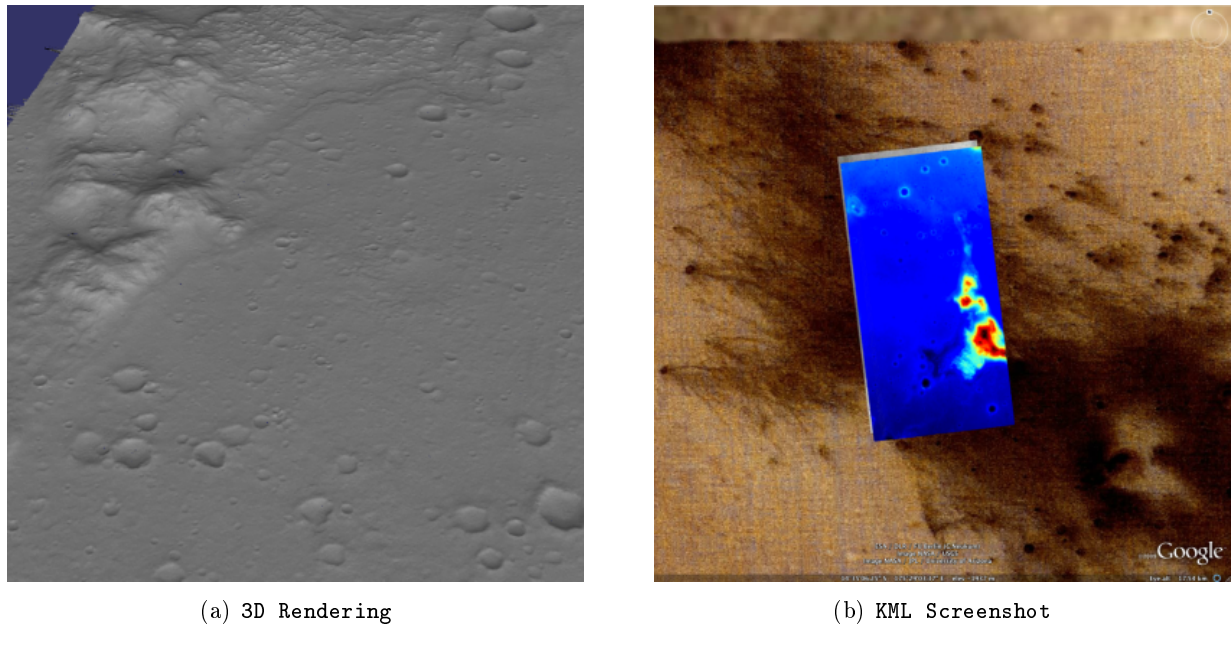


Figure 11.1: Example output using HiRISE images PSP_001513_1655 and PSP_001777_1650 of the Columbia Hills.

Commands

Download all 20 of the RED EDR .IMG files for each observation.

```
ISIS 3> hiedr2mosaic.py PSP_001513_1655_RED*.IMG
ISIS 3> hiedr2mosaic.py PSP_001777_1650_RED*.IMG
ISIS 3> cam2map4stereo.py PSP_001777_1650_RED.mos_hijitreged.norm.cub \
          PSP_001513_1655_RED.mos_hijitreged.norm.cub
ISIS 3> stereo PSP_001513_1655.map.cub \
          PSP_001777_1650.map.cub result/output
```

stereo.default

The stereo.default example file (appendix B) should apply well to HiRISE. Just set `alignment-method` to `none` if using map-projected imagery. If you are not using map-projected imagery, set `alignment-method` to `homography` or `affineepipolar`. The `corr-kernel` value can usually be safely reduced to 21 pixels to resolve finer detail and faster processing for images with good contrast.

11.3 Mars Reconnaissance Orbiter CTX

Context Camera (CTX) is a moderate camera to work with. Processing times for CTX can be pretty long when using Bayes EM subpixel refinement. Otherwise the disparity between images is relatively small, allowing efficient computation and a reasonable processing time.

11.3.1 North Terra Meridiani

In this example, we use map-projected images. Map-projecting the images is the most reliable way to align the images for correlation. However when possible, use non-map-projected images with the `alignment-method affineepipolar` option. This greatly reduces the time spent in triangulation. For all cases using linescan cameras, triangulation of map-projected images is 10x slower than non-map-projected images.

This example is distributed in the `examples/CTX` directory (type 'make' there to run it).

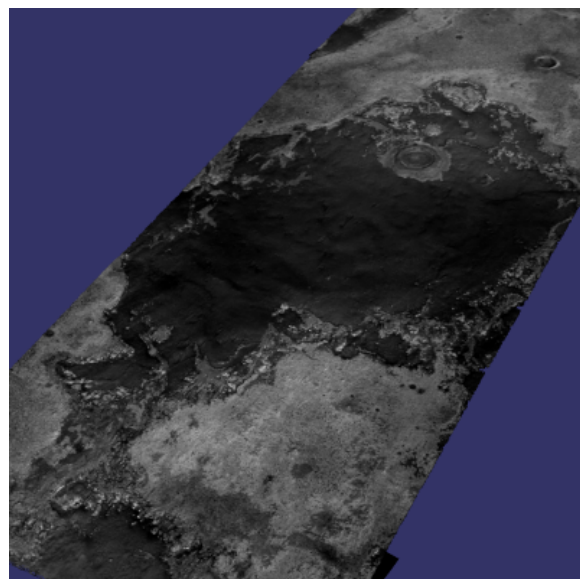
Commands

Download the CTX images P02_001981_1823_XI_02N356W.IMG and P03_002258_1817_XI_01N356W.IMG from the PDS.

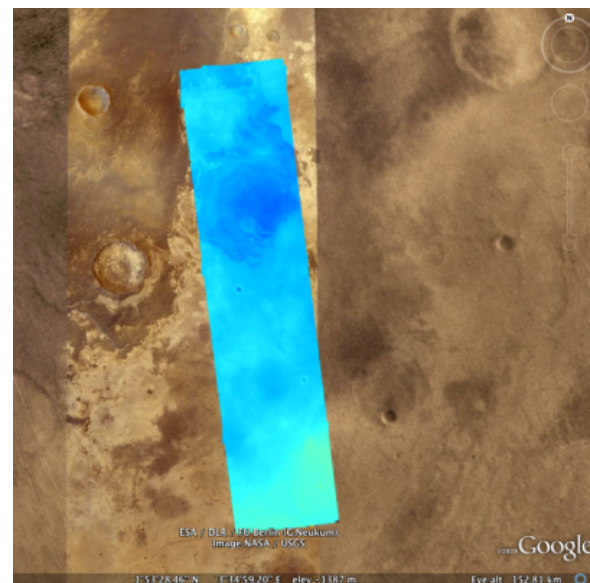
```
ISIS 3> mroctx2isis from=P02_001981_1823_XI_02N356W.IMG to=P02_001981_1823.cub
ISIS 3> mroctx2isis from=P03_002258_1817_XI_01N356W.IMG to=P03_002258_1817.cub
ISIS 3> spiceinit from=P02_001981_1823.cub
ISIS 3> spiceinit from=P03_002258_1817.cub
ISIS 3> ctxcal from=P02_001981_1823.cub to=P02_001981_1823.cal.cub
ISIS 3> ctxcal from=P03_002258_1817.cub to=P03_002258_1817.cal.cub
    you can also optionally run ctxevenodd on the cal.cub files, if needed
ISIS 3> cam2map4stereo.py P02_001981_1823.cal.cub P03_002258_1817.cal.cub
ISIS 3> stereo P02_001981_1823.map.cub P03_002258_1817.map.cub results/out
```

stereo.default

The `stereo.default` example file (appendix B) works generally well with all CTX pairs. Just set `alignment-method` to `homography` or `affineepipolar`.



(a) 3D Rendering



(b) KML Screenshot

Figure 11.2: Example output possible with the CTX imager aboard MRO.

11.4 Mars Global Surveyor MOC-NA

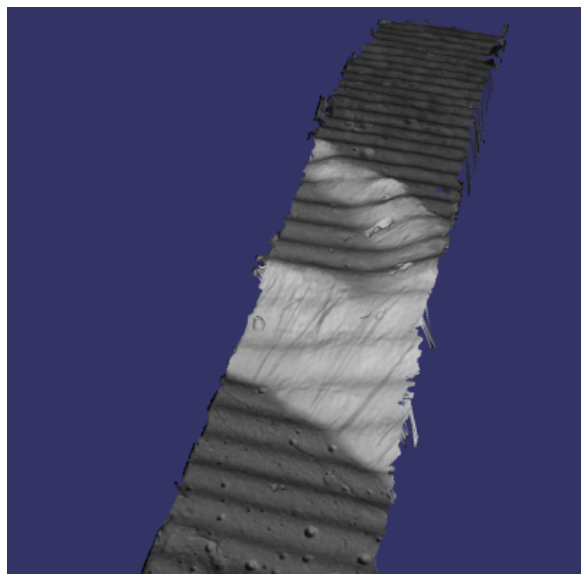
In the Stereo Pipeline Tutorial in Chapter 3, we showed you how to process a narrow angle MOC stereo pair that covered a portion of Hrad Vallis. In this section we will show you more examples, some of which exhibit a problem common to stereo pairs from linescan imagers: “spacecraft jitter” is caused by oscillations of the spacecraft due to the movement of other spacecraft hardware. All spacecraft wobble around to some degree but some are particularly susceptible.

Jitter causes wave-like distortions along the track of the satellite orbit in DEMs produced from linescan camera images. This effect can be very subtle or quite pronounced, so it is important to check your data products carefully for any sign of this type of artifact. The following examples will show the typical distortions created by this problem.

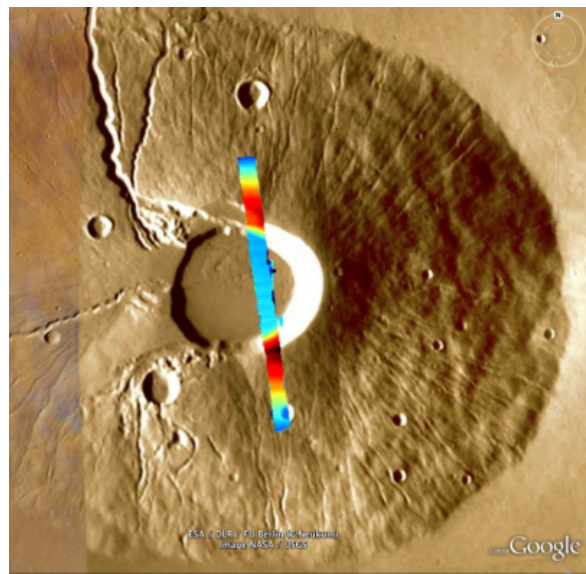
Note that the science teams of HiRISE and Lunar Reconnaissance Orbiter Camera (LROC) are actively working on detecting and correctly modeling jitter in their respective SPICE data. If they succeed in this, the distortions will still be present in the raw imagery, but the jitter will no longer produce ripple artifacts in the DEMs produced using ours or other stereo reconstruction software.

11.4.1 Ceraunius Tholus

Ceraunius Tholus is a volcano in northern Tharsis on Mars. It can be found at 23.96 N and 262.60 E. This DEM crosses the volcano’s caldera.



(a) 3D Rendering



(b) KML Screenshot

Figure 11.3: Example output for MOC-NA of Ceraunius Tholus. Notice the presence of severe washboarding artifacts due to spacecraft “jitter.”

Commands

Download the M08/06047 and R07/01361 images from the PDS.

```
ISIS 3> moc2isis f=M0806047.img t=M0806047.cub
```

```
ISIS 3> moc2isis f=R0701361.img t=R0701361.cub
ISIS 3> spiceinit from=M0806047.cub
ISIS 3> spiceinit from=R0701361.cub
ISIS 3> cam2map4stereo.py M0806047.cub R0701361.cub
ISIS 3> stereo M0806047.map.cub R0701361.map.cub result/output
```

stereo.default

The `stereo.default` example file (appendix B) works generally well with all MOC-NA pairs. Just set `alignment-method` to `none` when using map-projected imagery. If the images are not map-projected, use `homography` or `affineepipolar`.

11.5 Mars Exploration Rovers

The Mars Exploration Rovers (MER) have several cameras on board and they all seem to have a stereo pair. With ASP you are able to process the Pancam, Navcam, and Hazcam camera imagery. ISIS has no telemetry or camera intrinsic supports for these images. That however is not a problem as their raw imagery contains the cameras' information in JPL's CAHV, CAHVOR, and CHAVORE formats.

These cameras are all variations of a simple pinhole camera model so they are processed with ASP in the `Pinhole` session instead of the usual `ISIS`. ASP only supports creating of point clouds. *The *-PC.tif is a raw point cloud with the first 3 channels being XYZ in the rover site's coordinate frame.* We don't support the creation of DEMs from these images and that is left as an exercise for the user.

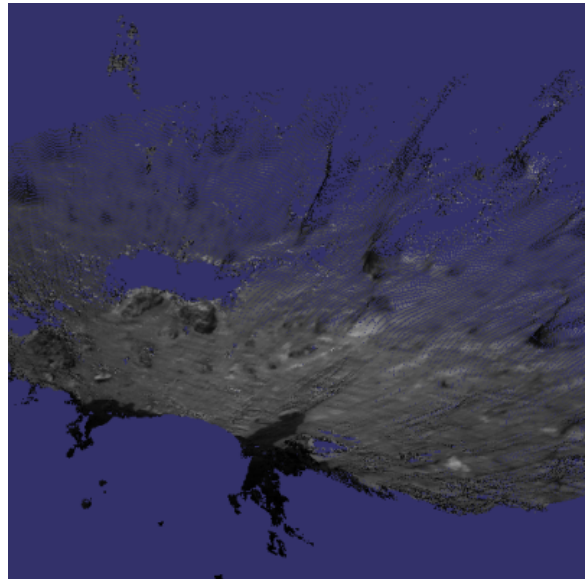
An example of using ASP with MER data is included in the `examples/MER` directory (just type 'make' there).

11.5.1 PANCAM, NAVCAM, HAZCAM

All of these cameras are processed the same way. We'll be showing 3D processing of the front hazard cams. The only new things in the pipeline is the new executable `mer2camera` along with the use of `alignment-method epipolar`. This example is also provided in the MER data example directory.



(a) Rectified Input



(b) Output Point Cloud

Figure 11.4: Example output possible with the front hazard cameras.

Commands

Download 2f194370083effap00p1214l0m1.img and 2f194370083effap00p1214r0m1.img from the PDS.

```
ISIS 3> mer2camera 2f194370083effap00p1214l0m1.img
ISIS 3> mer2camera 2f194370083effap00p1214r0m1.img
ISIS 3> stereo 2f194370083effap00p1214l0m1.img 2f194370083effap00p1214r0m1.img \
           2f194370083effap00p1214l0m1.cahvore 2f194370083effap00p1214r0m1.cahvore \
           fh01/fh01
```

stereo.default

The default stereo settings will work but change the following options. The universe option filters out points that are not triangulated well because they are too close *robot's hardware* or are extremely far away.

```
----- additional settings for MER -----
alignment-method epipolar
force-use-entire-range

# This deletes points that are too far away
# from the camera to truly triangulate.
universe-center Camera
near-universe-radius 0.7
far-universe-radius 80.0
```

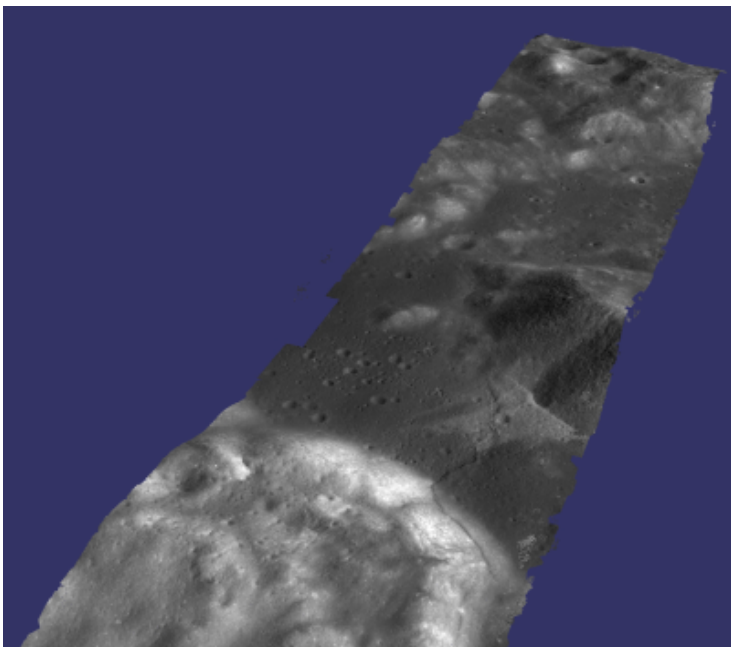
11.6 K10

K10 is an Earth-based research rover within the Intelligent Robotics Group at NASA Ames, the group ASP developers belong to. The cameras on this rover use a simple Pinhole model. The use of ASP with these cameras is illustrated in the `examples/K10` directory (just type 'make' there). Just as for the MER dataset (section 11.5), only the creation of a point cloud is supported.

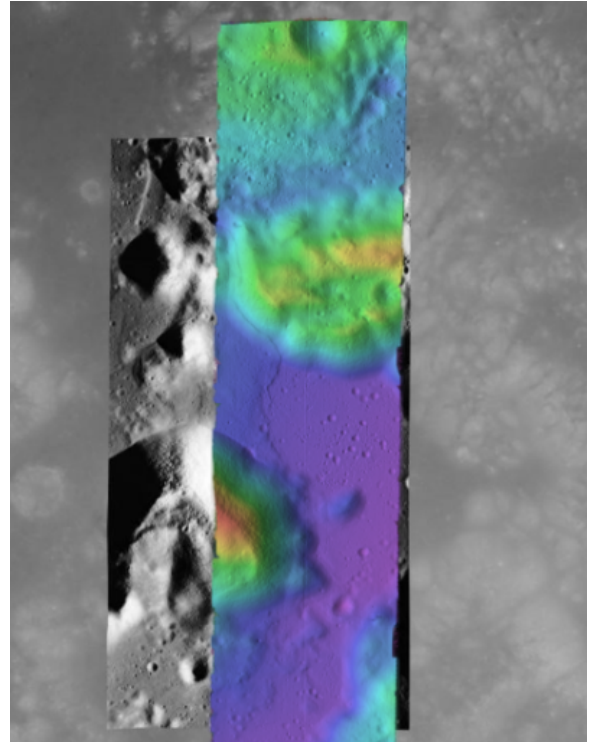
11.7 Lunar Reconnaissance Orbiter LROC NAC

11.7.1 Lee-Lincoln Scarp

This stereo pair covers the Taurus-Littrow valley on the Moon where, on December 11, 1972, the astronauts of Apollo 17 landed. However, this stereo pair does not contain the landing site. It is slightly west; focusing on the Lee-Lincoln scarp that is on North Massif. The scarp is an 80 m high feature that is the only visible sign of a deep fault.



(a) 3D Rendering



(b) KML Screenshot

Figure 11.5: Example output possible with a LROC NA stereo pair, using both CCDs from each observation courtesy of the `lronac2mosaic.py` tool.

Commands

Download the EDRs for the left and right CCDs for observations M104318871 and M104318871 from <http://wms.lroc.asu.edu/lroc/search>. Alternatively you can search by original IDs of 2DB8 and 4C86 in the PDS.

All ISIS preprocessing of the EDRs is performed via the `lronac2mosaic.py` command. This runs `lronac2isis`, `lronacall`, `lronacecho`, `spiceinit`, `noproj`, and `handmos` to create a stitched unprojected image for a single observation. In this example we don't map-project the images as ASP can usually get good results. More aggressive terrain might require an additional `cam2map4stereo.py` step.

```
ISIS 3> lronac2mosaic.py M104318871LE.img M104318871RE.img
ISIS 3> lronac2mosaic.py M104311715LE.img M104311715RE.img
ISIS 3> stereo M104318871LE*.mosaic.norm.cub M104311715LE*.mosaic.norm.cub \
           result/output --alignment-method affineepipolar
```

stereo.default

The defaults work generally well with LRO-NAC pairs, so you don't need to provide a `stereo.default` file. Map-projecting is optional. When map-projecting the images use `alignment-method none`, otherwise use `alignment-method affineepipolar`. Better map-project results can be achieved by projecting on a higher resolution elevation source like the WAC DTM. This is achieved using the ISIS command `demprep` and attaching to cube files via `spiceinit`'s `SHAPE` and `MODEL` options.

11.8 Apollo 15 Metric Camera Images

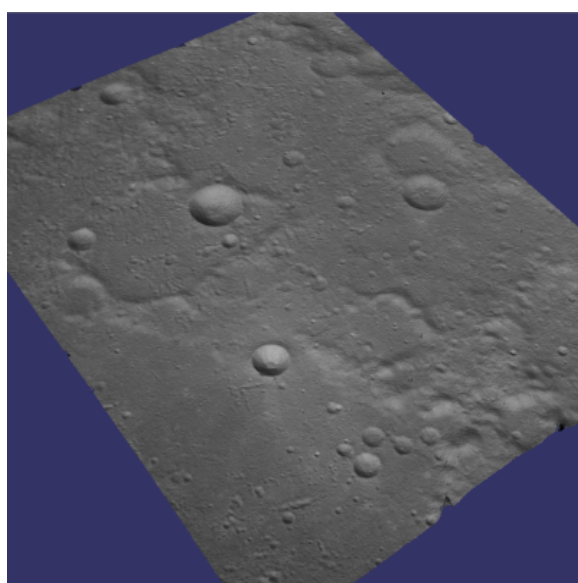
Apollo Metric images were all taken at regular intervals, which means that the same `stereo.default` can be used for all sequential pairs of images. Apollo Metric images are ideal for stereo processing. They produce consistent, excellent results.

The scans performed by ASU are sufficiently detailed to exhibit film grain at the highest resolution. The amount of noise at the full resolution is not helpful for the correlator, so we recommend subsampling the images by a factor of 4.

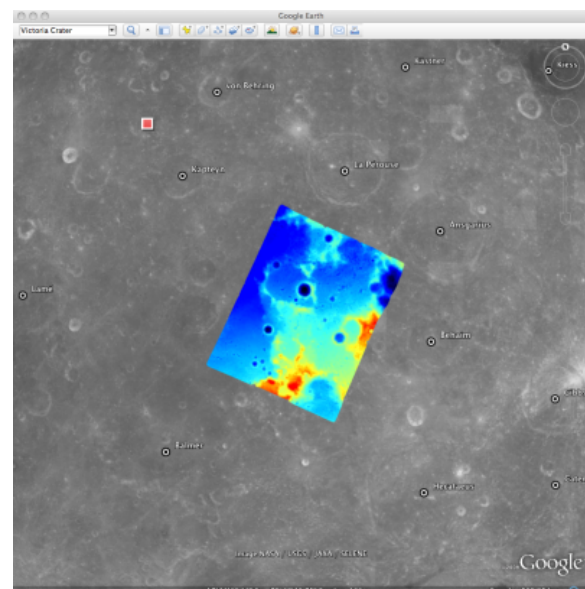
Currently the tools to ingest Apollo TIFFs into ISIS are not available, but these images should soon be released into the PDS for general public usage.

11.8.1 Ansgarius C

Ansgarius C is a small crater on the west edge of the far side of the Moon near the equator. It is east of Kapteyn A and B.



(a) 3D Rendering



(b) KML Screenshot

Figure 11.6: Example output possible with Apollo Metric frames AS15-M-2380 and AS15-M-2381.

Commands

Process Apollo TIFF files into ISIS.

```
ISIS 3> reduce from=AS15-M-2380.cub to=sub4-AS15-M-2380.cub sscale=4 lscale=4
ISIS 3> reduce from=AS15-M-2381.cub to=sub4-AS15-M-2381.cub sscale=4 lscale=4
ISIS 3> spiceinit from=sub4-AS15-M-2380.cub
ISIS 3> spiceinit from=sub4-AS15-M-2381.cub
ISIS 3> stereo sub4-AS15-M-2380.cub sub4-AS15-M-2381.cub result/output
```

stereo.default

The stereo.default example file (appendix B) works generally well with all Apollo pairs. Just set alignment-method to homography or affineepipolar.

11.9 Cassini ISS NAC

This is a proof of concept showing the strength of building the Stereo Pipeline on top of ISIS. Support for processing ISS NAC stereo pairs was not a goal during our design of the software, but the fact that a camera model exists in ISIS means that it too can be processed by the Stereo Pipeline.

Identifying stereo pairs from spacecraft that do not orbit their target is a challenge. We have found that one usually has to settle with images that are not ideal: different lighting, little perspective change, and little or no stereo parallax. So far we have had little success with Cassini's data, but nonetheless we provide this example as a potential starting point.

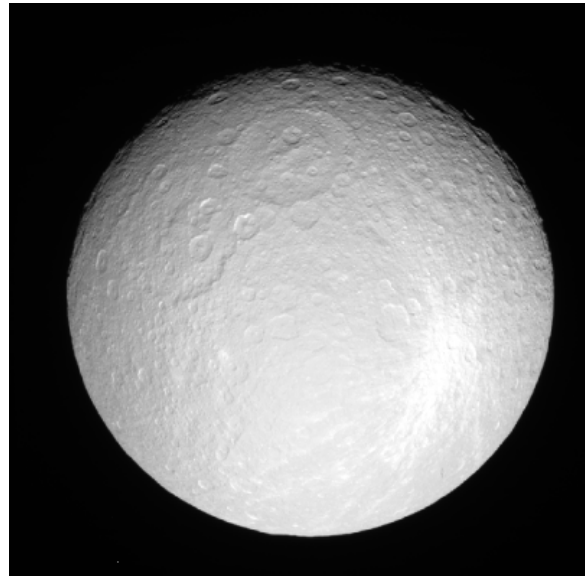
11.9.1 Rhea

Rhea is the second largest moon of Saturn and is roughly a third the size of our own Moon. This example shows, at the top right of both images, a giant impact basin named Tirawa that is 220 miles across. The bright white area south of Tirawa is ejecta from a new crater. The lack of texture in this area poses a challenge for our correlator. The results are just barely useful: the Tirawa impact can barely be made out in the 3D data while the new crater and ejecta become only noise.

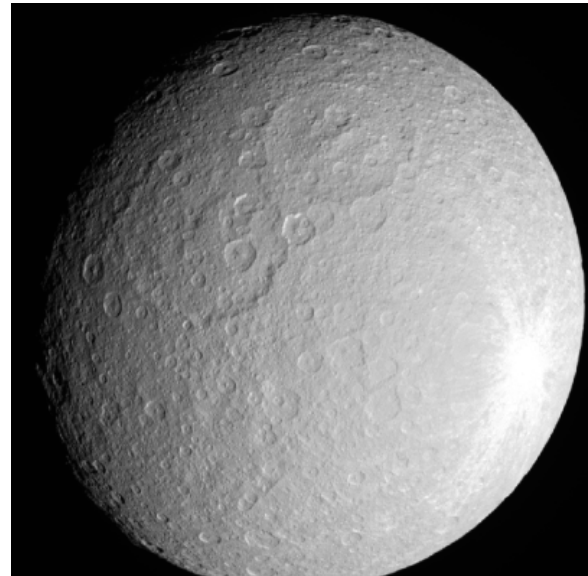
Commands

Download the N1511700120_1.IMG and W1567133629_1.IMG images and their label (.LBL) files from the PDS.

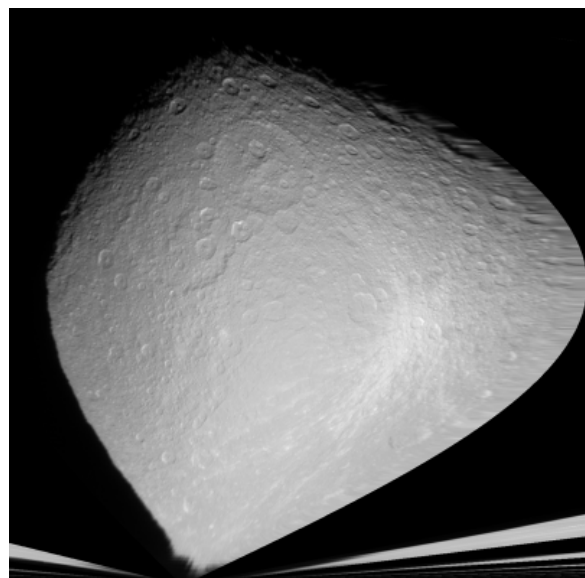
```
ISIS 3> ciess2isis f=N1511700120_1.LBL t=N1511700120_1.cub
ISIS 3> ciess2isis f=W1567133629_1.LBL t=W1567133629_1.cub
ISIS 3> ciesscal from=N1511700120_1.cub to=N1511700120_1.lev1.cub
ISIS 3> ciesscal from=W1567133629_1.cub to=W1567133629_1.lev1.cub
ISIS 3> fillgap from=W1567133629_1.lev1.cub to=W1567133629_1.fill.cub %Only one image
                                         %exhibits the problem
ISIS 3> cubenorm from=N1511700120_1.lev1.cub to=N1511700120_1.norm.cub
ISIS 3> cubenorm from=W1567133629_1.fill.cub to=W1567133629_1.norm.cub
ISIS 3> spiceinit from=N1511700120_1.norm.cub
ISIS 3> spiceinit from=W1567133629_1.norm.cub
ISIS 3> cam2map from=N1511700120_1.norm.cub to=N1511700120_1.map.cub
ISIS 3> cam2map from=W1567133629_1.norm.cub map=N1511700120_1.map.cub \
ISIS 3>           to=W1567133629_1.map.cub matchmap=true
ISIS 3> stereo N1511700120_1.map.equ.cub W1567133629_1.map.equ.cub result/rhea
```



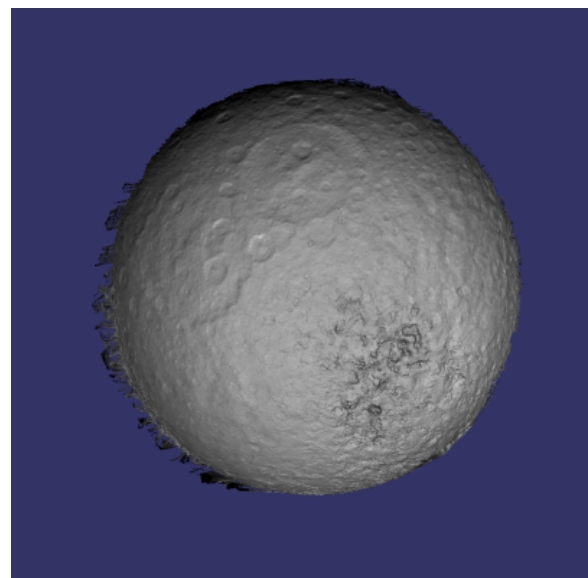
(a) Original Left Image



(b) Original Right Image



(c) Map-Projected Left



(d) 3D Rendering

Figure 11.7: Example output of what is possible with Cassini's ISS NAC

stereo.default

```
stereo.default for Cassini ISS
#####
### PREPROCESSING
alignment-method none
force-use-entire-range
individually-normalize

#####
### CORRELATION
prefilter-mode 2
prefilter-kernel-width 1.5

cost-mode 2

corr-kernel 25 25
corr-search -55 -2 -5 10

subpixel-mode 3
subpixel-kernel 21 21

#####
### FILTERING
rm-half-kernel 5 5
rm-min-matches 60 # Units = percent
rm-threshold 3
rm-cleanup-passes 1
```

11.10 Digital Globe Imagery

Processing of Digital Globe images is described extensively in the tutorial in chapter 4.

11.11 GeoEye and Astrium Imagery / RPC Imagery

GeoEye provides imagery from Ikonos and the two GeoEye satellites. Astrium provides imagery from SPOT and Pleiades satellites. Both companies provide only Rational Polynomial Camera (RPC) models. RPC represents four 20-element polynomials that map geodetic coordinates to image coordinates. Since they are easy to implement, RPC represents a universal camera model and can be had from many imaging providers; Digital Globe also provides them. The only downside is that it has less precision in our opinion compared to the linear camera model provided by Digital Globe. For GeoEye and Astrium, the only option is using RPC.

Our RPC read driver is GDAL. If the command `gdalinfo` can identify the RPC information inside the headers of your files, ASP will likely be able to see it as well. This means that sometimes we can get away with only providing a left and right image, with no extra files containing camera information. This is specifically the case for GeoEye.

You can download an example stereo pair from GeoEye's website at [27]. When we accessed the site, we downloaded a GeoEye-1 image of Hobart, Australia. As previously stated in the Digital Globe section, these types of images are not ideal for ASP. This is both a forest and a urban area which makes correlation difficult. ASP was designed more for modeling bare rock and ice. Any results we produce in other environments is a bonus but is not our objective.

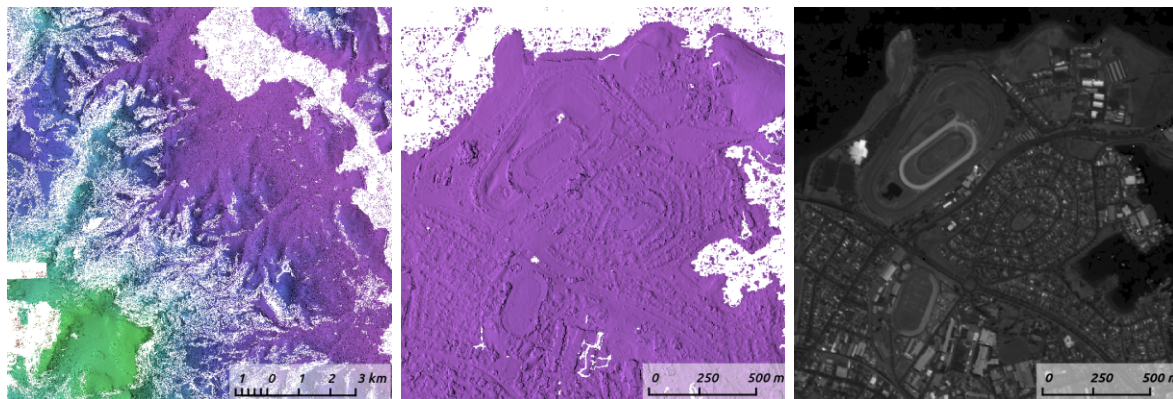


Figure 11.8: Example colorized height map and ortho image output.

Commands

```
> stereo -t rpc po_312012_pan_0000000.tif po_312012_pan_0010000.tif geoeye/geoeye
```

In case the image files do not contain the RPC models, separate XML files having this information need to be provided, as done for Digital Globe images (section 4.1).

For terrain having steep slopes, we recommend that images be map-projected onto an existing DEM before running stereo. This is described in section 5.1.6.

stereo.default

The `stereo.default` example file (appendix B) works generally well with all GeoEye pairs. Just set `alignment-method` to `affineepipolar` or `homography`.

11.12 SPOT5 Imagery

SPOT5 is a CNES (Space Agency of France) satellite launched on May 2002 and decommissioned in March 2015. SPOT5 contained two High Resolution Stereoscopic (HRS) instruments with a ground resolution of 5 meters. These two cameras were pointed forwards and backwards, allowing capture of a stereo image pair in a single pass of the satellite.

ASP supports only images from the HRS sensors on SPOT5. These images come in two parts, the data file (extension `.bil` or `.tif`) and the header file the data file (extension `.dim`). The data file can be either a plain binary file with no header information or a GeoTIFF file. The header file is a plain text XML file. When using SPOT5 images with ASP tools pass in the data file as the image file and the header file as the camera model file. ASP tools which do not accept camera model files as inputs do not support SPOT5 imagery.

You can find a sample SPOT5 image at <http://www.geo-airbusds.com/en/23-sample-imagery>.

One issue to watch out for is that SPOT5 data typically comes in a standard directory structure where the image and header files always have the same name. The header (camera model) files cannot be passed into the `bundle_adjust` tool with the same file name even if they are in different folders. A simple workaround is to create symbolic links to the original header files with different names:

```
> ln -s METADATA.DIM front/SEGMENT01/METADATA_FRONT.DIM
> ln -s METADATA.DIM back/SEGMENT01/METADATA_BACK.DIM
> bundle_adjust -t spot5 front/SEGMENT01/IMAGERY.BIL back/SEGMENT01/IMAGERY.BIL \
  front/SEGMENT01/METADATA_FRONT.DIM back/SEGMENT01/METADATA_BACK.DIM -o ba_run/out
> stereo -t spot5 front/SEGMENT01/IMAGERY.BIL back/SEGMENT01/IMAGERY.BIL \
  front/SEGMENT01/METADATA_FRONT.DIM back/SEGMENT01/METADATA_BACK.DIM \
  st_run/out --bundle-adjust-prefix ba_run/out
```

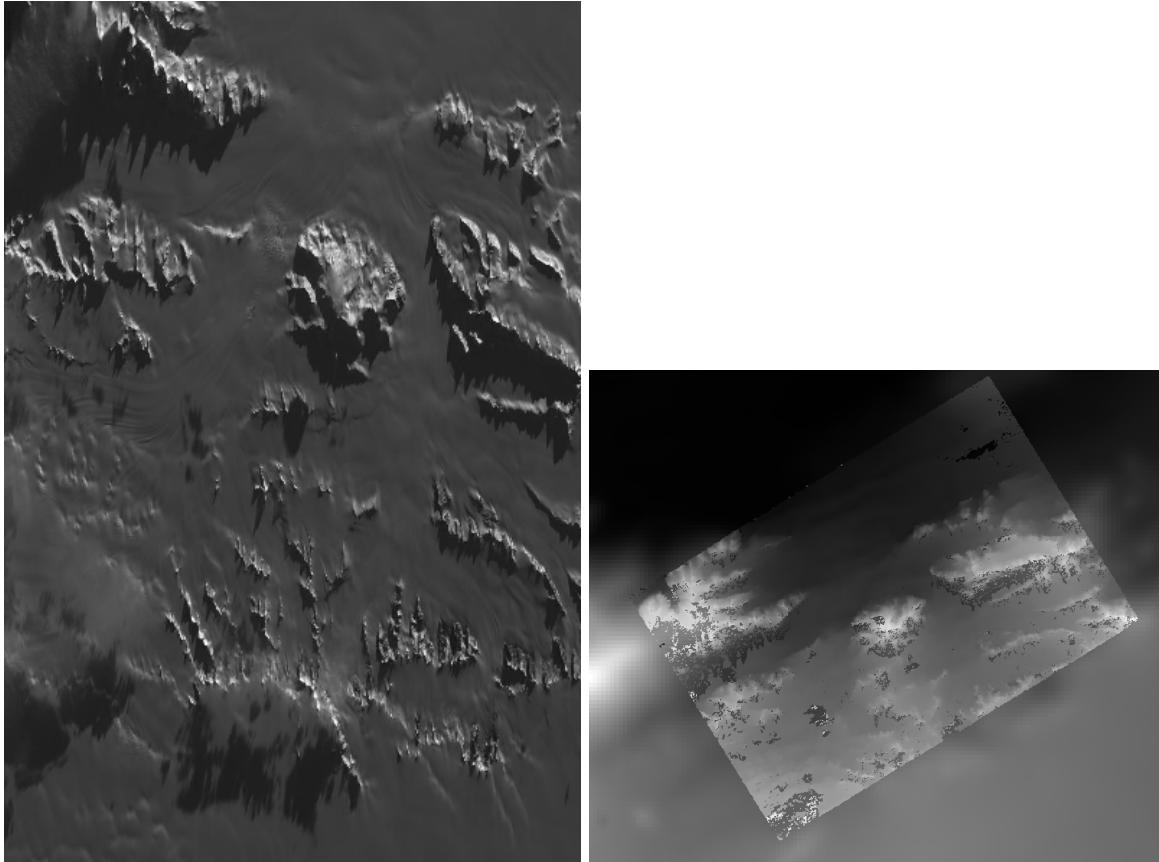


Figure 11.9: Cropped region of SPOT5 image and a portion of the associated stereo DEM overlaid on a low resolution Bedmap2 DEM.

11.13 Dawn (FC) Framing Camera

This is a NASA mission to visit two of the largest objects in the asteroid belt, Vesta and Ceres. The framing camera on board Dawn is quite small and packs only a resolution of 1024x1024 pixels. This means processing time is extremely short. To its benefit, it seems that the mission planners leave the framing camera on taking shots quite rapidly. On a single pass, they seem to usually take a chain of FC images that have a high overlap percentage. This opens the idea of using ASP to process not only the sequential pairs, but also the wider baseline shots. Then someone could potentially average all the DEMs together to create a more robust data product.

For this example, we downloaded the images

FC21A0010191_11286212239F1T.IMG and FC21A0010192_11286212639F1T.IMG

which show the Cornelia crater. We found these images by looking at the popular anaglyph shown on the Planetary Science Blog [57].

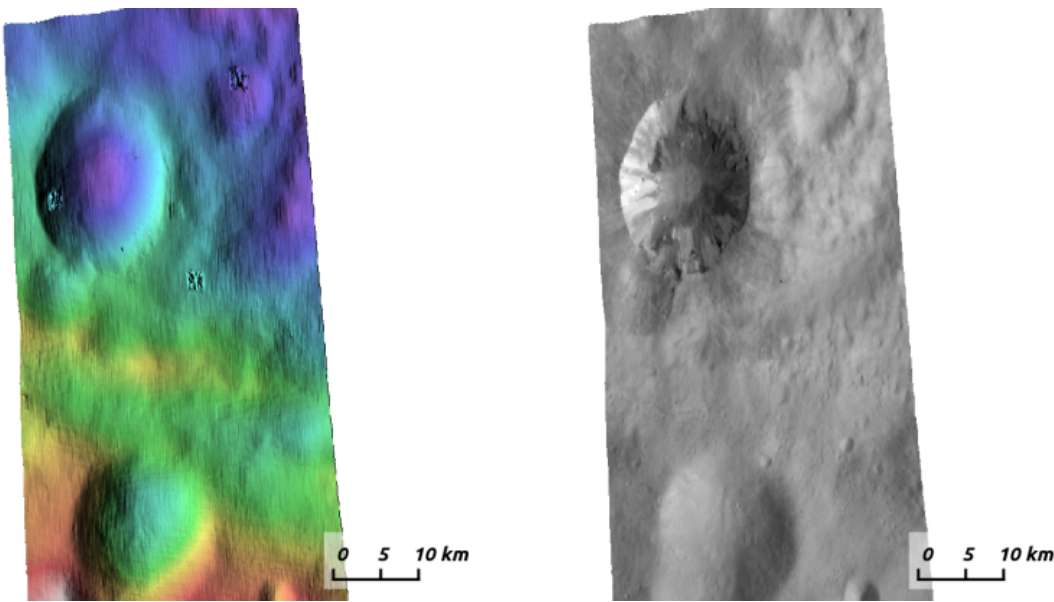


Figure 11.10: Example colorized height map and ortho image output.

Commands

First you must download the Dawn FC images from PDS.

```
ISIS3 > dawnfc2isis from=FC21A0010191_11286212239F1T.IMG \
          to=FC21A0010191_11286212239F1T.cub
ISIS3 > dawnfc2isis from=FC21A0010192_11286212639F1T.IMG \
          to=FC21A0010192_11286212639F1T.cub
ISIS3 > spiceinit from=FC21A0010191_11286212239F1T.cub
ISIS3 > spiceinit from=FC21A0010192_11286212639F1T.cub
ISIS3 > stereo FC21A0010191_11286212239F1T.cub \
          FC21A0010192_11286212639F1T.cub stereo/stereo
ISIS3 > point2dem stereo-PC.tif --orthoimage stereo-L.tif \
--t_srs "+proj=eqc +lat_ts=-11.5 +a=280000 +b=229000 +units=m"
```

stereo.default

The `stereo.default` example file (appendix B) works well for this stereo pair. Just set `alignment-method` to `affineepipolar` or `homography`.

11.14 ASTER Imagery

In this example we will describe how to process ASTER Level 1A VNIR imagery. The data can be obtained for free from <http://reverb.echo.nasa.gov>. Select a region on the map, search for `AST_L1A`, and choose “ASTER L1A Reconstructed Unprocessed Instrument Data”. (The same interface can be used to obtain pre-existing ASTER DEMs.)

There are two important things to keep in mind when ordering the data. First, at the very last step, when finalizing the order options, click on “change” and choose GeoTIFF as the data format, rather than HDF-EOS. This way the imagery and metadata will come already extracted from the HDF file.

Second, note that ASP cannot process ASTER Level 1B imagery, as those images lack camera information.

Below, we will use the dataset AST_L1A_00307182000191236_20160404141337_21031 near San Luis Reservoir in Northern California. This dataset will come as a directory containing TIFF imagery and meta-information as text files. We use the tool `aster2asp` (section A.26) to parse it (also there is described the data contained in this directory):

```
aster2asp 030353697511879 -o out
```

This command will create 4 files, named

```
out-Band3N.tif out-Band3B.tif out-Band3N.xml out-Band3B.xml
```

We refer again to the tool’s documentation page regarding details of how these files were created.

Next, we run stereo. We can use either the exact camera model (`-t aster`), or its RPC approximation (`-t rpc`). The former is much slower but more accurate.

```
stereo -t aster --subpixel-mode 3 out-Band3N.tif out-Band3B.tif \
out-Band3N.xml out-Band3B.xml out_stereo/run
```

or

```
stereo -t rpc --subpixel-mode 3 out-Band3N.tif out-Band3B.tif \
out-Band3N.xml out-Band3B.xml out_stereo/run
```

This is followed by DEM creation:

```
point2dem -r earth --tr 0.000277777777778 out_stereo/run-PC.tif
```

The value 0.000277777777778 is the desired output DEM resolution, specified in degrees. It is approximately 31 meters/pixel, the same as the publicly available ASTER DEM, and about twice the 15 meters/pixel image resolution.

Much higher quality results, but still not as detailed as the public ASTER DEM can be obtained by doing stereo as before, followed by map-projection onto a coarser and smoother version of the obtained DEM, and then redoing stereo with map-projected images (per the suggestions in chapter 6). Using `--subpixel-mode 2`, while much slower, yields the best results. The flow is as follows:

```
# Initial stereo
stereo -t aster --subpixel-mode 3 out-Band3N.tif out-Band3B.tif \
out-Band3N.xml out-Band3B.xml out_stereo/run

# Create a coarse and smooth DEM at 300 meters/pixel
point2dem -r earth --tr 0.0026949458523585 out_stereo/run-PC.tif \
-o out_stereo/run-300m
```

```
# Map-project onto this DEM at 10 meters/pixel
mapproject --tr 0.0000898315284119 out_stereo/run-300m-DEM.tif \
    out-Band3N.tif out-Band3N.xml out-Band3N_proj.tif
mapproject --tr 0.0000898315284119 out_stereo/run-300m-DEM.tif \
    out-Band3B.tif out-Band3B.xml out-Band3B_proj.tif

# Run stereo with the map-projected images with subpixel-mode 2
stereo -t aster --subpixel-mode 2 out-Band3N_proj.tif out-Band3B_proj.tif \
    out-Band3N.xml out-Band3B.xml out_stereo_proj/run \
    out_stereo/run-300m-DEM.tif

# Create the final DEM
point2dem -r earth --tr 0.000277777777778 out_stereo_proj/run-PC.tif
```

Here we could have again used `-t rpc` instead of `-t aster`. The map-projection was done using `--tr 0.0000898315284119` which is about 10 meters/pixel.

It is possible to increase the resolution of the final DEM slightly by instead map-projecting at 7 meters/pixel, hence using

```
--tr .0000628820698883
```

or smaller correlation and subpixel-refinement kernels, that is

```
--corr-kernel 15 15 --subpixel-kernel 25 25
```

instead of the defaults (21 21 and 35 35) but this comes with increased noise as well, and using a finer resolution results in longer run-time.

We also tried to first bundle-adjust the cameras, using ASP's `bundle_adjust`. We did not notice a noticeable improvement in results.

Part III

Appendices

Appendix A

Tools

This chapter provides a overview of the various tools that are provided as part of the Ames Stereo Pipeline, and a summary of their command line options.

A.1 stereo

The **stereo** program is the primary tool of the Ames Stereo Pipeline. It takes a stereo pair of images that overlap and creates an output point cloud image that can be processed into a visualizable mesh or a DEM using **point2mesh** (section A.6) and **point2dem** (section A.5), respectively.

Usage:

```
ISIS 3> stereo [options] <images> [<cameras>] output_file_prefix
```

Example (for ISIS):

```
stereo file1.cub file2.cub results/run
```

For ISIS, a .cub file has both image and camera information, as such no separate camera files are specified.

Example (for Digital Globe Earth images):

```
stereo file1.tif file2.tif file1.xml file2.xml results/run
```

Multiple input images are also supported (section 5.1.7).

This tool is primarily designed to process USGS ISIS .cub files and Digital Globe data. However, Stereo Pipeline does have the capability to process other types of stereo image pairs (e.g., image files with a CAHVOR camera model from the NASA MER rovers). If you would like to experiment with these features, please contact us for more information.

The *output_file_prefix* is prepended to all output data files. For example, setting *output_file_prefix* to ‘out’ will yield files with names like out-L.tif and out-PC.tif. To keep the Stereo Pipeline results organized in sub-directories, we recommend using an output prefix like ‘results-10-12-09/out’ for *output_file_prefix*. The **stereo** program will create a directory called **results-10-12-09/** and place files named out-L.tif, out-PC.tif, etc. in that directory.

Table A.1: Command-line options for stereo

Option
--help -h
--session-type -t pinhole isis dg rpc spot5 aster pinholemapinhole isismapisis dgmaprpc rpcmaprpc
--stereo-file -s <i>filename</i> (=./stereo.default)
--entry-point -e integer(=0 to 4)
--stop-point -e integer(=1 to 5)
--corr-seed-mode integer(=0 to 3)
--threads <i>integer</i> (=0)
--no-bigtiff
--tif-compress None LZW Deflate Packbits

More information about additional options that can be passed to `stereo` via the command line or via the `stereo.default` configuration file can be found in Appendix B on page 145. `stereo` creates a set of intermediate files, they are described in Appendix C on page 153.

A.1.1 Entry Points

The `stereo -e number` option can be used to restart a `stereo` job partway through the stereo correlation process. Restarting can be useful when debugging while iterating on `stereo.default` settings.

Stage 0 (Preprocessing) normalizes the two images and aligns them by locating interest points and matching them in both images. The program is designed to reject outlying interest points. This stage writes out the pre-aligned images and the image masks.

Stage 1 (Disparity Map Initialization) performs pyramid correlation and builds a rough disparity map that is used to seed the sub-pixel refinement phase.

Stage 2 (Sub-pixel Refinement) performs sub-pixel correlation that refines the disparity map.

Stage 3 (Outlier Rejection and Hole Filling) performs filtering of the disparity map and (optionally) fills in holes using an inpainting algorithm. This phase also creates a “good pixel” map.

Stage 4 (Triangulation) generates a 3D point cloud from the disparity map.

A.1.2 Decomposition of Stereo

The `stereo` executable is a python script that makes calls to separate C++ executables for each entry point.

Stage 0 (Preprocessing) calls `stereo_pprc`. Multi-threaded.

Stage 1 (Disparity Map Initialization) calls `stereo_corr`. Multi-threaded.

Stage 2 (Sub-pixel Refinement) class `stereo_rfne`. Multi-threaded.

Stage 3 (Outlier Rejection and Hole Filling) calls `stereo_fltr`. Multi-threaded.

Stage 4 (Triangulation) calls **stereo_tri**. Multi-threaded, except for ISIS input data.

All of the sub-programs have the same interface as **stereo**. Users processing a large number of stereo pairs on a cluster may find it advantageous to call these executables in their own manner. An example would be to run stages 0-3 in order for each stereo pair. Then run several sessions of **stereo_tri** since it is single-threaded for ISIS.

It is important to note that each of the C++ stereo executables invoked by **stereo** have their own command-line options. Those options can be passed to **stereo** which will in turn pass them to the appropriate executable. By invoking each executable with no options, it will display the list of options it accepts.

As explained in more detail in section 5.1.2, each such option has the same syntax as used in **stereo.default**, while being prepended by a double hyphen (--). A command line option takes precedence over the same option specified in **stereo.default**. Chapter B documents all options for the individual sub-programs.

Note that the stereo tools operate only on single channel (grayscale) images. If you need to run stereo on multi-channel images you must first convert them to grayscale or extract a single channel to operate on.

A.2 stereo_gui

The **stereo_gui** program is a GUI frontend to **stereo**, and has the same command-line options. It can display the input images side-by-side (and in other ways, as detailed later). One can zoom in by dragging the mouse from upper-left to lower-right, and zoom out via the reverse motion.

By pressing the Control key while dragging the mouse, regions can be selected in the input images, and then stereo can be run on these regions from the menu via Run→Stereo. The **stereo** command that is invoked (with parameters for the selected regions) will be displayed on screen, and can be re-run on a more powerful machine/cluster without GUI access.

Additional navigation options are using the mouse wheel or the +/- keys to zoom, and the arrow keys to pan (one should first click to bring into focus the desired image before using any keys).

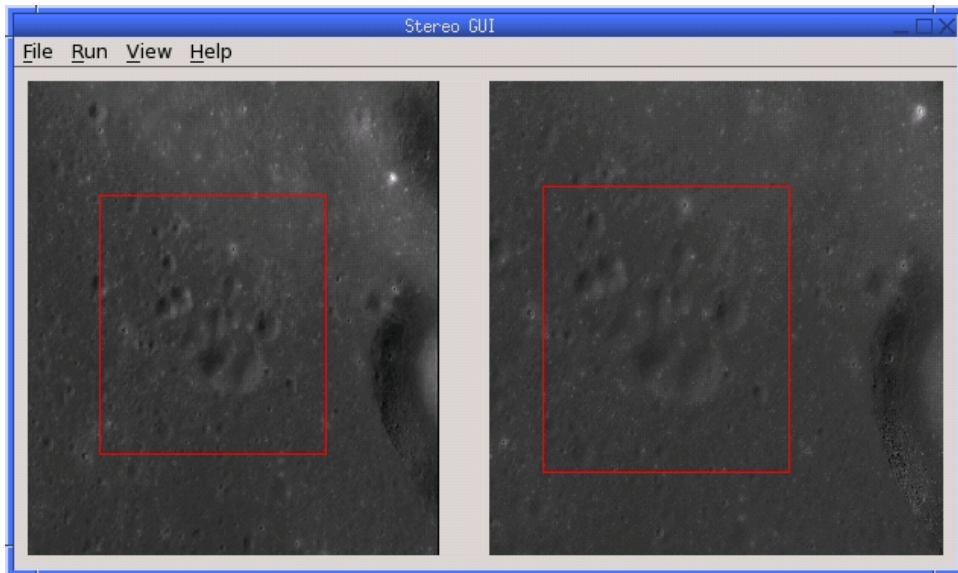


Figure A.1: An illustration of **stereo_gui**. The **stereo** command will be run on the regions selected by red rectangles.

Usage:

```
ISIS 3> stereo_gui [options] <images> [<cameras>] output_file_prefix
```

A.2.1 Use as an Image Viewer

This program can be also used as a general-purpose image viewer, case in which no stereo options or camera information is necessary. It can display arbitrarily large images with integer, floating-point, or RGB pixels, including ISIS .cub files and DEMs. It handles large images by building on disk pyramids of increasingly coarser subsampled images and displaying the subsampled versions that are appropriate for the current level of zoom.

The images can be shown either side-by-side, as tiles on a grid (using `--grid-cols integer`), or on top of each other (using `--single-window`), with a dialog to choose among them. In the last usage scenario, the option `--use-georef` will overlay the images correctly if georeference information is present. It is possible to switch among these modes once the GUI has been open, from the GUI View menu.

`stereo_gui` can show hillshaded DEMs, either via the `--hillshade` option, or by choosing from the GUI View menu the `Hillshaded images` option.

This program can also display the output of the ASP `colormap` tool (section A.22).

A.2.2 Other Functionality

View/create/delete/save interest point matches

`stereo_gui` can be used to view interest point matches (`*.match` files), such as generated by `bundle_adjust` and `stereo`. It can also manually create and delete matches (useful in situations when automatic interest point matching is unreliable due to large changes in illumination).

The match file to load can be specified via `--match-file`. It may also be auto-detected if `stereo_gui` was invoked like `stereo`, with an output prefix (auto-detection works only when images are not map-projected and alignment is homography or affine epipolar).

Create GCP

`stereo_gui` can be used to create ground control point (GCP) files for `bundle_adjust`. It is assumed that the user has two or more images and corresponding cameras that need adjustment. It is also assumed that there exists an additional reference image, possible from another source, that is georeferenced, and a reference DEM from which one can infer xyz coordinates. All these images, but not the cameras or the reference DEM, should be loaded in the GUI, with the reference georeferenced image being the last. For each output ground control point, an interest point must be picked manually in each of the images. When finished, use the "IP matches"->"Write GCP file" menu item to generate a ground control point file containing the selected points. You will be prompted for the reference DEM and for the desired output file name. The last image, that is the reference, is only used to find the positions on the ground, which in turn are used to find the heights for the GCPs from the DEM. The selected interest points from the reference image are not saved to the GCP file.

Shadow threshold

`stereo_gui` can be used to find the shadow threshold for each of a given set of images (useful for shape-from-shading (chapter 10). This can be done by turning on from the menu the `Shadow threshold detection`

mode, and then clicking on pixels in the shadow. The largest of the chosen pixel values will be set to the shadow threshold for each image and printed to the screen. To see the images with the pixels below the shadow threshold highlighted, select from the menu the `View shadow-thresholded images` option.

Listed below are the options specific to `stereo_gui`. It will accept all other `stereo` options as well.

Table A.2: Command-line options for `stereo_gui`

Option	Description
<code>-h --help</code>	Display this help message.
<code>--grid-cols arg</code>	Display images as tiles on a grid with this many columns. Default: Use one row.
<code>--window-size arg (=1200 800)</code>	The width and height of the GUI window in pixels.
<code>-w --single-window</code>	Show all images in the same window (with a dialog to choose among them) rather than next to each other.
<code>--use-georef</code>	Plot the images in the projected coordinate system given by image georeferences.
<code>--hillshade</code>	Interpret the input images as DEMs and hillshade them.
<code>--view-matches</code>	Locate and display the interest point matches.
<code>--match-file</code>	Display this match file instead of looking one up based on existing conventions (implies <code>--view-matches</code>).
<code>--delete-temporary-files-on-exit</code>	Delete any subsampled and other files created by the GUI when exiting.
<code>--create-image-pyramids-only</code>	Without starting the GUI, build multi-resolution pyramids for the inputs, to be able to load them fast later.

A.3 `parallel_stereo`

The `parallel_stereo` program is a modification of `stereo` designed to distribute the stereo processing over multiple computing nodes. It uses GNU Parallel to manage the jobs, a tool which is distributed along with Stereo Pipeline. It expects that all nodes can connect to each other using ssh without password. `parallel_stereo` can also be useful when processing extraterrestrial data on a single computer. This is because ISIS camera models are restricted to a single thread, but `parallel_stereo` can run multiple processes in parallel to reduce computation times.

At the simplest, `parallel_stereo` can be invoked exactly like `stereo`, with the addition of the list of nodes to use (if using multiple nodes).

```
parallel_stereo --nodes-list machines.txt <other stereo options>
```

It will create the same output files as `stereo`. (Internally some of them will be GDAL VRT files, that is, virtual mosaics of files created by individual processes; ASP and GDAL tools are able to use these virtual files in the same way as regular binary TIF files.)

If your jobs are launched on a cluster or supercomputer, the name of the file containing the list of nodes may exist as an environmental variable. For example, on NASA's Pleiades Supercomputer, which uses the Portable Batch System (PBS), the list of nodes can be retrieved as `$PBS_NODEFILE`.

It is important to note that when invoking this tool only stages 1, 2, and 4 of stereo (section A.1.2) are spread over multiple machines, with stages 0 and 3 using just one node, as they require global knowledge of the data. In addition, not all stages of stereo benefit equally from parallelization. Most likely to gain are stages 1 and 2 (correlation and refinement) which are the most computationally expensive.

For these reasons, while `parallel_stereo` can be called to do all stages of stereo generation from start to finish in one command, it may be more resource-efficient to invoke it using a single node for stages 0 and 3, many nodes for stages 1 and 2, and just a handful of nodes for stage 4 (triangulation). For example, to invoke the tool only for stage 2, one uses the options:

```
--entry-point 2 --stop-point 3
```

`parallel_stereo` accepts the following options (any additional options given to it will be passed to the stereo executables for each stage).

Table A.3: Command-line options for `parallel_stereo`

Options	Description
<code>--help -h</code>	Display the help message.
<code>--nodes-list</code> <i>filename</i>	The list of computing nodes, one per line. If not provided, run on the local machine.
<code>--entry-point -e</code> <i>integer</i> (=0 to 4)	Stereo Pipeline entry point (start at this stage).
<code>--stop-point -e</code> <i>integer</i> (=1 to 5)	Stereo Pipeline stop point (stop at the stage <i>right before</i> this value).
<code>--corr-seed-mode</code> <i>integer</i> (=0 to 3)	Correlation seed strategy (section B.2).
<code>--sparse-disp-options</code> <i>string</i>	Options to pass directly to <code>sparse_disp</code> (section 4.5).
<code>--verbose</code>	Display the commands being executed.

A.3.1 Advanced usage

The `parallel_stereo` tool tries to take advantage of its inside knowledge of the individual `stereo` subprograms to decide how many threads and processes to use at each stage, and by default, it will try to use all nodes to the fullest.

The advanced user can try to gain finer-level control of the tool, as described below. This may not necessarily result in improved performance compared to using the default settings.

As an example of using the advanced options, assume that we would like to launch the refinement and filtering steps only (stages 2 and 3). We will distribute the refinement over a number of nodes, using 4 processes on each node, with each process creating 16 threads. For the filtering stage, which is done in one process on one machine, we want to use 32 threads. The appropriate command is then:

```
parallel_stereo --nodes-list machines.txt --processes 4 --threads-multiprocess 16 \
--threads-singleprocess 32 --entry-point 2 --stop-point 4 <other stereo options>
```

To better take advantage of these options, the user should know the following. `parallel_stereo` starts a process for every image block, whose size is by default 2048×2048 (`job-size-w` by `job-size-h`). On such a block, the correlation, and subpixel refinement stages will use at most 4 and 64 threads respectively (1

and 16 threads for each 1024×1024 tile). Triangulation will use at most 64 threads as well, except for ISIS cameras, when it is single-threaded due to the limitations of ISIS (we account for the latter when the number of threads and processes are decided automatically, but not when these advanced options are used).

Table A.4: Advanced options for parallel_stereo

Options	Description
--job-size-w <i>integer</i> (=2048)	Pixel width of input image tile for a single process.
--job-size-h <i>integer</i> (=2048)	Pixel height of input image tile for a single process.
--processes <i>integer</i>	The number of processes to use per node.
--threads-multiprocess <i>integer</i>	The number of threads to use per process.
--threads-singleprocess <i>integer</i>	The number of threads to use when running a single process (for pre-processing and filtering).

A.4 bundle_adjust

The `bundle_adjust` program performs bundle adjustment on a given set of images and cameras. An introduction to bundle adjustment can be found in chapter 8, with an example of how to use this program in section 8.2.

This tool can use several algorithms for bundle adjustment. The default is to use Google's Ceres Solver (<http://ceres-solver.org/>).

Usage:

```
bundle_adjust <images> <cameras> <optional ground control points> \
-o <output prefix> [options]
```

Example (for ISIS):

```
bundle_adjust file1.cub file2.cub file3.cub -o results/run
```

Example (for Digital Globe Earth data, using ground control points):

```
bundle_adjust file1.tif file2.tif file1.xml file2.xml gcp_file.gcp \
--datum WGS_1984 -o results/run
```

Example (for generic pinhole camera data, using estimated camera positions):

```
bundle_adjust file1.JPG file2.JPG file1.tsai file2.tsai -o results/out \
-t pinhole --local-pinhole --datum WGS_1984 --camera-positions nav_data.csv \
--csv-format "1:file 6:lat 7:lon 9:height_above_datum"
```

The `stereo` program can then be told to use the adjusted cameras via the option `--bundle-adjust-prefix`.

Table A.5: Command-line options for `bundle_adjust`

Option	Description
<code>--help -h</code>	Display the help message.
<code>--output-prefix -o filename</code>	Prefix for output filenames.
<code>--bundle-adjuster string [default: Ceres]</code>	Choose a solver from: Ceres, RobustSparse, RobustRef, Sparse, Ref.
<code>--cost-function string [default: Cauchy]</code>	Choose a cost function from: Cauchy, PseudoHuber, Huber, L1, L2.
<code>--robust-threshold double(=0.5)</code>	Set the threshold for robust cost functions. Increasing this makes the solver focus harder on the larger errors.
<code>--datum string</code>	Use this datum (needed only if ground control points are used). Options: WGS_1984, D_MOON (1,737,400 meters), D_MARS (3,396,190 meters), MOLA (3,396,000 meters), NAD83, WGS72, and NAD27. Also accepted: Earth (=WGS_1984), Mars (=D_MARS), Moon (=D_MOON).

--semi-major-axis <i>double</i>	Explicitly set the datum semi-major axis in meters (needed only if ground control points are used).
--semi-minor-axis <i>double</i>	Explicitly set the datum semi-minor axis in meters (needed only if ground control points are used).
--session-type -t pinhole isis dg rpc spot5 aster	Select the stereo session type to use for processing. Usually the program can select this automatically by the file extension.
--min-matches <i>integer</i> (=30)	Set the minimum number of matches between images that will be considered.
--max-iterations <i>integer</i> (=100)	Set the maximum number of iterations.
--overlap-limit <i>integer</i> (=0)	Limit the number of subsequent images to search for matches to the current image to this value. By default try to match all images.
--camera-weight <i>double</i> (=1.0)	The weight to give to the constraint that the camera positions/orientations stay close to the original values (only for the Ceres solver). A higher weight means that the values will change less, a lower weight means more change.
--ip-per-tile <i>int</i>	How many interest points to detect in each 1024^2 image tile (default: automatic determination).
--ip-detect-method <i>string</i> [default: OBAloG]	Choose an interest point detection method from: 0=OBAloG, 1=SIFT, 2=ORB.
--local-pinhole	Optimize processing for inputs which are local coordinate pinhole models. Also writes out a standalone .tsai camera model file instead of adjust files.
--camera-positions <i>filename</i>	CSV file containing estimated positions of each camera. Only used with the local-pinhole setting to initialize global camera coordinates. If used, the csv-format setting must also be set. The "file" field is searched for strings that are found in the input image files to match locations to cameras.

<code>--csv-format string</code>	Specify the format of input CSV files as a list of entries column_index:column_type (indices start from 1). Examples: '1:x 2:y 3:z 4:file' (a Cartesian coordinate system with origin at planet center is assumed, with the units being in meters), '5:lon 6:lat 7:radius_m 2:file' (longitude and latitude are in degrees, the radius is measured in meters from planet center), '6:file 3:lat 2:lon 1:height_above_datum', '1:easting 2:northing 3:height_above_datum' (need to set <code>--csv-proj4</code> ; the height above datum is in meters). Can also use radius_km for column_type, when it is again measured from planet center.
<code>--csv-proj4 string</code>	The PROJ.4 string to use to interpret the entries in input CSV files, if those entries contain easting, northing, and height above datum.
<code>--position-filter-dist double(=1.0)</code>	If estimated camera positions are used, this option can be used to set a threshold distance in meters between the cameras. If any pair of cameras is farther apart than this distance, the tool will not attempt to find matching interest points between those two cameras.
<code>-min-triangulation-angle double(=0.1)</code>	The minimum angle, in degrees, at which rays must meet at a triangulated point to accept this point as valid.
<code>--lambda double</code>	Set the initial value of the LM parameter lambda (ignored for the Ceres solver).
<code>--threads integer(=0)</code>	Set the number threads to use. 0 means use the default defined in the program or in the .vwrc file.
<code>--report-level -r integer=(10)</code>	Use a value ≥ 20 to get increasingly more verbose output.

The `bundle_adjust` program will save the obtained adjustments (rotation and translation) for each camera in plain text files whose names start with the specified output prefix. This prefix can then be passed to `stereo` via the option `--bundle-adjust-prefix`.

A.4.1 Ground control points

A number of plain-text files containing ground control points (GCP) can be passed as inputs to `bundle_adjust`. These can either be created by hand, or using `stereo_gui` (section A.2.2).

A GCP file must end with a .gcp extension, and contain one ground control point per line. Each line must have the following fields:

- ground control point id (integer)

- latitude (in degrees)
- longitude (in degrees)
- height above datum (in meters), with the datum itself specified separately
- x, y, z standard deviations (three positive floating point numbers, smaller values suggest more reliable measurements)

On the same line, for each image in which the ground control point is visible there should be:

- image file name
- column index in image (float)
- row index in image (float)
- column and row standard deviations (two positive floating point numbers, smaller values suggest more reliable measurements)

The fields can be separated by spaces or commas. Here is a sample representation of a ground control point measurement:

```
5 23.7 160.1 427.1 1.0 1.0 1.0 image1.tif 124.5 19.7 1.0 1.0 image2.tif 254.3 73.9 1.0 1.0
```

A.5 point2dem

The `point2dem` program produces a GeoTIFF terrain model and/or an orthographic image from a set of point clouds. The clouds can be created by the `stereo` command, or be in LAS or CSV format.

Example:

```
point2dem output-prefix-PC.tif -o stereo/filename \
--nodata-value -10000 -n
```

This produces a digital elevation model. The program will infer the spheroid (datum) and the projection to use from the input images, if that information is present. Otherwise these can be set with `-r` and `--t_srs`.

Here, pixels with no data will be set to a value of -10000. Unless the input images have projection information, the resulting DEM will be saved in a simple cylindrical map-projection. The DEM is stored by default as a one channel, 32-bit floating point GeoTIFF file.

The `-n` option creates an 8-bit, normalized version of the DEM that can be easily loaded into a standard image viewing application for debugging.

Another example:

```
point2dem output-prefix-PC.tif -o stereo/filename -r moon \
--orthoimage output-prefix-L.tif
```

This command takes the left input image and orthographically projects it onto the 3D terrain produced by the Stereo Pipeline. The resulting `*-DRG.tif` file will be saved as a GeoTIFF image with the same geoheader as the DEM.

Here we have explicitly specified the spheroid (`-r moon`), rather than have it inferred automatically. The Moon spheroid will have a radius of 1737.4 km.

In the following example the point cloud is very close to the South Pole of the Moon, and for that reason we use the stereographic projection:

```
point2dem -r moon --stereographic --proj-lon 0 --proj-lat -90 output-prefix-PC.tif
```

Multiple point clouds can be passed as inputs, to be combined into a single DEM. If it is desired to use the `--orthoimage` option as above, the clouds need to be specified first, followed by the `L.tif` images. Here is an example, which combines together LAS and CSV point clouds together with an output file from `stereo`:

```
point2dem in1.las in2.csv output-prefix-PC.tif -o combined \
--dem-spacing 0.001 --nodata-value -32768
```

A.5.1 Comparing with MOLA Data

When comparing the output of `point2dem` to laser altimeter data, like MOLA, it is important to understand the different kinds of data that are being discussed. By default, `point2dem` returns planetary radius values in meters. These are often large numbers that are difficult to deal with. If you use the `-r mars` option, the output terrain model will be in meters of elevation with reference to the IAU reference spheroid for Mars: 3,396,190 m. So if a post would have a radius value of 3,396,195 m, in the model returned with the `-r mars` option, that pixel would just be 5 m.

You may want to compare the output to MOLA data. MOLA data is released in three ‘flavors,’ namely: Topography, Radius, and Areoid. The MOLA Topography data product that most people use is just the MOLA Radius product with the MOLA Areoid product subtracted. Additionally, it is important to note that all of these data products have a reference value subtracted from them. The MOLA reference value is NOT the IAU reference value, but 3,396,000 m.

In order to compare with the MOLA data, you can do one of two different things. You could operate purely in radius space, and have `point2dem` create radius values that are directly comparable to the MOLA radius data. You can do this by having `point2dem` subtract the MOLA reference value, by using either `-r mola` or setting `--semi-major-axis 3396000` and `--semi-minor-axis 3396000`.

Alternatively, to get values that are directly comparable to MOLA *Topography* data, you’ll need to run `point2dem` with either `-r mars` or `-r mola`, then run the ASP tool `dem_geoid` (section A.8). This program will convert the DEM height values from being relative to the IAU reference spheroid or the MOLA spheroid to being relative to the MOLA Areoid.

The newly obtained DEM will inherit the datum from the unadjusted DEM, so it could be either of the two earlier encountered radii, but of course the heights in it will be in respect to the areoid, not to this datum. It is important to note that one cannot tell from inspecting a DEM if it was adjusted to be in respect to the areoid or not, so there is the potential of mixing up adjusted and unadjusted terrain models.

A.5.2 Post Spacing

Recall that `stereo` creates a point cloud file as its output and that you need to use `point2dem` on to create a GeoTIFF that you can use in other tools. The point cloud file is the result of taking the image-to-image matches (which were created from the kernel sizes you specified, and the subpixel versions of the same, if used) and projecting them out into space from the cameras, and arriving at a point in real world coordinates. Since `stereo` does this for every pixel in the input images, the *default* value that `point2dem` uses (if you don’t specify anything explicitly) is the input image scale, because there’s an ‘answer’ in the point cloud file for each pixel in the original image.

However, as you may suspect, this is probably not the best value to use because there really isn’t that much ‘information’ in the data. The true ‘resolution’ of the output model is dependent on a whole bunch of

things (like the kernel sizes you choose to use) but also can vary from place to place in the image depending on the texture.

The general ‘rule of thumb’ is to produce a terrain model that has a post spacing of about 3x the input image ground scale. This is based on the fact that it is nearly impossible to uniquely identify a single pixel correspondence between two images, but a 3x3 patch of pixels provides improved matching reliability. As you go to numerically larger post-spacings on output, you’re averaging more point data (that is probably spatially correlated anyway) together.

So you can either use the `--dem-spacing` argument to `point2dem` to do that directly, or you can use your favorite averaging algorithm to reduce the `point2dem`-created model down to the scale you want.

If you attempt to derive science results from an ASP-produced terrain model with the default DEM spacing, expect serious questions from reviewers.

A.5.3 Using with LAS or CSV Clouds

The `point2dem` program can take as inputs point clouds in LAS and CSV formats. These differ from point clouds created by stereo by being, in general, not uniformly distributed. It is suggested that the user pick carefully the output resolution for such files (`--dem-spacing`). If the output DEM turns out to be sparse, the spacing could be increased, or one could experiment with increasing the value of `--search-radius-factor`, which will fill in small gaps in the output DEM by searching further for points in the input clouds.

It is expected that the input LAS files have spatial reference information such as WKT data. Otherwise it is assumed that the points are raw x, y, z values in meters in reference to the planet center.

Unless the output projection is explicitly set when invoking `point2dem`, the one from the first LAS file will be used.

For LAS or CSV clouds it is not possible to generate intersection error maps or ortho images.

For CSV point clouds, the option `--csv-format` must be set. If such a cloud contains easting, northing, and height above datum, the option `--csv-proj4` containing a PROJ.4 string needs to be specified to interpret this data (if the PROJ.4 string is set, it will be also used for output DEMs, unless `--t_srs` is specified).

Table A.6: Command-line options for `point2dem`

Options	Description
<code>--help -h</code>	Display the help message.
<code>--nodata-value float (= -3.40282347e+38)</code>	Set the nodata value.
<code>--use-alpha</code>	Create images that have an alpha channel.
<code>--normalized -n</code>	Also write a normalized version of the DEM (for debugging).
<code>--orthoimage</code>	Write an orthoimage based on the texture files passed in as inputs (after the point clouds).
<code>--errorimage</code>	Write an additional image whose values represent the triangulation error in meters.
<code>--output-prefix -o output-prefix</code>	Specify the output prefix.
<code>--output-filetype -t type(=tif)</code>	Specify the output file type.
<code>--x-offset float (= 0)</code>	Add a horizontal offset to the DEM.
<code>--y-offset float (= 0)</code>	Add a horizontal offset to the DEM.
<code>--z-offset float (= 0)</code>	Add a vertical offset to the DEM.
<code>--rotation-order order(=xyz)</code>	Set the order of an Euler angle rotation applied to the 3D points prior to DEM rasterization.

--phi-rotation float(=0)	Set a rotation angle phi.
--omega-rotation float(=0)	Set a rotation angle omega.
--kappa-rotation float(=0)	Set a rotation angle kappa.
--t_srs string	Specify the output projection (PROJ.4 string).
--t_projwin xmin ymin xmax ymax	The output DEM will have corners with these georeferenced coordinates.
--datum string	Set the datum. This will override the datum from the input images and also --t_srs, --semi-major-axis, and --semi-minor-axis. Options: WGS_1984, D_MOON (1,737,400 meters), D_MARS (3,396,190 meters), MOLA (3,396,000 meters), NAD83, WGS72, and NAD27. Also accepted: Earth (=WGS_1984), Mars (=D_MARS), Moon (=D_MOON).
--reference-spheroid string	This is identical to the datum option.
--semi-major-axis float(=0)	Explicitly set the datum semi-major axis in meters.
--semi-minor-axis float(=0)	Explicitly set the datum semi-minor axis in meters.
--sinusoidal	Save using a sinusoidal projection.
--mercator	Save using a Mercator projection.
--transverse-mercator	Save using a transverse Mercator projection.
--orthographic	Save using an orthographic projection.
--stereographic	Save using a stereographic projection.
--oblique-stereographic	Save using an oblique stereographic projection.
--gnomonic	Save using a gnomonic projection.
--lambert-azimuthal	Save using a Lambert azimuthal projection.
--utm zone	Save using a UTM projection with the given zone.
--proj-lat float	The center of projection latitude (if applicable).
--proj-lon float	The center of projection longitude (if applicable).
--proj-scale float	The projection scale (if applicable).
--false-northing float	The projection false northing (if applicable).
--false-easting float	The projection false easting (if applicable).
--dem-spacing -s float(=0)	Set output DEM resolution (in target georeferenced units per pixel). If not specified, it will be computed automatically (except for LAS and CSV files). Multiple spacings can be set (in quotes) to generate multiple output files. This is the same as the --tr option.
--search-radius-factor float(=0)	Multiply this factor by <code>dem-spacing</code> to get the search radius. The DEM height at a given grid point is obtained as a weighted average of heights of all points in the cloud within search radius of the grid point, with the weights given by a Gaussian. Default search radius: <code>max(dem-spacing, default_dem_spacing)</code> , so the default factor is about 1.

--csv-format <i>string</i>	Specify the format of input CSV files as a list of entries column_index:column_type (indices start from 1). Examples: '1:x 2:y 3:z' (a Cartesian coordinate system with origin at planet center is assumed, with the units being in meters), '5:lon 6:lat 7:radius_m' (longitude and latitude are in degrees, the radius is measured in meters from planet center), '3:lat 2:lon 1:height_above_datum', '1:easting 2:northing 3:height_above_datum' (need to set --csv-proj4; the height above datum is in meters). Can also use radius_km for column_type, when it is again measured from planet center.
--csv-proj4 <i>string</i>	The PROJ.4 string to use to interpret the entries in input CSV files, if those entries contain easting, northing, and height above datum.
--rounding-error <i>float</i> (=1/2 ¹⁰ =0.0009765625)	How much to round the output DEM and errors, in meters (more rounding means less precision but potentially smaller size on disk). The inverse of a power of 2 is suggested.
--dem-hole-fill-len <i>int</i> (=0)	Maximum dimensions of a hole in the output DEM to fill in, in pixels.
--orthoimage-hole-fill-len <i>int</i> (=0)	Maximum dimensions of a hole in the output orthoimage to fill in, in pixels.
--remove-outliers-params <i>pct (float)</i> <i>factor (float)</i> [default: 75.0 3.0]	Outlier removal based on percentage. Points with triangulation error larger than pct-th percentile times factor will be removed as outliers.
--max-valid-triangulation-error <i>float</i> (=0)	Outlier removal based on threshold. Points with triangulation error larger than this (in meters) will be removed from the cloud.
--median-filter-params <i>window_size (int)</i> <i>threshold (double)</i>	If the point cloud height at the current point differs by more than the given threshold from the median of heights in the window of given size centered at the point, remove it as an outlier. Use for example 11 and 40.0.
--erode-length <i>length (int)</i>	Erode input point clouds by this many pixels at boundary (after outliers are removed, but before filling in holes).
--use-surface-sampling [default: false]	Use the older algorithm, interpret the point cloud as a surface made up of triangles and sample it (prone to aliasing).
--fsaa	Oversampling amount to perform antialiasing. Obsolete, can be used only in conjunction with --use-surface-sampling.
--threads <i>int</i> (=0)	Select the number of processors (threads) to use.
--no-bigtiff	Tell GDAL to not create bigtiffs.
--tif-compress None LZW Deflate Packbits	TIFF compression method.

A.6 point2mesh

The `point2mesh` tool produces a mesh surface that can be visualized in `osgviewer`, which is a standard 3D viewing application that is part of the open source OpenSceneGraph package. This viewer is bundled with Stereo Pipeline.¹

Unlike DEMs, the 3D mesh is not meant to be used as a finished scientific product. Rather, it can be used for fast visualization to create a 3D view of the generated terrain.

The `point2mesh` program requires a point cloud file or a DEM, and an optional texture file. For example, it can be used with `output-prefix-PC.tif` and `output-prefix-L.tif`, as output by `stereo`, or otherwise with `output-prefix-DEM.tif` and `output-prefix-DRG.tif`, with the latter two output by `point2dem`.

When a texture file is not provided, a 1D texture is applied in the local Z direction that produces a rough rendition of a contour map. In either case, `point2mesh` will produce a `output-prefix.osgb` file that contains the 3D model in OpenSceneGraph format.

Two options for `osgviewer` bear pointing out: the `-l` flag indicates that synthetic lighting should be activated for the model, which can make it easier to see fine detail in the model by providing some real-time, interactive hillshading. The `-s` flag sets the sub-sampling rate, and dictates the degree to which the 3D model should be simplified. For 3D reconstructions, this can be essential for producing a model that can fit in memory. The default value is 10, meaning every 10th point is used in the X and Y directions. In other words that mean only $1/10^2$ of the points are being used to create the model. Adjust this sampling rate according to how much detail is desired, but remember that large models will impact the frame rate of the 3D viewer and affect performance.

Examples:

```
point2mesh -s 2 -l output-prefix-PC.tif output-prefix-L.tif
point2mesh -s 2 -l output-prefix-DEM.tif output-prefix-DRG.tif
```

To view the resulting `output-prefix.osgb` file use `osgviewer`.

Fullscreen:

```
> osgviewer output-prefix.osgb
```

In a window:

```
> osgviewer output-prefix.osgb --window 50 50 1000 1000
```

Be sure to turn on lightning as soon as the model is loaded, by pressing on “L”. In addition, the keys T, W, and F can be used to toggle on and off texture, wireframe, and full-screen modes. The left, middle, and right mouse buttons control rotation, panning, and zooming of the model.

Table A.7: Command-line options for point2mesh

Options	Description
<code>--help -h</code>	Display the help message.
<code>--simplify-mesh float</code>	Run OSG Simplifier on mesh, 1.0 = 100%.
<code>--smooth-mesh</code>	Run OSG Smoother on mesh
<code>--use-delaunay</code>	Uses the delaunay triangulator to create a surface from the point cloud. This is not recommended for point clouds with noise issues.
<code>--step -s integer(=10)</code>	Sampling step size for the mesher.

¹The full OpenSceneGraph package can be installed separately from <http://www.openscenegraph.org/>.

--input-file <i>pointcloud-file</i>	Explicitly specify the input file.
--output-prefix -o <i>output-prefix</i>	Specify the output prefix.
--texture-file <i>texture-file</i>	Explicitly specify the texture file.
--output-filetype -t <i>type(=ive)</i>	Specify the output file type.
--enable-lighting -l	Enables shades and lighting on the mesh.
--center	Center the model around the origin. Use this option if you are experiencing numerical precision issues.

A.7 dem_mosaic

The program `dem_mosaic` takes as input a list of DEM files, optionally erodes pixels at the DEM boundaries, and creates a mosaic. By default, it blends the DEMs where they overlap.

Usage:

```
dem_mosaic [options] <dem files or -l dem_files_list.txt> -o output_file_prefix
```

The input DEMs can either be set on the command line, or if too many, they can be listed in a text file (one per line) and that file can be passed to the tool.

The output mosaic is written as non-overlapping tiles with desired tile size, with the size set either in pixels or in georeferenced (projected) units. The default tile size is large enough that normally the entire mosaic is saved as one tile.

Individual tiles can be saved via the `--tile-index` option (the tool displays the total number of tiles when it is being run). As such, separate processes can be invoked for individual tiles for increased robustness and perhaps speed.

The output mosaic tiles will be named `<output prefix>-tile-<tile index>.tif`, where `<output prefix>` is an arbitrary string. For example, if it is set to `results/output`, all the tiles will be in the `results` directory.

By the default, the output mosaicked DEM will use the same grid size and projection as the first input DEM. These can be changed via the `--tr` and `--t_srs` options.

The default behavior is to blend the DEMs everywhere. If the option `--priority-blending-length integer` is invoked, the blending behavior will be different. At any location, the pixel value of the DEM earliest in the list present at this location will be kept, unless closer to the boundary of that DEM than this blending length (measured in input DEM pixels), only in the latter case blending will happen. This mode is useful when blending several high-resolution “foreground” DEMs covering small regions with larger “background” DEMs covering a larger extent. Then, the pixels from the high-resolution DEMs are more desirable, yet at their boundary these DEMs should blend into the background.

To obtain smoother blending when the input DEMs are quite different at the boundary, one can increase `--weights-blur-sigma` and `--weights-exponent`. The latter will result in weights growing slower earlier and faster later. Some experimentation may be necessary, helped for example by examining the weights used in blending; they can be written out with `--save-dem-weight integer`.

Instead of blending, `dem_mosaic` can compute the image of first, last, minimum, maximum, mean, standard deviation, median, and count of all encountered valid DEM heights at output grid points. For the “first” and “last” operations, the order in which DEMs were passed in is used. With any of these options, the tile names will be adjusted accordingly. It is important to note that with these options blending will not happen, since it is explicitly requested that particular values of the input DEMs be used.

If the number of input DEMs is very large, the tool can fail as the operating system may refuse to load all DEMs. In that case, it is suggested to use the parameter `--tile-size` to break up the output DEM into several large tiles, and to invoke the tool for each of the output tiles with the option `--tile-index`. Later, `dem_mosaic` can be invoked again to merge these tiles into a single DEM.

If the DEMs have reasonably regular boundaries and no holes, smoother blending may be obtained by using `--use-centerline-weights`.

Example 1 (erode 3 pixels from input DEMs and blend them):

```
dem_mosaic --erode-length 3 dem1.tif dem2.tif -o blended
```

Example 2 (read the DEMs from a list, and apply priority blending):

```
echo dem1.tif dem2.tif > imagelist.txt
dem_mosaic -l imagelist.txt --priority-blending-length 14 -o priority_blended
```

Example 3 (Find the mean DEM, no blending is used):

```
dem_mosaic -l imagelist.txt --mean -o mosaic
```

Table A.8: Command-line options for dem_mosaic

Options	Description
--help -h	Display the help message.
-l --dem-list-file <i>string</i>	Text file listing the DEM files to mosaic, one per line.
-o --output-prefix <i>string</i>	Specify the output prefix.
--tile-size <i>integer</i> (=1000000)	The maximum size of output DEM tile files to write, in pixels.
--tile-index <i>integer</i>	The index of the tile to save (starting from zero). When this program is invoked, it will print out how many tiles are there. Default: save all tiles.
--erode-length <i>integer</i> (=0)	Maximum dimensions of a hole in the output DEM to fill in, in pixels.
--priority-blending-length <i>integer</i> (=0)	If positive, keep unmodified values from the earliest available DEM at the current location except a band this wide measured in pixels around its boundary where blending will happen.
--hole-fill-length <i>integer</i> (=0)	Erode input DEMs by this many pixels at boundary before mosaicking them.
--tr <i>double</i>	Output DEM resolution in target georeferenced units per pixel. Default: use the same resolution as the first DEM to be mosaicked.
--t_srs <i>string</i>	Specify the output projection (PROJ.4 string). Default: use the one from the first DEM to be mosaicked.
--t_projwin <i>xmin ymin xmax ymax</i>	Limit the mosaic to this region, with the corners given in georeferenced coordinates (<i>xmin ymin xmax ymax</i>). Max is exclusive.
--first	Keep the first encountered DEM value (in the input order).
--last	Keep the last encountered DEM value (in the input order).
--min	Keep the smallest encountered DEM value.
--max	Keep the largest encountered DEM value.
--mean	Find the mean DEM value.
--stddev	Find the standard deviation of DEM values.
--median	Find the median DEM value (this can be memory-intensive, fewer threads are suggested).
--count	Each pixel is set to the number of valid DEM heights at that pixel.
--georef-tile-size <i>double</i>	Set the tile size in georeferenced (projected) units (e.g., degrees or meters).
--output-nodata-value <i>double</i>	No-data value to use on output. Default: use the one from the first DEM to be mosaicked.

--weights-blur-sigma <i>integer</i> (=5)	The standard deviation of the Gaussian used to blur the weights. Higher value results in smoother weights and blending. Set to 0 to not use blurring.
--weights-exponent <i>integer</i> (=1)	The weights used to blend the DEMs should increase away from the boundary as a power with this exponent. Higher values will result in smoother but faster-growing weights.
--use-centerline-weights	Compute weights based on a DEM centerline algorithm. Produces smoother weights if the input DEMs don't have holes or complicated boundary.
--extra-crop-length <i>integer</i> (=200)	Crop the DEMs this far from the current tile (measured in pixels) before blending them (a small value may result in artifacts).
--save-dem-weight <i>integer index</i>	Save the weight image that tracks how much the input DEM with given index contributed to the output mosaic at each pixel (smallest index is 0).
--save-index-map	For each output pixel, save the index of the input DEM it came from (applicable only for --first, --last, --min, and --max). A text file with the index assigned to each input DEM is saved as well.
--threads <i>integer</i> (=4)	Set the number of threads to use.

A.8 dem_geoid

This tool takes as input a DEM whose height values are relative to the datum ellipsoid, and adjusts those values to be relative to the equipotential surface of the planet (geoid on Earth, and areoid on Mars). The program can also apply the reverse of this adjustment. The adjustment simply subtracts from the DEM height the geoid height (correcting, if need be, for differences in dimensions between the DEM and geoid datum ellipsoids).

Three geoids and one areoid are supported. The Earth geoids are: EGM96 and EGM2008, relative to the WGS84 datum ellipsoid (<http://earth-info.nga.mil/GandG/wgs84/gravitymod/egm96/egm96.html>, http://earth-info.nga.mil/GandG/wgs84/gravitymod/egm2008/egm08_wgs84.html) and NAVD88, relative to the NAD83 datum ellipsoid (<http://www.ngs.noaa.gov/GEOID/GEOID09/>).

The Mars areoid is MOLA MEGDR (<http://geo.pds.nasa.gov/missions/mgs/megdr.html>). When importing it into ASP, we adjusted the areoid height values to be relative to the IAU reference spheroid for Mars of radius 3,396,190 m. The areoid at that source was relative to the Mars radius of 3,396,000 m. Yet `dem_geoid` can adjust correctly Mars DEMs created in respect to either spheroid.

Table A.9: Command-line options for `dem_geoid`

Options	Description
<code>--help -h</code>	Display the help message.
<code>--nodata-value float (= -32768)</code>	The value of no-data pixels, unless specified in the DEM.
<code>--geoid string</code>	Specify the geoid to use for Earth WGS84 DEMs. Options: EGM96, EGM2008. Default: EGM96.
<code>--output-prefix -o filename</code>	Specify the output file prefix.
<code>--double</code>	Output using double precision (64 bit) instead of float (32 bit).
<code>--reverse-adjustment</code>	Go from DEM relative to the geoid/areoid to DEM relative to the datum ellipsoid.

A.9 dg_mosaic

This tool can be used when processing Digital Globe Imagery (chapter 4). A Digital Globe satellite may take a picture, and then split it into several images and corresponding camera XML files. `dg_mosaic` will mosaic these images into a single file, and create the appropriate combined camera XML file.

Digital Globe camera files contain, in addition to the original camera models, their RPC approximations (section 11.11). `dg_mosaic` outputs both types of combined models. The combined RPC model can be used to map-project the mosaicked images with the goal of computing stereo from them (section 5.1.6).

The tool needs to be applied twice, for both the left and right image sets.

`dg_mosaic` can also reduce the image resolution while creating the mosaics (with the camera files modified accordingly).

Some older (2009 or earlier) Digital Globe images may exhibit seams upon mosaicking due to inconsistent image and camera information. The `--fix-seams` switch can be used to rectify this problem. Its effect should be minimal if such inconsistencies are not present.

Table A.10: Command-line options for `dg_mosaic`

Options	Description
---------	-------------

--help -h	Display the help message.
--target-resolution	Choose the output resolution in meters per pixel on the ground (note that a coarse resolution may result in aliasing).
--reduce-percent <i>integer</i> (=100)	Render a reduced resolution image and XML based on this percentage.
--skip-rpc-gen [<i>default: false</i>]	Skip RPC model generation.
--rpc-penalty-weight <i>float</i> (=0.1)	The weight to use to penalize higher order RPC coefficients when generating the combined RPC model. Higher penalty weight results in smaller such coefficients.
--output-prefix <i>string</i>	The prefix for the output .tif and .xml files.
--band <i>integer</i>	Which band to use (for multi-spectral images).
--input-nodata-value <i>float</i>	Nodata value to use on input; input pixel values less than or equal to this are considered invalid.
--output-nodata-value <i>float</i>	Nodata value to use on output.
--fix-seams	Fix seams in the output mosaic due to inconsistencies between image and camera data using interest point matching.
--preview	Render a small 8 bit png of the input for preview.
--dry-run/-n	Make calculations, but just print out the commands.

A.10 mapproject

The tool `mapproject` is used to orthorectify (map-project) a camera image onto a DEM or datum. (ASP is able to use map-projected images to run stereo, section 5.1.6.)

The `mapproject` program can be run using multiple processes and can be distributed over multiple machines. This is particularly useful for ISIS cameras, as in that case any single process must use only one thread due to the limitations of ISIS. The tool splits the image up into tiles, farms the tiles out to sub-processes, and then merges the tiles into the requested output image. If your image is small, smaller tiles can be used as well to start more simultaneous processes (parameter `--tile-size`).

Examples:

Map-project a .cub file (it has both image and camera information):

```
mapproject -t isis DEM.tif image.cub output.tif --ppd 256
```

Map-project an image file with associated .xml camera file:

```
mapproject -t rpc DEM.tif image.tif image.xml output.tif --mpp 20
```

Mapproject onto a datum rather than a DEM:

```
mapproject WGS84 image.tif image.xml output.tif --mpp 10
```

The first argument can either be a path to a DEM file or the name of a standard datum. Valid datum names include WGS84, NAD83, NAD27, D_MOON, D_MARS, and MOLA.

It is very important to pick a good value for the grid size parameter, given by `--mpp`, `--ppd`, or `--tr`. Ideally it should be very close to the known image resolution as measured on the ground (in degree or meter units, depending on the projection).

If the imagery is from Digital Globe, both the exact DG model from the XML file can be used for map-projection (`-t dg`) and its RPC approximation (`-t rpc`). The former is more accurate but much smaller.

Table A.11: Command-line options for `mapproject`

Options	Description
<code>--help -h</code>	Display the help message.
<code>--nodata-value float (= -32768)</code>	No-data value to use unless specified in the input image.
<code>--t_srs</code>	Specify the output projection (PROJ.4 string). If not provided, use the one from the DEM.
<code>--mpp float</code>	Set the output file resolution in meters per pixel.
<code>--ppd float</code>	Set the output file resolution in pixels per degree.
<code>--tr float</code>	Set the output file resolution in target georeferenced units per pixel.
<code>--datum-offset float</code>	When projecting to a datum instead of a DEM, add this elevation offset to the datum.
<code>--session-type -t pinhole isis rpc</code>	Select the stereo session type to use for processing. Choose 'rpc' if it is desired to later do stereo with the 'dg' session.
<code>--t_projwin xmin ymin xmax ymax</code>	Limit the map-projected image to this region, with the corners given in georeferenced coordinates (xmin ymin xmax ymax). Max is exclusive.

--t_pixelwin <i>xmin ymin xmax ymax</i>	Limit the map-projected image to this region, with the corners given in pixels (<i>xmin ymin xmax ymax</i>). Max is exclusive.
--bundle-adjust-prefix <i>string</i>	Use the camera adjustment obtained by previously running bundle_adjust with this output prefix.
--num-processes	Number of parallel processes to use (default program chooses).
--nodes-list	List of available computing nodes.
--tile-size	Size of square tiles to break processing up into.
--suppress-output	Suppress output from sub-processes.
--threads <i>int (=0)</i>	Select the number of processors (threads) to use.
--no-bigtiff	Tell GDAL to not create bigtiffs.
--tif-compress None LZW Deflate Packbits	TIFF compression method.

A.11 disparitydebug

The **disparitydebug** program produces output images for debugging disparity images created from **stereo**. The **stereo** tool produces several different versions of the disparity map; the most important ending with extensions ***-D.tif** and ***-F.tif**. (see Appendix C for more information.) These raw disparity map files can be useful for debugging because they contain raw disparity values as measured by the correlator; however they cannot be directly visualized or opened in a conventional image browser. The **disparitydebug** tool converts a single disparity map file into two normalized TIFF image files (***-H.tif** and ***-V.tif**, containing the horizontal and vertical, or line and sample, components of disparity, respectively) that can be viewed using any image display program.

The **disparitydebug** program will also print out the range of disparity values in a disparity map, that can serve as useful summary statistics when tuning the search range settings in the **stereo.default** file.

If the input images are map-projected (georeferenced), the outputs of **disparitydebug** will also be georeferenced.

Table A.12: Command-line options for **disparitydebug**

Options	Description
--help -h	Display the help message
--input-file <i>filename</i>	Explicitly specify the input file
--output-prefix -o <i>filename</i>	Specify the output file prefix
--output-filetype -t <i>type</i> (= tif)	Specify the output file type
--float-pixels	Save the resulting debug images as 32 bit floating point files (if supported by the selected file type)

A.12 orbitviz

Produces a Google Earth Keyhole Markup Language (KML) file useful for visualizing camera position. The input for this tool is one or more ***.cub** files.

Table A.13: Command-line options for **orbitviz**

Options	Description
--help -h	Display the help message
--output -o <i>filename</i> (= orbit.kml)	Specifies the output file name
--scale -s <i>float</i> (=1)	Scale the size of the coordinate axes by this amount. Ex: To scale axis sizes up to Earth size, use 3.66
--use_path_to_dae_model -u <i>fullpath</i>	Use this dae model to represent camera location. <i>Google Sketch up</i> can create these.
--load-camera-solve	Use a specialized display for showing the results of the camera_solve tool. When using this option, only pass in the path to the camera_solve output folder as a positional argument. Green lines drawn between the camera positions indicate a successful interest point match between those two images.
--hide-labels	Hide image names unless the camera is highlighted.

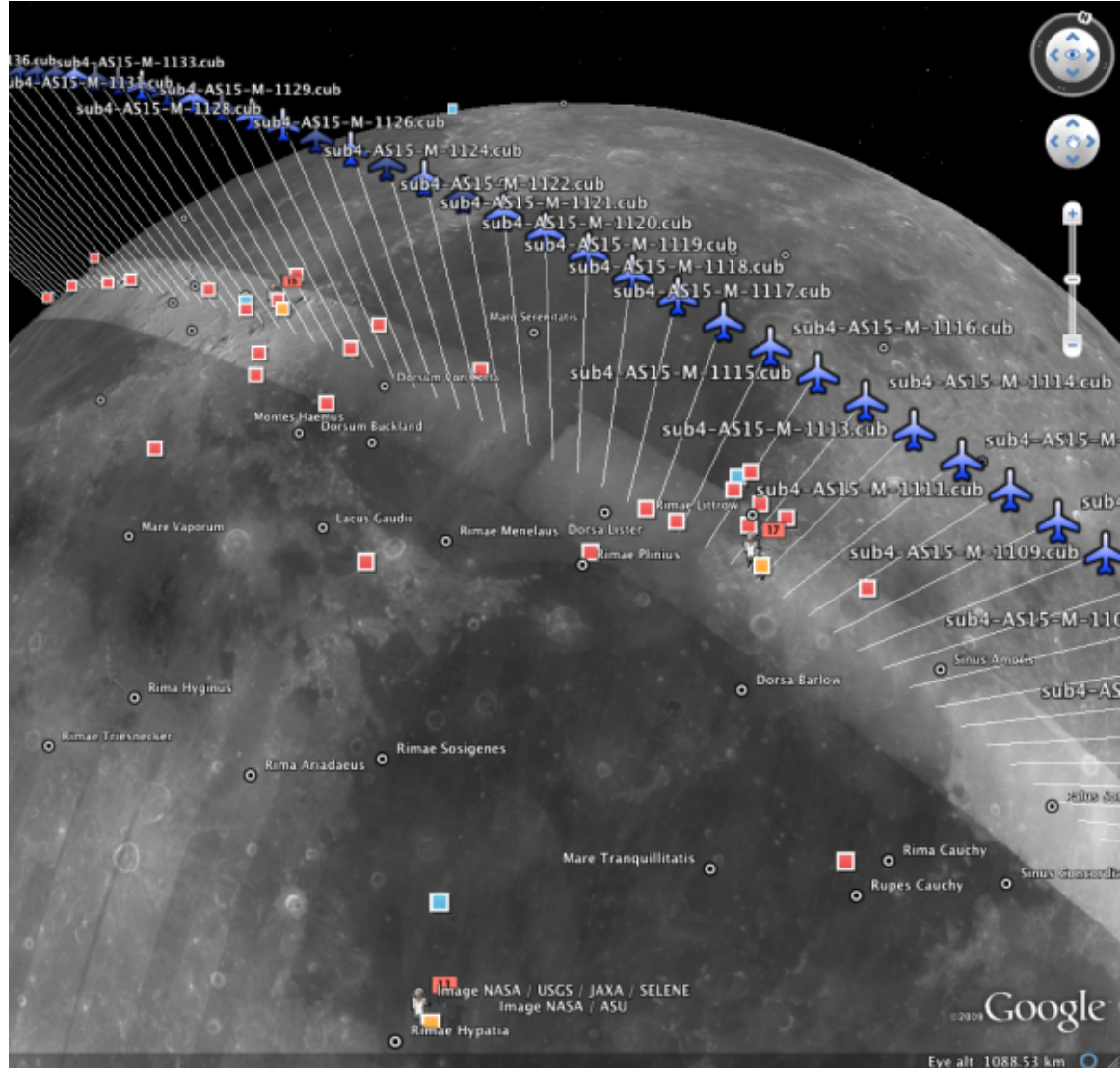


Figure A.2: Example of a KML visualization produced with `orbitviz` depicting camera locations for the Apollo 15 Metric Camera during orbit 33 of the Apollo command module.

A.13 cam2map4stereo.py

This program takes similar arguments as the ISIS3 `cam2map` program, but takes two input images. With no arguments, the program determines the minimum overlap of the two images, and the worst common resolution, and then map-projects the two images to this identical area and resolution.

The detailed reasons for doing this, and a manual step-by-step walkthrough of what `cam2map4stereo.py` does is provided in the discussion on aligning images on page 16.

The `cam2map4stereo.py` is also useful for selecting a subsection and/or reduced resolution portion of the full image. You can inspect a raw camera geometry image in `qview` after you have run `spiceinit` on it, select the latitude and longitude ranges, and then use `cam2map4stereo.py`'s `--lat`, `--lon`, and optionally `--resolution` options to pick out just the part you want.

Use the `--dry-run` option the first few times to get an idea of what `cam2map4stereo.py` does for you.

Table A.14: Command-line options for `cam2map4stereo.py`

Options	Description
<code>--help -h</code>	Display the help message.
<code>--manual</code>	Read the manual.
<code>--map=MAP -m MAP</code>	The mapfile to use for <code>cam2map</code> .
<code>--pixres=PIXRES -p PIXRES</code>	The pixel resolution mode to use for <code>cam2map</code> .
<code>--resolution=RESOLUTION -r RESOLUTION</code>	Resolution of the final map for <code>cam2map</code> .
<code>--interp=INTERP -i INTERP</code>	Pixel interpolation scheme for <code>cam2map</code> .
<code>--lat=LAT -a LAT</code>	Latitude range for <code>cam2map</code> , where <code>LAT</code> is of the form <code>min:max</code> . So to specify a latitude range between -5 and 10 degrees, it would look like <code>--lat=-5:10</code> .
<code>--lon=LON -o LON</code>	Longitude range for <code>cam2map</code> , where <code>LON</code> is of the form <code>min:max</code> . So to specify a longitude range between 45 and 47 degrees, it would look like <code>--lon=40:47</code> .
<code>--dry-run -n</code>	Make calculations, and print the <code>cam2map</code> command that would be executed, but don't actually run it.
<code>--prefix</code>	Make all output files use this prefix. Default: no prefix.
<code>--suffix -s</code>	Suffix that gets inserted in the output file names, defaults to 'map'.

A.14 pansharp

This tool reads in a high resolution grayscale file and a low resolution RGB file and produces a high resolution RGB file. The output image will be at the resolution of the grayscale image and will cover the region where the two images overlap. Both images must have georeferencing information. This can either be projection information in the image metadata or it can be a separate Worldview format XML camera file containing four ground control points (if using the tool with Digital Globe images).

Usage:

```
pansharp [options] <grayscale image file> <color image file> <output image file>
```

Table A.15: Command-line options for pansharp

Options	Description
--help	Display the help message.
--min-value	Manually specify the bottom of the input data range.
--max-value	Manually specify the top of the input data range.
--gray-xml	Look for georeference data here if not present in the grayscale image.
--color-xml	Look for georeference data here if not present in the RGB image.
--nodata-value	The nodata value to use for the output RGB file.

A.15 datum_convert

This tool is used to convert a DEM from one datum to another. For example, a UTM zone 10 DEM with an NAD27 datum can be converted to a UTM zone 10 DEM with a WGS84 datum. This tool does not convert between projections, another program such as `gdalwarp` or `dem_mosaic` should be used for that. `datum_convert` performs both horizontal and vertical conversion.

Intuitively, the input and output DEMs should correspond to the same point cloud in 3D space up to the interpolation errors required to perform the conversion.

Usage:

```
datum_convert [options] <input dem> <output dem>
```

Table A.16: Command-line options for datum_convert

Options	Description
--help	Display the help message.
--output-datum <i>string</i>	The datum to convert to. Supported options: WGS_1984, NAD83, WGS72, and NAD27.
--t_srs <i>string</i>	Specify the output datum via the PROJ.4 string.
--nodata-value	The value of no-data pixels, unless specified in the DEM.

A.16 point2las

This tool can be used to convert point clouds generated by ASP to the public LAS format for interchange of 3-dimensional point cloud data.

If the input cloud has a datum, or the `--datum` option is specified, then the output LAS file will be created in respect to this datum. Otherwise raw x, y, z values will be saved.

Table A.17: Command-line options for point2las

Options	Description
<code>--help -h</code>	Display the help message.
<code>--datum</code>	Create a geo-referenced LAS file in respect to this datum. Options: WGS_1984, D_MOON (1,737,400 meters), D_MARS (3,396,190 meters), MOLA (3,396,000 meters), NAD83, WGS72, and NAD27. Also accepted: Earth (=WGS_1984), Mars (=D_MARS), Moon (=D_MOON).
<code>--reference-spheroid string</code>	This is identical to the datum option.
<code>--t_srs string</code>	Specify the output projection (PROJ.4 string).
<code>--compressed</code>	Compress using laszip.
<code>--output-prefix -o filename</code>	Specify the output file prefix.
<code>--threads integer(=0)</code>	Set the number threads to use. 0 means use the default defined in the program or in the .vwrc file.
<code>--tif-compress None LZW Deflate Packbits</code>	TIFF compression method.

A.17 pc_align

This tool can be used to align two point clouds using Point-to-Plane or Point-to-Point Iterative Closest Point (ICP). With the latter method it can also handle a scale as part of the alignment transform, not just a rigid transformation. It uses the `libpointmatcher` library [82] (<https://github.com/ethz-asl/libpointmatcher>).

Usage:

```
pc_align --max-displacement <float> [other options] <reference cloud> <source cloud> \
-o <output prefix>}
```

An example of using this tool is in section 5.2.5.

Several important things need to be kept in mind if `pc_align` is to be used successfully and give accurate results, as described below.

A.17.1 The input point clouds

Due to the nature of ICP, the first input point cloud, that is, the reference (fixed) cloud, should be denser than the second, source (movable) point cloud, to get the most accurate results. This is not a serious restriction, as one can perform the alignment this way and then simply invert the obtained transform if desired (`pc_align` outputs both the direct and inverse transform, and can output the reference point cloud transformed to match the source and vice-versa).

In many typical applications, the source and reference point clouds are already roughly aligned, but the source point cloud may cover a larger area than the reference. The user should provide to `pc_align` the expected maximum distance (displacement) source points may move by as result of alignment, using the option `--max-displacement`. This number will help remove source points too far from the reference point cloud which may not match successfully and may degrade the accuracy. If in doubt, this value can be set to something large but still reasonable, as the tool is able to throw away a certain number of unmatched outliers. At the end of alignment, `pc_align` will display the *observed* maximum displacement, a multiple of which can be used to seed the tool in a subsequent run.

The user can choose how many points to pick from the reference and source point clouds to perform the alignment. The amount of memory and processing time used by `pc_align` is directly proportional to these numbers, ideally the more points the better. Pre-cropping to judiciously chosen regions may improve the accuracy and/or run-time.

A.17.2 Alignment method

Normally Point-to-Plane ICP is more accurate than Point-to-Point, but the latter can be good enough if the input point clouds have small alignment errors and it is faster and uses less memory as well. The tool also accepts an option named `--highest-accuracy` which will compute the normals for Point-to-Plane ICP at all points rather than about a tenth of them. This option is not necessary most of the time, but may result in better alignment at the expense of using more memory and processing time.

The default alignment transform is rigid, that is, a combination of rotation and translation. With Point-to-Point ICP, it is also possible to solve for a scale change (to obtain a so-called `similarity transform`). It is suggested this approach be used only when a scale change is expected. It can be turned on by using `--alignment-method similarity-point-to-point`.

A.17.3 File formats

The input point clouds can be in one of several formats: ASP's point cloud format (the output of `stereo`), DEMs as GeoTIFF or ISIS cub files, LAS files, or plain-text CSV files (with .csv or .txt extension).

By default, CSV files are expected to have on each line the latitude and longitude (in degrees), and the height above the datum (in meters), separated by commas or spaces. Alternatively, the user can specify the format of the CSV file via the `--csv-format` option. Entries in the CSV file can then be (in any order) (a) longitude, latitude (in degrees), height above datum (in meters), (b) longitude, latitude, distance from planet center (in meters or km), (c) easting, northing and height above datum (in meters), in this case a PROJ.4 string must be set via `--csv-proj4`, (d) Cartesian coordinates (x, y, z) measured from planet center (in meters). The precise syntax is described in the table below. The tool can also auto-detect the LOLA RDR PointPerRow format.

Any line in a CSV file starting with the pound character (#) is ignored.

If none of the input files have a geoheader with datum information, and the input files are not in Cartesian coordinates, the datum needs to be specified via the `--datum` option, or by setting `--semi-major-axis` and `--semi-minor-axis`.

A.17.4 The alignment transform

The transform obtained by `pc_align` is output to a text file as a 4×4 matrix with the upper-left 3×3 submatrix being the rotation (and potentially also a scale, per section A.17.2) and the top three elements of the right-most column being the translation. This transform, if applied to the source point cloud, will

bring it in alignment with the reference point cloud. The transform assumes the 3D Cartesian coordinate system with the origin at the planet center. This matrix can be supplied back to the tool as an initial guess (section A.17.5). The inverse transform is saved to a file as well.

The `pc_align` program outputs the translation component of this transform, defined as the vector from the centroid of the original source points to the centroid of the transformed source points. This translation component is displayed in three ways (a) Cartesian coordinates with the origin at the planet center, (b) Local North-East-Down coordinates at the centroid of the original source points, and (c) Latitude-Longitude-Height differences between the two centroids. If the effect of the transform is small (e.g., the points moved by at most several hundred meters) then the representation in the form (b) above is most amenable to interpretation as it is in respect to cardinal directions and height above ground if standing at a point on the planet surface.

The full transform itself, with its origin at the center of the planet, can result in large movements on the planet surface even for small angles of rotation. Because of this it may be difficult to interpret both its rotation and translation components.

A.17.5 Applying a previous transform

The transform output by `pc_align` can be supplied back to the tool as an initial guess via the `--initial-transform` option, with the same or different clouds. If it is desired to simply apply this transform to the clouds without further work, one can specify `--num-iterations 0`. This may be useful, for example, in first finding the alignment transform over a smaller, more reliable region (e.g., over rock, excluding moving ice), then extending it over the entire available dataset.

A.17.6 Error metrics and outliers

The tool outputs to CSV files the lists of errors together with their locations in the source point cloud, before and after the alignment of source points, where an error is defined as the distance from a source point used in alignment to the closest reference point. The format of output CSV files is the same as of input CSV files, or as given by `--csv-format`, although any columns of extraneous data in the input files are not saved on output.

The program prints to screen and saves to a log file the 16th, 50th, and 84th error percentiles as well as the means of the smallest 25%, 50%, 75%, and 100% of the errors.

When the reference point cloud is a DEM, a more accurate computation of the errors from source points to the reference cloud is used. A source point is projected onto the datum of the reference DEM, its longitude and latitude are found, then the DEM height at that position is interpolated. That way we determine a “closest” point on the reference DEM that interprets the DEM not just as a collection of points but rather as a polyhedral surface going through those points. These errors are what is printed in the statistics. To instead compute errors as done for other type of point clouds, use the option `--no-dem-distances`.

By default, when `pc_align` discards outliers during the computation of the alignment transform, it keeps the 75% of the points with the smallest errors. As such, a way of judging the effectiveness of the tool is to look at the mean of the smallest 75% of the errors before and after alignment.

A.17.7 Output point clouds and convergence history

The transformed input point clouds (the source transformed to match the reference, and the reference transformed to match the source) can also be saved to disk if desired. If an input point cloud is in CSV or ASP point cloud format, the output transformed cloud will be in the same format. If the input is a DEM,

the output will be an ASP point cloud, since a gridded point cloud may not stay so after a 3D transform. The `point2dem` program can be used to re-grid the obtained point cloud back to a DEM.

The convergence history for `pc_align` (the translation and rotation change at each iteration) is saved to disk and can be used to fine-tune the stopping criteria.

A.17.8 Manual alignment

If automatic alignment fails, for example, if the clouds are too different, or they differ by a scale factor, manual alignment can be used instead, either on its own, or as an initial guess for the automatic alignment transform. For that, the input point clouds should be first converted to DEMs using `point2dem`, unless in that format already. Then, `stereo_gui` can be invoked to create point correspondences (interest point matches) from the reference to the source DEM. Once these correspondences are saved to a match file, `pc_align` can be called with the reference and source DEMs and the `--match-file` option. This will compute and save to disk a rotation + translation + scale transform. A subsequent invocation of `pc_align`, either with the original clouds or the DEM created from them, can use this transform as an initial guess (section A.17.5).

A.17.9 Troubleshooting

Remember that filtering is applied only to the source point cloud. If you have an input cloud with a lot of noise, make sure it is being used as the source cloud.

If you are not getting good results with `pc_align`, something that you can try is to convert an input point cloud into a smoothed DEM. Use `point2dem` to do this and set `--search-radius-factor` if needed to fill in holes in the DEM. For some input data this can significantly improve alignment accuracy.

Table A.18: Command-line options for `pc_align`

Options	Description
<code>--help -h</code>	Display the help message.
<code>--threads integer(=0)</code>	Set the number threads to use. 0 means use the default as set by OpenMP. Only some parts of the algorithm are multi-threaded.
<code>--initial-transform string</code>	The file containing the transform to be used as an initial guess. It can come from a previous run of the tool.
<code>--num-iterations default: 1000</code>	Maximum number of iterations.
<code>--diff-rotation-error default: 10⁻⁸</code>	Change in rotation amount below which the algorithm will stop (if translation error is also below bound), in degrees.
<code>--diff-translation-error default: 10⁻³</code>	Change in translation amount below which the algorithm will stop (if rotation error is also below bound), in meters.
<code>--max-displacement float</code>	Maximum expected displacement of source points as result of alignment, in meters (after the initial guess transform is applied to the source points). Used for removing gross outliers in the source (movable) point cloud.

<code>--outlier-ratio default: 0.75</code>	Fraction of source (movable) points considered inliers (after gross outliers further than max-displacement from reference points are removed).
<code>--max-num-reference-points default: 10⁸</code>	Maximum number of (randomly picked) reference points to use.
<code>--max-num-source-points default: 10⁵</code>	Maximum number of (randomly picked) source points to use (after discarding gross outliers).
<code>--alignment-method default: point-to-plane</code>	The type of iterative closest point method to use. [point-to-plane, point-to-point, similarity-point-to-point]
<code>--highest-accuracy</code>	Compute with highest accuracy for point-to-plane (can be much slower).
<code>--datum string</code>	Use this datum for CSV files. Options: WGS_1984, D_MOON (1,737,400 meters), D_MARS (3,396,190 meters), MOLA (3,396,000 meters), NAD83, WGS72, and NAD27. Also accepted: Earth (=WGS_1984), Mars (=D_MARS), and Moon (=D_MOON).
<code>--semi-major-axis float</code>	Explicitly set the datum semi-major axis in meters.
<code>--semi-minor-axis float</code>	Explicitly set the datum semi-minor axis in meters.
<code>--csv-format string</code>	Specify the format of input CSV files as a list of entries column_index:column_type (indices start from 1). Examples: '1:x 2:y 3:z' (a Cartesian coordinate system with origin at planet center is assumed, with the units being in meters), '5:lon 6:lat 7:radius_m' (longitude and latitude are in degrees, the radius is measured in meters from planet center), '3:lat 2:lon 1:height_above_datum', '1:easting 2:northing 3:height_above_datum' (need to set --csv-proj4; the height above datum is in meters). Can also use radius_km for column_type, when it is again measured from planet center.
<code>--csv-proj4 string</code>	The PROJ.4 string to use to interpret the entries in input CSV files, if those entries contain easting, northing, and height above datum.
<code>--output-prefix -o filename</code>	Specify the output file prefix.
<code>--compute-translation-only</code>	Compute the transform from source to reference point cloud as a translation only (no rotation).
<code>--save-transformed-source-points</code>	Apply the obtained transform to the source points so they match the reference points and save them.
<code>--save-inv-transformed-reference-points</code>	Apply the inverse of the obtained transform to the reference points so they match the source points and save them.
<code>--no-dem-distances</code>	For reference point clouds that are DEMs, don't take advantage of the fact that it is possible to interpolate into this DEM when finding the closest distance to it from a point in the source cloud (the text above has more detailed information).

--match-file	Compute a translation + rotation + scale transform from the source to the reference point cloud using manually selected point correspondences (obtained for example using stereo_gui).
--config-file <i>file.yaml</i>	This is an advanced option. Read the alignment parameters from a configuration file, in the format expected by libpointmatcher, over-riding the command-line options.

A.18 pc_merge

This is a simple tool for combining multiple ASP-generated point cloud files into a single concatenated file. The output file will be float32 unless the input images are float64 or the user has specified the float64 option.

`pc_merge` can merge clouds with 1, 3, 4, and 6 bands. In particular, it can merge *output-prefix-L.tif* images created by `stereo`. This is useful if it is desired to create an ortho-image from a merged cloud with `point2dem`. In that case, one can invoke `pc_merge` on individual “L” files to create a merged texture file to pass to `point2dem` together with the merged point cloud tile.

Usage:

```
pc_merge [options] [required output file option] <multiple point cloud files>
```

Table A.19: Command-line options for pc_merge

Options	Description
--help	Display the help message.
--write-double -d	Force output file to be float64 instead of float32.
--output-file -o	Specify the output file (required).

A.19 wv_correct

An image taken by one of Digital Globe’s World View satellite cameras is formed of several blocks as tall as the image, mosaicked from left to right, with each block coming from an individual CCD sensor [29]. Either due to imperfections in the camera or in the subsequent processing the image blocks are offset in respect to each other in both row and column directions by a subpixel amount. These so-called *CCD boundary artifacts* are not visible in the images but manifest themselves as discontinuities in the DEMs obtained with ASP.

The tool named `wv_correct` is able to significantly attenuate these artifacts (see Figure 4.2 in the Digital Globe tutorial for an example). This tool should be used on raw Digital Globe images before calling `dg_mosaic` and `mapproject`.

It is important to note that both the positions of the CCD offsets and the offset amounts were determined empirically without knowledge of Digital Globe’s mosaicking process; this is why we are not able to remove these artifacts completely.

Presently, `wv_correct` works for WV01 images for TDI of 8, 16, 32, 48, 56 and 64, and for WV02 images for TDI of 8, 16, 48, and 64 (both the forward and reverse scan directions for both cameras). In addition,

the WV02 TDI 32 forward scan direction is supported. These are by far the most often encountered TDI. We plan to extend the tool to support other TDI when we get more such data to be able to compute the corrections. For WV03 images, CCD artifacts appear to not be significant, hence no corrections are planned for the near future.

Usage:

```
wv_correct [options] <input image> <input camera model> <output image>
```

Table A.20: Command-line options for wv_correct

Options	Description
--help -h	Display the help message.
--threads <i>integer</i> (=0)	Set the number threads to use. 0 means use the default defined in the program or in the .vwrc file.

A.20 lronac2mosaic.py

This tool takes in two LRONAC files (M*LE.IMG and M*RE.IMG) and produces a single noproj mosaic composed of the two inputs. It performs the following operations in this process: `lronac2isis`, `lronaccal`, `lronacecho`, `spiceinit`, `noproj`, and `handmos`. The offsets used in `handmos` are calculated using an ASP internal tool called `lronacjitreg` and is similar in functionality to the ISIS command `hijitreg`. Offsets need to be calculated via feature measurements in image to correct for imperfections in camera pointing. The angle between LE and RE optics changes slightly with spacecraft temperature.

Optionally, `lronac2mosaic.py` can be given many IMG files all at once. The tool will then look at image names to determine which should be paired and mosaicked. The tool will also spawn multiple processes of ISIS commands were possible to finish the task faster. The max number of simultaneous processes is limited by the `--threads` option.

Usage:

```
lronac2mosaic.py [options] <IMG file 1> <IMG file 2>
```

Table A.21: Command-line options for lronac2mosaic.py

Options	Description
--manual	Display the help message.
--output-dir -o	Set the output folder (default is input folder).
--stop-at-no-proj	Stops processing after the noproj steps are complete.
--resume-at-no-proj	Restarts processing using the results from 'stop-at-no-proj'.
--threads -t	Specify the number of threads to use.
--keep -k	Keep all intermediate files.

A.21 image_calc

This tool can be used to perform simple, per-pixel arithmetic on one or more input images. An arithmetic operation specified on the command line is parsed and applied to each pixel, then the result is written to disk. The tool supports multiple input images but each must be the same size and data type. Input images are restricted to one channel.

The following symbols are allowed in the arithmetic string: +, -, *, /, (), min(), max(), pow(), abs(), and var_N where N is the index of one of the input images. An example arithmetic string is: "-abs(var_2) + min(58, var_1, var_3) / 2". The tool respects the normal PEMDAS order of operations *except* that it parses equal priority operations from right to left, *not* the expected left to right. Parentheses can be used to enforce any preferred order of evaluation.

Usage:

```
image_calc [options] -c <arithmetic formula> <inputs> -o <output>
```

Example:

```
image_calc -c "pow(var_0/3.0, 1.1)" input_image.tif -o output_image.tif -d float32
```

Table A.22: Command-line options for image_calc

Options	Description
--help	Display the help message.
--calc -c	The arithmetic string in quotes (required).
--output-data-type -d	The data type of the output file (default is float64).
--input-nodata-value	Set an override nodata value for the input images.
--output-nodata-value	Manually specify a nodata value for the output image (default is data type min).
--output-file -o	Specify the output file instead of using a default.

A.22 colormap

The colormap tool reads a DEM and writes a corresponding color-coded height image that can be used for visualization.

Usage:

```
colormap [options] <input DEM>
```

Table A.23: Command-line options for colormap

Option	Description
--help	Display a help message.
-s [--shaded-relief-file] arg	Specify a shaded relief image (grayscale) to apply to the colorized image.
-o [--output-file] arg	Specify the output file.
--colormap-style arg	Specify the colormap style. Options: binary-red-blue (default), jet, or the name of a file having the colormap, similar to the file used by gdaldem.
--nodata-value arg	Remap the DEM default value to the min altitude value.
--min arg	Minimum height of the color map.
--max arg	Maximum height of the color map.
--moon	Set the min and max height to good values for the Moon.

--mars	Set the min and max height to good values for Mars.
--legend	Generate an unlabeled legend, saved as "legend.png".

A.23 hillshade

The `hillshade` tool reads in a DEM and outputs an image of that DEM as though it were a three-dimensional surface, with every pixel shaded as though it were illuminated by a light from a specified location.

Table A.24: Command-line options for `hillshade`

Option	Description
<code>--help</code>	Display a help message
<code>--input-file arg</code>	Explicitly specify the input file
<code>-o [--output-file] arg</code>	Specify the output file
<code>-a [--azimuth] arg (=300)</code>	Sets the direction that the light source is coming from (in degrees). Zero degrees is to the right, with positive degree counter-clockwise.
<code>-e [--elevation] arg (=20)</code>	Set the elevation of the light source (in degrees)
<code>-s [--scale] arg (=0)</code>	Set the scale of a pixel (in the same units as the DTM height values)
<code>--nodata-value arg</code>	Remap the DEM default value to the min altitude value
<code>--blur arg</code>	Pre-blur the DEM with the specified sigma

A.24 image2qtree

`image2qtree` turns a georeferenced image (or images) into a quadtree with geographical metadata. For example, it can output a kml file for viewing in Google Earth.

Table A.25: Command-line options for `image2qtree`

Option	Description
General Options	
<code>--help</code>	Display a help message
<code>-o [--output-name] arg</code>	Specify the base output directory
<code>-q [--quiet]</code>	Quiet output
<code>-v [--verbose]</code>	Verbose output
<code>--cache arg (=1024)</code>	Cache size, in megabytes
Input Options	
<code>--force-wgs84</code>	Use WGS84 as the input images' geographic coordinate systems, even if they're not (old behavior)
<code>--pixel-scale arg (=1)</code>	Scale factor to apply to pixels
<code>--pixel-offset arg (=0)</code>	Offset to apply to pixels
<code>--normalize</code>	Normalize input images so that their full dynamic range falls in between [0,255]
Output Options	
<code>-m [--output-metadata] arg (=none)</code>	Specify the output metadata type. One of [kml, tms, uniview, gmap, celestia, none]

--file-type arg (=png)	Output file type
--channel-type arg (=uint8)	Output (and input) channel type. One of [uint8, uint16, int16, float]
--module-name arg (=marsds)	The module where the output will be placed. Ex: marsds for Uniview, or Sol/Mars for Celestia
--terrain	Outputs image files suitable for a Uniview terrain view. Implies output format as PNG, channel type uint16. Uniview only
--jpeg-quality arg (=0.75)	JPEG quality factor (0.0 to 1.0)
--png-compression arg (=3)	PNG compression level (0 to 9)
--palette-file arg	Apply a palette from the given file
--palette-scale arg	Apply a scale factor before applying the palette
--palette-offset arg	Apply an offset before applying the palette
--tile-size arg (=256)	Tile size, in pixels
--max-lod-pixels arg (=1024)	Max LoD in pixels, or -1 for none (kml only)
--draw-order-offset arg (=0)	Offset for the <drawOrder> tag for this overlay (kml only)
--composite-multiband	Composite images using multi-band blending
--aspect-ratio arg (=1)	Pixel aspect ratio (for polar overlays; should be a power of two)
Projection Options	
--north arg	The northernmost latitude in degrees
--south arg	The southernmost latitude in degrees
--east arg	The easternmost longitude in degrees
--west arg	The westernmost longitude in degrees
--force-wgs84	Assume the input images' geographic coordinate systems are WGS84, even if they're not (old behavior)
--sinusoidal	Assume a sinusoidal projection
--mercator	Assume a Mercator projection
--transverse-mercator	Assume a transverse Mercator projection
--orthographic	Assume an orthographic projection
--stereographic	Assume a stereographic projection
--lambert-azimuthal	Assume a Lambert azimuthal projection
--lambert-conformal-conic	Assume a Lambert Conformal Conic projection
--utm arg	Assume UTM projection with the given zone
--proj-lat arg	The center of projection latitude (if applicable)
--proj-lon arg	The center of projection longitude (if applicable)
--proj-scale arg	The projection scale (if applicable)
--std-parallel1 arg	Standard parallels for Lambert Conformal Conic projection
--std-parallel2 arg	Standard parallels for Lambert Conformal Conic projection

--nudge-x arg	Nudge the image, in projected coordinates
--nudge-y arg	Nudge the image, in projected coordinates

A.25 geodiff

The **geodiff** program takes as input two DEMs, and subtracts the second from the first. The grid used is the one from the first DEM, so the second one is interpolated into it. The tool can also take the absolute difference of the two DEMs.

It is important to note that the tool is very sensitive to the order of the two DEMs, due to the fact that the grid comes from the first one. Ideally the grid of the first DEM would be denser than the one of the second.

Usage:

```
> geodiff [options] <dem1> <dem2> [ -o output_file_prefix ]
```

Table A.26: Command-line options for geodiff

Option	Description
--help -h	Display the help message.
--output-prefix -o <i>filename</i>	Specify the output prefix.
--absolute	Output the absolute difference as opposed to just the difference.
--float	Output using float (32 bit) instead of using doubles (64 bit).
--nodata-value <i>float</i> (=-32768)	The no-data value to use, unless present in the DEM geoheaders.
--threads <i>integer</i> (=0)	Set the number of threads to use. 0 means use as many threads as there are cores.
--no-bigtiff	Tell GDAL to not create bigtiffs.
--tif-compress None LZW Deflate Packbits	TIFF compression method.

A.26 aster2asp

The **aster2asp** tool takes as input a directory containing ASTER images and associated metadata, and creates TIF and XML files that can then be passed to **stereo** to create a point cloud.

An example for how to use this tool is given in section 11.14.

The tool can only process Level 1A ASTER images. The input should be a directory containing visible and near-infrared (VNIR) nadir (Band3N) and backward (Band3B) images, together with plain text files containing values for the satellite positions, sight vectors, longitudes, latitudes, lattice points, and radiometric correction tables. These files are described in [1].

Usage:

```
aster2asp <input directory> -o <output prefix>
```

The tool will apply the existing radiometric corrections to the the images, and save two images with Float32 pixels with names like `out-Band3N.tif` and `out-Band3B.tif`. Based on the metadata mentioned earlier, it will create approximate RPC camera models in XML format (section 11.11) for the left and right cameras, following [28], with names of the form `out-Band3N.xml` and `out-Band3B.xml` (we do not perform yet any jitter corrections as described in that paper).

These can then be passed to `stereo` as:

```
stereo -t rpc out-Band3N.tif out-Band3B.tif out-Band3N.xml out-Band3B.xml \
out_stereo/run
```

It is important to note that the tool expects the minimum and maximum simulation box heights (in meters, above the datum) in which to compute the RPC approximation. The defaults are 0 and 8000, corresponding to sea level and the highest location on Earth. Narrowing down these numbers (if it is known what range of terrain heights is expected) may result in slightly more accurate models.

Table A.27: Command-line options for aster2asp

Option	Description
<code>-o --output-prefix arg</code>	Specify the output prefix.
<code>--min-height arg (=0)</code>	The minimum height (in meters) above the WGS84 datum of the simulation box in which to compute the RPC approximation.
<code>--max-height arg (=8000)</code>	The maximum height (in meters) above the WGS84 datum of the simulation box in which to compute the RPC approximation.
<code>--num-samples arg (=100)</code>	How many samples to use between the minimum and maximum heights.
<code>--penalty-weight arg (=0.1)</code>	Penalty weight to use to keep the higher-order RPC coefficients small. Higher penalty weight results in smaller such coefficients.
<code>--no-bigtiff</code>	Tell GDAL to not create bigtiffs.
<code>--tif-compress arg (=LZW)</code>	TIFF Compression method. [None, LZW, Deflate, Packbits]
<code>-v --version</code>	Display the version of software.
<code>-h --help</code>	Display this help message.

A.27 sfs

The `sfs` tool can improve a DEM using shape-from-shading. Examples for how to use it are in chapter 10.

Table A.28: Command-line options for sfs

Option	Description
<code>-h --help</code>	Display this help message.
<code>-i --input-dem string</code>	The input DEM to refine using SfS.
<code>-o --output-prefix string</code>	Prefix for output filenames.
<code>-n --max-iterations int (=100)</code>	Set the maximum number of iterations.
<code>--reflectance-type int (=1)</code>	Reflectance type (0 = Lambertian, 1 = Lunar Lambertian).

--smoothness-weight <i>double</i> (=0.04)	A larger value will result in a smoother solution.
--coarse-levels <i>int</i> (=0)	Solve the problem on a grid coarser than the original by a factor of 2 to this power, then refine the solution on finer grids.
--max-coarse-iterations <i>int</i> (=50)	How many iterations to do at levels of resolution coarser than the final result.
--float-albedo	Float the albedo for each pixel. Will give incorrect results if only one image is present.
--float-exposure	Float the exposure for each image. Will give incorrect results if only one image is present.
--float-cameras	Float the camera pose for each image except the first one.
--model-shadows	Model the fact that some points on the DEM are in the shadow (occluded from the sun).
--shadow-thresholds <i>string</i>	Optional shadow thresholds for the input images (a list of real values in quotes).
--use-approx-camera-models	Use approximate camera models for speed.
--bundle-adjust-prefix <i>string</i>	Use the camera adjustments obtained by previously running bundle_adjust with this output prefix.
--init-dem-height <i>double</i>	Use this value for initial DEM heights. An input DEM still needs to be provided for georeference information.
--float-dem-at-boundary	Allow the DEM values at the boundary of the region to also float (not advised).
--camera-position-step-size <i>int</i> (=1)	Larger step size will result in more aggressiveness in varying the camera position if it is being floated (which may result in a better solution or in divergence).
--max-height-change <i>int</i> (=0)	How much the DEM heights are allowed to differ from the initial guess, in meters. The default is 0, which means this constraint is not applied.
--height-change-weight <i>int</i> (=0)	How much weight to give to the height change penalty (this penalty will only kick in when the DEM height changes by more than max-height-change).
--threads <i>int</i> (=0)	Select the number of processors (threads) to use.
--no-bigtiff	Tell GDAL to not create bigtiffs.
--tif-compress None LZW Deflate Packbits	TIFF compression method.

A.28 undistort_image

The `undistort_image` program takes as input an image and a pinhole model .tsai file describing the image. The tool will generate a copy of the input image with the lens distortion specified in the pinhole model file removed.

Usage:

```
> undistort_image [options] <input image> <camera model>
```

Table A.29: Command-line options for undistort_image

Option	Description
<code>--help -h</code>	Display the help message.
<code>--output-file -o filename</code>	Specify the output file.

A.29 camera_calibrate

The `camera_calibrate` tool can generate camera models suitable for use by `camera_solve` and other ASP tools. This tool only solves for intrinsic camera parameters; to obtain the camera pose you should use the `camera_solve` tool. This tool is a wrapper around the OpenCV (<http://opencv.org/>) checkerboard calibration tool which takes care of converting the output into readily usable formats. When you run the tool, three camera model files will be created in the output folder: `solve_cam_params.txt`, `vw_cam_params.tsai`, and `ocv_cam_params.yml`. The first file can be used as a camera calibration file for the `camera_solve` tool. The second file is a pinhole camera format that is recognized by ASP but remember that the extrinsic parameters were not solved for so ASP is limited in what it can do with the camera file. The last file contains the camera information as formatted by the OpenCV calibration tool. If you use the first file as an input to `camera_solve` you must remember to replace the wildcard image path in the file with the one to the images you want to use solve for (as opposed to the checkerboard images).

In order to use this tool you must provide multiple images of the same checkerboard pattern acquired with the camera you wish to calibrate. When calling the tool you must specify the number of internal square corners contained in your checkerboard pattern (width and height can be swapped) so that OpenCV knows what to look for. You must also specify an image wildcard path such as "`checkers/image_*.jpg`". You may need to enclose this parameter in quotes so that your command line does not expand the wildcard before it is passed to the tool. If you do not provide the `-box-size` parameter the output calibration numbers will be unitless.

Usage:

```
> camera_calibrate [options] <output folder> <Board Height> <Board Width> <Image Wildcard> ...
```

Table A.30: Command-line options for camera_calibrate

Option	Description
<code>-h --help</code>	Display this help message.
<code>--overwrite</code>	Recompute any intermediate steps already completed on disk.
<code>--suppress-output</code>	Reduce the amount of program console output.
<code>--box-size-cm float</code>	The size of the checkerboard squares in centimeters.
<code>--duplicate-files</code>	Make a copy of the vw param file for each input camera.

A.30 camera_solve

The `camera_solve` tool generates pinhole sensor models (frame cameras), including camera poses, for input images lacking metadata. See chapter 9 for an overview and examples of using the tool.

The camera calibration passed with the `--calib-file` option should be a .tsai pinhole camera model file in one of the formats compatible with ASP. Our supported pinhole camera models are described in appendix D.

You can use a set of estimated camera positions to register camera models in world coordinates. This method is not as accurate as using ground control points but it may be easier to use. To do this, use the `--camera-positions` parameter to `bundle-adjust` via the `--bundle-adjust-params` option similar to the example line below. If you see the camera models shifting too far from their starting positions try using the `--camera-weight` option to restrain their movement.

```
--bundle-adjust-params '--camera-positions nav.csv \
--csv-format "1:file 12:lat 13:lon 14:height_above_datum" --camera-weight 1.0'
```

This tool will generate two .tsai camera model files in the output folder per input image. The first file, appended with .tsai, is in a local coordinate system and does not include optimizations for intrinsic parameters but it may be useful for debugging purposes. The second file, appended with .final.tsai, contains the final solver results. If ground control points or estimated camera positions were provided then the second file will be in a global coordinate system.

Usage:

```
> camera_solve [options] <output folder> <Input Image 1> <Input Image 2> ...
```

Table A.31: Command-line options for `camera_solve`

Option	Description
<code>-h --help</code>	Display this help message.
<code>--datum string</code>	The datum to use when calibrating. Default is WGS84.
<code>--calib-file string</code>	Path to an ASP compatible pinhole model file containing camera model information. The position and pose information will be ignored. If you want to use a unique file for each input image, pass a space separated list of files surrounded by quotes.
<code>--gcp-file string</code>	Path to a ground control point file. This allows the tool to generate cameras in a global coordinate system.
<code>--bundle-adjust-params string</code>	Additional parameters (in single quotes) to pass to the <code>bundle_adjust</code> tool.
<code>--theia-flagfile string</code>	Path to a custom Theia flagfile to use settings from. File paths specified in this file are ignored.
<code>--overwrite</code>	Recompute any intermediate steps already completed on disk.

--reuse-theia-matches	Pass Theia's IP find results into ASP instead of recomputing them to reduce total processing time.
--suppress-output	Reduce the amount of program console output.

This tool is a wrapper that relies on two other tools to operate. The first of these is THEIA, as mentioned earlier, for computing the relative poses of the cameras. ASP's `bundle_adjust` tool is used to register the cameras in world coordinates using the ground control points. If the tool does not provide good results you can customize the parameters being passed to the underlying tools in order to improve the results. For `bundle_adjust` options, see the description in this document. For more information about THEIA flagfile options see their website or edit a copy of the default flagfile generated in the output folder

A.31 icebridge_kmz_to_csv

A simple tool for use with data from the NASA IceBridge program. Google Earth compatible .kmz files are available at <http://asapdata.arc.nasa.gov/dms/missions.html> which display the aircraft position at the point when each DMS frame image was captured. This tool exports those positions into a csv file which can be passed into `bundle_adjust` using the following parameters:

```
--camera-positions ../camera_positions.csv --csv-format "1:file 2:lon 3:lat 4:height_above_datum"
```

This may be useful in conjunction with the `camera_solve` tool to allow conversion of camera positions from local to global coordinates.

Usage:

```
> icebridge_kmz_to_csv <input kmz file> <output csv file>
```

A.32 lvis2kml

A simple tool for use with LVIS (Land, Vegetation, and Ice Sensor) lidar data from the NASA IceBridge program. Generates a Google Earth compatible .kml files from either an LVIS data file (.TXT extension) or an LVIS boundary file (.xml extension). Using this tool makes it easy to visualize what region a given LVIS file covers and what the shape of its data looks like. If the output path is not passed to the tool it will generate an output path by appending ".kml" to the input path. This tool requires the simplekml Python package to run. One way to get this is to install the ASP Python tools, described at the end of section 4.5.

Usage:

```
> lvis2kml [options] <input path> [<output path>]
```

Table A.32: Command-line options for lvis2kml

Option	Description
-h --help	Display this help message.
--name <i>string</i>	Assign a name to the KML file.
--color <i>string</i>	Draw plots in one of (red green blue)
--skip <i>int</i> (=1)	When loading a data file, plot only every N-th point. Has no effect on boundary files.

A.33 GDAL Tools

ASP distributes in the `bin` directory the following GDAL tools: `gdalinfo`, `gdal_translate` and `gdalbuildvrt`. These executables are used by a few ASP Python tools, are compiled with JPEG2000 and BigTIFF support, and can handle NTF images in addition to most image formats. They can be used to see image statistics, crop and scale images, and build virtual mosaics respectively. Detailed documentation is available on the GDAL web site, at <http://www.gdal.org/>.

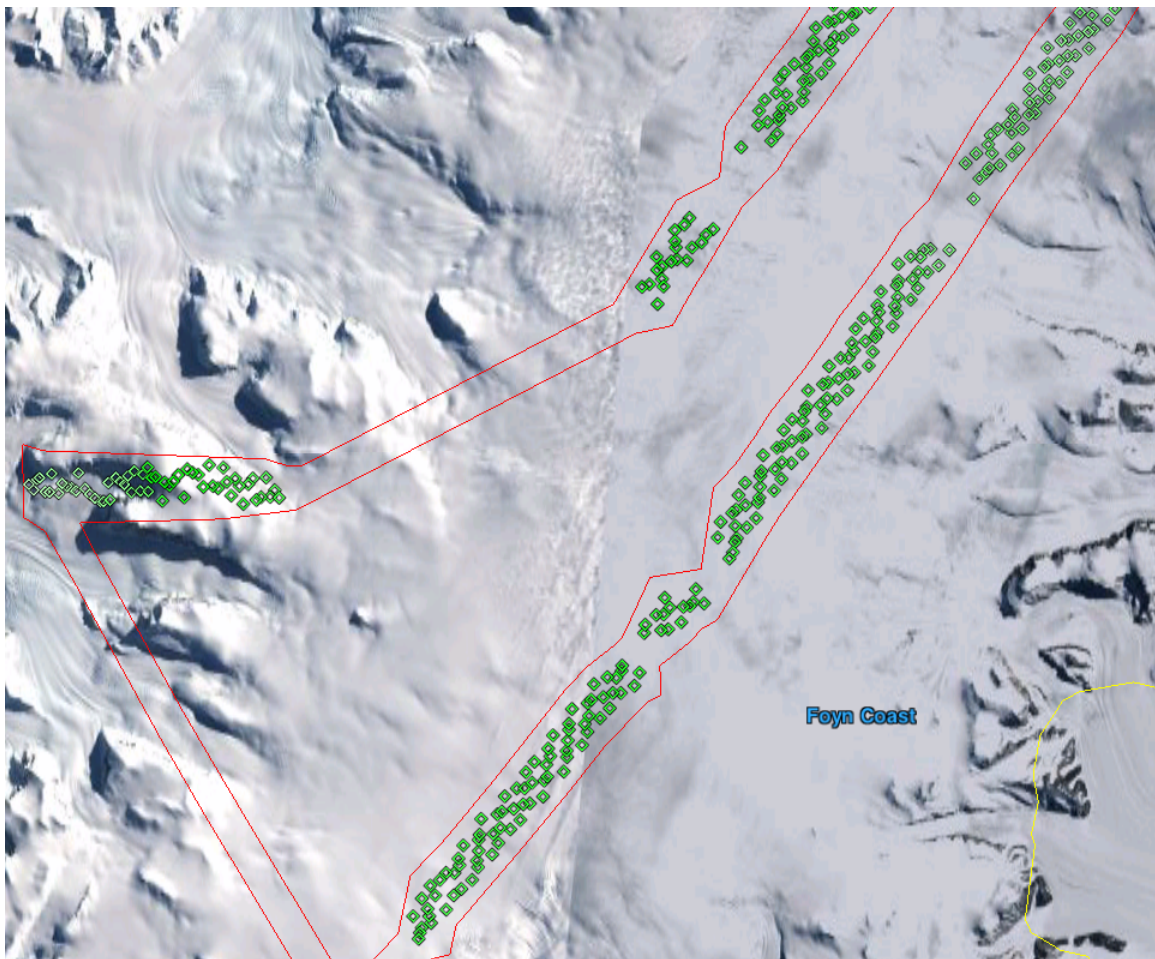


Figure A.3: Example of KML visualizations produced with `lvis2kml`. The output from both the boundary file (red) and the data file (green) with a point skip of 500 are shown in this image. The color saturation of data points is scaled with the elevation such that the points in the file with the least elevation show up as white and the highest points show up as the specified color.

Appendix B

The `stereo.default` File

The `stereo.default` file contains configuration parameters that the `stereo` program uses to process images. The `stereo.default` file is loaded from the current working directory when you run `stereo` unless you specify a different file using the `-s` option. Run `stereo --help` for more information. The extension is not important for this file.

A sample `stereo.default.example` file is included in the `examples/` directory of the Stereo Pipeline software distribution.

As mentioned in section 5.1.4, all the `stereo` parameters can also be specified on the command line.

Listed below are the parameters used by `stereo`, grouped by processing stage.

B.1 Preprocessing

alignment-method (= `affineepipolar`, `homography`, `epipolar`, `none`) (**default = affineepipolar**)

When `alignment-method` is set to `homography`, `stereo` will attempt to pre-align the images by automatically detecting tie-points between images using a feature based image matching technique. Tie points are stored in a `*.match` file that is used to compute a linear homography transformation of the right image so that it closely matches the left image. Note: the user may exercise more control over this process by using the `ipfind` and `ipmatch` tools.

When `alignment-method` is set to `affineepipolar`, `stereo` will attempt to pre-align the images by detecting tie-points, as earlier, and using those to transform the images such that pairs of conjugate epipolar lines become collinear and parallel to one of the image axes. The effect of this is equivalent to rotating the original cameras which took the pictures.

When `alignment-method` is set to `epipolar`, `stereo` will apply a 3D transform to both images so that their epipolar lines will be horizontal. This speeds of stereo correlation as it greatly reduces the area required for searching.

Epipolar alignment is only available when performing stereo matches using the pinhole stereo session (i.e. when using `stereo -t pinhole`), and cannot be used when processing ISIS images at this time.

left-image-crop-win `xoff` `yoff` `xsize` `ysize`

Do stereo in a sub-region of the left image [default: use the entire image].

right-image-crop-win `xoff` `yoff` `xsize` `ysize`

When combined with `left-image-crop-win`, do stereo in given subregions of left and right images.

It is important to note that when both of these are specified, we explicitly crop the input images to these regions, which does not happen when `left-image-crop-win` alone is specified. In that case we use the full images but only restrict the computation to the specified region.

force-use-entire-range (default = false)

By default, the Stereo Pipeline will normalize ISIS images so that their maximum and minimum channel values are ± 2 standard deviations from a mean value of 1.0. Use this option if you want to *disable* normalization and force the raw values to pass directly to the stereo correlations algorithms.

For example, if ISIS's `histeq` has already been used to normalize the images, then use this option to disable normalization as a (redundant) pre-processing step.

individually-normalize (default = false)

By default, the maximum and minimum valid pixel value is determined by looking at both images. Normalized with the same “global” min and max guarantees that the two images will retain their brightness and contrast relative to each other.

This option forces each image to be normalized to its own maximum and minimum valid pixel value. This is useful in the event that images have different and non-overlapping dynamic ranges. You can sometimes tell when this option is needed: after a failed stereo attempt one of the rectified images (`*-L.tif` and `*-R.tif`) may be either mostly white or black. Activating this option may correct this problem.

Note: Photometric calibration and image normalization are steps that can and should be carried out beforehand using ISIS's own utilities. This provides the best possible input to the stereo pipeline and yields the best stereo matching results.

ip-per-tile

How many interest points to detect in each 1024^2 image tile (default: automatic determination).

ip-detect-method

What type of interest point detection algorithm to use for image alignment. 0 = Custom OBAloG implementation (default) 1 = SIFT implementation from OpenCV 2 = ORB implementation from OpenCV If the default method does not perform well, try out one of the other two methods.

nodata-value (default = none)

Pixels with values less than or equal to this number are treated as no-data. This overrides the nodata values from input images.

B.2 Correlation

prefilter-mode (= 0,1,2,3) (default = 2)

This selects the pre-processing filter to be used to prepare imagery before it is fed to the initialization stage of the pipeline.

0 - None

1 - Subtracted Mean - This takes a preferably large Gaussian kernel and subtracts its value from the input image. This effectively reduces low frequency content in the image. The result is correlation that is immune to translations in image intensity.

2 - LoG Filter - Takes the Laplacian of Gaussian of the image, This provides some immunity to differences in lighting conditions between a pair of images by isolating and matching on blob features in the image.

For all of the modes above, the size of the filter kernel is determined by the `prefilter-kernel-width` parameter below.

The choice of pre-processing filter must be made with thought to the cost function being used (see `cost-mode`, below). LoG filter preprocessing provides good immunity to variations in lighting conditions and is usually the recommended choice.

`prefilter-kernel-width` (*float*) (default = 1.4)

This defines the diameter of the Gaussian convolution kernel used for the preprocessing modes 1 and 2 above. A value of 1.4 works well for LoG and 25-30 works well for Subtracted Mean.

`corr-seed-mode` (=0,1,2,3) (default = 1)

This integer parameter selects a strategy for how to solve for the low-resolution integer correlation disparity, which is used to seed the full-resolution disparity later on.

0 - None - Don't calculate a low-resolution variant of the disparity image. The search range provided by `corr-search` is used directly in computing the full-resolution disparity.

1 - Low-resolution disparity from stereo - Calculate a low-resolution version of the disparity from the integer correlation of subsampled left and right images. The low-resolution disparity will be used to narrow down the search range for the full-resolution disparity.

This is a useful option despite the fact that our integer correlation implementation does indeed use a pyramid approach. Our implementation cannot search infinitely into lower resolutions due to its independent and tiled nature. This low-resolution disparity seed is a good hybrid approach.

2 - Low-resolution disparity from an input DEM - Use a lower-resolution DEM together with an estimated value for its error to compute the low-resolution disparity, which will then be used to find the full-resolution disparity as above. These quantities can be specified via the options `disparity-estimation-dem` and `disparity-estimation-dem-error` respectively.

3 - Disparity from full-resolution images at a sparse number of points. This is an advanced option for terrain having snow and no large-scale features. It is described in section 4.5.

For large images, bigger than MOC-NA, using the low-resolution disparity seed is a definitive plus. Smaller images such as Cassini ISS or MER images should just shut this option off to save storage space.

`corr-sub-seed-percent` (*float*) (default=0.25)

When using `corr-seed-mode` 1, the solved-for or user-provided search range is grown by this factor for the purpose of computing the low-resolution disparity.

`cost-mode` (= 0,1,2) (default = 2)

This defines the cost function used during integer correlation. Squared difference is the fastest cost function. However it comes at the price of not being resilient against noise. Absolute difference is the next fastest and is a better choice. Normalized cross correlation is the slowest but is designed to be more robust against image intensity changes and slight lighting differences. Normalized cross correlation is about 2x slower than absolute difference and about 3x slower than squared difference.

0 - absolute difference

1 - squared difference

2 - normalized cross correlation

corr-kernel (*integer integer*) (**default = 25 25**)

These option determine the size (in pixels) of the correlation kernel used in the initialization step. A different size can be set in the horizontal and vertical directions, but square correlation kernels are almost always used in practice.

corr-search (*integer integer integer integer*)

These parameters determine the size of the initial correlation search range. The ideal search range depends on a variety of factors ranging from how the images were pre-aligned to the resolution and range of disparities seen in a given image pair. This search range is successively refined during initialization, so it is often acceptable to set a large search range that is guaranteed to contain all of the disparities in a given image. However, setting tighter bounds on the search can sometimes reduce the number of erroneous matches, so it can be advantageous to tune the search range for a particular data set.

Commenting out these settings will cause **stereo** to make an attempt to guess its search range using interest points.

These four integers define the minimum horizontal and vertical disparity and then the maximum horizontal and vertical disparity.

xcorr-threshold (*integer*) (**default = 2**)

Integer correlation to a limited sense performs a correlation forward and backwards to double check its result. This is one of the first filtering steps to insure that we have indeed converged to a global minimum for an individual pixel. The **xcorr-threshold** parameter defines an agreement threshold in pixels between the forward and backward result.

Optionally, this parameter can be set to a negative number. This will signal the correlator to only use the forward correlation result. This will drastically improve speed at the cost of additional noise.

rm-quantile-percentile (*double*) (**default = 0.85**)

See **rm-quantile-multiple** for details.

rm-quantile-multiple (*double*) (**default = -1**)

Used for filtering disparity values in **D_sub**. Disparities greater than **MULTIPLE*PERCENTILE** (of the histogram) will be discarded. If this value is set greater than zero, this filtering method will be used instead of the method using the values **RM_MIN_MATCHES** and **RM_THRESHOLD**. This method will help filter out clusters of pixels which are too large to be filtered out by the neighborhood method but that have disparities significantly greater than the rest of the image.

use-local-homography (**default = false**)

This flag, if provided, enables using local homography during correlation, as described in Section 7.2.3.

corr-timeout (*integer*) (**default = 1800**)

Correlation timeout for an image tile, in seconds. A non-positive value will result in no timeout enforcement. A value of 600 seconds should be sufficient in most cases.

B.3 Subpixel Refinement

subpixel-mode (= 0-5) (default = 1)

This parameter selects the subpixel correlation method. Parabola subpixel is very fast but will produce results that are only slightly more accurate than those produced by the initialization step. Bayes EM (mode 2) is very slow but offers the best quality. When tuning `stereo.default` parameters, it is expedient to start out using parabola subpixel as a “draft mode.” When the results are looking good with parabola subpixel, then they will look even better with subpixel mode 2. For inputs with little noise, the affine method (subpixel mode 3) may produce results equivalent to Bayes EM in a shorter time.

0 - no subpixel refinement

1 - parabola fitting

2 - affine adaptive window, Bayes EM weighting

3 - affine window

4 - Lucas-Kanade method (experimental)

5 - affine adaptive window, Bayes EM with Gamma Noise Distribution (experimental)

For a visual comparison of the quality of these subpixel modes, refer back to Chapter:7.

subpixel-kernel (integer integer) (default = 35 35) Specify the size of the horizontal and vertical size (in pixels) of the subpixel correlation kernel. It is advantageous to keep this small for parabola fitting in order to resolve finer details. However for the Bayes EM methods, keep the kernel slightly larger. Those methods weight the kernel with a Gaussian distribution, thus the effective area is small than the kernel size defined here.

B.4 Filtering

filter-mode (integer) (default = 1)

This parameter sets the filter mode. Three modes are supported as described below. Here, by neighboring pixels for a current pixel we mean those pixels within the window of half-size of `rm-half-kernel` centered at the current pixel.

0 - No filtering.

1 - Filter by discarding pixels at which disparity differs from mean disparity of neighbors by more than `max-mean-diff`.

2 - Filter by discarding pixels at which percentage of neighboring disparities that are within `rm-threshold` of current disparity is less than `rm-min-matches`.

rm-half-kernel (integer integer) (default = 5 5)

This setting adjusts the behavior of an outlier rejection scheme that “erodes” isolated regions of pixels in the disparity map that are in disagreement with their neighbors.

The two parameters determine the size of the half kernel that is used to perform the automatic removal of low confidence pixels. A 5×5 half kernel would result in an 11×11 kernel with 121 pixels in it.

max-mean-diff (integer) (default = 3)

This parameter sets the *maximum difference* between the current pixel disparity and the mean of disparities of neighbors in order for a given disparity value to be retained (for `filter-mode` 1).

rm-min-matches (integer) (default = 60)

This parameter sets the *percentage* of neighboring disparity values that must fall within the inlier threshold in order for a given disparity value to be retained (for **filter-mode 2**).

rm-threshold (integer) (default = 3)

This parameter sets the inlier threshold for the outlier rejection scheme. This option works in conjunction with RM_MIN_MATCHES above. A disparity value is rejected if it differs by more than RM_THRESHOLD disparity values from RM_MIN_MATCHES percent of pixels in the region being considered (for **filter-mode 2**).

rm-clean-passes (integer) (default = 1)

Select the number of outlier removal passes that are carried out. Each pass will erode pixels that do not match their neighbors. One pass is usually sufficient.

enable-fill-holes (default = false)

Enable filling of holes in disparity using an inpainting method. Obsolete. It is suggested to use instead point2dem's analogous functionality.

fill-holes-max-size (integer) (default = 100,000)

Holes with no more pixels than this number should be filled in.

erode-max-size (integer) (default = 0)

Isolated blobs with no more pixels than this number should be removed.

B.5 Post-Processing (Triangulation)

near-universe-radius (float) (default = 0.0)**far-universe-radius (float) (default = 0.0)**

These parameters can be used to remove outliers from the 3D triangulated point cloud. The points that will be kept are those whose distance from the universe center (see below) is between **near-universe-radius** and **far-universe-radius**, in meters.

universe-center (default = none)

Defines the reference location to use when filtering the output point cloud using the above near and far radius options. The available options are:

None - Disable filtering.

Camera - Use the left camera's center as the universe center.

Zero - Use the center of the planet as the universe center.

bundle-adjust-prefix (string)

Use the camera adjustments obtained by previously running bundle_adjust with this output prefix.

point-cloud-rounding-error (double)

How much to round the output point cloud values, in meters (more rounding means less precision but potentially smaller size on disk). The inverse of a power of 2 is suggested. Default: $1/2^{10}$ meters (about 1mm) for Earth and proportionally less for smaller bodies.

save-double-precision-point-cloud (default = false)

Save the final point cloud in double precision rather than bringing the points closer to origin and saving as float (marginally more precision at twice the storage).

compute-error-vector (default = false)

When writing the output point cloud, save the 3D triangulation error vector (the vector between the closest points on the rays emanating from the two cameras), rather than just its length. In this case, the point cloud will have 6 bands (storing the triangulation point and triangulation error vector) rather than the usual 4. When invoking `point2dem` on this 6-band point cloud and specifying the `--errorimage` option, the error image will contain the three components of the triangulation error vector in the North-East-Down coordinate system.

The next several parameters are used for jitter correction for Digital Globe imagery. A usage tutorial is given in section 4.4.

image-lines-per-piecewise-adjustment (integer) (default = 0) A positive value, e.g., 1000, will turn on using piecewise camera adjustments to help reduce jitter effects. Use one adjustment per this many image lines.

piecewise-adjustment-percentiles (float float) (default = 5 95) A narrower range will place the piecewise adjustments for jitter correction closer together and further from the first and last lines in the image.

piecewise-adjustment-interp-type (integer) (default = 1) How to interpolate between adjustments.
[1 Linear, 2 Using Gaussian weights]

piecewise-adjustment-camera-weight (float) (default = 1.0) The weight to use for the sum of squares of adjustments component of the cost function. Increasing this value will constrain the adjustments to be smaller.

num-matches-for-piecewise-adjustment (integer) (default = 90000) How many matches among images to create based on the disparity for the purpose of solving for jitter using piecewise adjustment.
These last two options are used internally.

compute-piecewise-adjustments-only (default = false)

Compute the piecewise adjustments as part of jitter correction, and then stop.

skip-computing-piecewise-adjustments (default = false)

Skip computing the piecewise adjustments for jitter, they should have been done by now.

Appendix C

Guide to Output Files

The **stereo** tool generates a variety of intermediate files that are useful for debugging. These are listed below, along with brief descriptions about the contents of each file. Note that the prefix of the filename for all of these files is dictated by the final command line argument to **stereo**. Run **stereo --help** for details.

*.**vwip** - image feature files

If **alignment-method** is not **none**, the Stereo Pipeline will automatically search for image features to use for tie-points. Raw image features are stored in *.vwip files; one per input image. For example, if your images are **left.cub** and **right.cub** you'll get **left.vwip** and **right.vwip**. Note: these files can also be generated by hand (and with finer grained control over detection algorithm options) using the **ipfind** utility.

*.**match** - image to image tie-points

The **match** file lists a select group of unique points out of the previous .vwip files that have been identified and matched in a pair of images. For example, if your images are **left.cub** and **right.cub** you'll get a **left_right.match** file.

The .vwip and .match files are meant to serve as cached tie-point information, and they help speed up the pre-processing phase of the Stereo Pipeline: if these files exist then the **stereo** program will skip over the interest point alignment stage and instead use the cached tie-points contained in the *.match files. In the rare case that one of these files did get corrupted or your input images have changed, you may want to delete these files and allow **stereo** to regenerate them automatically. This is also recommended if you have upgraded the Stereo Pipeline software.

*-**L.tif** - rectified left input image

The left input image of the stereo pair, saved after the pre-processing step. This image may be normalized, but should otherwise be identical to the original left input image.

*-**R.tif** - rectified right input image

Right input image of the stereo pair, after the pre-processing step. This image may be normalized and possibly translated, scaled, and/or rotated to roughly align it with the left image, but should otherwise be identical to the original right input image.

*-**lMask.tif** - mask for left rectified image

*-**rMask.tif** - mask for right rectified image

These files contain binary masks for the input images. These are used throughout the stereo process to mask out pixels where there is no input data.

*-**align-L.exr** - left pre-alignment matrix

***-align-R.exr** - right pre-alignment matrix

The 3×3 affine transformation matrices that are used to warp the left and right images to roughly align them. These files are only generated if `alignment-method` is not `none` in the `stereo.default` file. Normally, a single transform is enough to warp one image to another (for example, the right image to the left). The reason we use two transforms is the following: after the right image is warped to the left, we would like to additionally transform both images so that the origin (0, 0) in the left image would correspond to the same location in the right image. This will somewhat improve the efficiency of subsequent processing.

***-D.tif** - disparity map after the disparity map initialization phase

This is the disparity map generated by the correlation algorithm in the initialization phase. It contains integer values of disparity that are used to seed the subsequent sub-pixel correlation phase. It is largely unfiltered, and may contain some bad matches.

Disparity map files are stored in OpenEXR format as 3-channel, 32-bit floating point images. (Channel 0 = horizontal disparity, Channel 1 = vertical disparity, and Channel 2 = good pixel mask)

***-RD.tif** - disparity map after sub-pixel correlation

This file contains the disparity map after sub-pixel refinement. Pixel values now have sub-pixel precision, and some outliers have been rejected by the sub-pixel matching process.

***-F-corrected.tif** - intermediate data product

Only created when `alignment-method` is not `none`. This is ***-F.tif** with effects of interest point alignment removed.

***-F.tif** - filtered disparity map

The filtered, sub-pixel disparity map with outliers removed (and holes filled with the inpainting algorithm if `FILL_HOLES` is on). This is the final version of the disparity map.

***-GoodPixelMap.tif** - map of good pixels

An image showing which pixels were matched by the stereo correlator (gray pixels), and which were filled in by the hole filling algorithm (red pixels).

***-PC.tif** - point cloud image

The point cloud image is generated by the triangulation phase of Stereo Pipeline. Each pixel in the point cloud image corresponds to a pixel in the left input image (***-L.tif**). The point cloud has four channels, the first three are the Cartesian coordinates of each point, and the last one has the intersection error of the two rays which created that point (the intersection error is the closest distance between rays). By default, the origin of the Cartesian coordinate system being used is a point in the neighborhood of the point cloud. This makes the values of the points in the cloud relatively small, and we save them in single precision (32 bits). This origin is saved in the point cloud as well using the tag `POINT_OFFSET` in the GeoTiff header. To output point clouds using double precision with the origin at the planet center, call `stereo_tri` with the option `--save-double-precision-point-cloud`. This can effectively double the size of the point cloud.

All these images that are single-band can be visualized in `stereo_gui` (section A.2). The disparities can be first split into the individual horizontal and vertical disparity files using `disparitydebug`, then they can be seen in this viewer as well.

If the input images are map-projected (georeferenced) and the alignment method is `none`, all the output images listed above, will also be georeferenced, and hence can be overlayed in `stereo_gui` on top of the input imagery (the outputs of `disparitydebug` will then be georeferenced as well).

The point cloud file saves the datum (and projection if available) inferred from the input images, regardless of whether these images are map-projected or not.

The `point2mesh` and `point2dem` programs can be used to convert the point cloud to formats that are easier to visualize.

***-stereo.default** - backup of the Stereo Pipeline settings file

This is a copy of the `stereo.default` file used by `stereo`. It is stored alongside the output products as a record of the settings that were used for this particular stereo processing task.

Appendix D

Pinhole Models

Ames Stereo Pipeline supports a generic pinhole camera model with several generic lens distortion models which cover common calibration methods. The generic pinhole model uses the following parameters:

- f_x = The focal length in horizontal units.
- f_y = The focal length in vertical units.
- c_x = The horizontal offset of the principal point of the camera in the image plane.
- c_y = The vertical offset of the principal point of the camera in the image plane.
- $pitch$ = The size of each pixel in the units used to specify the four parameters listed above. This will usually either be 1.0 if they are specified in pixel units or alternately the size of a pixel in millimeters.

Along with the basic pinhole camera parameters, a lens distortion model can be added. Note that the units used in the distortion model must match the units used for the parameters listed above. For example, if the camera calibration was performed using units of millimeters the focal lengths etc. must be given in units of millimeters and the pitch must be equal to the size of each pixel in millimeters. The following lens distortion models are currently supported:

- **Null** = A placeholder model that applies no distortion.
- **Tsai** = A common distortion model similar to the one used by OpenCV and THEIA. This model uses the following parameters:

K_1, K_2 = Radial distortion parameters.

P_1, P_2 = Tangential distortion parameters.

The following equations describe the distortion:

$$r^2 = x^2 + y^2$$

$$x(\text{distorted}) = x * (K_1 r^2 + K_2 r^4 + 2P_1 y + P_2 \left(\frac{r^2}{x} + 2x \right))$$

$$y(\text{distorted}) = y * (K_1 r^2 + K_2 r^4 + 2P_2 x + P_1 \left(\frac{r^2}{y} + 2y \right))$$

References:

Roger Tsai, A Versatile Camera Calibration Technique for a High-Accuracy 3D Machine Vision Metrology Using Off-the-shelf TV Cameras and Lenses

Note that this model uses normalized pixel units.

- **Adjustable Tsai** = A variant of the Tsai model where any number of K terms and a skew term (alhpa) can be used. Can apply the AgiSoft Lens calibration parameters.
- **Brown-Conrady** = An older model based on a centering angle.

$K1, K2, K3$ = Radial distortion parameters.

$P1, P2$ = Tangential distortion parameters.

xp, yp = Principal point offset.

$B1, B2$ = Unused parameters.

The following equations describe the distortion:

$$x = x(\text{distorted}) - xp$$

$$y = y(\text{distorted}) - yp$$

$$r^2 = x^2 + y^2$$

$$dr = K_1 r^3 + K_2 r^5 + K_3 r^7$$

$$x(\text{undistorted}) = x + x \frac{dr}{r} + P_1(r^2 + 2x^2) + 2P_2xy$$

$$y(\text{undistorted}) = y + y \frac{dr}{r} + P_2(r^2 + 2y^2) + 2P_1xy$$

Note that this model uses non-normalized pixel units.

References:

Decentering Distortion of Lenses - D.C. Brown, Photometric Engineering, pages 444-462, Vol. 32, No. 3, 1966

Close-Range Camera Calibration - D.C. Brown, Photogrammetric Engineering, pages 855-866, Vol. 37, No. 8, 1971

- **Photometrix** = A model matching the conventions used by the Australis software from Photometrix. This model uses the following parameters:

$K1, K2, K3$ = Radial distortion parameters.

$P1, P2$ = Tangential distortion parameters.

xp, yp = Principal point offset.

phi = Tangential distortion angle in radians.

The following equations describe the distortion:

$$x = x(\text{distorted}) - xp$$

$$y = y(\text{distorted}) - yp$$

$$r^2 = x^2 + y^2$$

$$dr = K_1 r^3 + K_2 r^5 + K_3 r^7$$

$$x(\text{undistorted}) = x + x \frac{dr}{r} - (P_1 r^2 + P_2 r^4) \sin(\phi) +$$

$$y(\text{undistorted}) = y + y \frac{dr}{r} + (P_1 r^2 + P_2 r^4) \cos(\phi)$$

Note that this model uses non-normalized pixel units.

D.1 File Format

ASP pinhole model files are written in an easy to work with plain text format using the extension .tsai. A sample file is shown below:

```
VERSION_3
fu = 28.429
fv = 28.429
cu = 17.9712
cv = 11.9808
u_direction = 1 0 0
v_direction = 0 1 0
w_direction = 0 0 1
C = 266.943 -105.583 -2.14189
R = 0.0825447 0.996303 -0.0238243 -0.996008 0.0832884 0.0321213 0.0339869 0.0210777 0.9992
pitch = 0.0064
Photometrix
xp = 0.004
yp = -0.191
k1 = 1.31024e-04
k2 = -2.05354e-07
k3 = -5.28558e-011
p1 = 7.2359e-006
p2 = 2.2656e-006
b1 = 0.0
b2 = 0.0
```

The first half of the file is the same for all pinhole models:

- **VERSION_X** = A header line used to track the format of the file.
- ***f_u*, *f_v*, *c_u*, *c_v*** = The first four intrinsic parameters described in the previous section.
- ***u*, *v*, and *w_direction*** = These lines allow an additional permutation of the axes of the camera coordinates. By default, the positive column direction aligns with x, the positive row direction aligns with y, and downward into the image aligns with z.
- **C** = The location of the camera center, usually in the geocentric coordinate system (GCC).
- **R** = The rotation matrix describing the camera's pose in the coordinate system.
- ***pitch*** = The pitch intrinsic parameter described in the previous section.

The second half of the file describes the lens distortion model being used. The name of the distortion model appears first, followed by a list of the parameters for that model. The number of parameters may be different for each distortion type. Samples of each format are shown below:

- **Null**

```
NULL
```

- **Tsai**

```
TSAI
k1 = 1.31024e-04
k2 = -2.05354e-07
p1 = 0.5
p2 = 0.4
```

- **Adjustable Tsai**

```
AdjustableTSAI
Radial Coeff: Vector3(1.31024e-04, 1.31024e-07, 1.31024e-08)
Tangential Coeff: Vector2(-2.05354e-07, 1.05354e-07)
Alpha: 0.4
```

- **Brown-Conrady**

```
BrownConrady
xp = 0.5
yp = 0.4
k1 = 1.31024e-04
k2 = -2.05354e-07
k3 = 1.31024e-08
p1 = 0.5
p2 = 0.4
phi = 0.001
```

- **Photometrix**

```
Photometrix
xp = 0.004
yp = -0.191
k1 = 1.31024e-04
k2 = -2.05354e-07
k3 = -5.28558e-011
p1 = 7.2359e-006
p2 = 2.2656e-006
b1 = 0.0
b2 = 0.0
```

For several years Ames Stereo Pipeline generated pinhole files in the binary `.pinhole` format. That format has been deprecated and can be read but will no longer be written. At some point in the future support for that file format will be dropped.

Also in the past Ames Stereo Pipeline has generated a shorter version of the current file format, also with the extension `.tsai`, which only supported the TSAI lens distortion model. Existing files in that format can still be used by ASP.

Appendix E

Papers that used ASP

These works have made use of the Ames Stereo Pipeline to produce their results or enable their studies.

1. R. A. Beyer, B. Archinal, Y. Chen, K. Edmundson, D. Harbour, E. Howington-Kraus, R. Li, A. McEwen, S. Mattson, Z. Moratto, J. Oberst, M. Rosiek, F. Scholten, T. Tran, M. Robinson, and LROC Team. LROC Stereo Data—Results of Initial Analysis. In S. Mackwell and E. Stansbery, editors, *Lunar and Planetary Science Conference 41*, number #2678. Lunar and Planetary Institute, Houston, March 2010
2. T. R. Watters, M. S. Robinson, R. A. Beyer, J. F. Bell, M. E. Pritchard, M. E. Banks, E. P. Turtle, N. R. Williams, and LROC Team. Lunar Thrust Faults: Implications for the Thermal History of the Moon. In S. Mackwell and E. Stansbery, editors, *Lunar and Planetary Science Conference 41*, number #1863. Lunar and Planetary Institute, Houston, March 2010
3. C. B. Phillips, R. A. Beyer, F. Nimmo, J. H. Roberts, and G. Robuchon. Crater Relaxation and Stereo Imaging of the Icy Satellites of Jupiter and Saturn. *AGU Fall Meeting Abstracts*, (#P21B-1596), December 2010
4. N. P. Hammond, C. B. Phillips, G. Robuchon, R. A. Beyer, F. Nimmo, and J. Roberts. Crater relaxation and stereo imaging of rhea. In S. Mackwell and E. Stansbery, editors, *Lunar and Planetary Science Conference 42*, number #2633. Lunar and Planetary Institute, Houston, 2011
5. John Huffman, Andrew Forsberg, Andrew Loomis, James Head, James Dickson, and Caleb Fassett. Integrating advanced visualization technology into the planetary geoscience workflow. *Planetary and Space Science*, 59(11–12):1273 – 1279, 2011. ISSN 0032-0633. URL <http://www.sciencedirect.com/science/article/pii/S0032063310002175>
6. R. A. Beyer, B. Archinal, Y. Cheng, K. Edmundson, E. Howington-Kraus, R. L. Kirk, R. Li, A. S. McEwen, S. Mattson, X. Meng, Z. Moratto, J. Oberst, M. Rosiek, F. Scholten, T. Tran, O. Thomas, W. Wang, and the LROC Team. LROC DTM comparison effort. In S. Mackwell and E. Stansbery, editors, *Lunar and Planetary Science Conference 42*, number #2715. Lunar and Planetary Institute, Houston, 2011
7. Z. Moratto, A. Nefian, T. Kim, M. Broxton, R. A. Beyer, and T. Fong. Stereo reconstruction from apollo 15 and 16 metric camera. In S. Mackwell and E. Stansbery, editors, *Lunar and Planetary Science Conference 42*, number #2267. Lunar and Planetary Institute, Houston, 2011
8. A. Lefort, D. M. Burr, R. A. Beyer, and A. D. Howard. Topographic post-formation modifications of inverted fluvial features in the western Medusa Fossae formation, Mars. In S. Mackwell and E. Stans-

- bery, editors, *Lunar and Planetary Science Conference 42*, number #2418. Lunar and Planetary Institute, Houston, 2011
9. C. B. Phillips, N. P. Hammond, F. Nimmo, G. robuchon, R. A. Beyer, and J. H. Roberts. Crater Relaxation and Stereo Imaging of Icy Satellites. *AGU Fall Meeting Abstracts*, (#P41F-07), December 2011
 10. Vytas SunSpiral, D.W. Wheeler, Daniel Chavez-Clemente, and David Mittman. Development and field testing of the footfall planning system for the athlete robots. *Journal of Field Robotics*, 29(3): 483–505, 2012. ISSN 1556-4967. URL <http://dx.doi.org/10.1002/rob.20410>
 11. Cristina Re, Gabriele Cremonese, Elisa Dall'Asta, Gianfranco Forlani, Giampiero Naletto, and Riccardo Roncella. Performance evaluation of dtm area-based matching reconstruction of moon and mars. *Proc. SPIE 8537, Image and Signal Processing for Remote Sensing XVIII*, pages 85370V–85370V–12, 2012. URL <http://dx.doi.org/10.1117/12.974524>
 12. Teemu Öhman and David A. Kring. Photogeologic analysis of impact melt-rich lithologies in kepler crater that could be sampled by future missions. *Journal of Geophysical Research: Planets*, 117(E12): n/a–n/a, 2012. ISSN 2156-2202. URL <http://dx.doi.org/10.1029/2011JE003918>
 13. M. Golombek, J. Grant, D. Kipp, A. Vasavada, R. Kirk, R. Fergason, P. Bellutta, F. Calef, K. Larsen, Y. Katayama, A. Huertas, R. Beyer, A. Chen, T. Parker, B. Pollard, S. Lee, Y. Sun, R. Hoover, H. Sladek, J. Grotzinger, R. Welch, E. Noe Dobrea, J. Michalski, and M. Watkins. Selection of the mars science laboratory landing site. *Space Science Reviews*, 170(1-4):641–737, 2012. ISSN 0038-6308. URL <http://dx.doi.org/10.1007/s11214-012-9916-y>
 14. A. Lefort, D. M. Burr, R. A. Beyer, and A. D. Howard. Inverted fluvial features in the Aeolis-Zephyria Plana, western Medusae Fossae Formation, Mars: Evidence for post-formation modification. *Journal of Geophysical Research (Planets)*, 117:E03007, March 2012
 15. A. Lefort, D. M. Burr, R. A. Beyer, and A. D. Howard. Sinuous Ridges as Tools to Investigate Post-Flow Modification in the Aeolis-Zephyria Plana, Western Medusae Fossae Formation, Mars. In *Lunar and Planetary Science Conference 43*, number #1953, March 2012
 16. C. B. Phillips, N. P. Hammond, G. Robuchon, F. Nimmo, R. A. Beyer, and J. Roberts. Stereo Imaging, Crater Relaxation, and Thermal Histories of Rhea and Dione. In *Lunar and Planetary Science Conference 43*, number #2571, March 2012
 17. A. M. Morgan, R. A. Beyer, A. D. Howard, and J. M. Moore. The Alluvial Fans of Saheki Crater. In *Lunar and Planetary Science Conference 43*, number #2815, March 2012
 18. N.P. Hammond, C.B. Phillips, F. Nimmo, and S.A. Kattenhorn. Flexure on dione: Investigating subsurface structure and thermal history. *Icarus*, 223(1):418 – 422, 2013. ISSN 0019-1035. URL <http://www.sciencedirect.com/science/article/pii/S0019103513000043>
 19. Samantha E. Peel and Caleb I. Fassett. Valleys in pit craters on mars: Characteristics, distribution, and formation mechanisms. *Icarus*, (0):–, 2013. ISSN 0019-1035. URL <http://www.sciencedirect.com/science/article/pii/S0019103513001474>
 20. C. B. Phillips, N. P. Hammond, J. H. Roberts, F. Nimmo, R. A. Beyer, and S. Kattenhorn. Stereo Topography and Subsurface Thermal Profiles on Icy Satellites of Saturn. In *Lunar and Planetary Science Conference 44*, number #2766, March 2013
 21. T. Öhman and P. J. McGovern. Strain Calculations for Circumferential Graben on Alba Mons, Mars. *LPI Contributions*, 1719:2966, March 2013

22. W. A. Watters, L. Geiger, and M. Fendrock. Shape Distribution of Fresh Martian Impact Craters from High-Resolution DEMs. In *Lunar and Planetary Science Conference 44*, volume 44 of *Lunar and Planetary Institute Science Conference Abstracts*, March 2013
23. W. A. Watters and A. C. Radford. 3-D Morphometry of Martian Secondary Impact Craters from Zunil and Gratteri. In *Lunar and Planetary Science 45*, volume 45 of *Lunar and Planetary Institute Science Conference Abstracts*, March 2014
24. A. Lucchetti, R. Thomas, G. Cremonese, M. Massironi, D. A. Rothery, S. J. Conway, and M. Anand. Analysis and Numerical Modeling of a Pit Crater on Mercury. In *Lunar and Planetary Science Conference 45*, volume 45 of *Lunar and Planetary Institute Science Conference Abstracts*, March 2014
25. A. C. G. Hughes, E. Hauber, and A. P. Rossi. Geomorphology of Glacial and Periglacial Landforms Within a Small Crater in Terra Cimmeria, Mars: Stratigraphy and Inferred Chronology of Processes. In *Lunar and Planetary Science Conference 45*, volume 45 of *Lunar and Planetary Institute Science Conference Abstracts*, March 2014
26. A. Lucas, A. Mangeney, and J. P. Ampuero. Frictional velocity-weakening in landslides on Earth and on other planetary bodies. *Nature Communications*, 5:3417, March 2014
27. Laura A Stevens, Mark D Behn, Jeffrey J McGuire, Sarah B Das, Ian Joughin, Thomas Herring, David E Shean, and Matt A King. Greenland supraglacial lake drainages triggered by hydrologically induced basal slip. *Nature*, 522(7554):73–76, 2015
28. Michael J Willis, Andrew K Melkonian, and Matthew E Pritchard. Outlet glacier response to the 2012 collapse of the matusevich ice shelf, severnaya zemlya, russian arctic. *Journal of Geophysical Research: Earth Surface*, 120(10):2040–2055, 2015
29. David E Shean, Oleg Alexandrov, Zachary M Moratto, Benjamin E Smith, Ian R Joughin, Claire Porter, and Paul Morin. An automated, open-source pipeline for mass production of digital elevation models (dems) from very-high-resolution commercial stereo satellite imagery. *ISPRS Journal of Photogrammetry and Remote Sensing*, 116:101–117, 2016
30. Pascal Lacroix. Landslides triggered by the gorkha earthquake in the langtang valley, volumes and initiation processes. *Earth, Planets and Space*, 68(1):1–10, 2016
31. Allen Pope, TA Scambos, M Moussavi, M Tedesco, M Willis, D Shean, and S Grigsby. Estimating supraglacial lake depth in west greenland using landsat 8 and comparison with other multispectral methods. *The Cryosphere*, 10:15, 2016
32. Andrew K Melkonian, Michael J Willis, Matthew E Pritchard, and Adam J Stewart. Recent changes in glacier velocities and thinning at novaya zemlya. *Remote Sensing of Environment*, 174:244–257, 2016
33. Signe Hillerup Larsen, Shfaqat Abbas Khan, Andreas Peter Ahlstrøm, Christine Schøtt Hvidberg, Michael John Willis, and Signe Bech Andersen. Increased mass loss and asynchronous behavior of marine-terminating outlet glaciers at upernavik isstrøm, nw greenland. *Journal of Geophysical Research: Earth Surface*, 2016

Bibliography

- [1] Michael Abrams, Simon Hook, and Bhaskar Ramachandran. Aster user handbook, version 2. *Jet Propulsion Laboratory*, 4800:135, 2002.
- [2] C. H. Acton. Ancillary data services of NASA's Navigation and Ancillary Information Facility. *Planetary and Space Science*, 44:65–70, January 1996.
- [3] C. H. Acton. SPICE Products Available to the Planetary Science Community. In *Lunar and Planetary Science XXX*, number #1233. Lunar and Planetary Institute, Houston (CD-ROM), March 1999.
- [4] C. H. Acton, N. J. Bachman, J. A. Bytof, B. V. Semenov, W. Taber, F. S. Turner, and E. D. Wright. Examining Mars with SPICE. In *Fifth International Conference on Mars*, number #6042. Lunar and Planetary Institute, Houston (CD-ROM), July 1999.
- [5] J. A. Anderson, S. C. Sides, D. L. Soltesz, T. L. Sucharski, and K. J. Becker. Modernization of the Integrated Software for Imagers and Spectrometers. In S. Mackwell and E. Stansbery, editors, *Lunar and Planetary Science XXXV*, number #2039. Lunar and Planetary Institute, Houston (CD-ROM), March 2004.
- [6] J.A. Anderson. ISIS Camera Model Design. In *Proc of the Lunar and Planetary Science Conference (LPSC) XXXIX*, page 2159, March 2008.
- [7] Simon Baker, Ralph Gross, and Iain Matthews. Lucas-Kanade 20 Years On: A Unifying Framework. *International Journal of Computer Vision*, 56:221–255, 2004.
- [8] Herbert Bay, Andreas Ess, Tinne Tuytelaars, and Luc Van Gool. SURF: Speeded up robust features. In *Computer Vision and Image Understanding (CVIU)*, volume 110, pages 346–359, 2008. URL <http://www.vision.ee.ethz.ch/~surf/>.
- [9] R. A. Beyer, B. Archinal, Y. Chen, K. Edmundson, D. Harbour, E. Howington-Kraus, R. Li, A. McEwen, S. Mattson, Z. Moratto, J. Oberst, M. Rosiek, F. Scholten, T. Tran, M. Robinson, and LROC Team. LROC Stereo Data—Results of Initial Analysis. In S. Mackwell and E. Stansbery, editors, *Lunar and Planetary Science Conference 41*, number #2678. Lunar and Planetary Institute, Houston, March 2010.
- [10] R. A. Beyer, B. Archinal, Y. Cheng, K. Edmundson, E. Howington-Kraus, R. L. Kirk, R. Li, A. S. McEwen, S. Mattson, X. Meng, Z. Moratto, J. Oberst, M. Rosiek, F. Scholten, T. Tran, O. Thomas, W. Wang, and the LROC Team. LROC DTM comparison effort. In S. Mackwell and E. Stansbery, editors, *Lunar and Planetary Science Conference 42*, number #2715. Lunar and Planetary Institute, Houston, 2011.
- [11] Tye Brady. ALHAT Requirements. presentation at the Lunar Coordinate Systems Review Data Product Recommendation Meeting, NASA Ames Research Center, October 11.

- [12] Michael Broxton, Ara V. Nefian, Zachary Moratto, Taemin Kim, Michael Lundy, and Aleksandr V. Segal. 3D Lunar Terrain Reconstruction from Apollo Images . In *to appear in the Proceedings of the 5th International Symposium on Visual Computing*, 2009.
- [13] USGS Astrogeology Science Center. USGS ISIS Documentation. Isis 3 Application Documentation <http://isis.astrogeology.usgs.gov/Application/index.html>. URL <http://isis.astrogeology.usgs.gov/Application/index.html>.
- [14] Yanqing Chen, Timothy A. Davis, William W. Hager, and Sivasankaran Rajamanickam. Algorithm 887: Cholmod, supernodal sparse cholesky factorization and update/downdate. *ACM Trans. Math. Softw.*, 35(3):22:1–22:14, October 2008. ISSN 0098-3500. URL <http://doi.acm.org/10.1145/1391989.1391995>.
- [15] Li Cheng and T. Caelli. Bayesian stereo matching. *Computer Vision and Pattern Recognition Workshop, 2004. CVPRW '04. Conference on*, pages 192–192, June 2004.
- [16] G. Chin, A. Bartels, S. Brylow, M. Foote, J. Garvin, J. Kaspar, J. Keller, I. Mitrofanov, K. Raney, M. Robinson, D. Smith, H. Spence, P. Spudis, S. A. Stern, and M. Zuber. Lunar Reconnaissance Orbiter Overview: The Instrument Suite and Mission. In S. Mackwell and E. Stansbery, editors, *Lunar and Planetary Science XXXVII*, page #1949, March 2006.
- [17] G. Chin, S. Brylow, M. Foote, J. Garvin, J. Kasper, J. Keller, M. Litvak, I. Mitrofanov, D. Paige, K. Raney, M. Robinson, A. Sanin, D. Smith, H. Spence, P. Spudis, S. A. Stern, and M. Zuber. Lunar Reconnaissance Orbiter Overview: The Instrument Suite and Mission. *Space Science Reviews*, 129: 391–419, April 2007.
- [18] The Open Scene Graph Community. The open scene graph website. 2009. URL <http://www.openscenegraph.org/projects/osg>.
- [19] S. Debei, A. Aboudan, G. Colombatti, and M. Pertile. Lutetia surface reconstruction and uncertainty analysis. *Planetary and Space Science*, 71:64–72, October 2012.
- [20] Stefano Debei, Alessio Aboudan, Giacomo Colombatti, and Marco Pertile. Lutetia surface reconstruction and uncertainty analysis. *Planetary and Space Science*, 71(1):64 – 72, 2012. ISSN 0032-0633. URL <http://www.sciencedirect.com/science/article/pii/S0032063312002073>.
- [21] NASA ARC Intelligent Systems Division. NASA Vision Workbench. NASA Ames Research Center, Moffett Field, CA. <http://ti.arc.nasa.gov/visionworkbench/>. URL <http://ti.arc.nasa.gov/visionworkbench/>.
- [22] L. Edwards and M. Broxton. Automated 3D Surface Reconstruction from Orbital Imagery. In *Proceedings of AIAA Space 2006*, September 2006.
- [23] L. Edwards, J. Bowman, C. Kunz, D. Lees, and M. Sims. Photo-realistic Terrain Modeling and Visualization for Mars Exploration Rover Science Operations. In *Proceedings of IEEE SMC 2005*, October 2005.
- [24] Martin A. Fischler and Robert C. Bolles. Random Sample Consensus: A Paradigm for Model Fitting with Applications to Image Analysis and Automated Cartography. *Graphics and Image Processing*, 24(6), June 1981.
- [25] The CGIAR Consortium for Spatial Information. CGIAR-CSI SRTM 90m DEM Digital Elevation Database. URL <http://srtm.csi.cgiar.org>.

- [26] L. Gaddis, J. Anderson, K. Becker, T. Becker, D. Cook, K. Edwards, E. Eliason, T. Hare, H. Kieffer, E. M. Lee, J. Mathews, L. Soderblom, T. Sucharski, J. Torson, A. McEwen, and M. Robinson. An Overview of the Integrated Software for Imaging Spectrometers (ISIS). In *Lunar and Planetary Science Conference*, volume 28, page 387, March 1997.
- [27] GeoEye. Sample Imagery Request Form. GeoEye sample imagery request form <http://geoeye.com/CorpSite/solutions/learn-more/sample-imagery.aspx>. URL <http://geoeye.com/CorpSite/solutions/learn-more/sample-imagery.aspx>.
- [28] L Girod, C Nuth, and A Kääb. Improvement of dem generation from aster images using satellite jitter estimation and open source implementation. *The International Archives of Photogrammetry, Remote Sensing and Spatial Information Sciences*, 40(1):249, 2015.
- [29] Digital Globe. Radiometric Use of WorldView 2 Imagery. Description of the WV02 camera, . URL http://www.digitalglobe.com/sites/default/files/Radiometric_Use_of_WorldView-2_Imagery%20%281%29.pdf.
- [30] Digital Globe. Satellite Imagery and Geospatial Information Products. Digital Globe sample imagery <http://www.digitalglobe.com/product-samples>, . URL <http://www.digitalglobe.com/product-samples>.
- [31] M. Golombek, J. Grant, D. Kipp, A. Vasavada, R. Kirk, R. Fergason, P. Bellutta, F. Calef, K. Larsen, Y. Katayama, A. Huertas, R. Beyer, A. Chen, T. Parker, B. Pollard, S. Lee, Y. Sun, R. Hoover, H. Sladek, J. Grotzinger, R. Welch, E. Noe Dobrea, J. Michalski, and M. Watkins. Selection of the mars science laboratory landing site. *Space Science Reviews*, 170(1-4):641–737, 2012. ISSN 0038-6308. URL <http://dx.doi.org/10.1007/s11214-012-9916-y>.
- [32] Rajiv Gupta and Richard I. Hartley. Linear Pushbroom Cameras. *IEEE Transactions on Pattern Analysis and Machine Intelligence*, 19(9), September 1997.
- [33] Ebner H., Spiegel M., Albert B., Bernd G., and Neukum G. et. al. Improving The Exterior Orientation of Mars Express Hrsc Imagery. In *XXth ISPRS Congress, Commission IV*, 2004.
- [34] N. P. Hammond, C. B. Phillips, G. Robuchon, R. A. Beyer, F. Nimmo, and J. Roberts. Crater relaxation and stereo imaging of rhea. In S. Mackwell and E. Stansbery, editors, *Lunar and Planetary Science Conference 42*, number #2633. Lunar and Planetary Institute, Houston, 2011.
- [35] N.P. Hammond, C.B. Phillips, F. Nimmo, and S.A. Kattenhorn. Flexure on dione: Investigating subsurface structure and thermal history. *Icarus*, 223(1):418 – 422, 2013. ISSN 0019-1035. URL <http://www.sciencedirect.com/science/article/pii/S0019103513000043>.
- [36] R. I. Hartley and A. Zisserman. *Multiple View Geometry in Computer Vision*. Cambridge University Press, ISBN: 0521540518, second edition, 2004.
- [37] C. Heipke and J. Oberst et. al. The HRSC DTM Test. In *Symposium of ISPRS Commission IV - Geo Spatial Databases for Sustainable Development*, 2006.
- [38] John Huffman, Andrew Forsberg, Andrew Loomis, James Head, James Dickson, and Caleb Fassett. Integrating advanced visualization technology into the planetary geoscience workflow. *Planetary and Space Science*, 59(11–12):1273 – 1279, 2011. ISSN 0032-0633. URL <http://www.sciencedirect.com/science/article/pii/S0032063310002175>.
- [39] A. C. G. Hughes, E. Hauber, and A. P. Rossi. Geomorphology of Glacial and Periglacial Landforms Within a Small Crater in Terra Cimmeria, Mars: Stratigraphy and Inferred Chronology of Processes. In *Lunar and Planetary Science Conference 45*, volume 45 of *Lunar and Planetary Institute Science Conference Abstracts*, March 2014.

- [40] A. B. Ivanov and J. J. Lorre. Analysis of Mars Orbiter Camera Stereo Pairs. In *Lunar and Planetary Institute Conference Abstracts*, pages 1845–+, March 2002.
- [41] M. D. Johnston, J. E. Graf, R. W. Zurek, H. J. Eisen, and B. Jai. The Mars Reconnaissance Orbiter Mission. In *2003 IEEE Aerospace Conference*, pages 447–464, 2003.
- [42] J.R. Kim and J.-P. Muller. Multi-resolution topographic data extraction from martian stereo imagery. *Planetary and Space Science*, 57(14–15):2095 – 2112, 2009. ISSN 0032-0633. URL <http://www.sciencedirect.com/science/article/pii/S0032063309002888>.
- [43] R. L. Kirk, E. Howington-Kraus, D. Galuszka, B. Redding, T. M. Hare, C. Heipke, J. Oberst, G. Neukum, and HRSC Co-Investigator Team. Mapping Mars with HRSC, ISIS, and SOCET SET. In S. Mackwell and E. Stansbery, editors, *Lunar and Planetary Science XXXVII*, page #2050, March 2006.
- [44] R.L. Kirk, Laurence A. Soderblom, Elipitha Howington-Kraus, and Brent Archinal. USGS High-Resolution Topomapping of Mars with Mars Orbiter Camera Narrow-Angle Images. *IAPRS: GeoSpatial Theory, Processing and Applications*, 34, 2002.
- [45] Kurt Konolige. Sparse sparse bundle adjustment. In *British Machine Vision Conference*, Aberystwyth, Wales, 08/2010 2010.
- [46] C. Kunz and H. Singh. Stereo self-calibration for seafloor mapping using auvs. In *Autonomous Underwater Vehicles (AUV), 2010 IEEE/OES*, pages 1–7, 2010.
- [47] Pascal Lacroix. Landslides triggered by the gorkha earthquake in the langtang valley, volumes and initiation processes. *Earth, Planets and Space*, 68(1):1–10, 2016.
- [48] Signe Hillerup Larsen, Shfaqat Abbas Khan, Andreas Peter Ahlstrøm, Christine Schøtt Hvidberg, Michael John Willis, and Signe Bech Andersen. Increased mass loss and asynchronous behavior of marine-terminating outlet glaciers at upernavik isstrøm, nw greenland. *Journal of Geophysical Research: Earth Surface*, 2016.
- [49] S. J. Lawrence, M. S. Robinson, M. Broxton, J. D. Stopar, W. Close, J. Grunsfeld, R. Ingram, L. Jefferson, S. Locke, R. Mitchell, T. Scarsella, M. White, M. A. Hager, T. R. Watters ad E. Bowman-Cisneros, J. Danton, and J. Garvin. The Apollo Digital Image Archive: New Research and Data Products. In *Proc of the NLSI Lunar Science Conference*, page 2066, 2008.
- [50] A. Lefort, D. M. Burr, R. A. Beyer, and A. D. Howard. Topographic post-formation modifications of inverted fluvial features in the western Medusa Fossae formation, Mars. In S. Mackwell and E. Stansbery, editors, *Lunar and Planetary Science Conference 42*, number #2418. Lunar and Planetary Institute, Houston, 2011.
- [51] A. Lefort, D. M. Burr, R. A. Beyer, and A. D. Howard. Inverted fluvial features in the Aeolis-Zephyria Plana, western Medusae Fossae Formation, Mars: Evidence for post-formation modification. *Journal of Geophysical Research (Planets)*, 117:E03007, March 2012.
- [52] A. Lefort, D. M. Burr, R. A. Beyer, and A. D. Howard. Sinuous Ridges as Tools to Investigate Post-Flow Modification in the Aeolis-Zephyria Plana, Western Medusae Fossae Formation, Mars. In *Lunar and Planetary Science Conference 43*, number #1953, March 2012.
- [53] Rongxing Li, Juwon Hwangbo, Yunhang Chen, and Kaichang Di. Rigorous photogrammetric processing of hirise stereo imagery for mars topographic mapping. *Geoscience and Remote Sensing, IEEE Transactions on*, 49(7):2558–2572, 2011. ISSN 0196-2892.

- [54] David G. Lowe. Distinctive Image Features from Scale-Invariant Keypoints. *International Journal of Computer Vision*, 2004.
- [55] A. Lucas, A. Mangeney, and J. P. Ampuero. Frictional velocity-weakening in landslides on Earth and on other planetary bodies. *Nature Communications*, 5:3417, March 2014.
- [56] A. Lucchetti, R. Thomas, G. Cremonese, M. Massironi, D. A. Rothery, S. J. Conway, and M. Anand. Analysis and Numerical Modeling of a Pit Crater on Mercury. In *Lunar and Planetary Science Conference 45*, volume 45 of *Lunar and Planetary Institute Science Conference Abstracts*, March 2014.
- [57] Daniel Machacek. Images from the long-awaited Dawn Vesta data set. <http://www.planetary.org/blogs/guest-blogs/20121129-machacek-dawn-vesta.html>, 2012.
- [58] M. C. Malin and K. S. Edgett. Mars Global Surveyor Mars Orbiter Camera: Interplanetary cruise through primary mission. *Journal of Geophysical Research*, 106(E10):23429–23570, October 2001.
- [59] M. C. Malin, G. E. Danielson, A. P. Ingersoll, H. Masursky, J. Veverka, M. A. Ravine, and T. A. Soulanille. Mars Observer Camera. *Journal of Geophysical Research*, 97(E5):7699–7718, May 1992.
- [60] Alfred S McEwen. Photometric functions for photoclinometry and other applications. *Icarus*, 92(2):298–311, 1991.
- [61] Andrew K Melkonian, Michael J Willis, Matthew E Pritchard, and Adam J Stewart. Recent changes in glacier velocities and thinning at novaya zemlya. *Remote Sensing of Environment*, 174:244–257, 2016.
- [62] Christian Menard. *Robust Stereo and Adaptive Matching in Correlation Scale-Space*. PhD thesis, Institute of Automation, Vienna Institute of Technology (PRIP-TR-45), January 1997.
- [63] Zach Moore, Dan Wright, Chris Lewis, and Dale Schinstock. Comparison of bundle adjustment formulations. In *ASPRS Annual Conf., Baltimore, Maryland*, 2009.
- [64] Z. Moratto, A. Nefian, T. Kim, M. Broxton, R. A. Beyer, and T. Fong. Stereo reconstruction from apollo 15 and 16 metric camera. In S. Mackwell and E. Stansbery, editors, *Lunar and Planetary Science Conference 42*, number #2267. Lunar and Planetary Institute, Houston, 2011.
- [65] Zachary Moratto. Creating control networks and bundle adjusting with isis3. <http://lunokhod.org/?p=468>, 2012.
- [66] Zachary Moratto. Making well registered dems with isis and ames stereo pipeline. <http://lunokhod.org/?p=559>, 2012.
- [67] A. M. Morgan, R. A. Beyer, A. D. Howard, and J. M. Moore. The Alluvial Fans of Saheki Crater. In *Lunar and Planetary Science Conference 43*, number #2815, March 2012.
- [68] Ara V. Nefian, Kyle Husmann, Michael Broxton, Matthew D. Hancher, and Michael Lundy. A Bayesian Formulation for Subpixel Refinement in Stereo Orbital Imagery. In *to appear in the Proceedings of the 2009 IEEE International Conference on Image Processing*, 2009.
- [69] Diego Nehab, Szymon Rusinkiewicz, and James Davis. Improved sub-pixel stereo correspondences through symmetric refinement. *Computer Vision, IEEE International Conference on*, 1:557–563, 2005. ISSN 1550-5499.
- [70] G. Neukum and R. Jaumann. HRSC: the High Resolution Stereo Camera of Mars Express. In Andrew Wilson and Agustin Chicarro, editors, *Mars Express: the scientific payload*, number ESA SP-1240, pages 17–35. ESA Publications Division, Noordwijk, Netherlands, August 2004.

- [71] G. A. Neumann, F. G. Lemoine, E. Mazarico, J. F. McGarry, D. D. Rowlands, D. E. Smith, X. Sun, M. Torrence, T. Zagwodski, R. Zellar, and M. T. Zuber. Status of Lunar Reconnaissance Orbiter Laser Ranging and Laser Altimeter Experiments. *AGU Fall Meeting Abstracts*, pages B1419+, December 2008.
- [72] et al. Nguyen, L. Virtual reality interfaces for visualization and control of remote vehicles. *Autonomous Robots*, 11(1), 2001.
- [73] H.K. Nishihara. PRISM: A Practical real-time imaging stereo matcher. *Optical Engineering*, 23(5):536–545, 1984.
- [74] H.K. Nishihara. Practical real-time imaging stereo matcher. *Optical Engineering*, 23(5):536–545, 1984.
- [75] T. Öhman and P. J. McGovern. Strain Calculations for Circumferential Graben on Alba Mons, Mars. *LPI Contributions*, 1719:2966, March 2013.
- [76] Teemu Öhman and David A. Kring. Photogeologic analysis of impact melt-rich lithologies in kepler crater that could be sampled by future missions. *Journal of Geophysical Research: Planets*, 117(E12):n/a–n/a, 2012. ISSN 2156-2202. URL <http://dx.doi.org/10.1029/2011JE003918>.
- [77] Samantha E. Peel and Caleb I. Fassett. Valleys in pit craters on mars: Characteristics, distribution, and formation mechanisms. *Icarus*, (0):–, 2013. ISSN 0019-1035. URL <http://www.sciencedirect.com/science/article/pii/S0019103513001474>.
- [78] C. B. Phillips, R. A. Beyer, F. Nimmo, J. H. Roberts, and G. Robuchon. Crater Relaxation and Stereo Imaging of the Icy Satellites of Jupiter and Saturn. *AGU Fall Meeting Abstracts*, (#P21B-1596), December 2010.
- [79] C. B. Phillips, N. P. Hammond, F. Nimmo, G. robuchon, R. A. Beyer, and J. H. Roberts. Crater Relaxation and Stereo Imaging of Icy Satellites. *AGU Fall Meeting Abstracts*, (#P41F-07), December 2011.
- [80] C. B. Phillips, N. P. Hammond, G. Robuchon, F. Nimmo, R. A. Beyer, and J. Roberts. Stereo Imaging, Crater Relaxation, and Thermal Histories of Rhea and Dione. In *Lunar and Planetary Science Conference 43*, number #2571, March 2012.
- [81] C. B. Phillips, N. P. Hammond, J. H. Roberts, F. Nimmo, R. A. Beyer, and S. Kattenhorn. Stereo Topography and Subsurface Thermal Profiles on Icy Satellites of Saturn. In *Lunar and Planetary Science Conference 44*, number #2766, March 2013.
- [82] François Pomerleau, Francis Colas, Roland Siegwart, and Stéphane Magnenat. Comparing ICP Variants on Real-World Data Sets. *Autonomous Robots*, 34(3):133–148, February 2013.
- [83] Allen Pope, TA Scambos, M Moussavi, M Tedesco, M Willis, D Shean, and S Grigsby. Estimating supraglacial lake depth in west greenland using landsat 8 and comparison with other multispectral methods. *The Cryosphere*, 10:15, 2016.
- [84] Cristina Re, Gabriele Cremonese, Elisa Dall'Asta, Gianfranco Forlani, Giampiero Naletto, and Riccardo Roncella. Performance evaluation of dtm area-based matching reconstruction of moon and mars. *Proc. SPIE 8537, Image and Signal Processing for Remote Sensing XVIII*, pages 85370V–85370V–12, 2012. URL <http://dx.doi.org/10.1117/12.974524>.
- [85] M. S. Robinson, E. M. Eliason, H. Hiesinger, B. L. Jolliff, A. S. McEwen, M. C. Malin, M. A. Ravine, D. Roberts, P. C. Thomas, and E. P. Turtle. LROC – Lunar Reconnaissance Orbiter Camera. In S. Mackwell and E. Stansbery, editors, *Lunar and Planetary Science XXXVI*, number #1576. Lunar and Planetary Institute, Houston (CD-ROM), March 2005.

- [86] M.S. Robinson, E.M. Eliason, H. Hiesinger, B.L. Jolliff, A.S. McEwen, M.C. Malin, M.A. Ravine, D. Roberts, P.C. Thomas, and E.P. Turtle. LROC - Lunar Reconnaissance Orbiter Camera. In *Proc of the Lunar and Planetary Science Conference (LPSC) XXXVI*, page 1576, March 2005.
- [87] Jakob Schwendner and Javier Hidalgo. Terrain aided navigation for planetary exploration missions. In *International Symposium on Artificial Intelligence, Robotics and Automation in Space (i-SAIRAS)*, September 2012.
- [88] David E Shean, Oleg Alexandrov, Zachary M Moratto, Benjamin E Smith, Ian R Joughin, Claire Porter, and Paul Morin. An automated, open-source pipeline for mass production of digital elevation models (dems) from very-high-resolution commercial stereo satellite imagery. *ISPRS Journal of Photogrammetry and Remote Sensing*, 116:101–117, 2016.
- [89] Greg Slabaugh, Ron Schafer, and Mark Livingston. Optimal ray intersection for computing 3d points from n-view correspondences. <http://www.soi.city.ac.uk/~sbbh653/publications/opray.pdf>, 2001.
- [90] D. E. Smith, M. T. Zuber, H. V. Frey, J. B. Garvin, J. W. Head, D. O. Muhleman, G. H. Pettengill, R. J. Phillips, S. C. Solomon, H. J. Zwally, W. B. Banerdt, T. C. Duxbury, M. P. Golombek, F. G. Lemoine, G. A. Neumann, and et al. Mars Orbiter Laser Altimeter: Experiment summary after the first year of global mapping of Mars. *Journal of Geophysical Research*, 106(E10):23689–23722, October 2001.
- [91] Andrew Stein, Andres Huertas, and Larry Matthies. Attenuating stereo pixel-locking via affine window adaptation. In *IEEE International Conference on Robotics and Automation*, pages 914 – 921, May 2006.
- [92] Laura A Stevens, Mark D Behn, Jeffrey J McGuire, Sarah B Das, Ian Joughin, Thomas Herring, David E Shean, and Matt A King. Greenland supraglacial lake drainages triggered by hydrologically induced basal slip. *Nature*, 522(7554):73–76, 2015.
- [93] C. et al. Stoker. Analyzing Pathfinder data using virtual reality and superresolved imaging. *Journal of Geophysical Research*, 104(E4):8889–8906, April 1999.
- [94] Changming Sun. Rectangular Subregioning and 3-D Maximum-Surface Techniques for Fast Stereo Matching. *International Journal of Computer Vision*, 47(1-3), 2002.
- [95] Vytas SunSpiral, D.W. Wheeler, Daniel Chavez-Clemente, and David Mittman. Development and field testing of the footfall planning system for the athlete robots. *Journal of Field Robotics*, 29(3): 483–505, 2012. ISSN 1556-4967. URL <http://dx.doi.org/10.1002/rob.20410>.
- [96] Richard Szeliski and Daniel Scharstein. Sampling the Disparity Space Image. *IEEE Transactions on Pattern Analysis and Machine Intelligence (PAMI)*, 26:419 – 425, 2003.
- [97] Bill Triggs, Philip F. McLauchlan, Richard I. Hartley, and Andrew W. Fitzgibbon. Bundle adjustment – a modern synthesis. *Lecture Notes in Computer Science*, 1883:298+, January 2000.
- [98] Tuscon University of Arizona. The high resolution imaging science experiment. 2009. URL <http://hirise.lpl.arizona.edu/>.
- [99] AZ U.S. Geological Survey, Flagstaff. Integrated software for imagers and spectrometers (ISIS). 2009. URL <http://isis.astrogeology.usgs.gov/>.
- [100] T. R. Watters, M. S. Robinson, R. A. Beyer, J. F. Bell, M. E. Pritchard, M. E. Banks, E. P. Turtle, N. R. Williams, and LROC Team. Lunar Thrust Faults: Implications for the Thermal History of the Moon. In S. Mackwell and E. Stansbery, editors, *Lunar and Planetary Science Conference 41*, number #1863. Lunar and Planetary Institute, Houston, March 2010.

- [101] W. A. Watters and A. C. Radford. 3-D Morphometry of Martian Secondary Impact Craters from Zunil and Gratteri. In *Lunar and Planetary Science 45*, volume 45 of *Lunar and Planetary Institute Science Conference Abstracts*, March 2014.
- [102] W. A. Watters, L. Geiger, and M. Fendrock. Shape Distribution of Fresh Martian Impact Craters from High-Resolution DEMs. In *Lunar and Planetary Science Conference 44*, volume 44 of *Lunar and Planetary Institute Science Conference Abstracts*, March 2013.
- [103] Michael J Willis, Andrew K Melkonian, and Matthew E Pritchard. Outlet glacier response to the 2012 collapse of the matusevich ice shelf, severnaya zemlya, russian arctic. *Journal of Geophysical Research: Earth Surface*, 120(10):2040–2055, 2015.
- [104] M. T. Zuber, D. E. Smith, S. C. Solomon, D. O. Muhleman, J. W. Head, J. B. Garvin, J. B. Abshire, and J. L. Bufton. The Mars Observer laser altimeter investigation. *Journal of Geophysical Research*, 97(E5):7781–7797, May 1992.